STANISŁAW Z. MIKULSKI

The late Variscan gold mineralization in the Kaczawa Mountains, Western Sudetes

Polish Geological Institute Special Papers, 22

WARSZAWA 2007

Polish Geological Institute Special Papers, 22 (2007): 1–162

Editorial Office: Polish Geological Institute, PL-00-975 Warszawa, Rakowiecka 4 (building A, room 409)
phone: (48-22) 849 53 51 ext. 480
fax: (48-22) 849 53 42
Website: http://www.pgi.gov.pl
Volumes can be ordered from Państwowy Instytut Geologiczny, Sekcja Dystrybucji Wydawnictw PIG, Rakowiecka 4, PL-00-975 Warszawa, e-mail: dystryb@pgi.gov.pl

Editors of the volume: Janina Małecka, Anna Maziarz

Layout: Anna Maziarz

The Polish Geological Institute Special Papers is abstracted and indexed in: American Geological Institute/Bibliography and Index of Geology, Elsevier/GeoAbstracts, GEOBASE and Geological Bibliography of Poland.

Printed by Remigraf Ltd., Warszawa, Poland
Issued: 375 copies

CONTENTS

Polish Geological Institute Special Papers, 22 (2007): 1–162

Stanis³aw Z. MIKULSKI — **The late Variscan gold mineralization in the Kaczawa Mountains, Western Sudetes.**
Polish Geological Institute Special Papers, 22 (2007): 1–162

Polish Geological Institute, Rakowiecka 4, PL-00-975, Warszawa, Poland; e-mail: stanislaw.mikulski@pgi.gov.pl

Abstract. Detailed characteristic of the Au-bearing arsenic-polymetallic deposits and a few prospects of the hydrothermal quartz-sulphide vein type from the Kaczawa Mountains are presented. The most important are the gold mineralization in Radzimowice which is classified as the transition from the porphyry to the epithermal type and in Klecza–Radomice described as the orogenic type. Auriferous mineralization is structurally controlled and hosted mainly by cataclased sericite-graphite schists from Pilchowice and Bolków units, which constitute the Paleozoic Kaczawa Metamorphic Complex. The fractured axial planes of F_2 open asymmetric folds built of graphite schist, and second-order fault structures of major W–E and NE–SW directions played significant role as structural and geochemical traps for migrating mineralized hydrothermal fluids. Gold mineralization post-dates the regional metamorphism of host rocks (greenschist facies), main phases of Variscan orogenic deformations (D_1 and D_2), and emplacement of the late Variscan igneous rock suites (ca. 320 Ma). Gold mineralization processes developed in the Kaczawa Mountains are comparable with gold formation stages in the European Variscan Belt (Au_1 to Au_4) during the time period from ca. 350 to 240 Ma, which were distinguished by the author. However, in the Kaczawa Mountains the Au_1 stage connected with the emplacement of syn-collisional granite (Tournaisian) has not been recognised yet. In the Kaczawa Mountains gold formation stages from Au_2 to Au_3 were connected with geodynamic transition from the post-collisional to the within-plate setting. Gold mineralization implies a change from mesothermal to epithermal conditions of Au precipitation after post-collisional granite emplacement and development post-magmatic processes, followed by orogenic uplift, deep fracturing, development of grabens (upper Namurian–Stephanian) and sub- and volcanic activity (Autunian). The first stage of ore precipitation in the coarse quartz veins were Fe–As sulphides (ca. 317 Ma) with submicroscopic gold. This mineralization was brecciated and cemented by the epithermal quartz-carbonate-base metal sulphide (ca. 294–280 Ma) – microscopic gold and locally also by Bi–Te mineral association. Younger stages of the low temperature hydrothermal types are of minor importance and are represent by chalcedony-kaolinite-pyrite/marcasite-gold association connected with volcanic processes in Autunian and by chalcedony-hematite-calcite-gold (Au_4) association precipitated later during the post-Variscan basin formations (Upper Permian–Triassic and ?Cretaceous). Mineralogical and geochemical features of ores, sulphur and oxygen isotopes, fluid inclusion data, and Re–Os age determinations of gold-bearing sulphides are also given. The obtained results suggest that potential for additional gold resources exists in the abandoned mining sites in Radzimowice and Klecza–Radomice, as well as in other areas of the Kaczawa Mountains.

Key words: gold, European Variscan Belt, Kaczawa Mountains, Western Sudetes, Poland.

Abstrakt. Szczegółowo scharakteryzowano złoża oraz przejawy mineralizacji arsenowo-polimetalicznej ze złotem w hydrotermalnych żyłach kwarcowych, zalegających najczęściej w skataklazowanych serycytowo-grafitowych łupkach, zaliczanych do jednostki Pilchowic i Bolkowa, należących do paleozoicznych skał kaczawskiego kompleksu metamorficznego. Do najważniejszych zaliczono złotonośną mineralizację w Radzimowicach sklasyfikowaną jako typ przejściowy pomiędzy mineralizacją porfirową a hydrotermalną i mineralizację w Kleczy–Radomicach opisaną jako typ orogeniczny. Spękane powierzchnie osiowe otwartych, asymetrycznych fałdów (F_2) w obrębie łupków grafitowych oraz spękania i uskoki o drugorzędnym znaczeniu i orientacji wzdłuż kierunku E–W i NE–SW odegrały doniosłą rolę jako strukturalne i geochemiczne pułapki dla migrujących roztworów hydrotermalnych. W Górach Kaczawskich złotonośna mineralizacja siarczkowa jest młodsza od procesów metamorficznych skał otaczających (facja zieleńcowa), głównych faz waryscyjskich deformacji orogenicznych (D_1 i D_2) i późno-waryscyjskich skał magmowych (ca. 320 Ma). Procesy mineralizacji złota w Górach Kaczawskich zostały porównane z wydzielonymi przez autora w europejskich waryscydach procesami tworzenia się złota od etapu Au_1 do Au_4 w czasie od około 350 do 240 mln lat. Przy czym w Górach Kaczawskich jak dotychczas nie rozpoznano etapu Au_1 związanego z rozwojem granitów synkolizyjnych. Etapy od Au_2 do Au_3 były związane ze zmianą środowiska geotektonicznego od post-kolizyjnego do wewnątrz płytowego. Związane z tym było głębokie spękanie wynoszonego orogenu,

utworzenie rowów tektonicznych (górny namur – stefan), rozwój procesów sub- i wulkanicznych (autun). Pierwszy etap mineralizacji rudnej w gruboziarnistym kwarcu reprezentują głównie siarczki As i Fe (wiek ok. 317 mln) zawierające złoto submikroskopowe. Mineralizacja ta, została skataklazowana i scementowana przez epitermalny kwarc-węglany-siarczki metali podstawowych (wiek 294–280 Ma) – złoto mikroskopowe i lokalnie także przez asocjacje minerałów Bi i Te. Młodsze etapy reprezentowane są przez niskotemperaturowe asocjacje hydrotermalne. Mają one mniejsze znaczenie i są reprezentowane przez asocjacje chalcedon-kaolinit-piryt/markasyt-złoto, których powstanie związane było z aktywnością wulkaniczną w autunie oraz asocjacje chalcedon-hematyt-kalcyt-złoto (Au_4), powstałe w czasie formowania się post-waryscyjskich zbiorników sedymentacyjnych od górnego permu do triasu, a może nawet w kredzie. Ponadto szczegółowo scharakteryzowano pod względem mineralogicznym oraz geochemicznym złotonośne rudy siarczkowe. Przedstawiono również dane izotopowe siarki siarczkowej oraz rezultaty badań inkluzji fluidalnych oraz izotopów tlenu w kwarcu a także wyniki oznaczeń wieku metodą Re–Os na złotonośnych siarczkach. Uzyskane rezultaty wskazują na dodatkowe zasoby złota w opuszczonych rejonach górniczych Radzimowic i Kleczy–Radomic, jak również w innych rejonach Gór Kaczawskich.

Słowa kluczowe: złoto, waryscydy, Góry Kaczawskie, Sudety Zachodnie, Polska.

INTRODUCTION

In the Kaczawa Mountains, several small size gold deposits were the targets of limited exploitation since medieval times. Historical gold production in this area, of about 30 t gold, came from placer deposits located mostly in the valleys of the Kaczawa and Bóbr rivers and from vein gold deposits. Among the vein gold deposits the highest production came from the Radzimowice and Klecza–Radomice ore districts. It is estimated that at least 5–7 t of gold was recovered from these deposits. In the 1950s, the prospecting works started again in the abandoned gold mining sites. They were followed in the 1960s by the surface geophysical and geochemical prospecting that defined several metal anomalies, although major exploration was not undertaken. During the last few years limited surface prospecting carried out by the Polish Geological Institute provided many new data, which are presented in the monograph.

PREVIOUS WORKS ON THE GOLD ORE MINERALIZATION IN THE KACZAWA MOUNTAINS

Traube (1888) was the one of the first geologist who studied the primary gold-bearing sulphide mineralization in quartz veins from the Kaczawa Mountains. He combined the list of minerals from the ore zones in Radzimowice. Kosmann (1891) and Sachs (1914) connected the genesis of gold-bearing quartz-sulphide veins from the Radzimowice deposit with formation of kersantites. Stauffacher (1914, 1915) described in surroundings of the ore-bearing veins intensive alteration of the porphyry type and considered the genesis of the ore mineral concentration as related to the Żeleźniak porphyry intrusion. He considered the occurrence of the native gold as finely disseminated in arsenopyrite. The first short description of the Radzimowice ores investigation under the reflected light microscope was presented by Petrascheck (1933). He correlated the gold appearance mainly with arsenopyrite and subordinately with pyrite and chalcopyrite, and presence of silver with galena and chalcopyrite. Petrascheck (1933) connected genesis of the ore mineralization at Radzimowice deposit with the magmatic activity of the Karkonosze granitoid intrusion which hypothetically occurs deeper as a batholith.

The genesis of gold-bearing ore mineralization at the Klecza–Radomice ore district was also commonly assumed as a hydrothermal type though the source of metals remain obscure (Krusch, 1907; Kosmann, 1930; Grimming, 1933; Stahl, 1935; Quiring, 1948). Krusch (1907) recognised close correlation between distribution of gold and pyrite and a weak correlation of gold with arsenopyrite in the Klecza deposit. Grimming (1933) noticed that in the main adit (Wilhelm) concentration of arsenic decreases with depth while the contents of pyrite increase. Stahl (1935) described the mineral potential of this area.

Descriptions of the mineral deposits of the Lower Silesia after the II World War were given first by Krajewski (1948) and later by Konstantynowicz (1960). In the years 1951–1957 geologists from the Złoty Stok industrial arsenic plant carried out the prospecting works in the Radzimowice deposit. The new results allowed to discover the extension of the some already known quartz-sulphide veins as well as new ones (Osmólski, pers. inf., 1993). Geochemical sampling of the lowest soil horizons as well as the outcrops of the solid bedrock occurring near the profile lines in the Radzimowice area was made by Pendias (1965). Lindner (1963) localized the several near-surface geochemical and geophysical anomalies extending from Rząsiny to Jeżów Sudecki. Manecki, Młodożeniec (1959; 1960) found in samples from the Wanda vein at the Radzimowice deposit cobaltite and Co admixture in arsenopyrite. Paulo (1962) found in the vicinity of Lipa additional new

occurrences of ore mineralization. The detailed information about the primary gold deposits and history of their exploration in the Lower Silesia region was summarized by Domaszewska (1965, 1965). Mineralogical and petrographical characteristics of the polymetallic veins of the Radzimowice deposit and ore minerals occurrences in the vicinity of Wojcieszów were presented by Manecki (1965). His examinations of the ores showed that pyrite is the gold-bearing mineral in the Wanda vein, and native gold occurs as submicroscopic inclusions in pyrite and/or solid solution with pyrite. Zimnoch (1965) had access only to the ore samples from the Miner consolation vein and concluded that ore genesis at the Radzimowice deposit should be classified as of the hydrothermal origin and of the high temperature type. Fedak, Lindner (1966) in their monographic publication – "The metallogeny of the Sudetes", presented also a short description of the auriferous sulphide deposits and occurrences from the Kaczawa Mountains. They classified the primary gold deposits from the Kaczawa Mountains into a broad group of the pneumatolytic, hydrothermal and metasomatic deposits formed in the Variscan epoch.

The history of the ore mining and working of nonferrous metals in Lower Silesia from the 13th to the 20th century, elaborated Dziekoński (1972). The first microscopic native gold from the Kaczawa Mountains was recognized in samples from the Klecza–Radomice ore district by Paulo, Salamon (1973a).

In the 1960s and 1970s the intensive barite prospecting in the Kaczawa Mountains allowed the elaboration of the various hypotheses of the genesis of vein type mineralization of barite and polymetallic sulphide in the connection with the magmatic and structural developments of the Western Sudetes (Jerzmański, 1958, 1976 a, b; Konstantynowicz, 1960, 1971; Kanasiewicz, Sylwestrzak, 1970; Paulo, 1973, 1994; Wajsprych, 1974 Kowalski, 1976, 1977). Kowalski (1977) distinguished in the Sudetes two separate mineralization cycles of post-magmatic type. On the metallogenic map of the Bohemian Massif at the scale 1:500 000 Lächelt *et al.* (1976) classified mineralization from Klecza–Radomice and Radzimowice to the vein type deposits in quartz and in association with arsenic sulphide. In the book "The minerals of the Lower Silesia" by Lis, Sylwestrzak (1986) the short descriptions of the native gold distribution in the Sudetes are presented. Osika (1987) and Lindner (1990) included gold deposits from the Kaczawa Mountains into the epithermal arsenic-pyritic formation with gold (Pławna, Klecza–Radomice–Pilchowice) and to the hydrothermal high temperature arsenic-polymetallic formation (Radzimowice).

In the 1980s, Rutkowski from Polish Geological Institute conducted prospecting and exploration of the placer gold in the Bóbr middle river basin. These areas have a very long history of exploration (Domaszewska, 1965; Dziekoński, 1972) and have been studied in details by Grodzicki (1960, 1967, 1971, 1972).

In the 1990s the PGI started also a surface geochemical prospecting works for gold in the Sudetes Mountains (Sokołowska, Wojciechowski, 1995). Siemiątkowski (1993) recognised differences between average distributions of metallic elements from the northern and southern parts of the old mining wastes at Radzimowice deposit. Additionally, the ore genesis studies of the gold mineralization, as well as the petrologic and geochemical investigation began in order to define further mineral exploration targets in the entire region. Recently, microscopic gold from Radzimowice was described by Pająk (1997) and Mikulski (1999) and from Klecza–Radomice by Olszyński, Mikulski (1997). Banaś and Mochnacka (1997) summarised results of different author's investigation on Au and Ag paragenetic mineralization from selected parts of the Sudetes. Mikulski *et al.* (1999), presenting the classification of gold deposits and occurrences in the Western Sudetes, included gold deposits from the Kaczawa Mountains. Gold as a trace element in the rocks of the Kaczawa Metamorphic Complex was reported by Kaliszuk (2000). The structural microscopic classification of gold from Au-bearing polymetallic ores in Lower Silesia was proposed by Mikulski (2000a). Genesis of the ore mineralization in Radzimowice and Klecza–Radomice was considered recently by Mikulski (2003a, b; 2005a). Secondary minerals formed during weathering processes at the Radzimowice deposit were described by Siuda (2005)

METHODS AND ANALYTICAL PROCEDURES

Detailed microscope studies in reflected light were carried out on the LEITZ microscope of ORTHOPLAN-PL type. Microscope photographs were made by use of the Leitz ORTHOMAT E automatic microscope camera. Scanning electron microscope (SEM) analyses were performed at the Polish Geological Institute on an electron microscope of Jeol JSM-35 in energy-dispersive mode (EDS Link Analytical ISIS). Operating conditions were 20 kV accelerating voltage, 5 μm spot size, and 6 nA sample current for gold, telluride's and other ore minerals. Well-characterized mineral standards used; the ZAF-4 correction program was applied.

Application of arsenopyrite geothermometer despite its limits allowed obtaining crystallization temperatures of various type arsenopyrite samples. The As/S ratio of the arsenopyrite coexisting with other phases in the system As–S–Fe has been proposed as a geothermometer (e.g. Kretschmar, Scott, 1976; modified by Shap *et al.*, 1985). An application of the elaborated diagrams request use of the international arsenopyrite standards (asp 57 and/or asp 200) and a very precise selection of materials before the microprobe measurements. Dr. Ulrich Kretschmar and Steven D. Scott are thanked for providing arsenopyrite standards.

Sulphur isotope compositions were measured in over 50 sulphide samples from the ore-bearing quartz veins from the northern and southern parts of the Radzimowice deposit, and from the Klecza–Radomice ore district. Sulphide minerals for

isotope analysis were separated from crushed specimens by handpicking under a binocular microscope. Up to 50 mg was finely milled in an agate mortar. About 100 μg of sulphide was combusted in an elemental analyser and the resulting SO_2 gas was analysed with continuous flow-isotope ratio mass spectrometry (MI 1305) technique at the Isotope Laboratory of Wrocław University (Jędrysek, 1990). Analytical precision determined from replicate runs of the NBS-121 standard ($\delta^{34}S_{CDT}$ = 0.00‰) is ±0.1 per mil.

Microthermometric measurements were carried out on fluid inclusions hosted by quartz from the ore-bearing veins and by quartz phenocryst from mineralized and barren rocks by A. Kozłowski at Warsaw University. Only primary inclusions were considered for this study. Routine heating-freezing microscope runs were performed according to the procedures described by Roedder (1984). The precision of the measurements was ±1°C for the homogenization temperatures during heating and ±0.1°C during freezing. The method of physic-chemical analysis of inclusion fluid behaviour during freezing down to –130°C was performed after Kozłowski (1984). The contents of the salts in the inclusion solutions were calculated with use of the standard physic-chemical plots and the programme *Fluids* supplied to A. Kozłowski by R. Bakker. The percentage of the individual salts in inclusion solutions was calculated as the part of the total salt dissolved. Similarly, the percent values of the gas refer to the total gas equal 100 percent.

A total of over 300 samples from Radzimowice deposit and Klecza–Radomice ore districts subjected to noble elements analyses. Chemical gold determination was made in the PGI Central Chemical Laboratory with detection limit of 1 ppb. Rock samples, after ignition at temperature range 450–640°C were digested with aqua regia. The received gold-bearing chloride complex was extracted to MIBK (methyl isobutyl ketone) form. All results were obtained using Graphite Furnace Atomic Absorption method (GF-AAS) by spectrometer Perkin Elmer model 4100 ZL.

Major elements in over 50 samples from the gold-bearing areas in the Kaczawa Mts. were measured at PGI, by wave lenses dispersive X-ray fluorescence techniques on glass beads, and minor and trace elements by WD-XRF on powder pellets on PW-2400 Philips and/or by digestion ICP-AES techniques. Measurement conditions: radiation – X-ray tube with rhodium anode (3 kW); crystals – LiF 200, PE, Ge, PX1; collimators: 0.15 mm, 0.30 mm; detectors: scintillation counter, flow proportional counter (Ar/CH_4) and Xe-sealed proportional counter. Total uncertainty of the whole procedure applied during the XRF analyses was estimated by Iwasińska-Budzyk to be ±5% for major oxides and ±8% for trace elements. Additionally, trace elements, including REE in 38 samples were analysed by inductively coupled-plasma mass spectrometry (ICP-MS) in Act Lab (Canada).

Rhenium and osmium concentrations in selected auriferous sulphides from the Kaczawa Mountains were determined by AIRIE low level laboratory at Colorado State University (USA) by R. Markey and H. Stein. Re–Os measurements were performed according to procedure described by Smoliar *et al.* (1996), Stein *et al.* (2000, 2001) and Markey *et al*. (2003). Auriferous sulphides from the Kaczawa Mountains characterized by extremely low-level concentration of Re and Os and to very high Re to Os ratio (so called low level highly radiogenic sulphides – LLHR, Stein *et al*., 2000). On very low-level samples Os is dominated by the procedural blanks (Os contributed by the analytical reagents; Markey *et al.*, 2003). Subtraction of blank contributions in such cases results in a very significant adjustment to the $^{187}Os/^{188}Os$ ratio, with a commensurate increase in the uncertainties of both the isotopic composition and the concentration of Os in the sample. LLHR are samples whose ^{187}Os compose more than half of the total Os. They characterised a hydrothermal environment, particularly for crustally derived deposits (Stein *et al.*, 2000). The results presented here are the first direct age determination of auriferous sulphides from the European Variscan Belt.

Seven quartz samples from the Radzimowice deposit were analysed by C. Lerouge in BRGM for oxygen composition by laser fluorination following the procedure of Fouillac, Girard (1996). The $\delta^{18}O$ of fluid in equilibrium with quartz was estimated with use of the quartz-water fractionation data of Matsuhisa *et al*. (1979), for a range of temperatures based on micro-thermometric data of fluid inclusions in the quartz.

In co-operation with M. Sikorska-Jaworowska from PGI the cathodoluminescence studies were performed on over 100 polished thin-sections by used of the CCL 8200 mk3 device (cold-cathode) mounted on polarising microscope.

GEOLOGICAL SETTING

MAJOR GEOLOGICAL EVENTS IN THE WESTERN SUDETES

The Kaczawa Mountains occur in the west-central part of the Western Sudetes. On the north they are separate by the Marginal Sudetic fault (MSF) from the Fore-Sudetic Block and on the south by the Intra-Sudetic fault (ISF) from the Izera–Karkonosze Block. The Fore-Sudetic Block is covered by thin sequence of Mesozoic and Cenozoic sediments. Its basement is considered on the lithological and metamorphic grounds as continuation of the Kaczawa Metamorphic Complex (Oberc, 1972). The Western Sudetes constitute the northeastern part of the Bohemian Massif, which is an exposed part of the European Variscides within Central Europe that includes part of Poland, the Czech Republic, Austria, and Germany. The basement of the Western Sudetes unit is considered as a continuation of the Saxothuringian Zone of the European Variscides. However, its

structural zones are disrupted and separated from the rest of the Variscides by major NW–SE-striking faults, in particular the Marginal Sudetic and Intra-Sudetic faults. The basement of the Western Sudetes consists of Neoproterozoic and Paleozoic rocks, affected by Cadomian and Hercynian metamorphism ranging from very low grade to eclogite facies, with peaks during Middle–Late Devonian and Early Carboniferous (Viséan) times (Franke, Żelaźniewicz, 2000).

The Paleozoic geological evolution of the Western Sudetes is characterized by rifting during (?)Cambrian–Ordovician to Devonian times, with a Late Devonian to Early Carboniferous subduction-collision setting (Franke, Żelaźniewicz, 2000; Kozdrój *et al.*, 2001). Carboniferous thermal events were caused by the emplacement of the granitoid intrusions during the Variscan orogeny (ca. 330–280 Ma by Rb–Sr method; Pin *et al.*, 1989). In the Sudetic area these Variscan granitoid intrusions consolidated several crystalline blocks that consist of metamorphosed sedimentary-submarine-volcanic series with well documented bimodal-volcanic and ophiolitic rocks (Teisseyre *et al.*, 1957; Oberc, 1972; Don, 1995; Żelaźniewicz, 1997). This mosaic geological structure of this area has been interpreted as a terrane assemblage (Matte *et al.*, 1990). This idea was later developed and the various concept of the Sudetes division into several terranes have been presented recently in several papers (e.g. Grocholski, 1986; Cymerman, Piasecki, 1994; Cymerman *et al.*, 1997; Cymerman, 1998a, 2000). The Sudetic terranes collage was formed during the Caledonian (probably Silurian) events and reconstructed during Variscan time (Cymerman, Piasecki, 1994). In Carboniferous major NW–SE trending dextral strike-slip regional faults developed (Aleksandrowski, 1995) as a result of the oblique convergence between the amalgamated Bohemian Massif with the blocks already accreted to the East European Craton (Seston *et al.*, 2000). Aleksandrowski (1995, 2003) postulated multiple displacements along the ISF from Upper Devonian to Lower Permian. Extension within the eastern part of the Variscan belt of Europe (the Central European province) during the Late Carboniferous and Permian resulted in volcanism, as a product of a late- to post-collisional tectonic setting (Awdankiewicz, 1999; Karnkowski 1999). In the Western Sudetes several volcanic centres and their successive eruptive products were controlled by NNW–SSE to NW–SE aligned fault zones. These faults bound the Hercynian depressions filled with flysch deposits and minor volcanic rocks (Dziedzic, 1996). Kozłowski, Parachoniak (1967) described two volcanic cycles, each beginning with predominant trachyandesite with dacite and ending with rhyolite. These volcanics and subvolcanics overly discordantly older sediments and are comparable in age with a younger type of the Strzegom granodiorite (ca. 280 Ma; Pin *et al.*, 1989) which might have acted as their magmatic deep source (Kozdrój *et al.*, 2001). The paleomagnetic studies of the Western Sudetes showed also important counter clockwise rotations of the microplate during the Permian. These rotations indicate a sinistral transtensional tectonic regime during Permian sedimentation in the Sudetes (Nawrocki, 1998). During subsequent Mesozoic extension, the Western Sudetes underwent also a transpression that caused a basin inversion. The recent exhumation of the Variscan structures was due to Alpine faulting during the Paleogene (Teisseyre *et al.*, 1957).

GEOLOGY OF THE KACZAWA MOUNTAINS

The geological structure of the Kaczawa Mountains is characterized by vertical bipartite. Two structural complexes have been distinguished: 1) the lower, basement complex (Kaczawa Metamorphic Complex) composed of Paleozoic epimetamorphosed, folded volcanic-sedimentary rocks, 2) the upper complex that covered unconformably the lower complex, comprising unmetamorphosed, slightly deformed platform-type sediments and volcanics of Late Carboniferous, Permian, Triassic and Late Cretaceous in age (Teisseyre *et al.*, 1957).

The rocks of the lower complex were exposed, due to a strong diastrophic processes during the Cretaceous–Paleocene times (Laramian phase) of the Alpine orogeny (Teisseyre *et al.*, 1957; Oberc, 1972). The platform sediments of intra-mountain fluvial to marine clastic sediments of Early Carboniferous to Early Permian age, accompanied by acid to intermediate volcanism occur mainly in the graben structures such as the North Sudetic Basin, Świerzawa graben, and Intra-Sudetic Basin, that are developed on the basement built of rocks belonging to the Kaczawa Metamorphic Complex.

The Kaczawa Metamorphic Complex has been divided into thirteen nappe-like units, however most of these tectonic units consist of various smaller tectonic elements such as thrust sheets, thrust folds and/or mélange bodies (Gierwielaniec, 1956; Teisseyre, 1956, 1963, 1967; Jerzmański, 1965; Haydukiewicz, 1977, 1987a, b; Baranowski *et al.*, 1990, 1998; Kryza, Muszyński, 1992; Mapa…, 2000; Seston *et al.*, 2000; Kozdrój *et al.*, 2001; Cymerman, 2002). North of the Świerzawa graben these units are: (from north to south) the Złotoryja–Luboradz, Chełmiec and Rzeszówek–Jakuszowa units (Fig. 1). South of the graben, these units are (from the west to east): the Lubań Śląski, Pilchowice, Świerzawa, Bolków, Dobromierz units, and the Cieszów unit at the top. Gierwielaniec (1956) who described the Wleń and Pilchowice units as nappe structures, considered the last unit that consists at least of two thrust-sheets. These units have been correlated with Świerzawa (Wleń unit) and Bolków unit (Pilchowice unit), (Szałamacha, 1971; Oberc, 1972). The main southern outcrop of the Świerzawa unit was interpreted as the overturned limb of a south verging anticline (Teisseyre, 1956). Previously, to the Bolków unit also included the Radzimowice schist subunit (Baranowski, 1988), which recently is considered as a separate tectonic unit of unknown position and age. Kryza, Muszyński (1992) proposed a new working stratigraphic scheme of the southern part of the Kaczawa Metamorphic Complex:

Miłek succession that consists of (?)Cambrian –Ordovician rocks represented by Podgórki volcanic complex, Wojcieszów limestones, Osełka rhyodacites, and Gackowa sandstones, gray slates (?Cambrian–Ordovician), Lubrza trachytes (Ordovician), black slates and cherts and siliceous slates (Silurian–Devonian).

Preliminary U–Pb dating of zircons from the meta-trachyte associated with alkaline metabasalts from the Świerzawa unit yielded a result of 511 ±39 Ma (Pin *et al.*, 1989). Only a small amount of rocks have age determinations based on paleontological or radiometric dating. However, Silurian graptolitic slates, Devonian slates and meta-cherts with a radiolarian and conodont fauna, and Carboniferous limestones are documented (Baranowski *et al.*, 1990). A new paleontologic findings in the Wojcieszów limestones (Skowronek, Steffahn, 2000) unequivocally excludes a Cambrian age and points to a Silurian or younger age for the Wojcieszów limestones. This fact allowed elaborating a new lithostratigraphic profile for the Kaczawa Metamorphic Complex (KMC) (Kozdrój, Skowronek, 1999; Kozdrój *et al.*, 2001). The profile started with Ordovician grey slates of Świerzawa Formation through the Podgórki metavolcanic complex (correlated with the Lower Silurian metabasics) to Wojcieszów limestones (Silurian) that is followed by the Radzimowice schists. The Radzimowice schists that in the base are composed of graphitic quartzites and metalydites are comparable with other deep water sediments of Silurian or younger age. Thus, the sedimentation of the KMC succession started not in Cambrian but in Ordovician (Kozdrój, Skowronek, 1999).

The transitional Silurian-Devonian boundary was documented in the Lubań Śląski unit (Jaeger, 1964; Chorowska *et al.*, 1981). These rocks contain less lydites and graphitic slates and more siliceous or clay-rich slates and mudstones with locally developed phosphatic nodules. Lower and Middle Devonian rocks are represented by phyllites and slates with metalydites, graphite schists and locally metacherts (Urbanek *et al.*, 1975; Chorowska *et al.*, 1981; Chorowska, 1982;). Upper Devonian rocks are represented by thinly laminated slates with calcareous quartzites, greenish, partly red phyllites, locally intercalations of metacherts (Urbanek, 1978; Haydukiewicz, Urbanek, 1986; Baranowski *et al.*, 1987; 1990).

A large part of the Kaczawa Complex is occupied by an undifferentiated, probably Devonian–Lower Carboniferous series, comprising gray phyllites and slates with intercalations of calcareous metasiltstones, arkoses, quartzites, limestones and rhyolitic tuffs (Baranowski, 1975; Chorowska, 1978; Haydukiewicz, 1987a; Baranowski *et al.*, 1990; 1998).

The Variscan basin was considered to have been opened on a Late Proterozoic orogenic Cadomian basement during Cambrian (Franke, Żelaźniewicz, 2000), however, according to new data, it should be open rather in Ordovician (Kozdrój, Skowronek, 1999; Kozdrój *et al.*, 2001). Trace element and Nd-isotope data from all tectonic units of the Kaczawa Complex suggest evolution from a within-plate, possibly initial-rift environment, to more evolved rifting regime, producing basalts of T-MORB and N-MORB characteristics (Baranowski *et al.*, 1990; Floyd *et al.*, 2000). Alkali metabasalts dominated volcanic rocks in the west of the area, mainly in the Świerzawa unit, and MORB-like metabasalts in the east, mainly in the Dobromierz unit (Floyd *et al.*, 2000). A similar distribution is seen in the units north of the Świerzawa graben (Seston *et al.*, 2000). Rift-drift environment underwent until Devonian, and then the accretion prism formed between the Late Devonian and Early Carboniferous as a result of subduction-collision geotectonic settings (Baranowski *et al.*, 1990; Franke, Żelaźniewicz, 2000). The mélange bodies recognised in the whole area of the Kaczawa Mountains represent a later stage of the evolution of the Kaczawa Metamorphic Complex (Fig. 1). According to Baranowski *et al.*, 1990, the mélange was deposited from gravity flows and slides in a trench or on a trench slope during the formation of an accretion prism.

Cymerman, Piasecki (1994) proposed to divide the different rock associations in the Kaczawa Metamorphic Complex along the Kaczawa tectonic line. According to these authors, it is a major structural element (a regional scale detachment) which acted as the basal decollement of thin- to thick-skinned orogenic wedge. According to the Cymerman's (2002) new structural model for the Variscan evolution of Kaczawa Metamorphic Complex, five tectonic units from the eastern part that are built of MORB-like-metabasalt rocks of oceanic crust have been overthrusted toward the west along the Kaczawa zone on the allochthonous units built of metasediments and alkali metabasalts that occurred in the western part of Kaczawa Metamorphic Complex. On the other hand, these units forming also imbricated thrust sheets were thrusted westwards on less deformed and metamorphosed parautochthonous units. The western part of the Kaczawa Metamorphic Complex (lower structural unit) belongs to the Saxothuringian terrane and those structural units are overriding by the Dobromierz and Jakuszowa units, which belong to the Central Sudetic terrane (Cymerman, 2002).

Kaczawa Complex underwent polyphase deformation and metamorphism ranging from very low grade to greenschist-facies metamorphism, with peaks during Late Devonian and Early Carboniferous (Viséan) time. Locally, there are relicts of a high-grade blue schist glaucophane-jadeite mineral assemblage (Kryza, Mazur, 1995). The rocks of the Kaczawa Metamorphic Complex experienced several stages of deformation during the Variscan orogeny (Teisseyre, 1963; Wajsprych, 1974; Haydukiewicz, 1987a). The older event, probably during Lower Devonian, resulted in a system of thrusts related to the formation of mélange metamorphism in blue schist condition (Baranowski *et al.*, 1990). According to Żelaźniewicz *et al.* (1997) the Kaczawa Mountains along the Intra-Sudetic fault have been thrusted southward and south-westward over the Izera–Karkonosze Block during greenschist metamorphism of the Kaczawa Metamophic Complex (ca. 340 Ma) and prior to intrusion of the Variscan Karkonosze granite at ca. 330–325 Ma (Duthou *et al.*, 1991). Seston *et al.* (2000) indicate for three deformation events in the KMC (D_1–D_3). D_1 of compression character directed towards the NW. The second deformation event (D_2), under greenschist facies metamorphism has extensional character with movements to south-east. The third deformation event probably in the Sudetic phase during Early

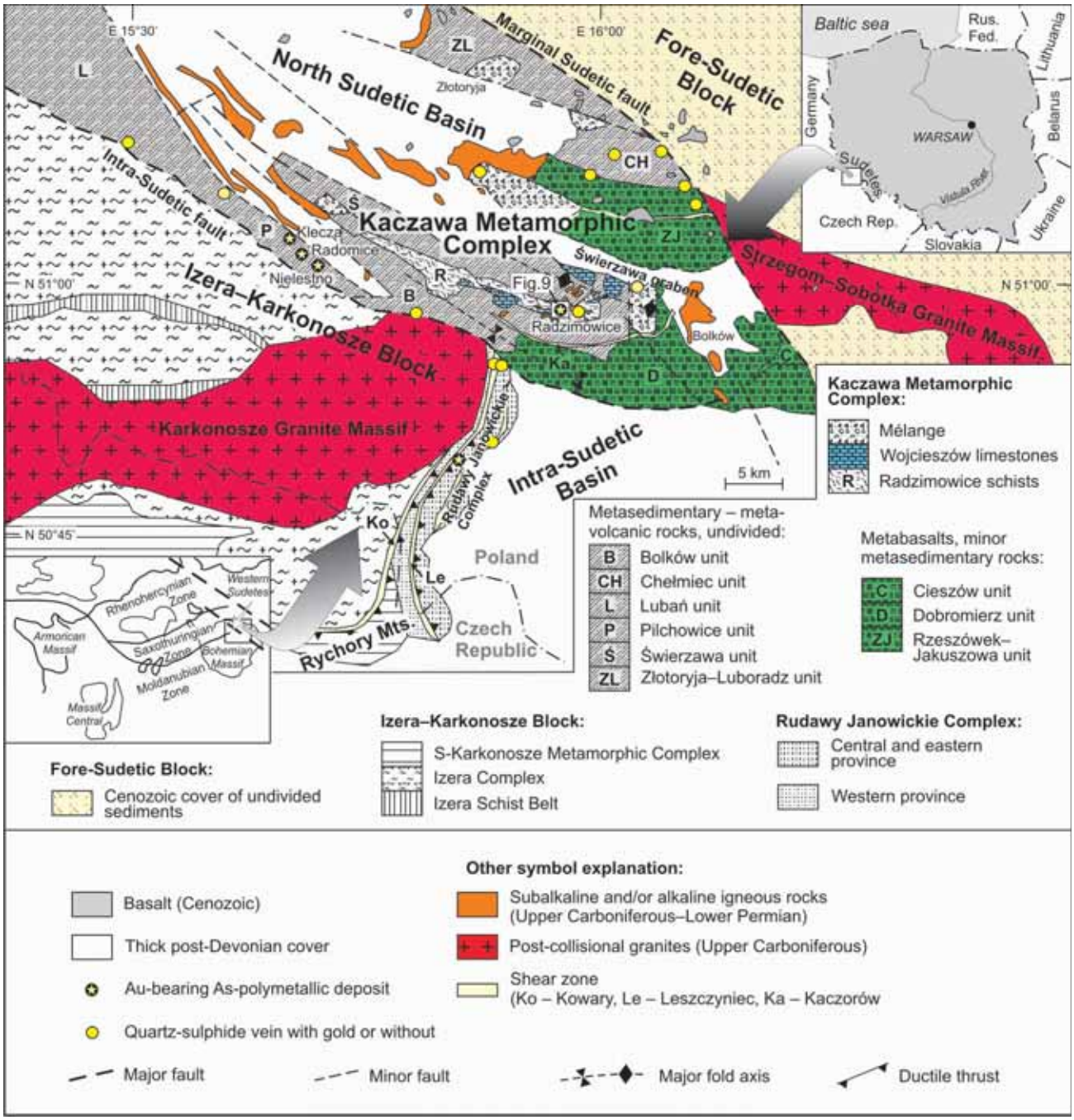

Fig. 1. The tectonic structural subdivisions of the Kaczawa Metamorphic Complex, and adjacent geological units (after Jerzmański, 1965; Baranowski *et al.* 1990; Seston *et al.* 2000; Winchester *et al.* 1995; Kozdrój, Skowronek, 1999; Cymerman, 2002) with distribution of Upper Paleozoic igneous rocks and Cenozoic basalts and location of abandoned major gold mines and prospects

Carboniferous resulted in a major and minor south-verging F_3 open, asymmetric folds, which trend WNW–ESE and verge towards the SW, such as the Bolków–Wojcieszów antiform or Chrośnica–Radomierz synform (Baranowski *et al.*, 1998; Seston *et al.*, 2000; Fig. 1). Cymerman (2002) revealed only two principal deformation events (D_1 and D_2). The D_1 deformation took place in a sinistral transpressional tectonic regime, where the regional-scale overriding ductile thrust sheets moved to the west and northwest in Late Devonian–Early Carboniferous. During the late Variscan orogeny (late Viséan) the D_2 deformation tectonic movements became extensional and more brittle in general towards the east. These extensional movements of D_2 deformation ended with development of extensive volcanism during the uppermost Carboniferous–Lower Permian as grabens and semi-grabens formed. Upper Viséan to Permian regional extension of the earlier, tectonically thickened crust produced high-angle normal and small displacement strike-slip faults in the Western Sudetes.

During the Upper Carboniferous the late to post-collisional intrusion of the Karkonosze granites, caused tilting the Kaczawa Metamorphic Complex and Rudawy Janowickie Complex and then took place faulting.

Block movements along the major faults in the Kaczawa Mountains have been of different character intensity. The Marginal Sudetic fault revealed rather advantage of a dip-slip movement instead of the strike-slip movement documented along the Intra-Sudetic fault (Aleksandrowski, 1995). Variscan structures of the Kaczawa Complex were also modified during the Laramian and young Alpine tectonic movements, mainly by rotation and tilting of small crustal blocks (Teisseyre, 1956; Oberc, 1972).

MAIN EVENTS OF ORE FORMATION IN THE KACZAWA MOUNTAINS

The Kaczawa Mountains since the early medieval time were the place of noble and base metals exploitation. Prospecting for ores and their mining, like in other areas of Europe, were carried out with many breaks and intensive development.

During the 20th century, only a few small deposits of vein type were the subjects of exploitation in the Kaczawa Mountains. Among them the most important are: Radzimowice Au–As–Cu deposit, Klecza–Radomice Au ore district, Wielisław Złotoryjski Au–Fe deposit, Pławna–Lubomierz Au deposit, Chełmiec Fe deposit, Męcinka Fe deposit, Stanisławów Ba deposit, Jeżów Sudecki Ba deposit (Fig. 2).

According to results presented by various geologists (e.g. Petrascheck 1933, 1943; Neuhaus, 1936; Quiring, 1948; Jerzmański, 1958, 1976a, b; Manecki, Młodożeniec, 1960; Manecki, 1965; Zimnoch, 1965, Fedak, Lindner 1966; Paulo, 1970, 1972, 1973, 1994; Paulo, Salamon, 1973a, b, 1974a, b; Kowalski, 1976; 1977; Grocholski, Sawicki, 1982; Sawłowicz, 1987; Olszyński, Mikulski, 1997; Mikulski, 1999, 2001, 2003a, b; 2005a Mikulski *et al*. 1999) it is possible to distinguished in the Kaczawa Mountains at least four principal genetic episodes of mineral deposition:

(1) Those related to sedimentary processes and submarine volcanism within a rifting environment (Ordovician–Silurian);

(2) Those associated with the main folding event and greenschist metamorphism (Upper Devonian–Lower Carboniferous);

(3) Variscan (Carboniferous–Permian; ca. 340–270 Ma) epigenetic gold-bearing As-polymetallic quartz ± carbonate vein mineralization;

(4) Younger post-Variscan barite-fluorite vein deposits formed during Triassic–Paleogene (ca. 245–65 Ma).

Ad. 1 and 2. Within elaborated rocks ore mineralization is not significant. Among the ore minerals dominate pyrite, chalcopyrite, magnetite, ilmenite and titanite. Late diagenetic framboidal pyrite appears in graphite schists. In some places

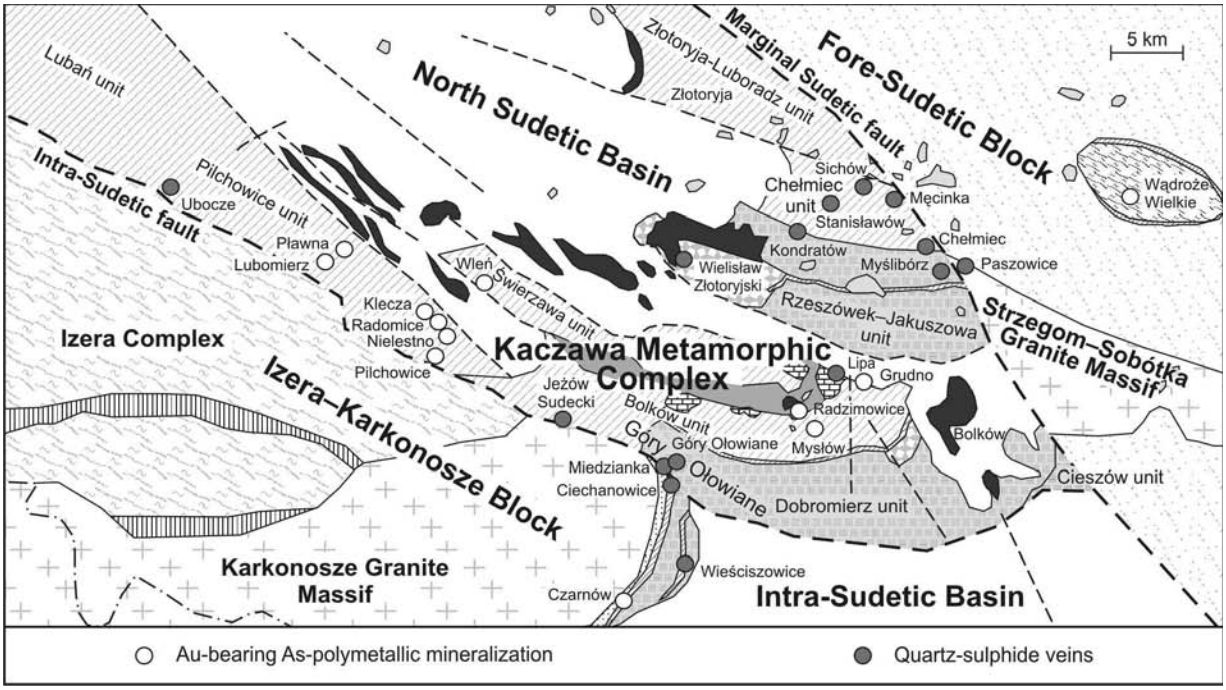

Fig. 2. The vein-type gold and other metals deposits in the Kaczawa Mountains and in the adjacent areas

contents of pyrite framboids may reach up to a several per cent of rock volume. In massive rocks pyrite forms euhedral and fractured grains that are randomly distributed. In chlorite schists pyrite grains of variable size occurred within laminae. Fine flakes of hematite accompany pyrite in chlorite schists. Contents of hematite may reach up to 12–15% of rock volume.

In the southern part of the Kaczawa Mountains, near Chrośnica village, hematite accumulations in greenstones and keratophyres were occasionally exploited.

Ad. 3 and 4. Most characteristic feature of these deposits is their form of occurrence as veins built of various gangue minerals such as quartz, carbonate, barite or siderite. These veins may contain variable grade of ore mineralization. Quartz ± carbonate-sulphide veins with auriferous mineralization are commonly considered as connected with post-Variscan hydrothermal processes around granitic intrusions. Post-Variscan barite and siderite veins originated during formation of deep-seated regional fractures.

THE RADZIMOWICE Au–As–Cu ORE DISTRICT

The Radzimowice Au–As–Cu ore district is located about 4 km eastward of Wojcieszów. In Radzimowice, exploitation works were carried out in the southern and eastern slopes of the Żeleźniak Hill (666 m a.s.l., Fig. 3).

THE HISTORY OF THE MINING EXPLORATION

The Radzimowice Au–As–Cu deposit comprises 11–13 ore veins (Tab. 1). However, only six of them were important ore sources. Materials about the mining activities in the Radzimowice ore district are based on the mining reports that were presented by Stauffacher (1914, 1915); Beyschlag *et al*. (1921); Hoehne, (1935); Quiring (1948); Domaszewska (1964, 1965); Manecki (1965); Zimnoch (1965); Fedak, Lindner (1966); Dziekoński (1972); Paulo, Salamon (1974b).

Extensive operation in the Radzimowice area was carried out since the end of 12th century until the middle of the 13th century when the most valuable parts of the weathering zone which contained from 15 to >100 ppm of Au, were exploited (Quiring, 1948). It is estimated that ca. 0.5–0.7 t of gold was received from the gossan type ore. Chalcocite, cuprite, azurite, malachite, limonite, and less frequently cerusite occurred inside oxidation zone.

Fig. 3. The landscape of the Żeleźniak Hill (666 m a.s.l.), view from the main road Bolków–Jelenia Góra

Table 1

The characteristic features of the ore veins at the Radzimowice deposit (data after various authors)

Name of vein	Length of vein [m]	Average thickness [m]	Main ore minerals	Average gold and silver contents according to various authors [ppm]			Average content of elements after Fedak, Lindner (1966)			
				Stauffacher (1915)	Beyschlag *et al*. (1921)	Manecki (1965)	Au [ppm]	Ag [ppm]	As [%]	Cu [%]
Miner consolation	2000	0.15 max. 1.4	asp, py, ga, sf, chp, fa	Au: traces – 5 Ag: 146 and 563	Au-low; Ag: 222	1.07 ±0.13 (n=3)	1.0	306	1.6	0.22
Wanda	320	0.14	asp, py, chp, sf, fa	Au: 5; Ag: 433	Au: 26.6; Ag: 221 mining reports Au: 27; Ag: 227 Au/Ag=1:8.3	19.58 ±8.46 (n=4)	18.0	180	7.6	6.0
Olga I Olga II	300	0.10–0.50	asp, ga, sf	Au: 3; Ag: 72	–	4.0 ±1.67 (n=3)	3.5	39	13.2	1.1
Maria I	300	0.20	asp, chp, ga, py, sf	W part: Au: 18; Ag: 174; S part: Au: 21; Ag: 73	Au: 16.5 Ag: 170 Au/Ag=1:10.8	6.32 ±4.26 (n=8)	6.4	84	9.5	1.9
Maria Buckeltraum	–	–	asp	Au: 3; Ag: 17	–	–	–	–	–	–
Aleksandra	320	0.16	chp	–	Au: none; Ag: 46	5.05 ±0.8 (n=15)	5.0	75	5.0	3.0
Klara	200	0.06		–	Au: ? Ag: ?	17.0	–	–	14.0	1.6
Arnold	–	–	barren nests of asp, ga	–	Au: ? Ag: ?	–	–	–	–	–
Wilhelm	–	–	–	–	–	–	–	–	–	–
Herman	–	–	coarse asp Au/Ag= 1:7	Au: 10; Ag: 34 Au: 13.5; Ag: 100	Au: 17 Ag: 165	–	–	–	–	–
New Vein	–	–	py, asp, chp, ga,	Au + Ag ?	–	–	–	–	–	–
Ludwig	–	0.40	chp, asp	Au: 3; Ag: 70	Au: low; Ag: 46	–	–	–	–	–

Abbreviations: asp – arsenopyrite; py – pyrite; chp – chalcopyrite; sf – sphalerite; ga – galena; fa – tetrahedrite group

The second period of the gold mining development was between 15th and 16th century, when the first adit about 100 m long was built on the eastern slope of Żeleźniak Hill and seven separate open pit mines operated (*op. cit.*). The rich nests of copper ores were the subject of surface exploitation. Supergene minerals of Cu and Ag-bearing ores contained enrichments in Au. Later exploitation was focused in the western side of the Żeleźniak Hill.

In the 17th century mining activity decreased. Since the beginning of the 19th century intensive development of exploitation and processing of copper, arsenic ores and gold extraction took place. In 1801 the first arsenic product (As_2O_3) was made in a new smelter. During 1803 mining works were carried out in the eastern slopes of the Żeleźniak Hill, and then in 1806 a new adit and exploitation shaft (Arnold) on southern slope begun to exploited the Miner consolation vein. The cooper ores were extracted from the eastern part and the arsenic ores from the southern part of the deposit located in Żeleźniak Hill. In order to extract the upper parts of primary ore the Wilhelm mine was opened, new adit and shaft Luis were built (Figs. 4, 5). At that time few ore-bearing veins were found. The Miner consolation vein was mined by two adits and shafts (Fig. 4).

In 1864 the joint venture of both mines started under the name Bergmanntrost. Moreover, few smaller mines operated in the Radzimowice ore district that time. Production increased again in the years 1870–1880 with output of ores about 3,000 t yearly. That time was most prosperous period, because rich arsenic-copper ores were found.

After opening at the railway between Marciszów, Wojcieszów and Legnica, production per year (1890– 1900) achieved 12,259 t of Cu and As ores.

According to mining reports in 19th century over 160,000 t of Cu and As ores were mined and about 1.3 t of gold produced from the ores of average grade of 5 to 8 ppm Au.

In 1907 underground workings of Bergmanntrost mine were connected together. At that time the mine had two exploitation shafts – Arnold about 104 m deep and – Luis 142 m deep. In 1908 the highest ore production was about 30 t of mainly Cu ore per day. The years 1904–1912 were also prosperous. Annual mining production was 10,200 t of ore, which after processing gave an average 2,400 t of copper and 1,300 t of arsenic concentrates (Fedak, Lindner, 1966). During 1912–1917 production decreased to 6,000 t of ore per year. In 1916, 995.2 t of Cu concentrate were produced from which 96.1 t of copper was received. An average content of 5.5 ppm Au and 122.9 ppm silver was found in copper ore. All five veins were exploited, and for instance, in 1917, during the period from January to May the production yielded about 650 t of Cu concentrate with average contents of 4.4 ppm Au and 95.3 ppm Ag, and about 350 t of arsenic concentrate with average contents of 9.2 ppm Au and 44.2 ppm Ag (Domaszewska, 1965). The Wanda vein was the richest in gold and the Miner consolation vein was the poorest. Between 1920 and 1925 the average production was 1,800 t of arsenic ore and 750 t of copper ore per year with the gold content 5–8 ppm. In 1925 the last mine in the Radzimowice ore district was closed due to low demand for arsenic products and very low price for arsenic flame (Dziekoński, 1972).

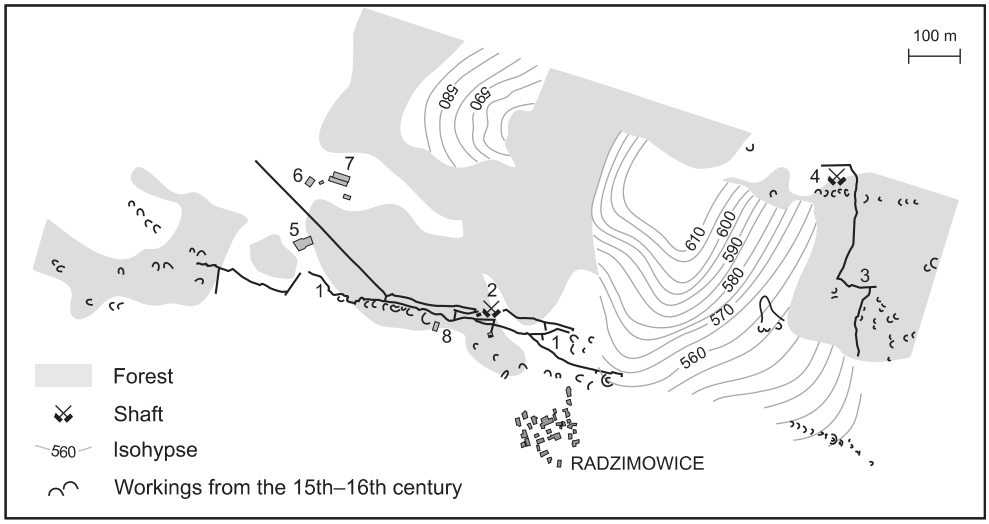

Fig. 4. The schematic plans of the mining activities at the Radzimowice Au-As-Cu deposit in 1826 (after Dziekoński, 1972, modified)

Explanation. 1 – Bergmanntrost adit; 2 – Arnold shaft; 3 – Heinitz adit; 4 – Gesellenzeche or Luis shaft; 5 – pond for jigging of ore; 6 – jigging of ore building; 7 – arsenic metallurgic plant; 8 – supply building

Fig. 5. Photograph of the underground working near the Luis shaft (–70 m b.s.l.)

Photo by P. Gut; summer 2000

It is estimated that total productions from the Radzimowice deposit in 19th and 20th century was from ca. 0.5 Mt of metal ores and ca. 4.2 t of gold. An average grade of metal ores was from 5 to 8 ppm of Au. The arsenic content in the ores widely ranged from 1.0 to 20.0%, copper from 0.8 to 8% and silver from 40.0 to 300 ppm.

In 1952–1953 prospecting works in mines and over 1,400 m of underground galleries were made. In 1957, the underground mining was abandoned. As the result of geophysical investigation performed in 1952–1953 and 1959, the area for further soil geochemical sampling was suggested. That prospecting revealed the extension along strike of old known veins (Lindner, 1963).

GEOLOGICAL SETTING OF THE DEPOSIT

The Radzimowice Au–As–Cu deposit is located in the south-eastern part of the Kaczawa Mountains (Fig. 1). Gold-bearing quartz-sulphide veins are related to Upper Carboniferous igneous rocks that comprise the Żeleźniak intrusion. The intrusion was emplaced into Paleozoic sedimentary-volcanic rock sequences of the Kaczawa Metamorphic Complex, the oldest of which is comprised of the Radzimowice schists in the southern part and the Chmielarz schists in the northern part (Fig. 6). The Chmielarz schists are tectonically overlain by the Lubrza trachytes and gray slates or phyllites (Kryza, Muszyński, 1992). The Radzimowice schists unit has thickness >1 km extending up to 2 km in width and about 17 km in length. This unit consists of rocks that have been documented by conodonts as no older than Ordovician but the upper age limit is still problematic (Urbanek, Baranowski, 1986). Baranowski *et al.* (1990) interpreted the northern and southern margins of the Radzimowice schists as tectonic with separate thrust sheet unit between the Bolków unit to the south and the Świerzawa unit to the north.

Kryza, Muszyński (1992) re-interpreted the central-southern part of the Kaczawa Metamorphic Complex as thrust sheet structures. They suggested that the southern part of the Świerzawa unit represents the overturned limb of a south verging anticline and the northern part of the Bolków unit defines fragments of normal (western part) and overturned limbs (eastern part) of the S-verging folds. In the deposit area the Radzimowice schists unit is thrust upon the Chmielarz schists. Hence, the Radzimowice schists have an uncertain position within the stratigraphic sequence of the Kaczawa Metamorphic Complex (Fig. 7).

The new structural and kinematics data presented by Cymerman (2002) indicate that the hinge zone of the regional-scale Bolków–Wojcieszów anticline, which has an east-plunging axis (e.g. Teisseyre, 1963) should rather be regarded as a set of flood ramps. Also the existence of hinge zone of recently suggested the Radzimowice syncline (Kryza, Muszyński, 1992; Kozdrój, 1995) is very questionable according to Cymerman (2002).

The primary thickness of the Radzimowice schists was probably at least one km (Baranowski, 1988). The dark colour of Radzimowice schists, and the abundance of graphite (Manecki, 1962a) and framboidal pyrite (Sawłowicz, 1987) indicate that the deposition took place on a basin floor where reducing conditions prevailed (Baranowski, 1988). The dominance of mudstone over sandstone and the development mode of the turbidite sequences of the Radzimowice schists are consistent with sedimentation in a trench-floor or trench-slope basin setting (Baranowski, 1988).

The Chmielarz schists consist of volcanoclastic sediments of Cambrian or Ordovician age (Kozdrój *et al.*, 2001). They are together with Lubrza trachytes, volcanoclastic rocks (Ordovician) and with black slates, and cherts and siliceous slates of Silurian–Devonian ages assigned by Seston *et al.* (2000) to the Świerzawa unit. The Chmielarz schists belong to a poorly exposed unit and its relationship to adjacent units is uncertain. The Lubrza trachytes usually comprise small but widespread high-level intrusions or extrusions (domes) of dominantly trachytic composition. They also contain up to 500 m variable maphic to felsic volcanoclastic rocks associated with tuffaceous units. The black slates and cherts, up to 100 m thick locally, contain Silurian graptolites and have not been distinguished from the siliceous slates on Figure 7. Siliceous slates are up to 100 m thick, and contain Late Devonian conodonts (Haydukiewicz, Urbanek, 1986). This assemblage of shaly flysch sediments recrystallized under greenschist facies to quartz-sericite and quartz-sericite-graphite schists, dark albitized phyllites with thin intercalations of siliceous and graphitic slates, metagreywackes, and quartzites. Together with the Chmielarz schists they have been affected by superimposed folding (F_3) and by faulting.

The structural-kinematics analysis of the Kaczawa Metamorphic Complex indicates that in the Radzimowice region the D_1 deformation have opposite direction of shearing (transport of the top to the E and only in a few cases to SW and to W or NE; Cymerman, 2002). It was probably a result of the later re-folding of this unit associated by shearing, rotation and tilting of blocks. The D_2 deformation is characterised by orientation of shearing to NE and E. In this region F_{2A} folds dominate with axial planes almost perpendicular to L_1 lineation and with the prevailing vergence to the south. The F_{2B} fan-shaped folds with axial dip to SE characterised by vergence to the south-west (Cymerman, 2002).

In the Radzimowice deposit area this part of the Kaczawa Mountains formed a horst structure between the North-Sudetic Basin to the northwest and the Intra-Sudetic Basin to south-east (Fig. 1). These areas belong to the Central-European province of the Permian–Carboniferous volcanism of bimodal character forming a zone 400 km long from Germany to Poland (Dziedzic, 1996). In the Kaczawa Mountains these intrusive rocks form a row of dykes and radial apophyses generally discordant to the surrounding bedding. The largest body constitutes the Żeleźniak intrusion that has the shape of a laccolith and comprises of igneous rocks of various textures, including xenoliths, maphic or acid dykes and quartz veins

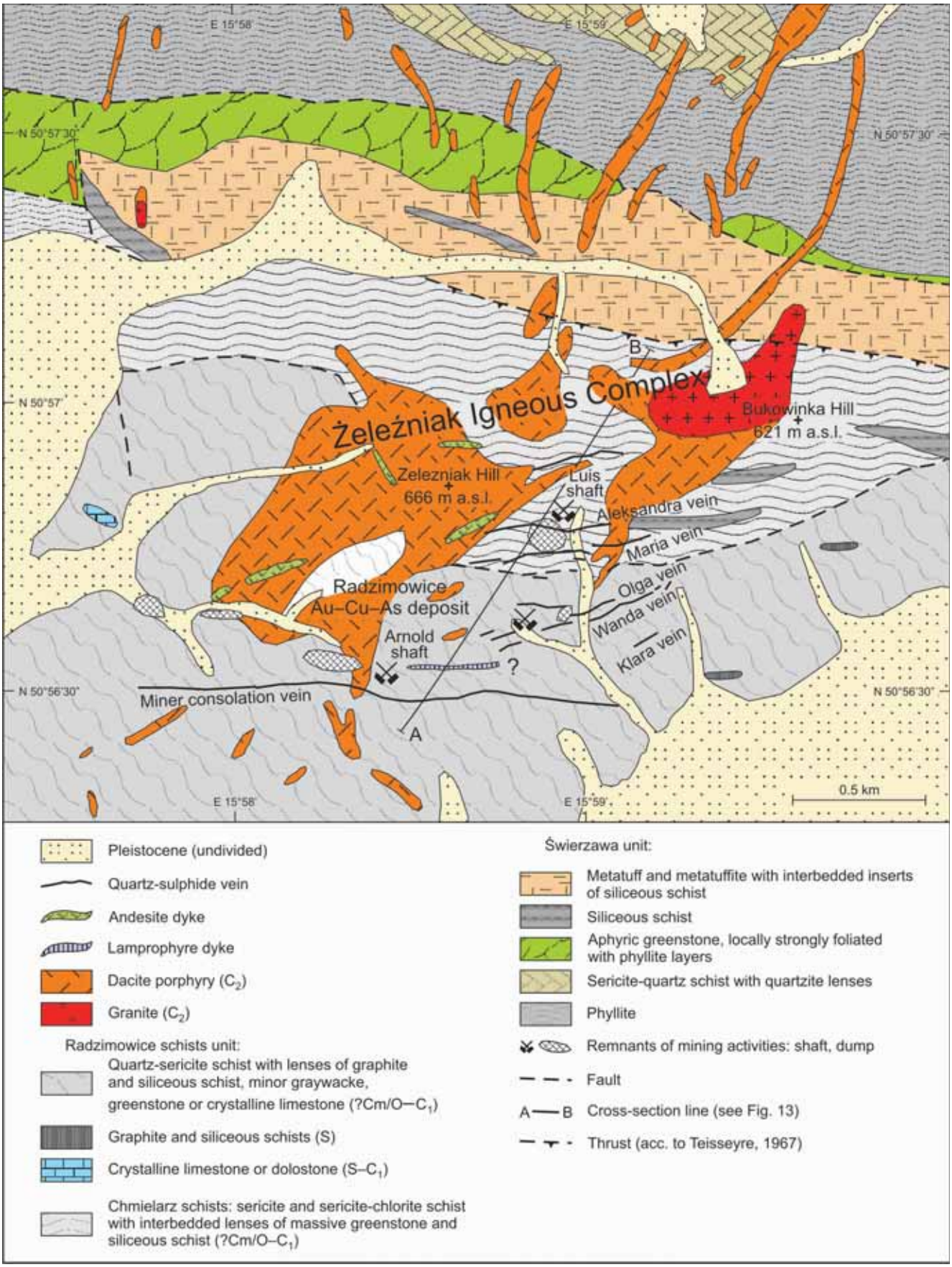

Fig. 6. Compiled geological map of the area of the Au–Cu–As Radzimowice deposit (after Baranowski, 1988; Kryza, Muszyński, 1992; Cwojdziński, Kozdrój, 1994; the ore veins location at a level of +430 m a.s.l. after Paulo, Salamon, 1974b)

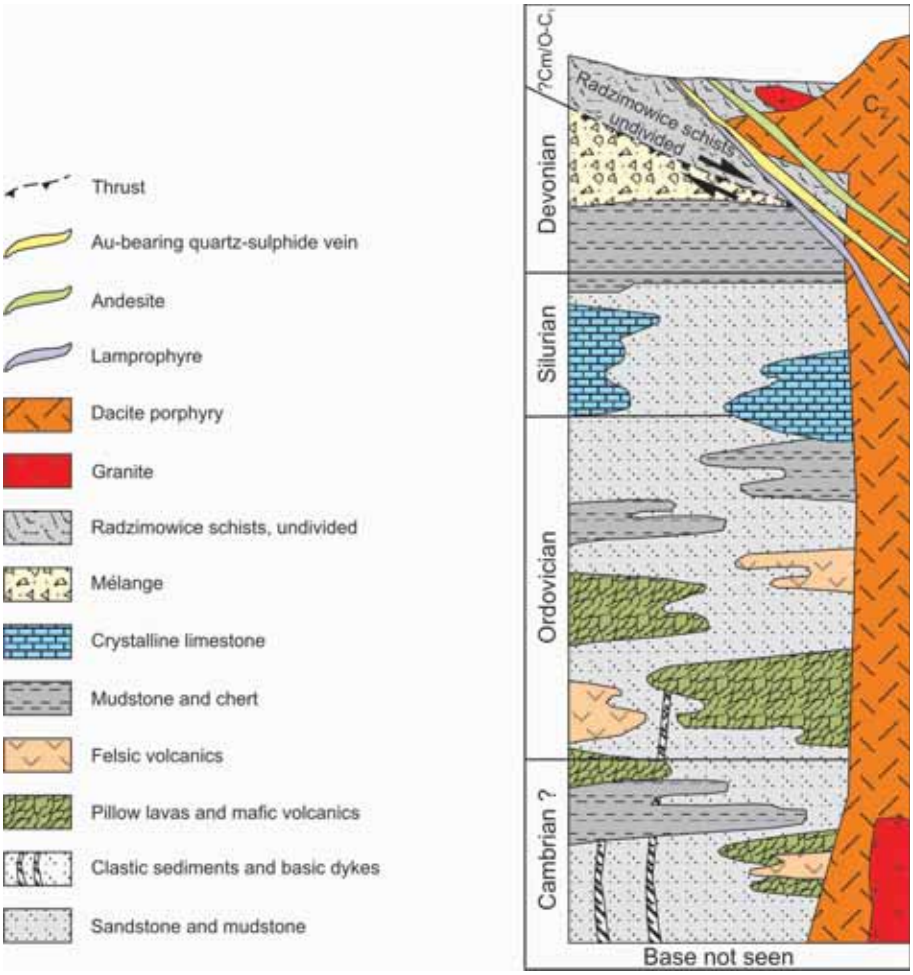

Fig. 7. Relation of the quartz-sulphide and lamprophyre veins to the Upper Paleozoic igneous rock suites and to the geological profile of the Świerzawa unit and the Radzimowice schists (undivided) (compiled from Kryza, Muszyński, 1992; Cwojdziński, Kozdrój, 1994; Seaston *et al.*, 2000)

(Skurzewski, 1984; Kozdrój, 1995). Igneous rocks of the Żeleźniak and the Bukowinka intrusions, the latter located east from Żeleźniak intrusion (ZI), probably intruded along W–E oriented faults.

The Żeleźniak intrusion is irregularly shaped with a core that is ca. 3–4 km^2 and several of radial dykes that surround the core (Fig. 6). Rhyodacite dykes have a thickness from several to hundreds of meters and a length up to 6–7 km. Petrographically the ZI body mainly consists of aphanitic rocks with minor porphyritic ones. Emplacement of the Żeleźniak intrusion post-dates the regional metamorphism (blue schist and subsequent greenschist facies) and main deformation events in the Kaczawa Metamorphic Complex. The SHRIMP age values of zircon grains from the fine-grained rhyolite are similar to the medium-grained microgranites and indicate that the main magmatic event was restricted to the late Namurian, at about 315 ±1 Ma as determined by the Pb/U method (Muszyński *et al.*, 2002). The Żeleźniak intrusion rocks bear strongly sericitized plagioclase, chloritized biotite and other maphic minerals and they host ore mineralization.

The Bukowinka rhyolite has a more uniform texture, equigranular structure and a higher content of biotite; ore mineralization is absent (Manecki, 1962b; Skurzewski, 1984).

GEOCHEMICAL CHARACTERISTICS OF THE IGNEOUS ROCK SUITES OF THE ŻELEŹNIAK INTRUSION

The geochemistry of the Upper Paleozoic igneous rock complex can be divided into three groups: (1) hypabyssal calc-alkaline micro-, and medium-grained granites with porphyritic textures (tonalite, monzogranite, and granodiorite), (2) calc-alkaline felsic rocks with porphyritic to aphyric textures of subvolcanic facies (dacite, rhyolite, andesite and trachyte), and (3) dykes or veins of fine-, and coarse-grained alkaline rocks (lamprophyre) with porphyritic texture.

In Table 2 only a several most representative igneous rocks geochemistry are shown from the total set of 44 samples that were analysed by the ICP-AES, ICP-MS, and XRF methods.

CALC-ALKALINE SUITE – GRANITE

Granites represent the first episode of magmatic activity, they were documented in drill holes of Żeleźniak intrusion, (Majerowicz, Skurzewski, 1987) and mapped in the northern part of the Bukowinka Hill (Cwojdziński, Kozdrój, 1994; Fig. 6). Light-grey granite that occurs in core has been classified as medium to fine-grained monzogranite (Majerowicz, Skurzewski, 1987). In the Bukowinka Hill, gray-pink porphyritic microgranite (tonalitie) representing hypabyssal rocks transition between granite crystallizing in plutonic condition and subvolcanic rhyolite porphyry. The tonalite is composed of quartz, plagioclase, biotite and accessory zircon and apatite. Żeleźniak intrusion granite occurs between the quartz-sericite schists and the rhyolite (Kozdrój, 1995). The xenoliths of granite suggest that it is connected with a deep-seated granitic pluton (Majerowicz, Skurzewski, 1987). According to these authors, a magma chamber for the granite probably underlies the Żeleźniak intrusion and other intrusions that are up to 15 km from the Żeleźniak Hill.

The Żeleźniak intrusion granite contains about 72 wt % SiO_2, 8–9 wt % total alkalis and 2.4 wt % total Fe_2O_3 (Table 2; Fig. 8A). The Żeleźniak intrusion granite belongs to the calc-alkaline series and on the Nb–Zr plot after Leat *et al.* (1986) these granites are located close to the Nb/Zr = 10 line that separates calc-alkaline and transitional fields (Fig. 9). They are peraluminous, with K_2O/Na_2O ratios from 1.3 to 1.8 (Fig. 10). On the Nb–Y–Ce and Nb–Y–3xGa plots of Eby's (1992) they plot in the fields of crustally derived A-type felsic rocks (Fig. 11). The monzogranites from the Żeleźniak intrusion display rare earth elements enrichment, average initial $^{87}Sr/^{86}Sr$ ratios of ≥0.708 (to 0.728), normative corundum contents >1%, and ratio of Al_2O_3 / total alkali oxides + CaO >1.1 (Machowiak, Muszyński, 2000). The geochemical characteristics indicate that these granites are of the *S*-type and that they were derived from inhomogeneous crustal sources (Muszyński *et al.*, 2002).

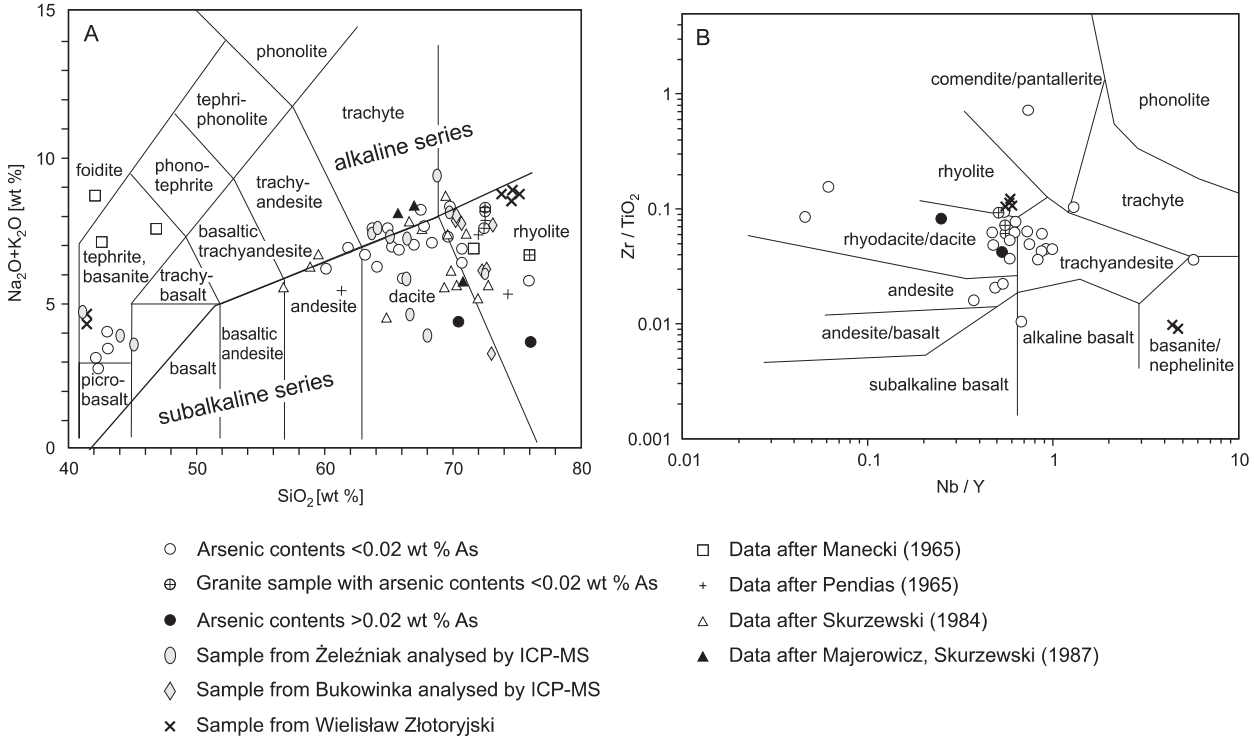

Fig. 8. Classification of the Upper Carboniferous igneous rock suites of the Żeleźniak and Bukowinka intrusions from the Radzimowice Au–Cu–As deposit and Permian igneous rocks from Wielisław Złotoryjski

A – diagram of the Na_2O+K_2O versus SiO_2 (after Le Maitre *et al.*, 1989); **B** – plot of the Zr/TiO_2 –Nb/Y (after Winchester, Floyd, 1977)

Table 2

Representative major and trace element contents in selected igneous rock samples from the northern and southern ore fields of the Radzimowice Au–Cu–As deposit

	Microgranite			Rhyolite porphyry		Dacite porphyry					And. porph.	Trachyte porphyry			Lamprophyre		
	Bk1	Bk3	Bk5	R29	Bk4	R5	R13	R20	R21	R22	R7	R32	Bk2	Bk6	R8	R25	R38
Major elements [wt %]																	
SiO_2	72.49	72.33	72.56	76.04	69.8	68.20	68.74	66.12	71.48	66.98	61.80	63.75	65.87	68.40	44.31	45.06	44.10
Al_2O_3	13.48	13.09	13.52	11.94	14.96	14.27	14.08	14.17	14.55	13.70	15.16	13.81	16.63	16.21	11.28	13.80	12.98
Fe_2O_3	2.46	2.17	2.38	3.91	2.24	3.68	1.39	2.25	5.52	5.82	3.74	1.90	3.41	3.21	8.29	8.97	9.67
MgO	0.43	0.57	0.34	0.55	1.03	1.11	0.88	1.15	0.92	0.50	1.63	1.46	1.45	1.26	8.36	8.58	9.01
CaO	1.41	1.53	1.37	0.44	0.94	1.11	1.36	1.79	0.54	0.28	2.70	2.70	0.71	0.36	7.15	6.84	8.87
Na_2O	3.50	3.02	3.52	0.14	3.83	0.09	2.70	2.16	0.13	0.09	2.66	3.10	3.76	3.40	0.96	1.56	1.46
K_2O	4.67	4.58	4.69	3.56	4.57	4.51	4.95	3.73	4.25	4.23	3.77	4.50	3.93	4.74	1.84	2.49	2.01
TiO_2	0.26	0.30	0.25	0.09	0.33	0.29	0.21	0.31	0.27	0.27	0.37	0.31	0.51	0.44	0.78	1.04	0.97
P_2O_5	0.09	0.11	0.08	0.04	0.14	0.10	0.07	0.10	0.10	0.08	0.13	0.11	0.17	0.16	0.32	0.31	0.36
MnO	0.04	0.05	0.04	0.01	0.02	0.12	0.02	0.10	0.02	0.02	0.13	0.03	0.02	0.02	0.20	0.19	0.16
S	<0.01	<0.01	<0.01	0.20	<0.01	0.23	0.47	0.22	0.20	0.14	1.08	0.15	<0.01	<0.01	0.20	0.25	0.18
Cl	0.02	0.02	0.01	0.01	0.02	0.02	0.02	0.01	0.01	0.01	0.02	0.02	0.03	0.06	0.02	0.02	0.01
F	0.02	0.04	0.08	0.01	0.10	0.07	0.09	0.15	0.02	0.01	0.13	0.10	0.06	<0.01	0.02	0.03	0.01
LOI	0.73	1.66	0.49	1.03	1.71	1.67	1.87	4.43	1.05	4.13	5.57	4.49	2.30	1.61	12.13	10.25	8.05
Total	99.59	99.47	99.33	97.97	99.69	95.47	96.85	96.69	99.04	96.26	98.89	96.43	98.85	99.87	95.82	99.39	97.84
Trace elements [ppm]																	
Au	0.001	<0.001	0.001	0.104	0.010	0.034	0.011	0.003	0.054	0.008	0.005	0.001	0.001	<0.001	0.001	0.003	0.005
Ag	5	2	3	9	8	15	7	5	13	11	4	1.5	3	4	6	8	4
Cu	7	7	9	1298	320	11	23	42	222	126	134	29	92	82	105	59	92
Pb	20	20	18	43	690	188	2	24	32	108	27	13	24	11	62	48	22
Zn	47	31	39	48	32	226	5	78	159	119	82	20	17	21	178	186	122
As	3	<3	4	2986	278	687	168	48	3602	634	191	39	65	65	1070	597	567
Bi	<3	<3	<3	<3	<3	<3	<3	<3	4	9	<3	<3	13	7	<3	<3	5
Co	<5	<5	5	67	<5	5	11	6	4	1.5	7	4	6	9	38	30	64
Cr	51	22	19	3	113	6	13	8	20	7	9	18	9	<5	802	510	749
Mo	6	5	5	4	6	4	4.6	4.5	5	5.1	4.2	5.1	7	2	<2	<2	31.8
Ni	3	5	3	7	8	1.5	3	6	11	6	7	6	4	<3	247	145	329
V	12	20	12	6	32	29	17	22	28	27	29	29	40	41	146	162	168
W	1	<5	28	24	6	9	19	8	<5	<5	11	10	<5	<5	<5	<5	<5
Ba	509	471	501	751	777	374	1090	419	340	473	352	856	765	726	656	586	721
Ga	17	15	17	16	18	13	15	17	18	14	19	17	20	19	13	14	15
Hf	5	4	4	5	5	4	4	4	5	5	5	4	4	5	5	4	4
Nb	23	16	21	12	13	12	14	12	14	13	12	12	12	9	11	9	<2
Rb	185	142	168	92	88	157	155	141	163	160	152	126	151	157	88	93	34
Sr	84	120	79	391	303	368	191	163	552	582	122	213	339	256	385	205	735
Th	26	24	25	15	16	16	19	16	20	15	19	15	19	24	6	8	<3
U	4	4	6	5	5	7	6.5	6.9	7.1	6.5	7	4.6	5	5	<2	2.1	4.5
Y	38	25	35	16	17	10	16	13	16	15	20	12	13	<3	21	24	<3
Zr	226	156	222	158	162	130	124	135	138	133	191	135	205	179	163	170	100
La	62	45	58	29	21	28	31	29	40	29	40	26	20	25	26	24	5
Ce	112	95	117	60	55	70	92	74	59	95	95	70	37	56	54	56	17

And. porph. – andesite porphyry; Bk1,..., R38 – number of sample

CALC-ALKALINE SUITE – PORPHYRIES

The second group of the igneous rocks that constitute the bulk of the outcropping Żeleźniak intrusion belongs to the subvolcanic facies. These aphyric to porphyritic felsic rocks are represented by the sub-alkaline and alkaline series (Fig. 8).

Most of the rocks have rhyodacite-dacite, trachyandesite and andesite compositions with Nb/Y ratios of <0.67 that are characteristic of the calc-alkaline series or transitional rocks between the calc-alkaline and tholeiitic series (Fig. 9). Most of the igneous rock samples from Żeleźniak massif fall in peraluminous field except for lamprophyre samples, which are in metaluminous field (Fig. 10A). Most of these rocks have potassic characteristics (Fig. 8B). Barren or slightly mineralized porphyries from the Żeleźniak intrusion have variable contents of SiO_2 (66–72 wt %) and alkalies and rather high Al_2O_3 contents (up to ca. 17 wt %; Table 2). The Na_2O and K_2O contents vary from 0.1 up to ~4 wt % and from 3 up to 5 wt %, respectively.

Two groups of the dacite porphyries with different Na_2O contents were found: moderate (>2.0 wt %) and low (<0.15 wt %). Calcite and sericite formed pseudomorphs after biotite. Macroscopically, the high Na dacite has characteristic pink colour and the K_2O/Na_2O ratios of 1.1 up to 2.2. The Na poor dacite is of gray or light beige colour and contain abundant disseminated sulphides (mainly pyrite) and has very high alkali ratios of >25. In the both type dacites the K_2O/Al_2O_3 ratios are <0.4. Both series have variable magnesium numbers of 25–75 (*mg#* = Mg/(Mg+Fe), and low concentrations of mantle-compatible trace elements (e.g. <20 ppm Cr, <15 ppm Ni). They are characterized by high concentrations of large ion lithophile elements (LILE; e.g. up to 5 wt % K_2O, up to ~160 ppm Rb,~ 600 ppm Sr, and ~0.1 wt % Ba), moderate light rare earth element concentrations (LREE; e.g. up to 40 ppm La, 95 ppm Ce), and low field strength elements (HFSE; e.g. <0.5 wt % TiO_2, <200 ppm Zr, <15 ppm Nb). The HFSE (Nb, Ta, Ga, Zr, Hf, and Y) contents are low to moderate and typical of volcanic-arc rocks with *I*-type affinities. High contents of Th up to 20 ppm and U up to 7 ppm suggest some crustal contamination during magma ascent, which is characteristic feature for continental arc associations (Müller, Groves, 2000).

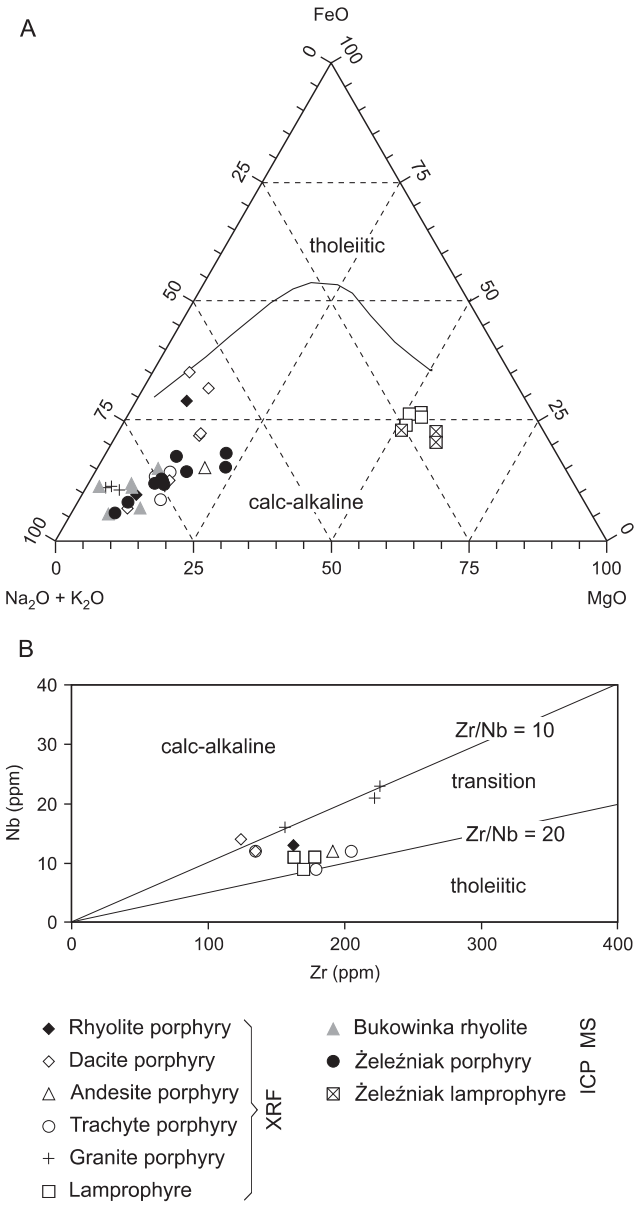

Fig. 9. Diagrams of calc-alkalinity of the Żeleźniak intrusion igneous rock suites

A – plot of AFM with tholeiitic and calc-alkaline fields (from Irvine, Baragar, 1971); **B** – plot of high field strength element Nb *versus* Zr (after Leat *et al.*, 1986)

ALKALINE SUITE – LAMPROPHYRES

Hypabyssal lamprophyre dykes represent the third group of Żeleźniak intrusion igneous rock suites. Field observations indicate that they are younger in comparison with other ingeous rocks. Lamprophyric rocks have usually been found in waste from the southern part of the Radzimowice deposit or they were reported in unpublished mining materials as diorite porphyry or as kersantite that intruded the Radzimowice schists (Manecki, 1963, 1965; Zimnoch, 1965; Paulo, Salamon, 1974b). On the detailed geological map of the Radzimowice area the lamprophyres cut Żeleźniak dacites and hence postdate them in age (Cwojdziński, Kozdrój, 1994).

Two types of kersantites, both with porphyritic textures, are recognised. The first type shows typical coarse-grained textures, with biotite phenocrysts (<0.5 mm) and phenocrysts of secondary minerals after olivine in a crystalline groundmass containing plagioclase (andesine), quartz, biotite and carbonates. The second type is characterized by fine-grained porphyritic textures and carbonate, chalcedony, and chlorite pseudomorphically replacing primary olivine in a fine-grained groundmass comprising sericitized plagioclase and biotite. The second type of lamprophyres is strongly affected by carbonatization. On the geochemical diagram showing K_2O versus SiO_2 after Peccerillo, Taylor (1976) the lamprophyres are located in the field of shoshonites and ultrapotassic lampro-

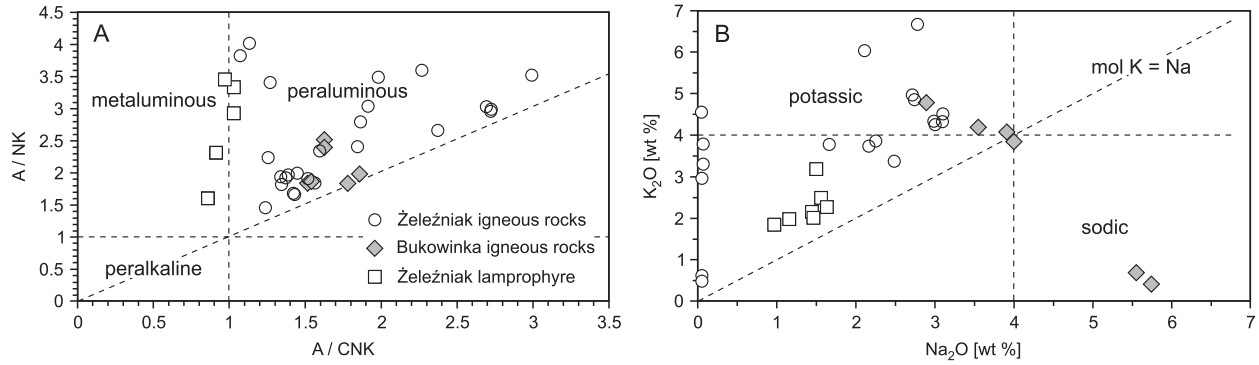

Fig. 10. Diagrams of alkali oxides composition of the Żeleźniak igneous rock suites from the Radzimowice Au–Cu–As deposit (after Irvine, Baragar, 1971)

A – plot of Al/Na+K *versus* Al/(Ca+Na+K); **B** – plot of K_2O *versus* Na_2O

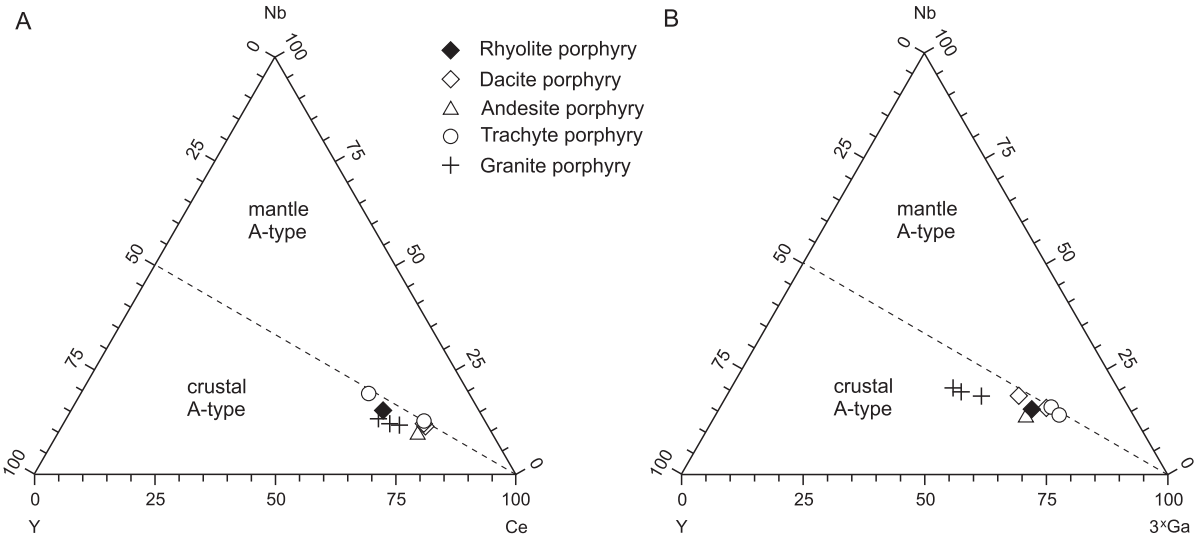

Fig. 11. Eby's (1992) plots applied for the Nb–Y–Ce (A), and for the Nb–Y–3xGa (B) illustrating the crustal A-type nature of the felsic rocks of the Żeleźniak intrusion

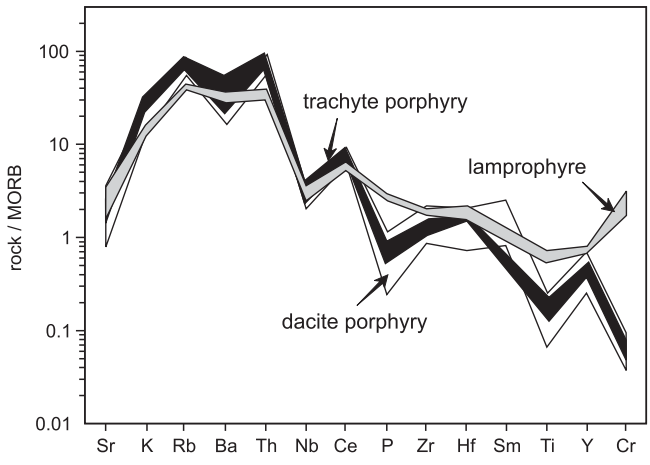

Fig. 12. MORB-normalized (after Pearce, 1983) trace element patterns for the rocks of Żeleźniak intrusion

phyres. On the diagram showing K_2O–MgO after Rock *et al.* (1991) they are plot in the fields of kersantite and spessartite.

Geochemically, the lamprophyres have low SiO_2 (44–47 wt %), high Na_2O (up to 1.6 wt %), and high MgO (8–10 wt %) contents. Their K_2O/Na_2O ratios range between 1.1 and 1.9, which are typical for the shosonitie association (Müller, Groves, 2000). These rocks have mg# from 77 to 79 and high concentrations of mantle-compatible trace-elements indicating a relatively primitive character of the parent magma. It should be noted that the arsenic contents of the lamprophyre samples is highly elevated (0.05–0.1 wt % As) due to hydrothermal processes. They have relatively high LILE, low LREE and low HFSE contents. The MORB-normalized patterns of the porphyries are relatively smooth and similar to each other but highly different from the pattern of lamprophyres (Fig. 12). Intermediate volcanic rocks show strong Cr depletions and P and Ti depletions. Lamprophyres have relatively more smooth signatures with well-pronounced Cr enrichments.

TYPE AND GRADE OF ORE

At the Radzimowice Au–As–Cu deposit the following types of gold-bearing sulphide ores are distinguished:

1. Quartz veins with variable contents of sulphide minerals (from massive to poor ones; Pl. I, 1, 2);
2. Stockworks and veinlets associated with quartz and carbonates (Pl. I, 3, 4);
3. Sulphide impregnation±veinlet of dacite porphyry (Pl. I, 4–6);
4. Disseminated sulphides in vein selvages (Pl. I, 7, 8);
5. Weathered ores.

The main ore mineralization is found in 6 major quartz-sulphide±carbonate veins that cut the Upper Carboniferous Żeleźniak intrusion and Paleozoic flysch-like rocks. These veins strike E–W and dip about 60–85° to the N or S (Figs. 6, 13, 14). The quartz-sulphide±carbonate vein thickness range from 0.06 to 1.4 m. They are typically from 300 up to 350 m long with the exception of the Miner consolation vein, which measures about 2 km in length, and up to 1.4 m in thickness. Most of those veins run concordantly with the direction of the anticlinal axis of the Radzimowice schists. The veins are cut by transverse faults displacing them up to several meters. In porphyries and metamorphic schists, sulphide impregnation up to several meters broad occurs in the walls adjacent to the veins (Fig. 15).

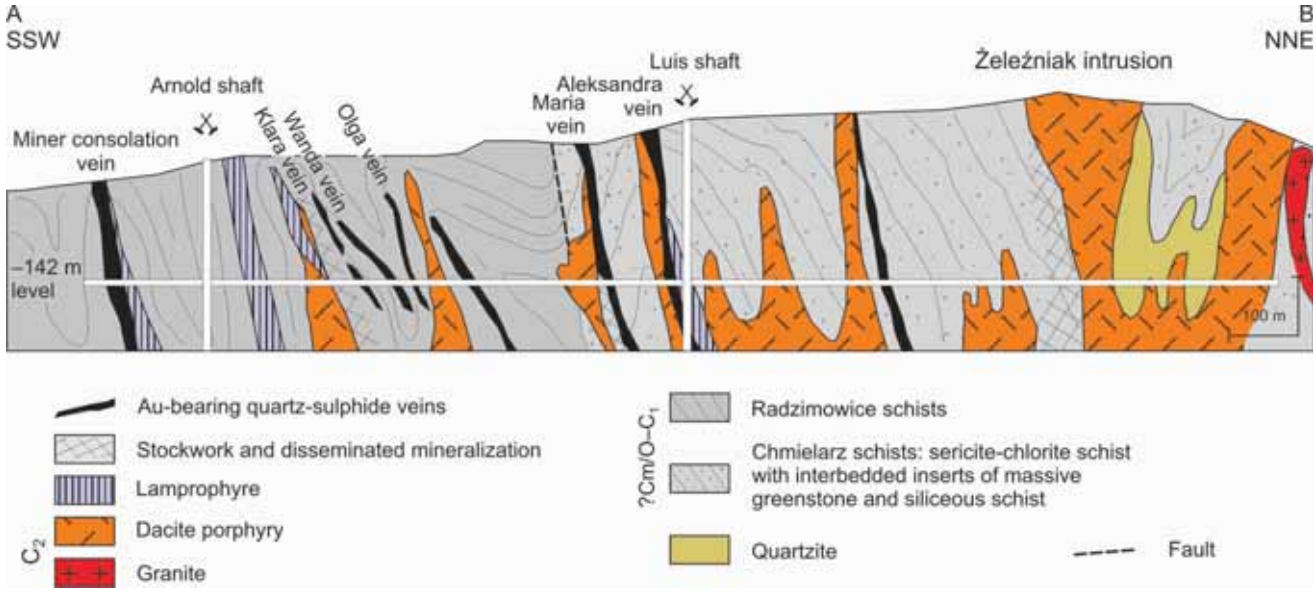

Fig. 13. Geological cross-section along A–B profile on the Fig. 6 (modified after Mikulski *et al.*, 1999)

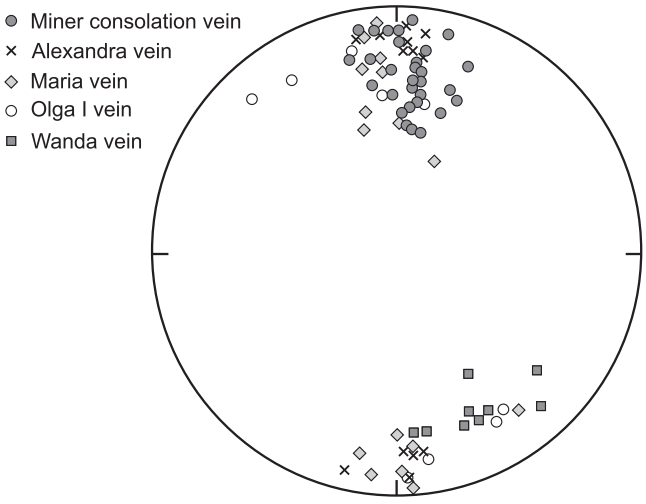

Fig. 14. Diagrams of the various vein orientations at the Radzimowice Au–As–Cu deposit (after Paulo, Salamon, 1974b)

According to old mining records, average gold contents vary between veins, but up to hundreds of grams per ton of gold (typically about 5–8 ppm). The richest Au-bearing ores were from the Klara and Wanda veins with an average Au concentration of 17 and 19.58 ppm, respectively (Manecki, 1965). Some sporadically or never exploited veins such as the New Vein or Herman have fissures and gaps filled with sulphidized tectonic clays. The contents of gold in the vein selvages of the Miner consolation vein ranged from traces up to several ppm. In the dacite porphyries, the highest ore grades occur in zones with stockworks that underwent pervasive hydrothermal alteration. The stockworks consist of sulphides or quartz±carbonate-sulphide veinlets with thicknesses from several mm up to 3–5 cm. It is accompanied by disseminated sulphides in the wallrock zone up to 15–20 cm

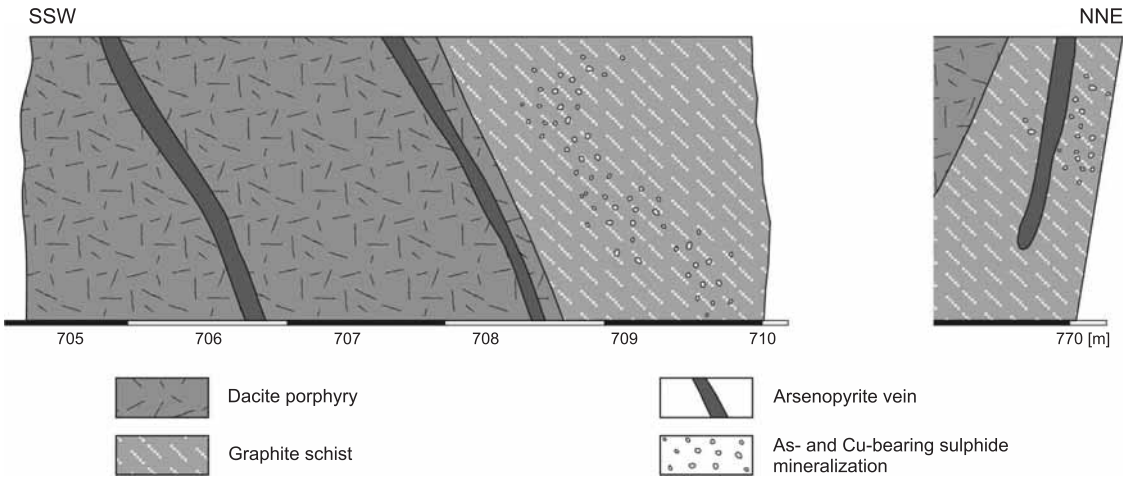

Fig. 15. The cross-section through the vein ore body number 1 at the Radzimowice Au–As–Cu deposit (after Krajewski, 1960)
The main adit +430 m a.s.l.

thick. Stockworks are irregularly distributed and have almost vertical dips. Besides, brecciated lamprophyre veins that are cemented by sulphides were described during exploration of the Miner consolation vein by Manecki (1963, 1965). These lamprophyre dykes trend parallel to the Miner consolation vein, and they attain up to several hundreds of meters in length and 2.5–3.0 m in thickness. The central part of the Miner consolation quartz vein occasionally consisted also of kersantite that was mineralized on both sides by ores (Zimnoch, 1965). The kersantite additionally observed in the northern part of the deposit where was cut by the Maria vein (Paulo, Salamon, 1974b; Fig. 16).

ORE MINERALIZATION IN QUARTZ-SULPHIDE-CARBONATE VEINS

In the main quartz veins (e.g. Miner consolation) two prevailing generations of sulphides occur. The first one contains Co-arsenopyrite and pyrite, and the second one contains base metal sulphides. The sulphides of the oldest generation are strongly brecciated and cemented by quartz, carbonates and sulphides of the younger generations (Fig. 17A, B). The barren parts of the veins consist mainly of quartz and in the central and brecciated zones they also contain calcite, ankerite, dolomite, siderite and barite of younger generations. In the high-grade part of the veins, the sulphide ores are intergrown as massive and coarse network patches up to several centimetres in diameter. They also form aggregates, veinlets and impregnations in gangue quartz and carbonates. Arsenopyrite and pyrite are usually dominant, however, locally chalcopyrite may become more abundant. Arsenopyrite occurs separately as massive euhedral crystals, strongly brecciated and intergrown with pyrite, chalcopyrite and minor loellingite. This arsenopyrite, especially from the richest gold sulphide ores in the northern part of the deposit, reveals constant cobalt content of up to ca. 6.5 atom. % (atomic percent) and shows a compositional variability in its As contents ranging from 32.2 up to 37.5 atom. %.

The other minerals that have been recognised in the main quartz vein are cobaltite, gersdorffite, linnaeite and scheelite. The minerals of the As–Co–Ni association occur mainly as fine inclusions in Co-bearing arsenopyrite; however, gersdorffite was also observed as separate anhedral crystals. Cobaltite was also described from the Wanda vein (Manecki, Młodożeniec, 1959).

Euhedral scheelite crystals are characteristically zoned and up to 1 mm in size in gold-rich samples (Mikulski, 1999). Scheelite forms either growths on the Co-arsenopyrite or inclusions.

Pyrite occurs mainly as anhedral crystals forming coarse aggregates up to several centimetres in size or as euhedral poikilitic crystals of variable size. Pyrrhotite appears usually as globular blebs within pyrite, chalcopyrite, or arsenopyrite.

The younger base metal sulphide stage contains chalcopyrite, sphalerite, galena, and minerals from the tetrahedrite-tennantite group with carbonates (Fig. 17C–G, I). Among these minerals, chalcopyrite is most abundant and forms anhedral aggregates up to several centimetres in size and tiny veinlets that cement fractured sulphides of the older generation. Chalcopyrite occurs in several successive generations (Manecki, 1965; Zimnoch, 1965; Mikulski, 1999). Sphalerite forms aggregates of fine- to medium-size grains or individual grains up to 3 mm in diameter. Three varieties of sphalerite occur. The first variety is black with high Fe (~10 wt %) and Cd (1.3 wt %), and low Ge, In and Ag contents. Sphalerite I crystallized at temperatures of 370–430°C according to Kullerud's sphalerite geothermometer (1953; *in* Manecki, 1965). The second variety of sphalerite occurs in star-like shapes within chalcopyrite what may indicate solid state exsolution, simultaneous crystallization of similarly oriented nuclei (Ramdohr, 1969; Piestrzyński, 1992) or replacement of chalcopyrite by sphalerite (Augustithis, 1995). However,

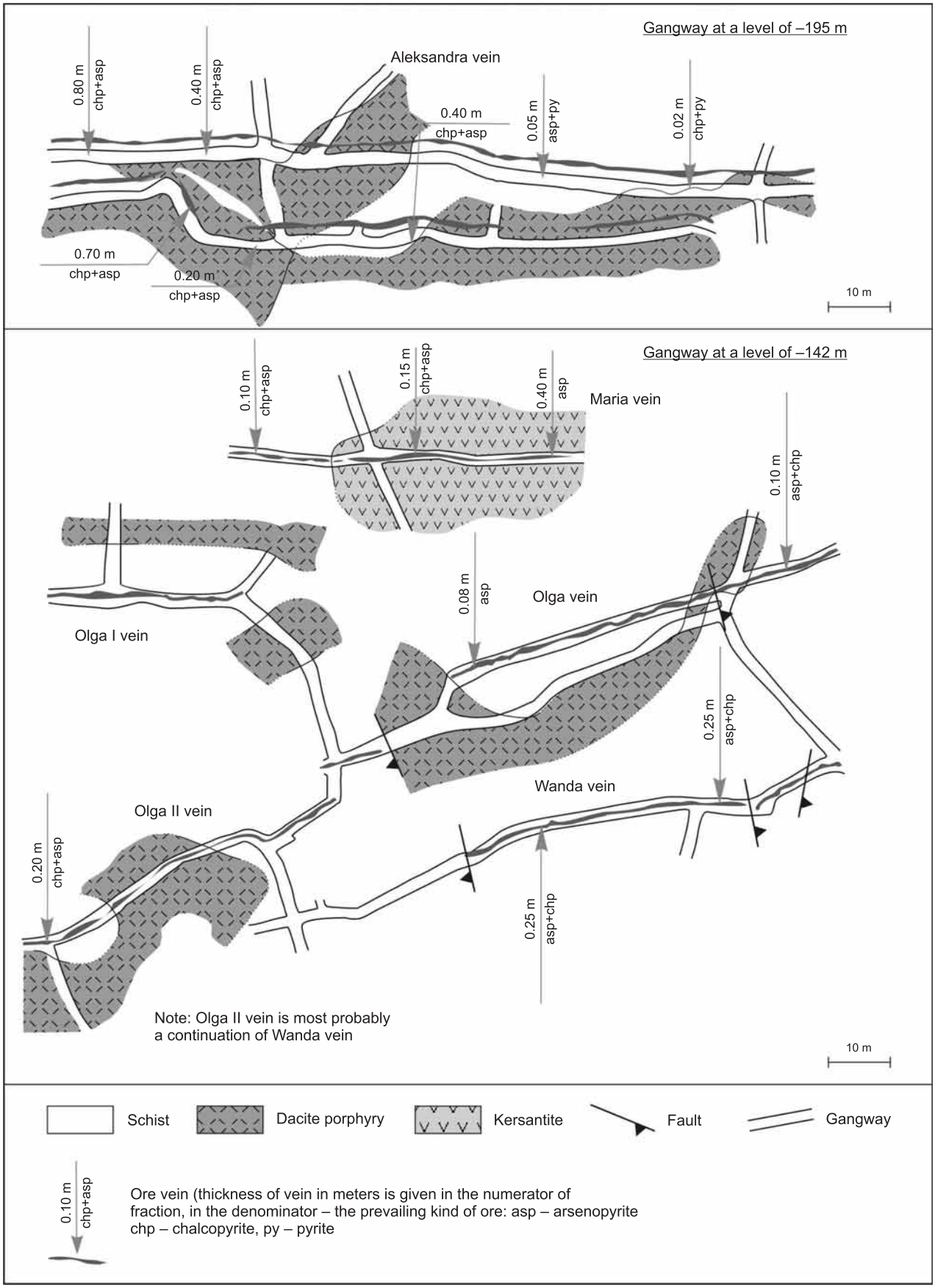

Fig. 16. Fragments of the Radzimowice Au–As–Cu deposit at –142 m and –195 m exploitation levels (after Paulo, Salamon, 1974b)

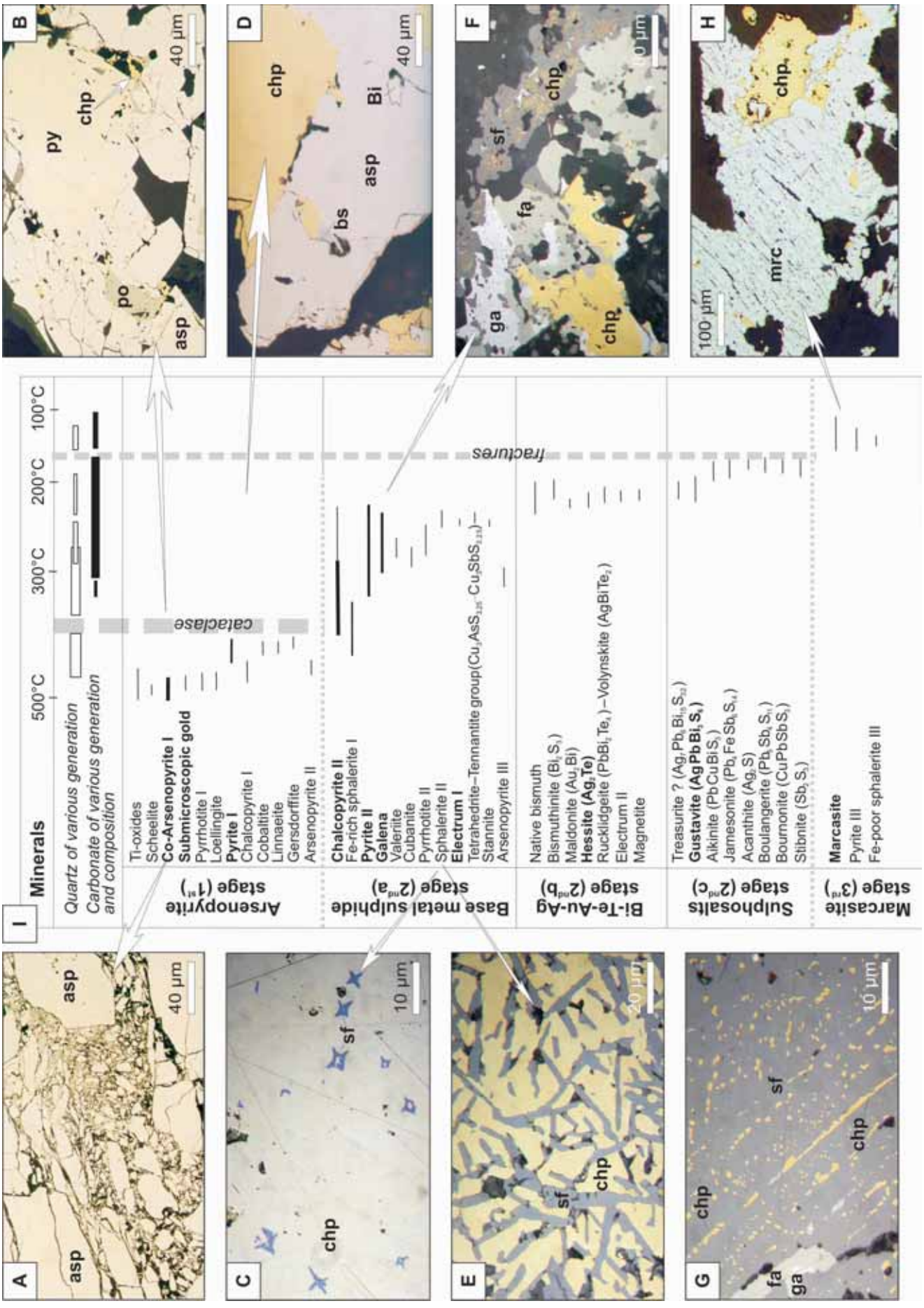
A
asp
asp
40 µm
B
py
chp
po
asp
40 µm
C
chp
sf
10 µm
D
chp
bs
asp
Bi
40 µm
E
sf
chp
20 µm
F
sf
fa
chp
ga
chp
0 µm
G
chp
fa
sf
chp
ga
10 µm
H
chp
mrc
100 µm
I
Minerals
500°C
300°C
200°C
100°C
Quartz of various generation
Carbonate of various generation and composition
cataclase
fractures
Arsenopyrite stage (1st)
Ti-oxides
Scheelite
Co-Arsenopyrite I
Submicroscopic gold
Pyrrhotite I
Loellingite
Pyrite I
Chalcopyrite I
Cobaltite
Linnaeite
Gersdorffite
Arsenopyrite II
Base metal sulphide stage (2nd a)
Chalcopyrite II
Fe-rich sphalerite I
Pyrite II
Galena
Valeriite
Cubanite
Pyrrhotite II
Sphalerite II
Electrum I
Tetrahedrite–Tennantite group(Cu3AsS3.25–Cu3SbS3.25)–
Stannite
Arsenopyrite III
Bi-Te-Au-Ag stage (2nd b)
Native bismuth
Bismuthinite (Bi2S3)
Maldonite (Au2Bi)
Hessite (Ag2Te)
Rucklidgeite (PbBi2Te4)–Volynskite (AgBiTe2)
Electrum II
Magnetite
Sulphosalts stage (2nd c)
Treasurite ? (Ag7Pb6Bi19S32)
Gustavite (AgPbBi3S6)
Aikinite (PbCuBiS3)
Jamesonite (Pb4FeSb6S14)
Acanthite (Ag2S)
Boulangerite (Pb5Sb4S11)
Bournonite (CuPbSbS3)
Stibnite (Sb2S3)
Marcasite stage (3rd)
Marcasite
Pyrite III
Fe-poor sphalerite III

Fig. 17. Reflected light microphotographs of ore minerals and the table of the mineral sequence of the Radzimowice deposit

A – strongly fractured and cataclased Co-arsenopyrite cemented by quartz and carbonates (black); **B** – fractured aggregate of Co-arsenopyrite cemented by pyrite, chalcopyrite, pyrrhotite, and quartz and carbonates (black); **C** – sphalerite star-like inclusions in chalcopyrite (sample no. Rdz 6a); **D** – Co-arsenopyrite replaced by chalcopyrite; **E** – inclusions of sphalerite in chalcopyrite; **F** – chalcopyrite replacement by minerals from the tetrahedrite group, galena and sphalerite in association with carbonates; **G** – linear inclusions of chalcopyrite in association with galena, tetrahedrite in sphalerite (sample no. S-5b); **H** – marcasite replacements of anhedral coarse-grained chalcopyrite (sample no. R29); **I** – the ore mineral succession in the main quartz-sulphide veins at the Radzimowice Au–As–Cu deposit. Note: the range of quartz temperature crystallization according to fluid inclusion measurements.

Abbreviations: asp – arsenopyrite, Bi – native bismuth, bs – bismuthinite, chp – chalcopyrite, fa – tetrahedrite group, ga – galena, mrc – marcasite, po – pyrrhotite, py – pyrite, sf – sphalerite.

the presence in the samples of star-shaped and skeletal exsolutions of sphalerite or lamellar exsolutions of cubanite in chalcopyrite suggests high temperatures of precipitation (Barton, 1973; Barton, Skinner, 1979). Cubanite exsolution lamellae define minimum temperatures ranging from 250 to 300°C. The third variety of sphalerite is commonly found in "spotty dolomite" samples from the central parts of the Miner consolation vein. It is pale-brown to honey-yellow. Electron microprobe analysis indicates iron contents of lower than 1.5 wt %. Fine-grained sphalerite III, up to 0.4 mm in size, overgrows boulangerite and bournonite. In other parts of the deposit the base-metal sulphides are associated with calcite instead of dolomite and may be surrounded by siderite.

Galena occurs mainly in the Miner consolation vein where it forms pockets weighting up to several kilograms. Galena is intergrown with sphalerite and/or chalcopyrite or as small inclusions, or as veinlets in older-generation sulphides. Galena may contain inclusions (up to 0.03 mm in size) of bournonite ($CuPbSbS_3$), boulangerite ($Pb_5Sb_4S_{11}$), acanthite (Ag_2S) and aikinite ($PbCuBiS_3$).

Marcasite is commonly present in samples associated with pyrite and in veinlets (up to few millimetres thick) or less commonly replacing older sulphides (Fig. 17H). In some ore-bearing quartz sample veinlets of chalcedony and/or alkalic feldspar (orthoclase or adularia) associated with fine-grained sulphides, occur randomly.

SULPHUR ISOTOPE DISTRIBUTION PATTERN

The sulphur isotopic compositions of 43 sulphide (pyrite, arsenopyrite, chalcopyrite, galena and sphalerite) samples range from –2.44 to +3.63 ‰ $\delta^{34}S_{CDT}$ with characteristic values for pyrite from 0.15 to 1.65 ‰ $\delta^{34}S_{CDT}$ (arithmetic average = 0.93, n = 20; standard deviation (std.) = 0.44, Fig. 18). Coarse-grained pyrites from massive ores have sulphur isotopic compositions from 0.29 to 0.73 ‰ $\delta^{34}S_{CDT}$, whereas those that are associated with base metal and arsenic sulphides range from 0.93 to 1.65 ‰. Chalcopyrite reveals similar value range of $\delta^{34}S_{CDT}$ from 0.38 to 0.98 (arithmetic average = 0.65, n = 5, std. = 0.23). By contrast, the sulphur isotopic compositions of galena from the pyrite-sphalerite-chalcopyrite-galena ore range from –0.23 to –1.13 ‰ and those of sphalerite from 2.76 to 3.63 ‰.

Arsenopyrite samples derived from massive arsenopyrite ores have a wide range of the sulphur isotopic compositions from –2.44 to 2.29 ‰, with exclusion of arsenopyrite sample from a quartz vein crosscutting dacite with value of –0.16 ‰. Single arsenopyrite crystals up to 2 mm in diameter and their characteristic twins have the sulphur isotopic compositions from 0.85 to 1.13 ‰. The average sulphur isotope composition of pyrite, chalcopyrite, galena and the most arsenopyrite clusters compose values $\delta^{34}S_{CDT}$ from –1 to + 2 ‰ (arithmetic average = 0.84, n = 37, std. = 0.44), which may indicate a magmatic source of sulphur (Ohmoto, 1986). Higher values of sulphur isotope composition in sphalerite (up to 3.6 ‰) may indicate the sulphur contribution from the country rocks (Ohmoto, Goldhaber, 1997).

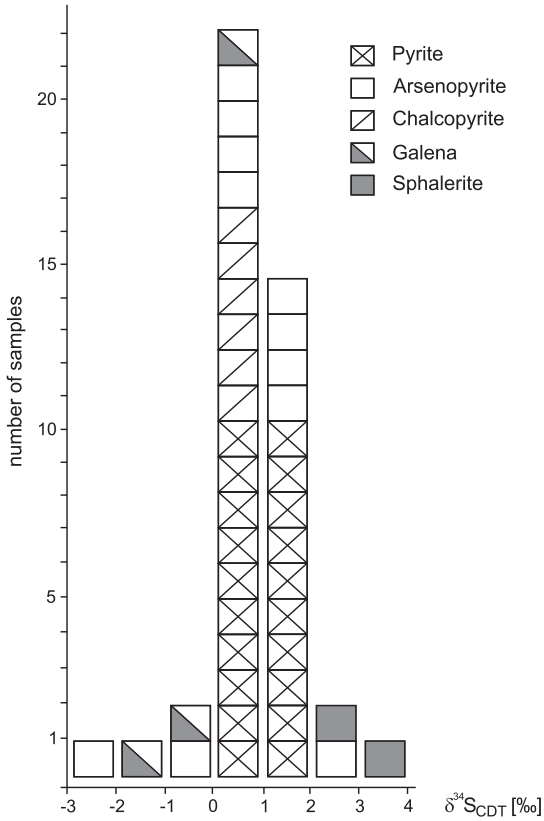

Fig. 18. Sulphur isotope composition of sulphide minerals within the gold-bearing ores from Radzimowice

ARSENOPYRITE GEOTHERMOMETER DATA

Three varietes of arsenopyrite with different contents of As and S from the Radzimowice deposit have been recognized (Fig. 19; Tab. 3). Arsenopyrite I occurs as fractured single large grains of a prismatic habit from 0.3 mm up to a several mm in size and as massive aggregates intergrown with or replacing pyrite. In some samples arsenopyrite forms intergrowths with loellingite. Moreover, inside arsenopyrite, it is possible to find

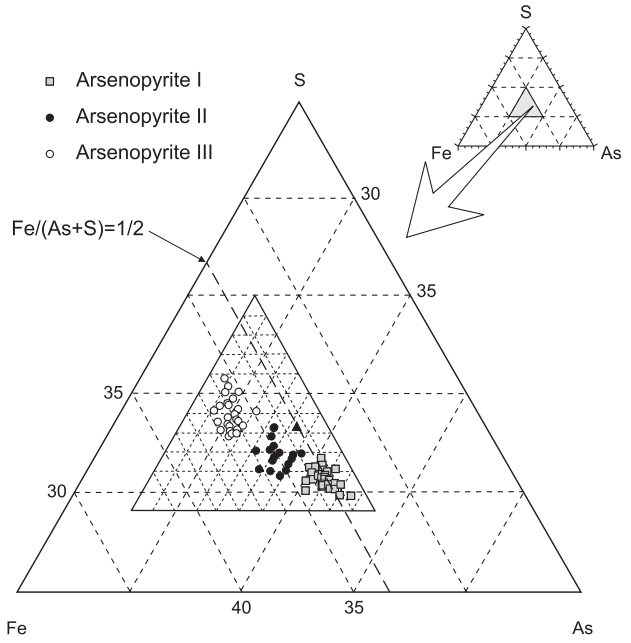

Fig. 19. Plot of the atomic percent composition of arsenopyrites from the Radzimowice Au–Cu–As deposit

fine relics of loellingite or inclusions of other sulphides (pyrrhotite or chalcopyrite). This arsenopyrite may also contain inclusions of gold, native bismuth and tellurium minerals. Arsenopyrite I, especially from the richest in gold sulphide ores of the northern part of the deposit, revealed a constant cobalt admixture from 0.5 up to 6.5 atom. % Co (arithmetic average $x_{n=28}$ = 3.3 atom. % Co). Some grains of this Co-bearing arsenopyrite revealed up to 71 ppm Au (determined by GF-AAS methods) and about 1 wt % Co (by XRF method). This Au±Co-bearing arsenopyrite shows compositional variation ranging from 34.8 to 37.5 atom. % As with an arithmetic average of 35.8 atom. % As, ($\sigma = \pm 1.4$); n = 28 measurements. It has a deficiency of sulphur from 2 to over 3 atom. % . The majority of these arsenopyrites are not suitable for geothermometry except for 3 arsenopyrite grains that have Co-admixture below 1 atom. % (As content 34.8–35.5 atom. %). To establish the temperature range for this arsenopyrite, it should be assumed that the beginning of its crystallization took place at the arsenopyrite-pyrrhotite-loellingite buffer of $f(S_2)$ due to pyrrhotite and loellingite presence. However, the presence of pyrrhotite is limited only to small inclusions in arsenopyrite. According to the isopleths of arsenopyrite composition in the log$f(S_2)$ – T plot from Kretschmar, Scott (1976), modified by Sharp *et al*., (1985), the temperature ranges between 495 and 535°C, and sulphur fugacity – log$f(S_2)$ for arsenopyrite I varies from –6.5 to –8.2 (Fig. 20; field A).

Arsenopyrites II form single grains of rhombohedric habits up to 1 mm in size or aggregates intergrown with quartz. It may contain also Co admixtures similar to arsenopyrites of the first variety. However, arsenopyrite II contains usually lower Co admixture, <1 atom. %. The composition of this arsenopyrite is ranging between 32.0 and 34.1 wt. % As. Arithmetic average of these arsenopyrites is 33.1 atom. % As (std. = ±1.2) close to stochiometric value. Their sulphur content, like arsenopyrite of the first variety, characterized by a decrease of sulphur from 1 up to 2 atom. %. Conditions close to arsenopyrite-pyrrhotite-loellingite buffer of $f(S_2)$ have been assumed only for these arsenopyrites that contain Co-admixture less than 1 atom. % Co (As content varies from 32.2 to 33.8 atom. % As). Arsenopyrite II could have originated at temperature from 345 to 455°C (arithmetic average = 400°C) and sulphur fugacity – log$f(S_2)$ for the range of arsenopyrite II (Fig. 20; field B) varies from –8.2 to –12.9. A similar range of temperatures of arsenopyrite and pyrite crystallization from 428 to 368°C was obtained by Machowiak, Weber-Weller (2003) from sulphur isotope geothermometry.

Arsenopyrite III is different from the previous ones. Arsenopyrite 3rd occurs as fine-grained euhedral crystals in thin quartz veinlets cutting dacite porphyries. This arsenopyrite may be associated with pyrite or/and galena veinlets and sulphosalts. Arsenopyrites III are of rhombohedric or acicular habits and may form cross twins of crystals. This arsenopyrite represents the youngest generation. It contains less than 31 atom. % As and has the arithmetic average value of 29.9 atom. % As (std. =

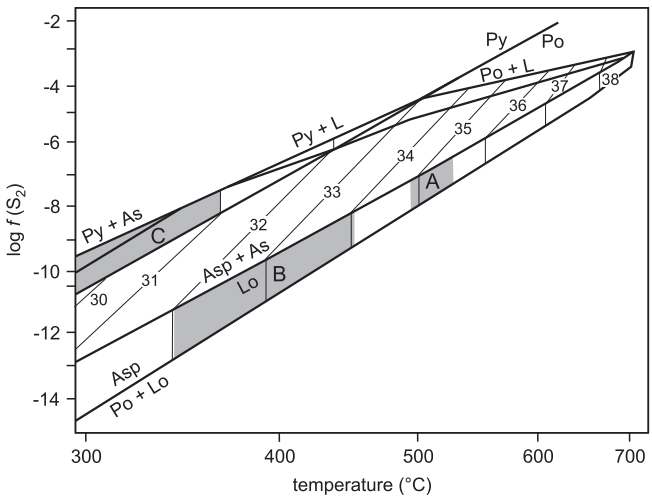

Fig. 20. Projection on log $f(S_2)$ *versus* temperatures diagram of the arsenopyrite microprobe analyses (from Kretschmar, Scott, 1976; modified by Sharp *et al.*, 1985)

Shaded area shows range of arsenopyrite compositions from Radzimowice deposit; As – arsenic, Asp – arsenopyrite, L – liquid sulphur, Lo – loellingite, Po – pyrrhotite, Py – pyrite

Table 3

Statistic parameters of the As contents in arsenopyrite from the Radzimowice deposit and their crystallization temperatures (ac. to arsenopyrite geothermometer by Kretschmar and Scott, 1976)

Location	Arsenopyrite type	As [atom. %]				Number of samples	Interval of arsenopyrite crystallization [°C]
		minimum	maximum	arithmetic mean	standard deviation		
Radzimowice Co<1 atomic%	Arsenopyrite I	34.81	37.45	35.81	1.43	28	535–495
	Arsenopyrite II	32.01	34.13	33.11	1.21	9	445–345
	Arsenopyrite III	28.75	30.98	29.95	0.58	25	370–<300

±0.6); n = 25 and is free of admixtures. This arsenopyrite composition ranges from 28.8 to 31.0 atom. % As, equivalent to the temperature ranges between 370°C and below 300°C (outside the stability field of arsenopyrite) along the arsenopyrite-pyrite buffering curve. Sulphur fugacity – log $f(S_2)$ for the range of arsenopyrite III varies from –7.5 to –11.2 (Fig. 20; field C).

GOLD MINERALIZATION

Gold contained in the structure of the common sulphide minerals (as a result of solid solution decomposition or chemically bound) and present as a discrete inclusions smaller than 1000Å are collectively termed "submicroscopic gold", "invisible gold" or nanogold not detectable by optical and scanning electron microscopy (Bürg, 1930; Boyle, 1979; Gasparrini, 1983; Cook, Chryssoulis, 1990). In opposite, gold observed under microscopy (>1µm in size) is defined as visible gold or microscopic gold. In the metallurgy term refractory gold beside invisible gold is also used for gold which is refractory to conventional cyanidation (Johan *et al.*, 1989).

Previous investigators (Cabri *et al.*, 1989; Cathelineau *et al.*, 1989; Cook, Chryssoulis, 1990; Fleet *et al.*, 1989) demonstrated that submicroscopic gold exists mostly in arsenopyrite and arsenian pyrite both in solid solution in the crystal lattice and as discrete colloidal particles. Gold is preferentially concentrated within As-rich zones of arsenian pyrite (Fleet, Mumin, 1997) and in As-rich and (Sb+Fe)-poor zones of arsenopyrite.

According to the analytical techniques used to detect gold in sulphide samples from the Kaczawa Mountains gold mineralization occurs as microscopic and submicroscopic ones. Based on those results Mikulski (2000a) proposed the classification of the microscopic gold from the Western Sudetes (Fig. 21). Electron microprobe investigation and GF-AAS methods detected the bulk gold in arsenopyrite and As-rich pyrite. At the Radzimowice deposit concentration of gold in Co-bearing arsenopyrite is over one order higher than in pyrite as evidenced by GF-AAS methods (71 ppm and 5.1 ppm, respectively).

In Radzimowice electrum, native gold and maldonite represent the microscopic gold. Electrum occurs as inclusions or micro-veinlets associated with pyrrhotite or chalcopyrite filling fractures in Co-arsenopyrite (Pl. II). Electrum grains (0.25 mm) were also observed among quartz fibres or as intergrowths with tellurium and bismuth minerals. Electron micro-probe revealed several gold grains, containing significant amounts of silver, with Au:Ag ratio varying from 0.62 to 0.75, thus corresponding to electrum. Electrum forms also composite inclusions built of native bismuth, bismuthinite or hessite intergrowths (Pl. II, 1–6).

Maldonite (Au_2Bi) was also recognized in association with gold, native bismuth, bismuthinite, hessite, and sulphotellurides forming inclusions in Co-arsenopyrite.

Bismuthinite is scarcer and mainly occurs together with native bismuth. In places polar inclusions of gold-bismuth myrmekites formed as a result of solid solution decomposition of maldonite at temperature of about 270°C (Elliot, 1965 *in* Afifi *et al.*, 1988). Its polar zones may contain up to 34 wt % of Bi and 64–66 wt % of Au, respectively (Tab. 4).

Besides electrum and silver-bearing tetrahedrite, other Ag-rich minerals such as acanthite (β–Ag_2S) and Ag, Pb and Bi sulphosalts occur in fractures in galena in association with carbonates. Silver, lead and bismuth sulphosalts are present, with members of the gustavite-lilianite-galenobismuthite group (Fig. 22).

Hessite (Ag_2Te) is the main tellurium mineral present, with members of the rucklidgeite ($PbBi_2Te_4$) – volynskite ($AgBiTe_2$) solid solution series (Pl. II, 1). Hessite typically occurs in fractured Co-arsenopyrite as globular inclusions up to 40 µm in diameter, although it can form larger grains intergrown with calcite and Ag, Pb and Bi sulphosalts. The composition of the hessite grains ranges from 54 to 63 wt % Ag and from 31 to 37 wt % Te (Tab. 4). Hessite contains up to several wt % Au and Pb, indicating the presence of the different phases of the solid solution. Moreover, Ag, Pb and Bi sulphotellurides occur as fine intergrowths with magnetite and ankerite that are replace arsenopyrite-chalcopyrite aggregates.

Available geothermometric data indicate that most tellurides in veins were deposited at temperatures less than 350°C (Afifi *et al.*, 1988). The deposition of tellurides is restricted to

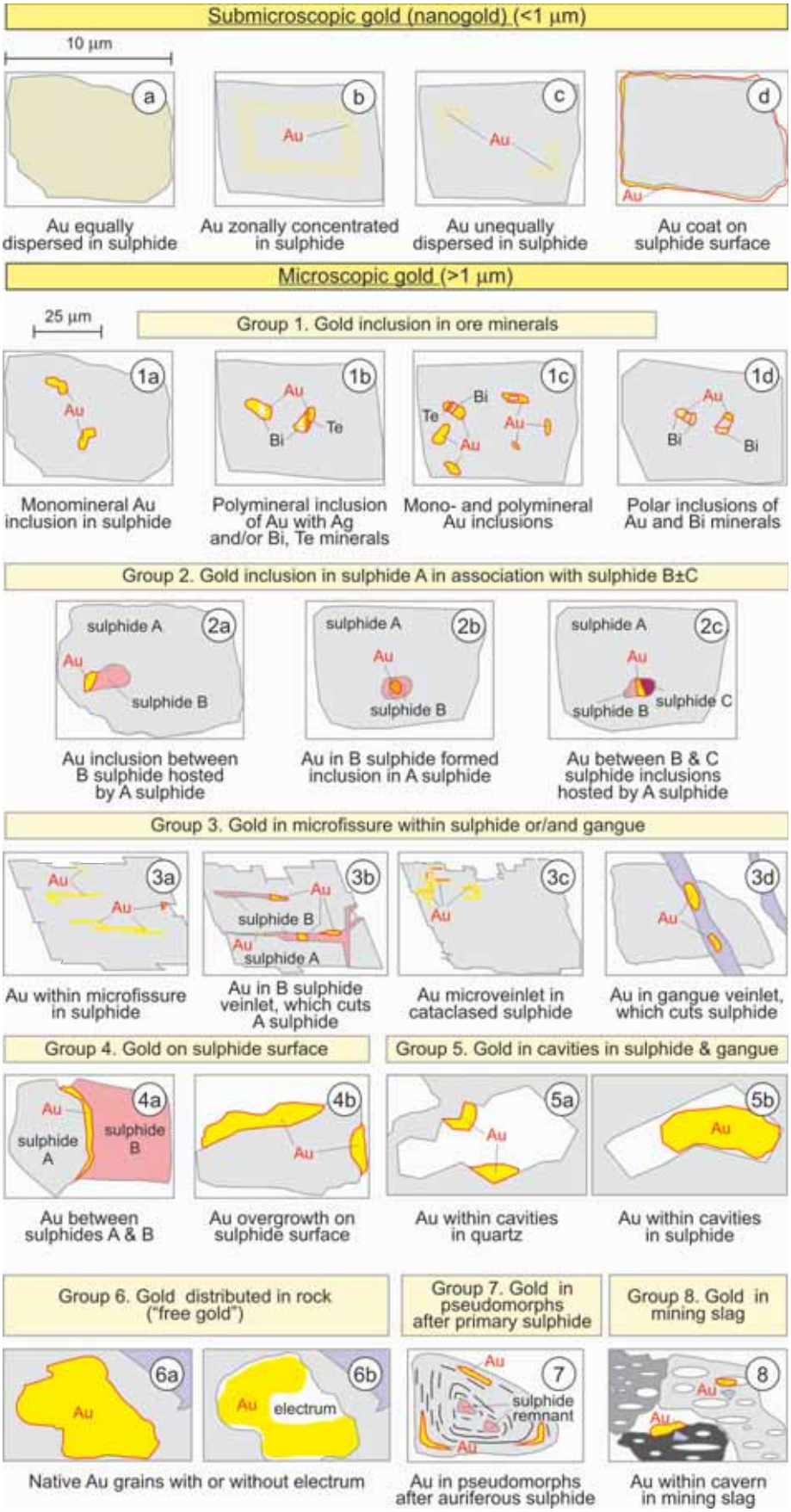

Fig. 21. The classification of sub- and microscopic gold forms in gold-bearing As-polymetallic ores in the Western Sudetes (after Mikulski, 2000a)

Table 4

Chemical compositions of minerals from the Au–Ag–Te–Bi–Pb–S associations from the Radzimowice deposit, electron-microprobe analyses

Element	Electrum (Au,Ag)			Maldonite (Au_2Bi)		Hessite (Ag_2Te)			Rucklidgeite-volynskite ($PbBi_2Te_4$–$AgBiTe_2$)			Gustavite ($AgPbBi_3S_6$)			Treasurite (?) ($Ag_7Pb_6Bi_{15}S_{32}$)		
Au	68.59	65.20	61.13	65.6	64.79	–	1.05*	0.04*	0.36*	1.75	–	–	0.89	1.45	–	–	–
Ag	29.56	35.32	37.19	–	–	62.53	53.99	61.51	29.08	36.35	47.91	11.03	9.51	9.77	32.28	28.45	30.78
Te	1.68	–	–	–	–	36.23	30.81	34.76	13.52	16.68	27.72	–	–	–	15.74	14.28	15.01
Bi	–	–	–	31.0	31.80	–	9.02	–	33.64	26.57	12.17	48.09	55.48	52.72	30.99	35.12	34.19
Pb	–	–	–	–	–	–	3.76*	2.58*	20.62	18.50	12.69	22.57	20.55	21.11	10.30	12.70	13.14
Fe	–	–	–	1.09	2.10	1.00	0.33*	0.84	1.10	1.43	1.71	1.75	2.46	5.25	2.58	0.44	0.29*
Cu	–	–	–	–	–	–	–	–	–	–	–	–	–	–	3.06*	0.24*	0.26*
As	–	–	–	–	–	–	1.43*	1.75*	–	–	–	–	–	–	–	–	–
Se	–	–	–	–	–	–	–	–	0.12*	–	–	–	–	–	–	–	–
Co	–	–	–	0.61	0.09*	–	–	–	–	–	–	–	–	–	–	–	–
S	–	–	–	–	–	0.32	1.09	0.26	–	–	–	14.50	11.80	11.10	6.93	7.21	6.06
Total	99.83	100.52	98.71	98.3	102.40	100.08	101.32	101.69	98.44	101.23	100.95	97.90	99.98	101.46	101.89	98.09	99.54

* error > 1 std.

one or two stages that always follow initial crystallization of sulphides. The bismuth-tellurium-gold-silver-lead minerals of Radzimowice deposit are all characterised by low melting points; maldonite melts at 371°C and acanthite crystallizes below 194°C (Afifi *et al*. 1988; Barton, Skinner, 1979). The experimental data of Cabri (1965) shows that the limits of electrum composition for the assemblage electrum – hessite are Ag_{100}–$Au_{26}Ag_{74}$ at 356°C and Ag_{100}–$Au_{21}Ag_{79}$ at 290°C. Consequently, the Au–Ag–Bi–Te–Pb±S mineral association belongs to the hydrothermal low temperature mineralization in which the appearance of tellurides after initial deposition of sulphides reflects an increase in the tellurium/sulphur fugacity ratio due to input of H_2Te from a magmatic source (Barton, Skinner, 1979; Afifi *et al.*, 1988; Fig. 23).

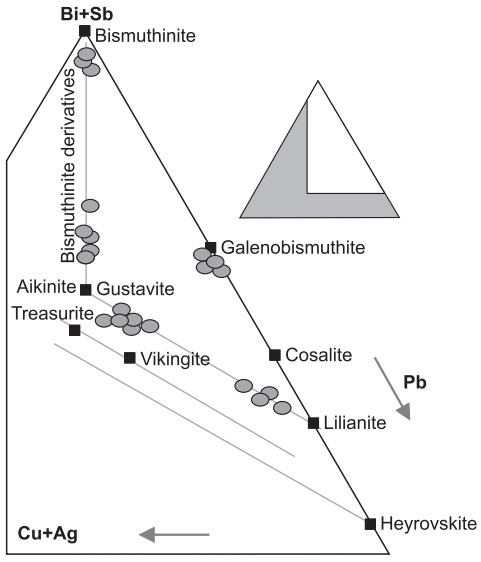

Fig. 22. Pseudo-ternary plot of (Cu+Ag)–Pb–(Bi+Sb) mineral compositions from the Radzimowice Au–As–Cu deposit (mineral division after Cook, Ciobanu, 2004)

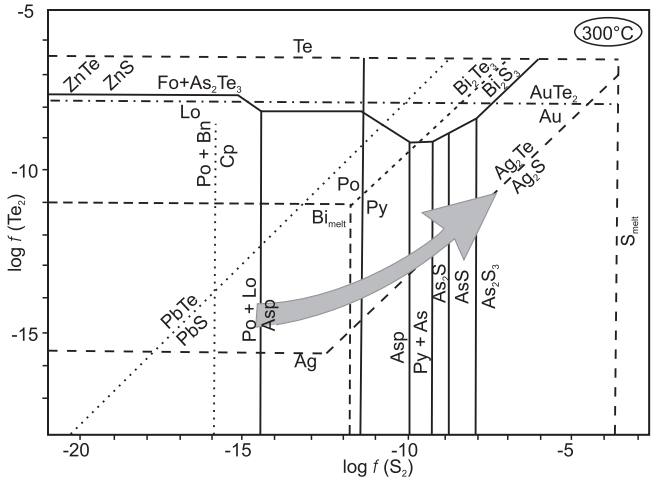

Fig. 23. Telluride-sulphide stability diagram of $f(Te_2)$ versus $f(S_2)$, at 300°C (after Afifi *et al.*, 1988) for mineral phases relevant to the Radzimowice Au–As–Cu deposit

ORE MINERALIZATION IN THE COUNTRY ROCKS

Ore mineralization occurs also in the country rocks of the Żeleźniak intrusion. In dacite porphyry pyrite occurs mainly as euhedral crystals up to 1 mm in size, and as coarse aggregates of variable grain size. Pyrite has of poikilitic cores with abundant quartz, and rare galena, sphalerite, chalcopyrite or rutile inclusions and massive inclusion-free rims (Pl. III, 1). The pyrite may be intergrown with gangue minerals and it commonly forms pseudomorphs after biotite or plagioclase phenocrysts (Pl. III, 3–4). Coarse or fine-grained euhedral arsenopyrite crystals precipated with pyrite but they appear less commonly. They contain inclusions of globular pyrrhotite and irregularly shaped base metal sulphides (Pl. III, 2). Pyrite and arsenopyrite crystals are fractured and cemented by Cu–Zn–Pb sulphides. Pyrite and sphalerite are usually replaced by marcasite. Marcasite also occurs as thin veinlets that cut earlier sulphides or gangue. Ti-oxides appear mostly as fine-grains associated with calcite or epidote pseudomorphs after biotite phenocrysts, or as crystals of up to 2 mm in size (rutile, titanite, anatase, and brookite) that are intergrown with carbonates and replace rock forming minerals (e.g. biotite) (Pl. III, 1, 4–5). Hydrothermal muscovite-rutile-leucoxene assemblages have symptoms of the sericite alteration. Siderite anhedral crystals occur in association with pyrite and calcite, indicating Fe remobilization from primary sulphides (Pl. III, 6). In some dacite samples, crown-like structures consisting of fine acicular silica crystals occur around quartz phenocrysts, indicating the presence of chalcedony (Pl. III, 3).

The lamprophyres contain fine-grained (0.01 to 0.3 mm) disseminated sulphides mainly within the groundmass, but also in pseudomorphs after phenocrysts (Pl. III, 7). The sulphides are represented mainly by marcasite and arsenopyrite with minor pyrite, chalcopyrite, pentlandite and pyrrhotite. Ti-oxides formed pseudomorphs after biotite and hornblende crystals (Pl. III, 8).

In quartz-sericite-graphitic schists mineralization consists of calcite-sulphide veinlets and irregularly distributed fine- or medium-grained disseminated sulphides and Fe-hydroxides, and Ti-oxides. The oldest pyrite generation has a framboidal texture and occurs as impregnations (Sawłowicz, 1987).

ORE GEOCHEMISTRY

A total 178 rock samples, in part sulphide-bearing, collected from the mine dumps and the rock outcrops were subject of investigation for contents of over 50 elements (Tab. 5). They include samples from the northern (99) and the southern (69) parts of deposit, as well as from underground workings of the Luis shaft surroundings (10 samples). Mineralized rock samples are represented by the following ore types: massive sulphide, quartz-sulphide veins, sulphide impregnated rocks and quartz stockworks.

CORRELATIONS

According to the old mining reports the Wanda and Klara veins (N ore field) have the highest gold contents, and the Miner consolation vein (S ore field) has the lowest gold contents. Chemical determinations made for this study confirmed this observation. The average Au concentration in samples from the northern area is 6.9 ppm for n = 109 samples, and from the southern area 1.7 ppm (n = 69; Tab. 6). The massive arsenopyrite-pyrite-chalcopyrite ores with copper contents ≤4 % are richest in gold (20–135 ppm). Distribution of metals is not uniform in the whole deposit (Fig. 24, 25). Arithmetic average values of Au, Te, and Co are higher in the northern part and of Sb, Pb, As, and Cu in the southern part of the deposit (Tab. 6). Contents of Pb and Sb are several times higher values in the southern ore field. Ag and Bi arithmetic average values are relatively similar in the both ore fields of the deposit (northern area: –33.0 ppm Ag for n = 109, –135.6 ppm Bi for n = 101, and in the southern area: –32.9 ppm Ag for n = 69, and –128.5 ppm Bi for n = 51).

(1) Gold correlation is very strong with silver (northern area: r = 0.94; southern area: r = 0.84; Tab. 7), suggesting the presence of electrum. This is confirmed by mineralogical studies, which yield a general gold fineness of 600–750. The correlation with Cu (r – correlation coefficient = 0.60 and r = 0.66, respectively) is explained by the fact that the presence of gold is often associated with chalcopyrite. In the northern area the correlations between gold and typical indicator elements, namely As, Sb, Bi and Te, show differences but are distinctly visible (Fig. 25A, C, D, F). It is very strong Au correlation with Bi and Te (r = 0.94) and weaker with As, Sb and Pb (r = 0.4). Here, the younger stage of Au mineralization overprinted the older generation of Co-bearing arsenopyrite-sulphide association and form mineral assemblage of Au–Ag–Bi–Te–Pb–Fe–S (galena, pyrite, tetrahedrite, native bismuth, bismuthinite, gold, electrum, hessite, gustavite, tellurides and sulphotellurides) and carbonate minerals that occur much frequently in the southern part. Carbonates are represented by fine veinlets with different proportions of calcite, dolomite, ankerite and siderite. It was previously reported that Au correlates here with CaO and MgO – r = 0.46 and 0.47, respectively (Mikulski, 1999). The strong correlation between Au and Cd (r = 0.57) indicates a constant cadmium admixture in sphalerite and pyrites and most probably is related to Au affiliation with those minerals. Gold correlation with Co (r = 0.40) is not clear due to a limited quantity of samples (n = 27).

Table 5

Representative geochemical composition of ore and rock samples from the Radzimowice deposit

	Sulphide ore					Q.vein	Sulphide ore						Schist		
	S-13	S-15	S-27	S-10	S-25	S-20	M-19	M-22	MS-2	MS-7	MS-36	M-21	R35	R9	S-5
Major elements [wt %]															
SiO_2	35.00	35.00	5.00	70.00	45.00	79.93	13.00	4.00	9.45	5.54	46.00	68.00	61.09	57.25	63.10
Al_2O_3	0.86	0.06	0.76	4.98	0.35	0.83	0.12	0.46	2.23	0.49	0.32	9.24	12.17	10.26	4.38
Fe_2O_3	19.10	28.3	48.6	6.06	33.3	6.8	41.9	51.2	48.59	41.5	25.00	9.88	7.76	14.74	12.42
MgO	0.22	0.24	0.33	0.44	2.48	0.29	0.96	0.80	1.57	1.26	0.98	0.40	1.10	0.66	1.22
CaO	0.46	0.85	0.73	0.45	1.27	0.61	2.21	1.06	2.43	4.08	2.31	0.281	0.67	0.087	2.83
Na_2O	0.05	0.01	0.01	0.05	0.05	0.02	0.01	0.01	0.01	0.01	0.01	0.07	0.16	0.18	0.10
K_2O	0.48	0.02	0.39	2.95	0.03	0.59	0.03	0.16	0.44	0.17	0.17	3.29	5.41	2.37	2.42
TiO_2	0.02	0.01	0.04	0.14	0.05	0.02	0.01	0.01	0.02	0.013	0.01	0.12	0.52	0.31	0.21
P_2O_5	0.01	0.01	0.01	0.03	0.01	0.01	0.01	0.01	–	0.01	0.01	0.001	0.13	0.02	0.04
MnO	0.03	0.02	0.01	0.02	0.08	0.02	0.04	0.02	0.04	0.05	0.04	0.02	0.04	0.01	0.23
S	19.42	17.80	26.67	3.74	15.71	3.75	28.79	27.13	30.47	31.42	12.89	4.43	0.13	0.3	4.26
LOI	3.00	5.00	2.00	5.1	3.00	5.00	5.00	5.00	2.00	3.00	–	–	5.26	12.00	5.00
As	19.10	6.81	13.4	5.34	0.0256	0.26	2.86	6.68	0.86	4.82	0.345	3.41	0.0713	0.161	0.79
Cu	0.3210	6.11	1.01	0.0386	0.0868	0.807	3.3	3.71	0.6059	6.43	11.9	0.0435	1.4258	0.0157	0.277
Pb	0.7610	0.0076	0.0230	0.406	0.0534	0.0085	0.0437	0.0296	0.05	0.0685	0.0218	0.0058	0.0027	0.1584	0.915
Zn	0.0492	0.0746	0.0197	0.0304	0.116	0.0268	0.121	0.13	0.0163	0.261	0.256	0.0225	0.0222	0.006	0.193
Total	98.90	100.31	99.00	99.81	101.62	98.96	98.39	100.41	98.78	99.12	100.26	99.21	95.95	99.94	98.37
Trace elements [ppm]															
Au	1.7	27.1	1.09	0.622	0.05	0.246	119	21.3	50	67.8	2.28	0.24	0.254	0.122	0.565
Ag	93	206	27	18	5.1	12	436	63.2	155	169.8	152.4	6	18	86	79.0
Bi	124.7	351.7	552.2	49.3	43.7	22.9	1050	221.8	475	558.3	38.8	50	–	–	128.3
Co	6	2560	113	5	17	94	2060	4560	224	3400	148	14.2	27	1.5	6
Cd	13.4	17.4	4.2	3.9	2.1	4.8	20.8	25.29	53	41.05	46.9	2.5	–	–	30.7
Cr	31	<5	21	23	16	41	–	–	–	–	–	–	–	45	125
Hg	<1	<1	<1	<1	<1	<1	–	–	–	–	–	–	–	–	<1
Mo	4	6	5	2.1	1	6	–	–	–	–	–	–	–	–	4
Ni	3.2	42.4	95.1	4.1	8.1	41.7	13.6	28.6	–	14.2	30.4	2.0	21.0	13.0	28.9
Sb	2650	120	145	491	14.1	51.5	61.1	103	–	81	23.3	–	–	–	1510
Sn	10.6	30.6	8.2	17.7	54.1	10.8	15.8	18.2	–	30.6	63.6	–	–	–	18.8
Te	1.6	72.2	17.6	0.2	<0.1	3.9	149.0	82.2	–	105.9	10.0	–	–	–	0.3
V	3.8	<2	15.5	19.5	5.8	17.5	11.9	7.9	–	15.4	<2	12	141	57	51.7
Ba	110	<50	580	520	<50	340	<50	<50	–	<50	120	–	1352	371	380
Be	0.4	<0.1	0.34	2.05	6.43	0.41	0.16	0.27	–	0.29	0.23	–	–	–	1.34
Cs	1.09	0.22	0.92	3.75	0.87	1.69	0.40	1.13	–	1.28	0.39	–	–	–	4.16
Ga	3.5	1.3	4.5	20.0	6.2	4.0	3.2	10.5	–	10.7	3.1	–	–	–	15.5
Ge	1.7	1.4	1.9	0.7	0.3	0.2	0.6	0.8	–	0.7	0.5	–	–	–	1.0
W	<15	77	12	<1	37	<1	–	–	–	–	–	–	–	–	<1
In	1.1	75.2	3.6	0.3	14.3	3.5	33.4	29.7	–	59.7	87.8	–	–	–	1.4
Li	6.3	3.1	2.7	11.3	11.3	12.6	9.3	14.7	–	12.0	5.9	–	–	–	21.4
Nb	1.7	0.2	1.4	9.9	1.8	0.9	0.3	0.4	1.5	0.5	0.1	9	–	–	5.8
Rb	40	1.7	30	135	2.3	51	35	35	65	30	12.2	141	–	–	130
Re	0.003	0.003	0.004	0.003	0.002	0.004	0.003	0.002	–	0.002	0.002	–	–	–	0.003
Sr	3.9	4.9	33.4	28.3	2.4	23.0	9.4	4.6	1.5	12.6	195.9	7	7.8	14.7	83.6
Sc	0.7	0.2	2.5	3.3	1.5	1.4	19.6	2.6	–	1.7	0.8	–	–	–	6.8
Se	26.3	58.9	123.8	5.4	< 0.1	8.4	50.0	55.6	–	54.2	40.7	–	–	–	2.8
Ta	0.13	<0.1	0.11	0.84	0.15	<0.1	< 0.1	<0.1	–	<0.1	<0.1	–	–	–	0.41
Tl	0.5	0.1	0.6	2.2	0.8	0.5	0.3	0.4	–	0.5	0.6	–	–	–	1.3
Th	2.3	<0.1	1.1	10.3	1.7	0.3	<0.1	<0.1	–	0.3	0.6	–	–	–	6.8
U	0.7	0.8	1.6	4.7	0.8	9.1	0.4	0.3	–	1.8	2.0	–	–	–	2.4
Y	2.2	3.8	7.8	7.6	3.0	2.9	4.5	2.8	9	5.6	4.3	11	–	–	8.8
Zr	179.3	149.4	243.2	139.5	18.5	30.7	30.4	67.9	9	50.9	8.5	73	–	–	96
La	5.5	4.2	11.4	31.8	12.916	12.4	3.2	1.5	–	6	12	–	–	–	10.6
Ce	10.5	7.7	24.7	59.9	23.5	20.2	5.7	3.3	–	9.3	25.9	–	–	–	20.9

Q. vein – quartz vein; S-13,..., S-5 – number of sample

Table 6

Statistic parameters for comparison of the selected elements distribution within the northern (N) and southern (S) ore fields of the Radzimowice deposit

Element	Minimum		Maximum		Arithmetic average		Standard deviation		Number of samples	
[ppm]	N	S	N	S	N	S	N	S	N	S
Au	0.001	0.001	135	33.8	6.91	1.70	22.72	5.23	109	69
Ag	1.41	1.5	436	227	33.03	32.89	71.78	42.04	109	69
Bi	7.4	0.01	1397	1860	135.56	128.52	237.35	310.25	101	51
Sb	0	0.01	105.54	2650	17.00	348.47	22.39	479.48	91	41
Co	1.5	1.5	4800	4398	1254.08	312.76	1601.22	936.30	22	35
Ni	2	1.5	248	247	37.61	40.56	57.90	63.79	16	25
V	1	1	178	163	55.11	45.08	67.65	50.51	16	25
Cd	0.22	0.43	63	30.774	6.07	5.87	14.95	7.26	101	51
Te	10.039	0.05	149.02	72.203	86.79	13.68	58.16	26.55	4	7
Sn	11.03	0	86.54	67.46	30.32	26.99	18.65	18.83	32	41
Ba	25	25	1749	1090	605.00	402.28	642.26	269.90	12	25
[wt%]										
Cu	0.003	0.003	11.900	17.124	0.742	0.877	1.88	3.20	109	69
Pb	0.001	0.002	0.096	1.227	0.025	0.207	0.02	0.26	109	69
Zn	0.002	0.005	0.261	0.228	0.083	0.061	0.09	0.07	22	35
As	0.004	0.005	6.680	27.866	1.733	4.351	1.44	7.45	109	69
S	0.130	0.140	36.980	28.580	18.189	6.539	14.49	8.93	20	29

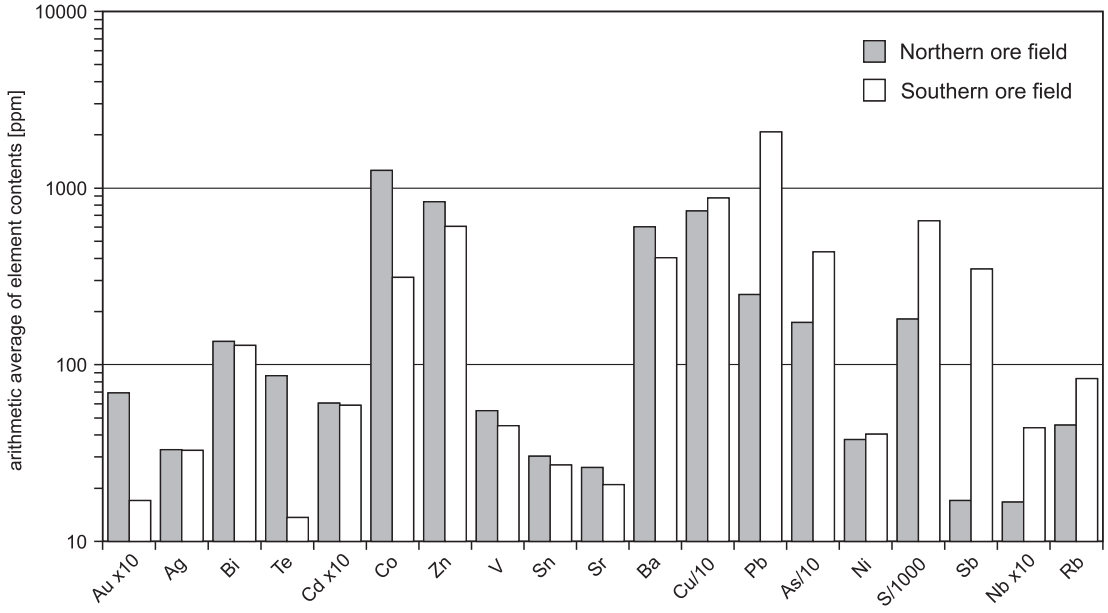

Fig. 24. The arithmetic average comparison of selected elements content in ppm between the northern and southern ore fields at the Radzimowice deposit

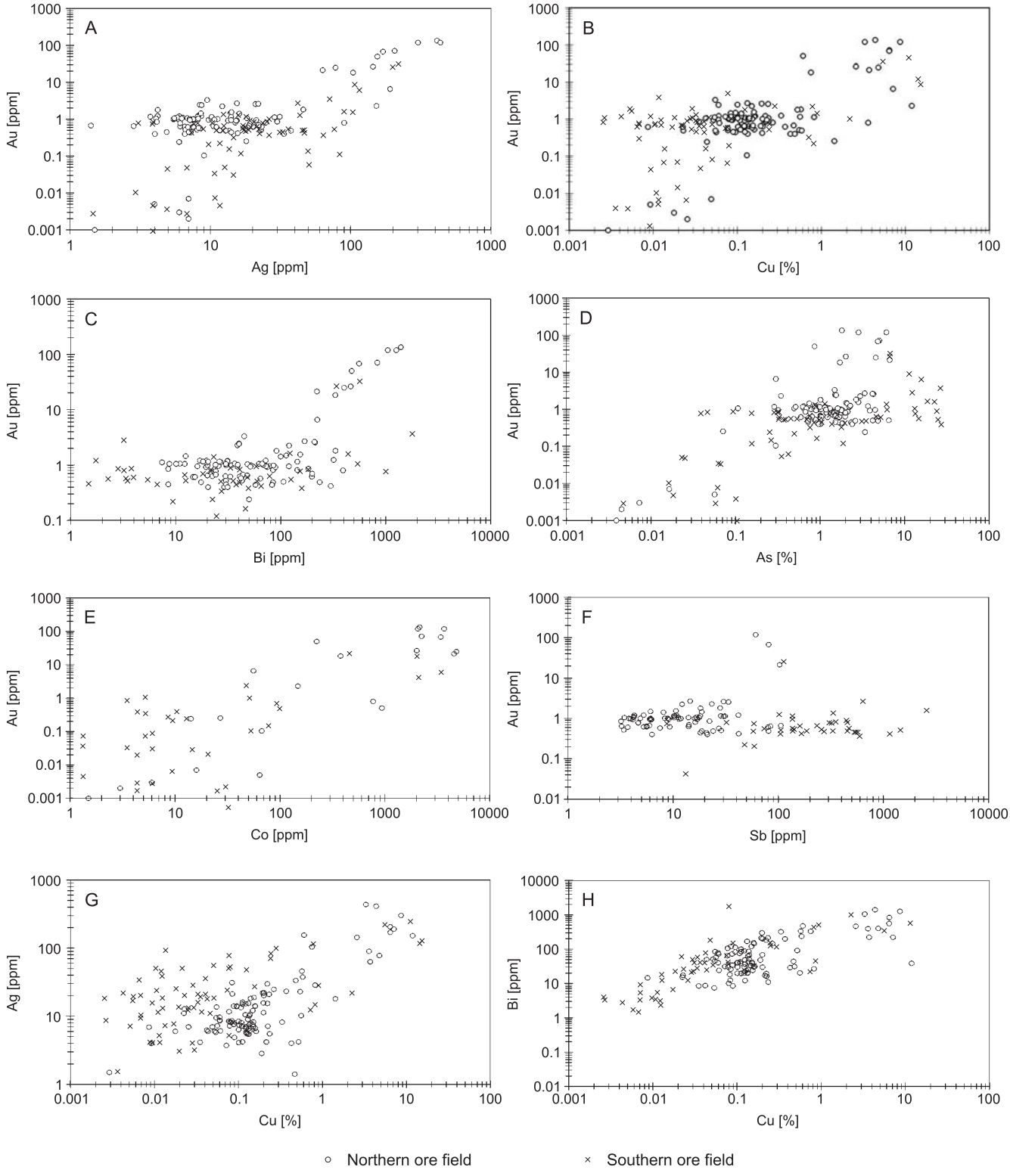

Fig. 25. The variation logarithmic plots of the selected trace and metallic elements in the northern and southern ore fields of the Radzimowice deposit

Microprobe measurements indicated an association of Co-bearing arsenopyrite with gold, however, Co correlation with As is strong only in the N part of the deposit. Gold and silver negatively correlates with SiO_2, K_2O, TiO_2 and Al_2O_3, indicating rather development of alteration processes such as sericitization, argillization, and silicification not coeval with noble metals precipitation. The Au-bearing ores closer correlate with sulphidization (Au–S, r = 0.5).

Table 7

Correlation matrix of selected elements for the rock samples from the northern and southern ore fields at the Radzimowice deposit

Northern ore field / Southern ore field		Au	Ag	As	Cu	Pb	Bi	Cd	Sb	Sn
		n=106	n=106	n=106	n=106	n=106	n=101	n=91	n=91	n=32
Au	n=69	1.000	**.9382**	.3779	**.6045**	.3982	**.9400**	**.5782**	.3868	.0886
Ag	n=69	**.8438**	1.000	.3038	**.7175**	.3795	**.9139**	**.6672**	.3781	.1608
As	n=69	.1702	.3451	1.000	.3166	**.6810**	.4533	.2560	.3794	–.1680
Cu	n=69	**.6575**	**.6782**	.2557	1.000	.2880	**.6063**	**.9629**	.3153	.3263
Pb	n=69	–.1093	.1966	.1871	–.1810	1.000	.4332	.1571	–.0108	–.1818
Bi	n=51	.2927	.3851	**.4975**	.3279	–.0559	1.000	.4567	.3606	–.0834
Cd	n=51	.0765	.2596	–.0351	.0567	.2333	–.0060	1.000	.4068	.2975
Sb	n=41	–.0418	.4199	.3230	–.0430	**.5499**	.1023	.3547	1.000	.3372
Sn	n=41	.0098	–.0393	–.0951	–.0279	–.0667	–.2042	.1210	–.1746	1.000

Bold written digit indicates moderate and/or strong (underline) correlation value between selected elements; n – number of samples

(2) Silver displays also a strong correlation with Cu (r = 0.68–0.72) and Te (r = 0.80) in the whole deposit areas. In the northern part of the deposit Ag has a strong correlation with Bi (r = 0.92) and Cd (r = 0.67) and a weaker correlation with Pb, As, Zn, and Sb (r = ~0.4) suggesting not only a base metal sulphide association. In the southern part silver correlates with Bi, Cd and Sb (r = 0.38; 0.26 and 0.42, respectively). An arithmetic average of silver concentration is 33.0 ppm for n = 178 samples (range 1.4–436 ppm) is a highest value among the late Variscan gold deposits in the Western Sudetes (Mikulski, 2001).

(3) Copper correlates additionally, in the northern part of the deposit, with Cd (r = 0.96), Bi (r = 0.61), and Sr, and much weaker with As, Pb, Zn, Sb, and Sn. In the southern part Cu correlates only with Bi, Zn and Co. Correlation of Cu with Cd, As and Co indicate for association of chalcopyrite with Cd-bearing pyrite and Co-bearing arsenopyrite. Arithmetic average of Cu is 0.74 % (n = 109) in the northern area and 0.88 % (n = 69) in southern part of deposit. Cu concentration is from 0.003 up to 17.1 %.

(4) Arsenic has a correlation with Pb, Bi, Cd and Co. The arithmetic average of arsenic concentration in ore samples is 1.7 % As (range from 0.04 to 6.7 % As) in northern area, and in the southern part of the deposit reveals higher arsenic average value –4.3 % (for n = 41 samples; range 0.004 – 27.9 % As).

(5) Bismuth displays in the northern area a strong correlation with Au and Ag (r ≥ 0.91; n = 101), and weaker with Cu, Cd, and As (r = 0.61; 0.46 and 0.45, respectively). Bi has also significant correlation with Te (r = 0.6; n = 11) and negative correlation with SiO_2 (r = –0.70; n = 21). An arithmetic average of Bi concentration in the northern part of the deposit is 135.6 ppm (range 7.4–1397.4 ppm; n = 101) and in the southern area 128.5 ppm (range 10–1860 ppm; n = 51; Fig. 25C). The average Bi concentration within the Radzimowice deposit is ca. 133 ppm (n = 152). Distribution of Bi in the deposit is mostly connected with appearance of native bismuth, bismuthinite, and Bi, Ag and Pb sulphosalts.

(6) The range of tellurium concentration is from 0.05 to 149 ppm (n = 11). Arithmetic average is 49.3 ppm for the whole area. The presence of tellurium within Radzimowice deposit is very important feature that should be considered during the geochemical and mineralogical divagation. Preliminary results of Te geochemical investigation are limited by small numbers of analysed samples.

(7) Sb concentration within deposit varies significantly between the northern and southern parts of the Radzimowice deposit. An arithmetic average of Sb in gold-bearing samples at Radzimowice deposits is 134.9 ppm. Positive correlation of Sb with Pb and As indicate for tetrahedrite-tennantite distribution, especially in the southern part where Sb an arithmetic average value (348.5 ppm for n = 41) is almost 20 times higher than in the northern area (17 ppm for n = 91). Sb has positive correlation with Au (r = 0.39).

(8) Cobalt within sulphide ores, especially in the northern part of the deposit, has arithmetic average = 0.13%. However, generally it may reach up to 0.48%. Presence of Co is connected with its own minerals and with its admixture in arsenopyrite (Mikulski, 2001). Cobalt has a positive correlation with Au (r = 0.51; n = 57), Ag (r = 0.52), Bi (r = 0.33; n = 32), Fe_2O_3 (r = 0.48), and S (r = 0.4; n = 50) and negative correlation with SiO_2 (r = –0.65; n = 43). There are also correlations of Co with other metallic elements such as: As (r = 0.04; n = 57) and Cu (r = 0.13). Cobalt distribution within deposit was earlier reported from the Wanda vein from 0.084 do 0.91% (Manecki, Młodożeniec, 1959). A very strong correlation of cobalt with

gold high-grade samples is well visible on the Figure 25E. In samples with Au contents >100 ppm, Co concentrations are reaching up to 0.25%.

Sulphur displays strong correlation with total iron that confirms its strong affinity to sulphides and weaker correlation with Bi and Cd.

Position of most ore samples on the pseudo--ternary diagram of Au–Ag-base metals (acc. to Poulsen *et al.*, 2000) falls in the epithermal gold deposit field, strongly indicating low temperature ore-forming processes within the Radzimowice deposit (Fig. 26).

GOLD TO SILVER RATIO IN ORES

Gold to silver ratios are highly variable, and according to mining reports, may change vertically and laterally within the specific veins. A total of 132 auriferous samples with gold contents ≥ 0.5 ppm were selected from the entire set of samples collected in the deposit area (Fig. 27). In this sample population, the gold to silver ratio is between 1:2 and 1:8, with an average arithmetic value about 1:8 (geometric average is about 1:12).

The average arithmetic value of Au:Ag in the northern and southern areas are 1:6.6 (n = 90; geometric average is 1:8.9), and 1:15.8 (n = 42; geometric average 1:22.2), respectively.

In the gold-rich samples > 3 ppm Au (n = 17) the average ratio is about 1:4 (geometric average is about 1:5). The highest Au:Ag ratio, about 1:2 occurs in brecciated massive pyrite-arsenopyrite ores that are overprinted by base-metal sulphides (mainly chalcopyrite) and later cut by carbonate veins associated with tellurides.

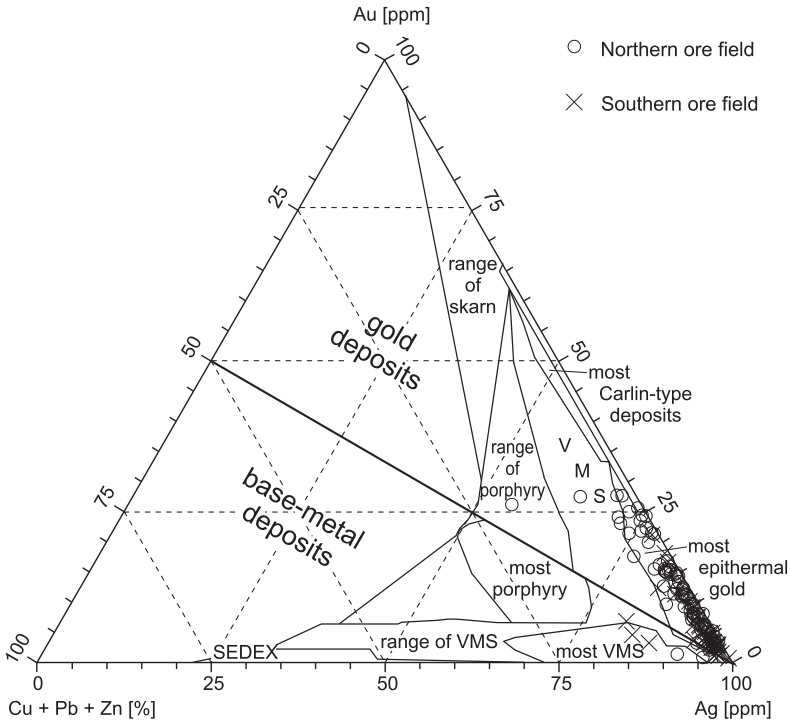

Fig. 26. Pseudo-ternary diagram of gold-silver-base metals (after Poulsen *et al.*, 2000) illustrating the estimated compositions of Au-bearing ores in Radzimowice

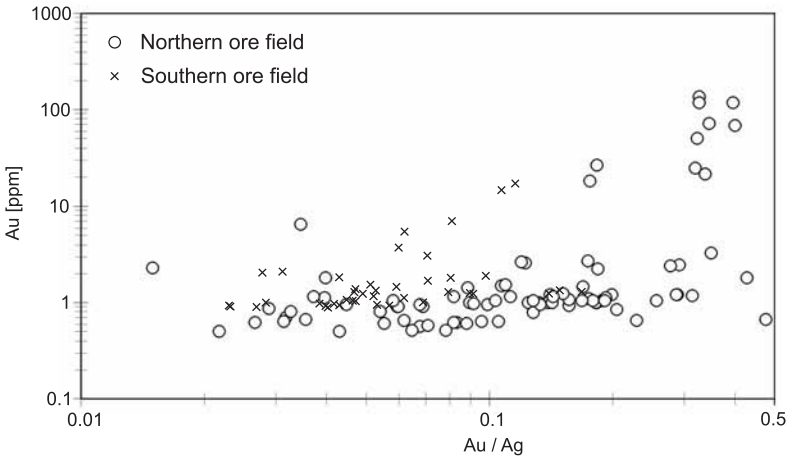

Fig. 27. Logarithmic plot of gold and silver ratio versus gold contents within the ore samples of grade ≥ 0.5 ppm Au from the northern and southern ore fields at the Radzimowice deposit

GOLD AND BASE METAL CONCENTRATIONS IN BARREN ROCKS

Geochemical data set contains additional information concerning gold and base metals assays of over 40 barren rock samples comprising Radzimowice schists and igneous rock suites. The barren Radzimowice schists were collected from the Radzimowice deposit, the Wojcieszów IG 1 borehole and surface outcrops located about 3 km to NW from the deposit. The igneous rocks comprise of dacite, rhyolite and lamprophyre from the country rocks in the Radzimowice deposit.

Gold contents in the rocks from Radzimowice schists from the considering here areas are very similar and range from below 1 ppb up to 8 ppb with an arithmetic average about 3 ppb.

The average concentrations of other elements within the Radzimowice schists from the studied deposit (n = 5) and from the Wojcieszów IG 1 borehole (n = 9, in brackets) are evidently different, as shown here: Cu – 212 (55) ppm, As – 102 (24) ppm, Pb – 64 (20) ppm, Zn – 124 (103) ppm, Cr – 75 (42) pm, Ni – 22 (30) ppm and Co – 9 (42) ppm, Co/Ni = ~1:2 (1.5:1). The highest As concentrations were determined in metasandstones and graphite schists from Radzimowice – ca. 400 ppm and 200 ppm, respectively.

In the group of barren potassic igneous rocks an arithmetic average of gold for dacite porphyry is at 4.5 ppb (n = 6, range 1–11 ppb) and for lamprophyre at 3.3 ppb (n = 5, range 1–5 ppb). The other elements arithmetic average values for dacite and lamprophyre (in brackets) are as follows: As – 242 (816) ppm, Cu – 120 (97) ppm, Zn – 46 (157) ppm, Pb – 16 (50) ppm, Co 6 (42) ppm, Cr 18 (686) ppm, Ni – 7 (208) ppm and V – 30 (160) ppm. These metal concentrations are typical of such rocks excluding As contents. Arsenic concentration in igneous rocks is high, especially in lamprophyres (0.05 to 0.1 wt %). The ratio of Co/Ni in dacite porphyries and lamprophyres is ~1:1 and 1:5, respectively.

REE DISTRIBUTION IN ORES

Non mineralized porphyry samples were considered as representative of the fresh members of the K igneous suite from the Żeleźniak and Bukowinka intrusions (Ze 13..., and Bu 8... samples, Tab. 8). Chondrite-normalized (cn) REE patterns after Taylor, McLennan (1985) was applied to the host rocks and ores from the Radzimowice deposit (Fig. 28). The Żeleźniak and Bukowinka porphyries REE patterns plot within a narrow range. They exhibit light REE (LRRE) enrichment (Ce/Yb_{cn} = 8–14 and 10–13, respectively) and no Eu anomaly. Two samples of Bukowinka porphyries show low Ce/Yb_{cn} ratio of ca. 5. Żeleźniak lamprophyres have Ce/Yb_{cn} ratio = ca. 6. In comparison to the Żeleźniak porphyry patterns, the lamprophyres exhibit slight depletion in the light REE, and almost similar concentration of the heavy REE (HRRE), and also lack of Eu anomaly.

The chondrite-normalized trace elements patterns of ores exhibit different REE enrichment (Ce/Yb_{cn} = 2–27), strong negative Eu anomaly and variable value of Eu related to ore grade. Eu concentrations in hydrothermal sulphide ore samples are strongly depleted in comparison with igneous rock. The mineralizing processes which caused formation of high grade ores were also responsible for depletion of Eu contents within hosts rocks (Fig. 28E). This observation is supported by REE patterns of massive ores and mineralized quartz veins that exhibit a strong negative Eu anomaly. The quartz veins with minor sulphide mineralization show even higher enrichment of light REE (Ce/Yb_{cn} = up to 27). Compared to mineralized porphyries, they are depleted in both the HREE and LREE and have strong negative Eu anomalies. REE patterns of massive ores also exhibit a strong negative Eu anomaly and a weak LREE enrichments (Ce/Yb_{cn} = 2–3). In comparison to the quartz veins, the massive ores exhibit very similar REE patterns with a negative Eu anomaly but they are depleted in the light REE (Fig. 28D–E).

The Radzimowice schists are represented by two samples (Fig. 28F). The S-5 sample contains smaller amount of disseminated pyrite and shows a REE pattern very similar to PAAS (Post-Archean Average Shales; Taylor, McLennan, 1985) and ES (European Shales; Haskin, Haskin, 1966) with REE depletions of up to one order of magnitude. The second sample of the Radzimowice schists (S-27) is strongly mineralized by sulphides. The both Radzimowice schists samples have relatively flat heavy REE with Tb/Yb_{cn} approximating 1 and Ce/Yb_{cn} ratios of 5 and 8 correspond with the PAAS and ES ratios 6 and 7, respectively.

The total REE content of the selected samples displays some variations. The highest ΣREE (308 ppm) is contained in an unmineralized dacite. Quartz veins have ΣREE from 50 to 140 ppm and moderate enrichment in LREE. This may suggests hydrothermal origin of apatite, zircon and/or monazite. This is consistent with the observation of apatite and zircon by cathodoluminescence methods (Pl. XIV, 7).

WALL-ROCK ALTERATION

At the Radzimowice deposit, hydrothermal alteration occurs particularly within dacite porphyries surrounding the ore-bearing veins (Pl. IV). Dacites that are rich in disseminated sulphides (mainly pyrite) have characteristically grey or light beige colour and have high alkali ratios (K_2O/Na_2O>25). By contrast, unmineralized dacites have pink colour and K_2O/Na_2O ratios of 1.1 to 2.2. Slightly altered porphyries contain K-feldspar and/or Na-bearing plagioclase phenocrysts. Sericite, calcite, Ti-oxides and sulphide commonly formed pseudomorphs after biotite and feldspar phenocrysts in altered porphyries (Pl. IV, 1, 2, 5). Plagioclase destruction reactions result in the loss of alkalis (particularly Na) and Ca during the formation of sericite.

Hydrothermal alteration started with strong acidic and argillic reactions (sericitization, pyritization, and kaolinitization), as reflected in vein selvages, followed by alkaline hydrothermal alteration (illitization) with albitization and carbonatization (Pl. IV, 3, 4, 7). Kaolinitization postdating sericitization occurs only in narrow zones adjacent to the contact with the ore veins (Manecki, 1965). Pyrite precipitation ac-

REE content (in ppm) in the rocks and sulphide ores from the Radzimowice deposit

Sample	La	Ce	Pr	Nd	Sm	Eu	Gd	Tb	Dy	Ho	Er	Tm	Yb	Lu	Ce/Yb_{cn}
S 5 py impregnation in Radzimowice schists	10.649	20.943	2.558	9.16	1.929	0.448	2.004	0.311	1.733	0.372	0.993	0.166	1.129	0.172	4.69
S 10 asp ore as impregnation in porphyry	31.793	59.943	7.238	22.819	3.945	1.091	3.217	0.414	2.073	0.397	0.99	0.16	1.024	0.154	14.18
S 27 asp + chp ores in Radzimowice schists	11.42	24.696	2.943	9.766	1.388	0.112	1.281	0.189	1.208	0.307	0.843	0.124	0.818	0.124	7.63
S 25 asp impregnation in porphyry	12.916	23.511	2.606	7.612	0.947	0.503	0.724	<0.1	0.535	0.139	0.386	<0.1	0.411	<0.1	14.49
S 20 Q vein with poor sulphide contents	12.433	20.224	2.099	6.606	1.048	0.126	1.013	0.126	0.587	0.114	0.256	<0.1	0.188	<0.1	27.35
S 15 massive chp-asp ore in Q vein	4.154	7.728	0.922	3.352	0.721	0.114	0.793	0.141	0.765	0.148	0.334	<0.1	0.243	<0.1	8.07
S 13 asp ore in Q vein cuts porphyry	5.481	10.493	1.185	3.995	0.716	0.101	0.628	<0.1	0.457	<0.1	0.224	<0.1	0.249	<0.1	10.67
M 19 massive chp-py-asp ore	3.201	5.754	0.68	2.605	0.705	0.129	0.832	0.124	0.688	0.151	0.383	<0.1	0.655	0.207	2.21
M 22 massive asp-py-chp ore	1.531	3.339	0.444	1.695	0.447	0.085	0.527	<0.1	0.452	<0.1	0.217	<0.1	0.273	<0.1	3.09
M 22’ massive asp-py-chp ore	1.587	3.499	0.448	1.716	0.452	0.09	0.522	<0.1	0.464	<0.1	0.209	<0.1	0.279	<0.1	3.16
MS 7chp-asp-py ore in greenstone	5.057	9.285	1.14	4.174	1.017	0.185	1.235	0.167	0.859	0.157	0.318	<0.1	0.251	<0.1	9.35
MS 36 chp ore	11.963	25.921	3.42	13.15	2.462	0.395	2.14	0.287	1.258	0.206	0.401	<0.1	0.254	<0.1	25.9
Bu (Bukowinka) 7/2 granite	95.368	66.876	–	36.568	18.039	10.920	–	6.897	–	–	–	–	6.204	6.299	10.780
Bu 8 granite	89.373	55.381	–	26.723	13.506	11.609	–	6.897	–	–	–	–	5.518	5.512	10.036
Bu 6/4 rhyolite	43.052	32.393	–	22.504	11.082	12.184	–	6.897	–	–	–	–	6.238	6.299	5.193
Bu 6/1 rhyolite	120.163	72.100	–	35.162	15.152	13.448	–	8.621	–	–	–	–	6.272	6.299	11.495
Bu 5 rhyolite	48.229	35.528	–	21.097	11.082	9.310	–	6.897	–	–	–	–	6.272	6.299	5.664
Bu 4 rhyolite	88.828	53.292	–	30.942	12.554	9.195	–	6.897	–	–	–	–	5.313	5.512	10.031
Bu 1/2 rhyolite	107.357	70.010	–	43.601	18.831	14.253	–	8.621	–	–	–	–	5.381	5.512	13.011
Ze (¯eleŸniak) 13/5 rhyolite	106.354	71.055	–	39.381	16.580	12.529	–	6.897	–	–	–	–	6.375	6.299	11.146
Ze 13/3 rhyolite	95.640	59.561	–	32.349	13.377	8.046	–	6.897	–	–	–	–	4.627	4.462	12.872
Ze 15/2 rhyolite	70.845	47.022	–	25.316	11.861	8.391	–	5.172	–	–	–	–	4.627	4.462	10.162
Ze 15/1 rhyolite	132.970	76.280	–	42.194	17.965	12.759	–	8.621	–	–	–	–	6.718	6.562	11.355
Ze 14/3 rhyolite	147.411	91.954	–	50.633	19.870	14.023	–	8.621	–	–	–	–	6.375	6.037	14.424
Ze 14/2 rhyolite	73.297	45.977	–	26.723	13.420	10.000	–	6.897	–	–	–	–	5.724	5.512	8.033
Ze 13/4 rhyolite	97.548	60.606	–	36.568	17.056	13.563	–	6.897	–	–	–	–	7.129	6.824	8.501
Ze 13/9 rhyolite	108.447	65.831	–	36.568	16.147	12.299	–	8.621	–	–	–	–	6.546	6.299	10.056
Ze 10/1 rhyolite	79.564	50.157	–	28.129	13.030	10.345	–	5.172	–	–	–	–	5.690	5.512	8.816
Ze 13/8 rhyolite	103.542	67.921	–	42.194	21.688	15.747	–	8.621	–	–	–	–	8.226	7.874	8.257
Ze 14/5 lamprophyre	79.564	61.651	–	42.194	24.372	20.575	–	6.897	–	–	–	–	9.768	9.449	6.311
Ze 13/10 lamprophyre	78.747	59.561	–	42.194	22.424	18.966	–	8.621	–	–	–	–	9.665	9.449	6.162
Ze 14/4 lamprophyre	78.474	55.381	–	39.381	21.351	18.506	–	15.517	–	–	–	–	8.740	8.399	6.337

Ce/Yb_{cn} normalized to chondrite after Taylor, McLennan, 1985; n.d. – not determined; asp – arsenopyrite, chp – chalcopyrite, py – pyrite, Q – quartz; M, MS, S and Ze – symbol of samples colected from the area of Żeleźniak Hill; Bu – symbol of samples colected from the area of Bukowinka Hill

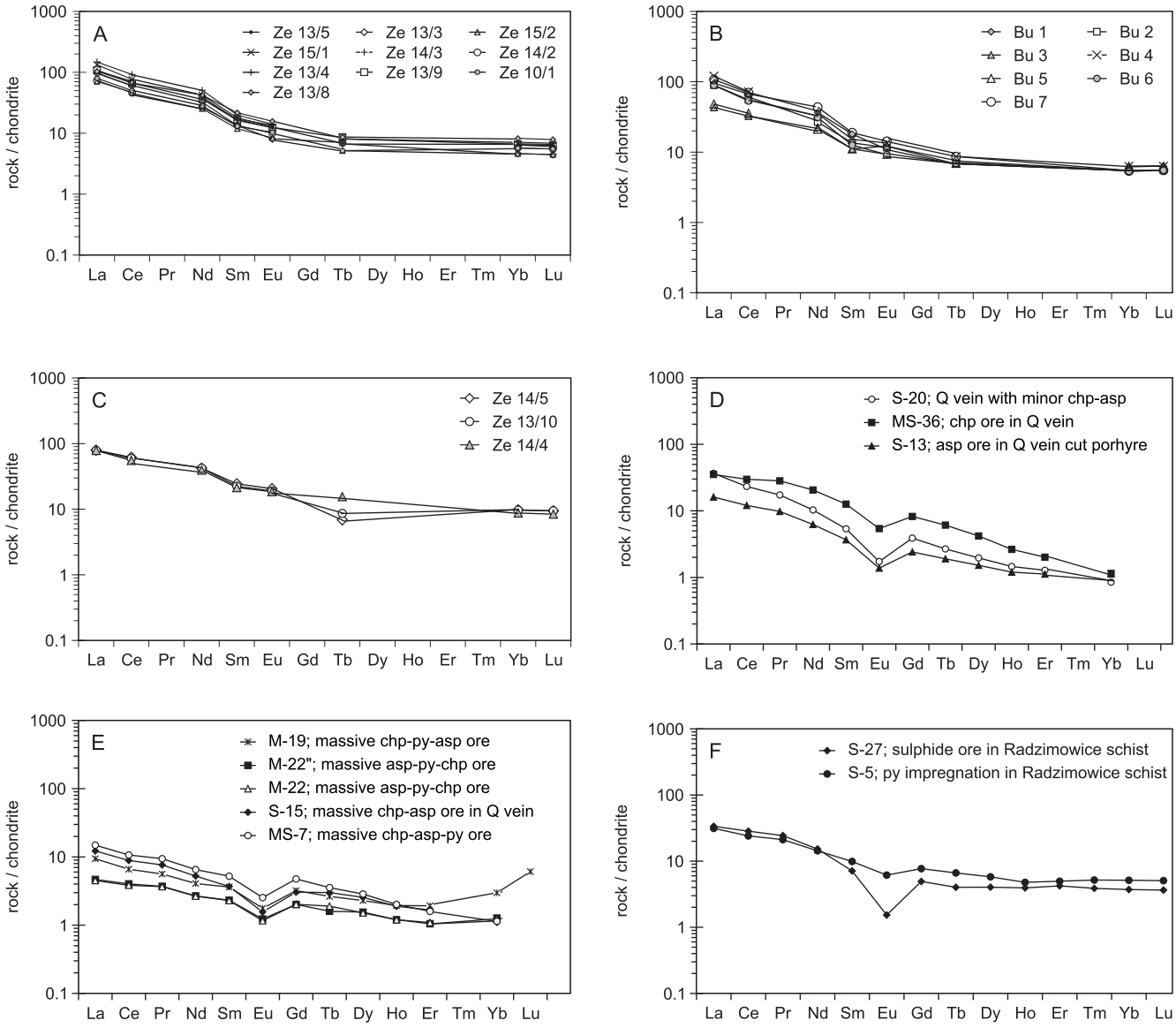

Fig. 28. Chondrite-normalized rare earth element diagram (after Taylor, McLennan, 1985) for representative igneous rocks from the ¯eleŸniak and Bukowinka intrusions, and ore samples from the Radzimowice deposit

A – ¯eleŸniak porphyry; **B** – Bukowinka porphyry; **C** – ¯eleŸniak lamprophyre; **D** – sulphide in quartz veins; **E** – massive ores; **F** – sulphide impregnation in the Radzimowice schists

Abbreviations: asp – arsenopyrite, chp – chalcopyrite, py – pyrite, Q – quartz. Ze 13/5, Bu 1, M-19, S-5 – number of sample

companied by sericitization is widespread beyond the selvages. Additionally, the appearance of dickite in association with sericite and pyrite suggests successive hydrothermal alterations in rhyolite porphyries around the ore veins (Manecki, 1964). Illite concentration appears in altered rocks as veinlets and infills commonly replacing biotite or plagioclase phenocrysts. Among the chlorites, post-biotite chlorite of ripidolite and brunshvigite composition and spherolitic, oxidized chamosite were recognized (Machowiak, Weber-Weller, 2003). Post-biotite chlorite is also subject of later replacement by muscovite/sericite. Carbonates (calcite, dolomite, ankerite, and siderite), marcasite, Ti-oxides, Fe-hydroxides, and locally low temperature quartz, orthoclase and/or adularia are common (Pls. III, 6; IV, 5–8). In the contact zones between dacite with the Radzimowice schists, the alteration is weak developed and typically representing by chalcedony-opal mineralization with medium- and fine-grained disseminated pyrite, and minor calcite.

Altered lamprophyres are characterized by the presence of sericite replacing plagioclase, calcite, prehnite, muscovite, pumpeliite, and chalcedony replacing olivines and by secondary biotite and phlogopite. The lamprophyres also contain fine-grained disseminated sulphides and Ti-oxides (Pl. III, 7, 8).

The correlations between calc-alkali oxides and sulphur indicate that during processes of ore precipitation took place gain of CaO and lose of alkalies content (K_2O and Na_2O; Fig. 29). Bukowinka porphyries contained very low concentration of

sulphur what clearly excludes them as a source of sulphur. Even barren ¯eleŸniak porphyries have at least 2 order higher sulphur concentration.

Geochemical assays of ores and country rocks from the northern and southern areas indicate that K_2O have a high correlation coefficient ($r \geq 0.92$) with Al_2O_3, TiO_2, Nb and Rb and with SiO_2 ($r = 0.66$; $n = 20$). However, silica and Fe–Mg, as well as the large ion lithophile elements (LILE: Ba, Rb, Cs, Sr) are considered mobile during hydrothermal alteration. Other major compounds such as TiO_2 and Al_2O_3 and the HFSE appear to be immobile (MacLean, 1990).

Average values of alkali content in gold-bearing ores (Au ≥0.5 ppm) for the northern part of deposits (K_2O – 0.23 wt % and Na_2O – 0.01 wt %; n=13), is several times lower than for the southern part (K_2O – 1.54 wt % and Na_2O – 0.05 wt %; n=13). It is evident that significant amounts of potassium were lost in ¯eleniak porphyries during later hydrotermal stages especially in the northern part, close to the source of post-magmatic fluids.

The REE can be mobile during intense hydrothermal alteration, but under low-grade alteration conditions they remain immobile. The results of this study present evidence that rocks underwent pervasive hydrothermal alteration have noticeably depleted REE patterns relative to slightly mineralized rocks (Fig. 28A, E). Enrichment of LREE in quartz veins can be accounted for high activity of K^+ in the hydrothermal fluids (Bierlein *et al*., 1999). Correlation coefficients for REE and Si, K and Al oxides ($n = 11$; $r = 0.95$) are strongly positive as contrasted to elements such as S, As, Au, and other metals.

Total REE concentrations in the mineralized Radzimowice schists (127–134 ppm) are 3 or 4 times lower in comparison with ΣREE values for PAAS and ES. REE enrichment of mineralized quartz veins and depletion of mineralized meta-turbidities (Radzimowice schists) may also indicate the mobilization of REE (mainly LREE) from country rocks adjacent to ore mineralization. However, Alderton *et al.* (1980) suggested that no significant change of REE is likely to occur during sericitic alteration beyond a negative Eu anomaly.

Eu anomaly is the most characteristic effect of sericitization of siliclastic sediments that is also present among alteration assemblages at Radzimowice. As illustrated by Bau (1991), Eu anomaly depends strongly on temperature and slightly on pH. Under nearly neutral to mildly basic conditions the REE concentration in fluids is dominated by carbonate, fluoride and hydroxide complexes that at the high temperatures (500–600°C) may effect negative Eu anomaly and REE concentration, unless the water/rock ratio is $>10^2$–10^3. Results of fluid inclusion studies of ores from the Radzimowice deposit revealed that the ore-bearing fluids have a temperatures ranging from 150 to 420°C, and generally moderate salinities of less than 16 wt % NaCl equivalent and under these conditions REE mobility is expected to remain low, even in conditions involving relatively high fluid/rock ratios (>100; Bau, 1991).

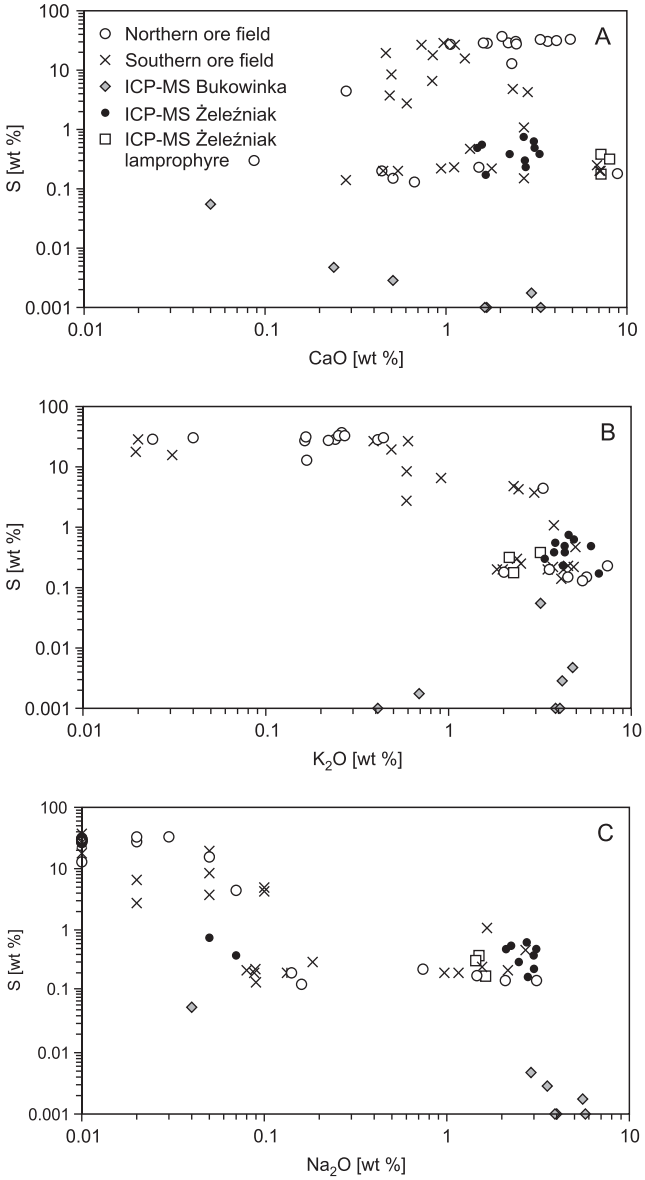

Fig. 29. Lose of alkalis and gain of CaO content due to alteration processes within the northern and southern ore fields at the Radzimowice deposit, and in Bukowinka porphyry

Plots of sulphur *vs*. CaO (**A**), K_2O (**B**), and Na_2O (**C**)

STUDIES OF FLUID INCLUSIONS IN QUARTZ

Four types of samples with various quartz generations associated with ore mineralization were selected for fluid inclusion studies (Fig. 30). The first type represents gray quartz veins in altered dacite porphyries of different Au grade (36 ppb – 1.83 ppm Au) and type of ore mineralization (Fig. 30A, B). The second type consists of samples with domination of white quartz generation veinlets and with gold-bearing chalcopyrite and chalcopyrite-arsenopyrite ores (up to 9.3 ppm

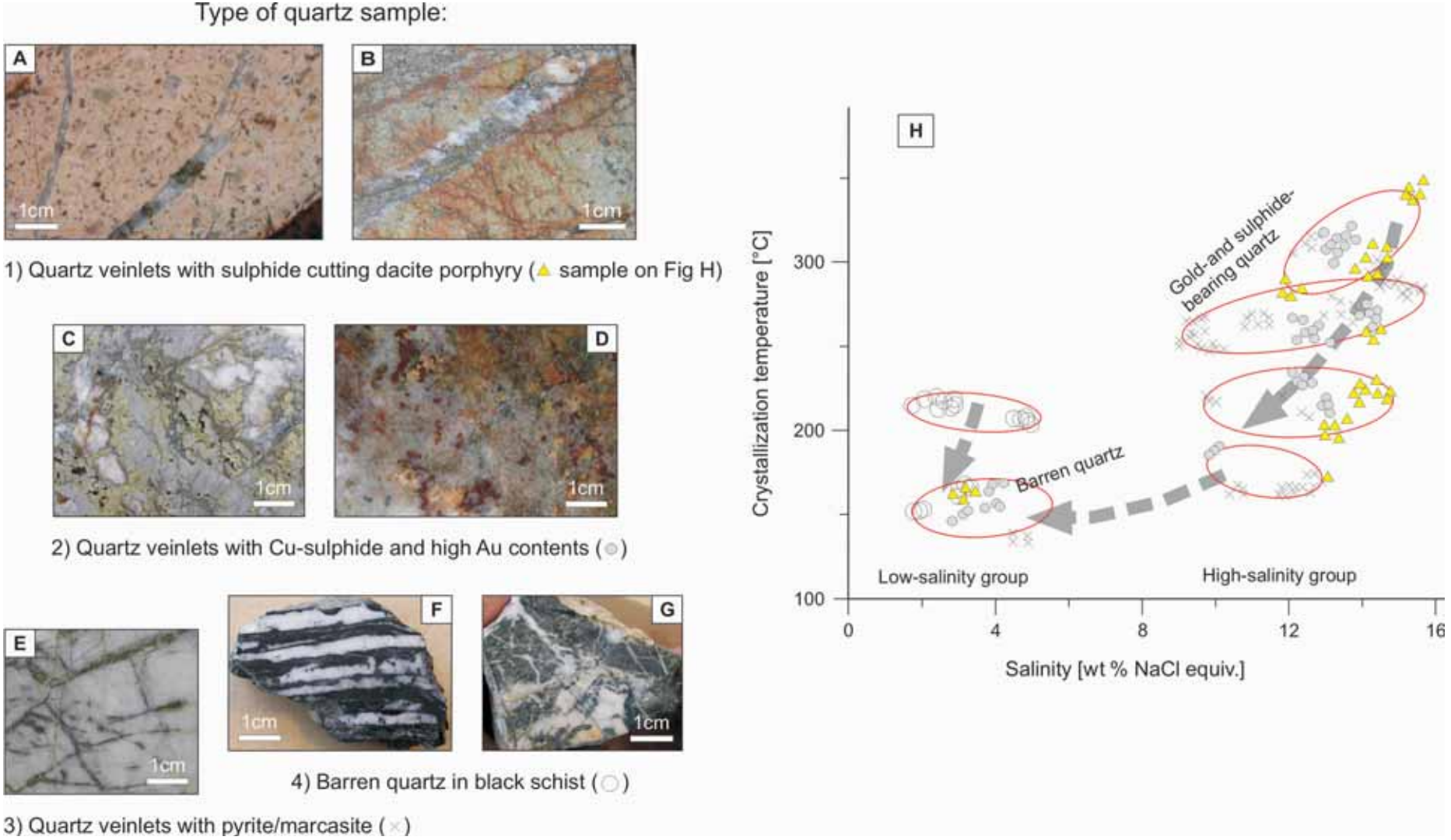

Fig. 30. The various generation quartz veinlets from the Radzimowice Au–As–Cu deposit which were subject of fluid inclusion studies.

The microphotographs in reflected light; **A** – dacite porphyry with gold-bearing quartz-sulphide veinlets; **B** – altered dacite porphyry cutting by gold-bearing quartz-sulphide veinlets; **C** – fractured coarse-crystalline gray-white quartz vein with arsenopyrite and chalcopyrite cemented by carbonates and marcasite; **D** – quartz-sulphide vein and various generations carbonate (beige – dolomite and dark red – siderite); **E** – the successive coarse- and fine-crystalline quartz generations with the youngest marcasite/pyrite veinlets (dark); **F** – barren milky-white quartz in quartz-graphite schists from the surroundings of the Miner consolation vein; **G** – cataclased barren milky-white quartz veinlets cutting graphite schist; **H** – plot of crystallization temperatures versus salinity of fluid inclusions in quartz veinlets

Au; Fig. 30C, D). The third type contains samples with mostly white quartz with a late generation of pyrite or marcasite in fractures (Fig. 30E), that reveal only traces of Au concentrations. The fourth type is represented by barren milky-white quartz veinlets in silicified black schists of the flysch unit (Fig. 30F, G).

In general, primary fluid inclusions are small, usually not exceeding 10 μm in length. Typically, they are two-phase liquid-rich inclusions with a small vapour bubble. They were frequently isometric of euhedral quartz habit. The salinity of the primary fluid inclusions in quartz of various generations splits into two distinct salinity groups: a low salinity group (3 ±2 wt % NaCl equivalent), and a moderate salinity group (12 ±4 wt % NaCl equivalent; Fig. 30H). Four ranges of the calculated temperature of crystallization for various generations of quartz may be defined, which partly overlap the two distinct salinity groups: A high-temperature range from 350 to 270°C (Fig. 30H – adequate ellipse); a second range from 290 to 250°C, a third range from 240 to 190°C, and a low-temperature range from 170 to 140°C. Fluid pressure during quartz crystallization shows a decrease from 1.2 to 0.8 kb. The high temperature high-salinity group of quartz may correspond to the stage of base metal sulphides mineralization associated with the next generation of quartz and carbonates (stage 2; Fig. 17I). According to fluid inclusion results the second and third temperature ranges of high salinity fluids can be related to Au–Ag–Te–Bi–Pb±S minerals assemblage and sulphosalts mineralization (stages 3–4). The lowest-temperature range of fluid inclusion corresponds to barren quartz with marcasite/pyrite mineralization (stage 5). Fluid inclusions in quartz veinlets or schistosity-parallel lamination in the schists indicate quartz crystallization in temperature ranges: 220–200°C for clear glassy quartz and 170–140°C for fine-grained quartz-feldspar veinlets with pyrite from fluids with salinity about 3 wt % NaCl equivalents.

OXYGEN ISOTOPES OF QUARTZ

The preliminary results of oxygen isotopes of quartz from Radzimowice deposit have been presented by Mikulski *et al.* (2003). Calculated $\delta^{18}O_{fluid}$ of various type (from I to IV) vary between –3.3 to +7.4 ‰ (Tab. 9). Oxygen isotope data indicate mixing of an ^{18}O-depleted fluid (surface-derived waters, meteoric waters) and an ^{18}O-rich fluid (of magmatic and/or metamorphic origin). The highest values are estimated for quartz of the earliest vein stages, lower ones were recorded by later vein stages, indicating a gradual increase in the proportion of meteoric water. Mineralizing fluids responsible for the richest gold mineralization that is associated with epithermal overprint of the early As- and Fe- sulphide mineralization seem to be characterized by higher values of salinities and the $\delta^{18}O_{fluid}$ oxygen compositions of vein quartz.

Table 9

Results of $\delta^{18}O$ composition in quartz from Radzimowice deposit (after Mikulski *et al.*, 2003)

Sample	Type of quartz*	$\delta^{18}O_{quartz}$ [%]	T [°C]	$\delta^{18}O_{fluid}$ [%]
R17	I	+13.1	225 and 250	+2.9 to +4.2
R1	II	+13.9	225 and 300	+3.7 to +7
R10		+14.1	225 and 300	3.9 to +7.4
R4	III	+12.7	225 and 300	+2.5 to +5.8
R16		+15.0	120 to 275	–3.3 to +7.2
R28		+13.8	175 and 300	+0.5 to +6.9
R11	IV	+12.5	150 and 200	–2.8 to –0.6

Abbreviations: * Type I–IV –separation of samples into four types based on grade and ore composition, similar like for the fluid inclusion study; for more details see Fig. 30

THE Re–Os AGE VALUES OF GOLD-BEARING SULPHIDE AT THE RADZIMOWICE DEPOSIT

The several Co-bearing arsenopyrite samples for Re–Os dating were collected from the underground workings of the Luis shaft in the northern part of the abandoned Radzimowice deposit and from the old mining wastes of the Miner consolation vein in the southern part of the deposit. Only a medium-, and fine-grained (0.5–3 mm in size) euhedral Co-arsenopyrite, pyrite and chalcopyrite non-fractured crystals of the first generation from the veinlet-impregnation zones were selected for the Re–Os measurements (Pl. V, 1–6). Short characteristic of host rocks and mineral association is presented in Table 10.

Arsenopyrite crystals from Radzimowice display a compositional variability in arsenic contents (34.8–37.4 atom. %) and high admixture of cobalt (up to 6.4 atom. %) and refractory gold. Refractory gold (ca. 70 ppm) appears as submicroscopic inclusions within Co-bearing arsenopyrite and less abundant in pyrite.

Analyses of auriferous Co-arsenopyrite from the Radzimowice deposit yielded Re concentrations of 0.13–3.5 ppb with total Os in the ppt range (Tab. 11). The arsenopyrite (sample LL-99) from Radzimowice with the highest Re con-

Table 10

Short description of sulphide samples from the Radzimowice deposit for the age determination by Re–Os methods

Sample symbol	Location	Rock description	Ore mineral description	
			major minerals	minor minerals
M-22	Radzimowice deposit, Luis shaft – northern ore field	Massive aggregate of sulphides in quartz vein cutting greenstone	Massive aggregate and single coarse – and medium –grained crystals of pyrite and Co-arsenopyrite, fractured and cemented by quartz, calcite and base metal sulphides	Medium-grained crystals of chalcopyrite may contain sphalerite intergrowths or sphalerite star-like inclusions. Subordinate galena and tetrahedrite occur as fine crystals. Micro-fractures are filled by carbonate associated with tellurides and Bi and Au minerals
Wil/2		Massive aggregate of Co-arsenopyrite in quartz-carbonate vein cutting dacite	Medium- and coarse-grained Co-arsenopyrite crystals up to several mm occurring separately or as aggregates locally with pyrite	Rare anhedral chalcopyrite up to 0.1 mm in diameter
R 2	Radzimowice deposit the Miners consolation vein – southern ore field	Dacite porphyre strongly sericitized and illitized with pyrite impregnation	Pyrite euhedral crystals up to 1.5 mm in size replacing phenocrysts of biotite or plagioclase	Base metal sulphides and rutile in pyrite
StG3/4	Radzimowice deposit – southern ore field	Quartz-sulphide vein cutting dark gray sericite-graphite schists	Massive aggregate of coarse- and medium-grained crystals of Co-arsenopyrite, in part fractured and cemented by quartz	Fine-crystalline base metal sulphides
StG - 6		Massive base metal sulphides in quartz-carbonate vein	Massive intergrowths of pyrite and base metal sulphides	Galena contains Bi–Ag sulphosalts

Table 11

Low level Re-Os data for Co-arsenopyrite, chalcopyrite and pyrite from the Radzimowice Au-As-Cu deposit

PGI sample number	AIRE sample number	Location	Mineral	Re, ppb (± 2δ)	^{187}Os, ppb (± 2δ)	Model Age[3] [Ma]
M-22	LL-28	Luis shaft –70 m b.s.l.	Co-asp[2]	0.129(2)	0.0013(1)	ca. 320
StG3/4	LL-29	Southern ore field	Co-asp[2]	0.3448(4)	0.0019(1)	ca. 316
Wil/2	LL-30	Luis shaft –70 m b.s.l.	Co-asp[2]	0.357(6)	0.0028(2)	ca. 387
M-22	LL-97		cp[3]	0.0072(4)	0.00022(2)	ca. 425
M-22	LL-98		py[3]	0.0253(7)	0.0048(2)	ca. 294
posy533M-22	LL-99		Co-asp[3]	3.51(9)	0.01327(6)	317

Abbreviations: Co-asp — Co-bearing arsenopyrite; cp — chalcopyrite; py — pyrite

Notes: **1** – All samples analyzed using a Carius tube dissolution and Re–Os data are blank corrected; **2** – Assuming an initial $^{187}Os/^{188}Os$ ratio of 0.2 after Mikulski *et al.* (2005a); **3** – Analytical blanks: Re = 1.97 (2) pg, Os = 4.68 (5) pg with $^{187}Os/^{188}Os = 0.182(4)$; (4) Analytical blanks: Re = 2.5 (1) pg; Os = 0.635 (6) pg with $^{187}Os/^{188}Os = 0.190(8)$

tents yielded Re–Os age of ca. 317 Ma that was fairly insensitive to the change of the assumed initial ratios.

The four-point isochron based on auriferous Co-arsenopyrite yielded a Re–Os age of 314 ±31 Ma (initial ratio = 0.8 ±2.2, MSWD = 2.1). Large uncertainties on the final results for the two Co-arsenopyrite analyses (LL-28, 29) is due to low Re contents, however there is general agreement between model ages for these samples when a low initial ratio was used. Assuming an initial ratio of 0.2, LL-28 and LL-29 yield model ages of 320 and 316 Ma, respectively (Mikulski *et al*., 2005a, d). Additional analyses of Re and Os concentrations in pyrite and chalcopyrite samples from the Radzimowice deposit were made. Unfortunately, these sulphides revealed extremely low contents of Re – 0.025 ppb, and 0.007 ppb, and Os – 0.0048 ppb, and 0.00022 ppb, respectively. These results allowed constructing a six-point isochron that gives a Re–Os age of 317 ±17 Ma (Mikulski *et al.*, 2005a; Fig. 31). This isochron has a better uncertainty to compare to four-point isochron based only on Co-arsenopyrite. However, still relatively large uncertainty is due to the very low Os concentrations of most of the samples (<5 ppt total Os in all cases exclude one). Nevertheless, a model age of 317 Ma for sample LL-99 with an $^{187}Re/^{188}Os > 10^5$ is fairly insensitive to the assumed initial ratio and supports the isochron age (R. Markey, pers. inform., 2004).

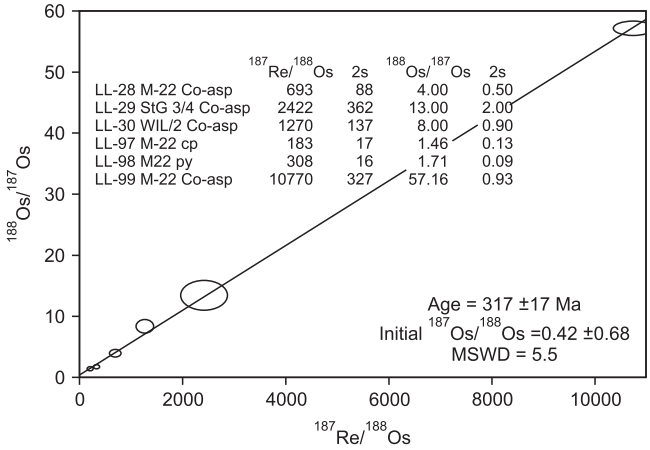

Fig. 31. The six-point isochron of auriferous sulphide from the Radzimowice deposit (after Mikulski *et al.*, 2005a)

Co-asp – Co-bearing arsenopyrite, cp – chalcopyrite, py – pyrite

DISCUSSION OF THE ORE MINERALIZATION GENESIS OF THE RADZIMOWICE DEPOSIT

The studied economic gold mineralization is related to sheeted quartz-sulphide veins which occur peripherally (east- and southward) to the Upper Carboniferous Żeleźniak intrusion. The arc setting, multiple magmatism and hydrothermal episodes, as well as the ore vein mineralogy are similar to other gold systems related to alkalic magmatism (Richards, 1995; Jensen, Barton, 2000; Kelley, Ludington, 2002).

Two main stages of ore mineralization are recognised at the Radzimowice deposit. The first stage is of mesothermal character and consists of strongly brecciated quartz–Fe–As sulphides that according to calculations based on the arsenopyrite geothermometer crystallized at temperatures 535–345°C (485–368°C on sulphur isotope fractionation geothermometer acc. to Machowiak, Weber-Weller, 2003). The second stage has low sulphidation epithermal character with base-metal sulphides and carbonates. The lower temperature ~300°C of base metal sulphide crystallization, were calculated on the basis of the fractionation of sulphur isotopes between the cogenetic sulphide minerals (Ohmoto, 1986). According to these calculations the temperatures, obtained from the two pairs studied, range from 322 (sphalerite 2.76 $\delta^{34}S_{CDT}$ – galena 0.23 $\delta^{34}S_{CDT}$) to 289°C (pyrite 1.65 $\delta^{34}S_{CDT}$ – chalcopyrite 0.38 $\delta^{34}S_{CDT}$) (Mikulski 2005a).

Machowiak, Muszyński (2005) reported on the base of the rock thin section research the presence of ignimbrites and diatremes from the Żeleźniak massif. It indicates the presence of complex magmatic system with active arid volcano. Mikulski (2003a) identified multiple stages of magmatic activities characterised in the end by post-tectonic lamprophyre and andesite formation followed by strong hydrothermal quartz-sulphide mineralization of vein-impregnated type. Figure 32 shows schematic model of the ore formation at the Radzimowice Au–As–Cu deposit.

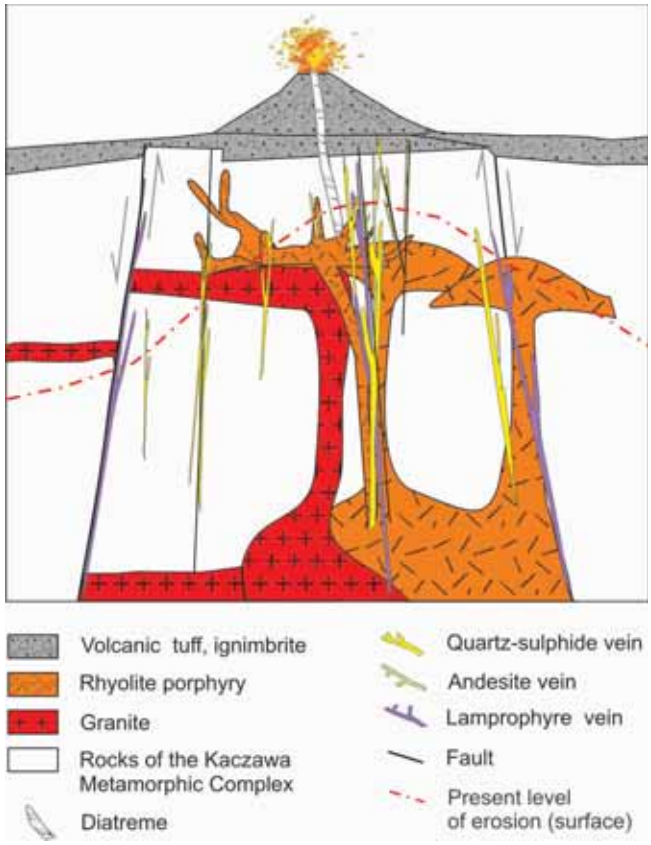

Fig. 32. The schematic model of the complex magmatic bodies and related ore mineralization at the Radzimowice Au–As–Cu deposit in Upper Carboniferous

Hedenquist *et al.* (2000) subdivided low sulphidation deposits into intermediate-sulphidation and end-member low sulphidation groups that are related to various magmatic affiliations reflecting the different tectonic settings. The typical sulphide assemblage of end-member low sulphidation epithermal deposits is pyrite-pyrrhotite-arsenopyrite and Fe-rich sphalerite, corresponding to mesothermal and the intermediate assemblage between the low sulphidation and high-sulphidation end-members is represented by tennantite-tetrahedrite-chalcopyrite and Fe-poor sphalerite which corresponds to the younger stage at Radzimowice.

Primary gold mineralization of submicroscopic type crystallized during rapid cooling as submicroscopic inclusions or as a solid solution or chemically bound admixture within Co-bearing arsenopyrite. The second type of gold – the microscopic gold, formed during slower cooling as inclusions and micro-veinlets associated with base metals and Bi–Te minerals. The average purity of gold at the Radzimowice deposit is low (about 685) and characteristic for gold deposits formed at shallow epithermal levels similar to the purity of gold in carbonate-base metal gold systems (Corbett, Leach, 1998).

The presence of tellurides with electrum and bismuth, and other Ag–Bi–Pb±S minerals associated with carbonate minerals in Radzimowice indicates their crystallization in close to neutral conditions at temperatures <354°C and probably <250°C (Cabri, 1965; Afifi *et al.*, 1988). Carbonates vary in composition (ankerite, dolomite, siderite, and calcite) and they are typically zoned with depth (siderite-rhodochrosite with kaolinite occur at shallow levels, calcite and Mg-carbonates at depth, and mixed Fe–Mn–Ca–Mg carbonates in the mineralized intermediate zones) which are characteristic for low sulphidation epithermal mineralization (Hedenquist *et al*., 1998). The zoning indicates fluid mixing as the probable mechanism for mineralization. Reconnaissance oxygen isotopic analyses of quartz samples from the Radzimowice deposit showed that calculated $\delta^{18}O_{fluid}$ values vary between –3.3 to +7.4 ‰ (Mikulski *et al*. 2003). These data indicate mixing of a $\delta^{18}O$-depleted fluid (surface-derived waters, meteoric waters) and an ^{18}O-rich fluid (of magmatic and/or metamorphic origin). The highest values are estimated for quartz of the earliest vein stages ($\delta^{18}O_{fluid}$ = +2.9 to +4.2‰), and the lower ones are recorded by later vein stages, indicating a gradual increase in the proportion of meteoric water ($\delta^{18}O_{fluid}$ = –2.8 to –0.6‰).

According to Hedenquist *et al.* (1998), the injections of magmatic fluids of low- to moderate salinity, metal-rich and oxidized into ground water during the late stages of magma crystallization may lead to the formation of base metal and silver-rich low sulphidation deposits within distal parts of high-sulphidation deposits. At Radzimowice this is confirmed by measurements of fluid inclusions in sulphide bearing quartz ± carbonate veinlets (Mikulski *et al*., 2003). The P–T conditions of formation of gangue minerals (quartz, carbonate) that are associated with base-metal sulphides suggest temperature range of 300 to <200°C at pressures of 1.2 to 0.8 kbar and a moderate salinity fluids (13 ±3 wt % NaCl equivalent). Most of the epithermal gold-silver-bismuth-tellurides took places at about 240–190°C from fluids with salinity about 12–15 wt % NaCl equivalent. Moderate temperatures of late hydrothermal solutions from 207 to 177°C are also indicated by chlorite geothermometry on chlorite from altered peraluminous rocks from the Radzimowice deposit as estimated by Machowiak, Weber-Weller (2003).

The gold to silver ratios in sulphide ores are generally low; however, the geometric average for ore samples grading >3 ppm Au is about 1:5. Mikulski (2001) suggested that all ore samples from the both areas of the Radzimowice deposit are located within the epithermal gold field on the Au–Ag-base metals pseudo-ternary diagram of Poulsen *et al.* (2000). The base-metal contents in the ore samples may be up to several weight percent. The Cu contents in all igneous rocks are high (about 200 ppm) excluding the granite. The correlation of gold and copper is associated with positive correlations of gold with other elements such as Ag, S, Bi, Te, Pb, Sb, Co, Cd, As, CaO, and MgO (Mikulski, 1999; confirmed by the present study). Paragenetic studies suggest that arsenic and cobalt were introduced by hydrothermal fluids only during the early stage and other elements such as base metals; bismuth, silver, tellurium and antimony came only during younger stages. Iron, sulphur and gold were supplied by hydrothermal fluids even multiple.

The hydrothermal alteration started with strong acidic and argillic reactions (sericitization, pyritization, and kaolinitization) followed by propylitic alteration (illitization, chloritization), albitization and carbonatization. Sericitization is widely distributed. Other hydrothermal alterations are restricted in area around quartz-sulphide±carbonate veins. The earliest alterations may indicate presence of porphyry copper and/or high sulphidation systems at depth (Hedenquist *et al*., 2000). The first mineralizing fluids were rich in SO_2 and formed argilitic alteration and acid-leaching characteristics. The comparison of LREE (Ce/Yb_{cn} ratio 5–8) and HREE (Tb/Yb_{cn} approximating 1.1) in Radzimowice schists with their concentration in PAAS (Post-Archean Average Shales; Taylor, McLennan, 1985) and ES (European Shales; Haskin, Haskin, 1966) shows significant depletion of the wall rocks immediately adjacent to the gold-bearing sulphide mineralization. The HREE depletion in the schists is comparable to the meta-turbidities that underwent a strong hydrothermal pervasive alteration by high temperature fluids responsible for some of the mesothermal gold mineralization in the central Victoria in Australia (Bierlein *et al*., 1999).

The sulphur isotope compositions of the sulphides range from –1.13‰ (in galena) to +2.29‰ (in Co-bearing arsenopyrite), indicating a magmatic source of sulphur at the Radzimowice deposit. At the Radzimowice deposit typical porphyry Cu–Au mineralization has not been recognized, but they may be concealed beneath younger igneous and unmineralized rocks. Located to the east of Radzimowice, prospects with hematite veins at Lipa and quartz-sulphide veins at Grudno are supporting evidence that a district-scale hydrothermal event of different character (oxidized fluids) occurred in association with Upper Carboniferous potassic magmas. One source of metals may be felsic magmas of crustal origin with contribution of mantle elements. This fact is supported by the REE patterns of mas-

sive ores and mineralized quartz veins that are very similar and have strong negative Eu anomalies. Moreover, massive ores are depleted in the light REE (Ce/Yb_{cn} = 2–10) and only positive Eu anomaly or its lack exhibit rhyodacite porphyries that host any appreciable mineralization.

Alkaline magmas are hydrous and oxidized, and have the ability to produce hydrothermal systems with a suitable chemical features for transporting gold (Connors *et al*., 1993; Jensen, Barton, 2000). According to Heinrich *et al*. (1999) in oxidizing magmas the partitioning of copper and gold into a vapour is high relative to a brine phase but in reduced magmas, the resulting brine may cool to form porphyry Cu–Au mineralization. Cu-rich alkaline deposits are primarily found in arc environments and are associated with intrusive phases with <60 wt percent SiO_2 (Jensen, Barton, 2000). According to Müller, Groves (2000), shoshonitic magma may be responsible for noble metal supply in several world-class deposits genetically associated with potassic igneous rock suites. Similar to a number of subalkaline systems, at Radzimowice there is evidence for the late-stage injection of maphic alkaline magmas as manifested by the presence of lamprophyre dykes. Locally, they are spatially related to quartz-sulphide veins. According to Keith *et al*. (1998) and Maughan *et al*. (2002) maphic melts play a critical role in generating large mineral deposits such as at Bingham, Utah, where mixing between late-stage maphic alkaline magmas and sub-alkaline granitic melts supplied a substantial portion of sulphur, copper and gold. Late maphic magma (*e.g.* producing lamprophyre) may has introduce metals or trigger volatile release from a large magmatic reservoir at depth (Wyman, Kerrich, 1989). Some of the Radzimowice lamprophyres contain quartz xenocrysts that are indicative of volatile – driven rapid up-rise of the lamprophyric magma (Rock *et al*. 1991).

The Żelaźniak intrusion geotectonic setting, ore vein mineralogy, Au/Ag ratio, base-metal contents, and associated alteration are similar to epithermal Au–Ag deposits accompanied by felsic volcanic rock suites that formed in Cenozoic continental arc-settings along the Western United States (John, 2001; Kelley, Ludington, 2002).

The mineralization of the Radzimowice deposit is considered as related to alkaline magmatism and is characterized by superposition of low sulphidation epithermal mineralization on higher-temperature and deeper-seated mesothermal mineralization. It is classified as of the transition from porphyry to epithermal type.

THE KLECZA–RADOMICE ORE DISTRICT WITH QUARTZ-SULPHIDE-GOLD VEINS

The Klecza–Radomice ore district was located inside the area of the rectangle shape (6.2 km by 1.4 km; Domaszewska, 1964). It starts near the Pilchowice–Nielestno railway line on its southeastern side and runs through Radomice and Klecza up to Golejów village on the northwestern corner (Fig. 33). This ore district consisted of the main four mining fields: Klecza I, and II, Radomice I, and Golejów (*op. cit.*).

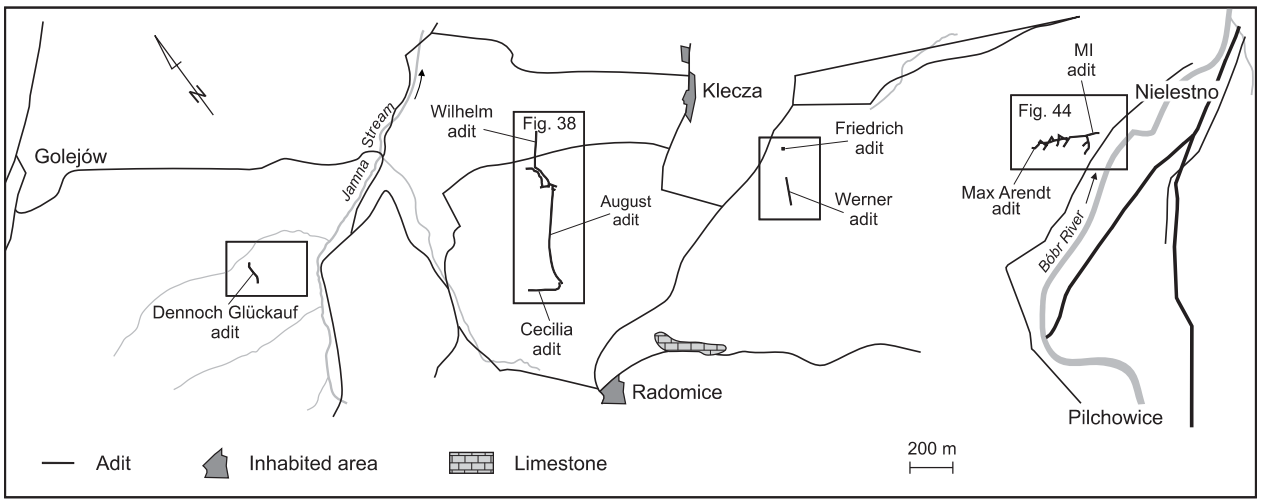

Fig. 33. The old mining situation plans of the German adits in the Klecza–Radomice gold ore district (acc. to Grimming, 1933)

THE HISTORY OF THE MINING EXPLORATION

The oldest notes about the surface exploration of the richest part of outcropped veins in the period from 1425 to 1625 are given by Möller (1911). However, there are no data about a total quantity of ore production or gold contents during this time. During the Middle Ages exploration was carried out from the open pit, later by use of shallow shafts and short adits. The new, more advanced gold prospecting began in the years 1896–1909 when the old mining workings and underground channels were found. According to Krusch (1907), gold contents from the trench samples, collected in 1898 usually were below 6 ppm. However, in some samples, they reaching up to 96 ppm of Au. The silver content in the samples was usually about 6 ppm, and only in some samples reached up to 50 ppm Ag. Gold ore also contained arsenic (in Klecza ca. 2% As and in Radomice 10–12% As). Samples from Klecza were richest in Au with an average content 13.3 ppm and low in arsenic (Krusch, 1907; Materiały..., 1923). Despite good gold contents, investigation work stopped in 1909 in the Klecza–Radomice ore district. This was mainly due to tectonic disturbances of veins, small ore reserves and lack of financial support.

In the period 1916–1921 short production of arsenic took place. Exploitation was carried out by use of 4 adits. The strong inflow of water was a main reason for closing the mine. Since 1922 to 1933 some exploitation were active under the management of new owners. During this time period the ore production from Klecza–Radomice mines was only 120 t, which contained an average 28.6 ppm Au (Domaszewska, 1964). According to Grimming (1933) one of the samples from the Klecza deposit revealed almost 120 ppm Au and the exploitation was focused on the most valuable part of the veins. In 1933 production was finished due to difficult condition of ore exploitation. Gold mining activities have never been carried again, despite positive report elaborated by Grimming (1933).

Gold contents in the ore from the Klecza–Radomice district had the highest value among known deposits in the Western Sudetes (Mikulski, 2001). Here, the main gold-bearing mineral was pyrite instead of arsenopyrite (Krusch, 1907). At Klecza arithmetic average of Au within 18 big technological samples was high – 13.3 ppm (Krusch, 1907). Lower grade of Au ores was at Radomice deposit where in samples from the Cecilia adit an average gold concentration was only ca. 1.2 ppm and in samples from the August adit about 5.8 ppm and about 11% As. In general gold content in the ores ranged from a few to around 40 ppm (Tab. 12).

Table 12

The characteristic of the ore veins features from different workings of the Klecza–Radomice ore district (after various authors)

Area	Name of adit	Quantity & quality of exploited veins				Average contents of element			Reference
		Number of veins	Length of vein [m]	Average thickness [m]	Main ore minerals	Au [ppm]	Ag [ppm]	As [% wt]	
Klecza	Wilhelm adit # 1	2 major	>90	0.25 max. 1.2	asp, py	13.3	5.1	2.82	Krusch, 1907
						39.86 (max. 48)	–	5	Grimming, 1933
						19.87	–	–	
		1 diagonal		<0.1		40 (max. 120)	–	3	
Radomice	Cecilia adit # 2	2 major	>100	min. 0.25	asp, py,ga	16.0	–	10–15	
		5 minor	–	–		1.2	–	12–15	Krusch, 1907
	August adit # 3	1	>120	max. 1.5	asp	5.80	–	11	
						8.0	–	25	Grimming, 1933
		–	–	–	–	5.8	–	11	Domaszewska, 1964
Golejów	Dennoch Glückauf adit	2 major	>140	0.3 0.12	asp , ga asp	2.4	90	35	Fedak, Lindner, 1966
		2 minor	–	0.06–0.08	asp	2.1	–	–	Domaszewska, 1964
Nielestno	Max Arendt adit	(?)1 +	120	up to 2.0	asp	30.0	–	3	Grimming,1933
		–	–	–	–	37.7	–	–	Domaszewska, 1964

asp – arsenopyrite (main ore mineral); py – pyrite; chp – chalcopyrite; ga – galena

GEOLOGIC STRUCTURE OF GOLD DEPOSITS

Gierwielaniec (1956) was the first who described two main tectonic units in the Klecza–Radomice ore district. The Wleń tectonic unit that is separated from the second Pilchowice unit by the Wleń trough. The upper structural position occupies the Wleń unit that in comparison with Pilchowice unit does not reveal such strong tectonic deformation.

Teisseyre (1967), Szałamacha (1971) and Szałamacha (1974; 1978) did not exclude possibility that Pilchowice unit may be an equivalent of deeper and distal part of the Bolków unit and as well as the Wleń unit an equivalent of the Świerzawa unit (Fig. 1).

Auriferous mineralization occurs in flysch-like rocks of the Pilchowice unit localized between gneisses of the Karkonosze-Izera Block on the south and Rotliegende sediments that filled Wleń trough on the north (Fig. 34). At the Klecza-Radomice ore district gold bearing quartz-sulphide mineralization consist of veins, and vein arrays in folds (saddle reefs), faults and brittle-ductile shear zones in flysch-like sedi-

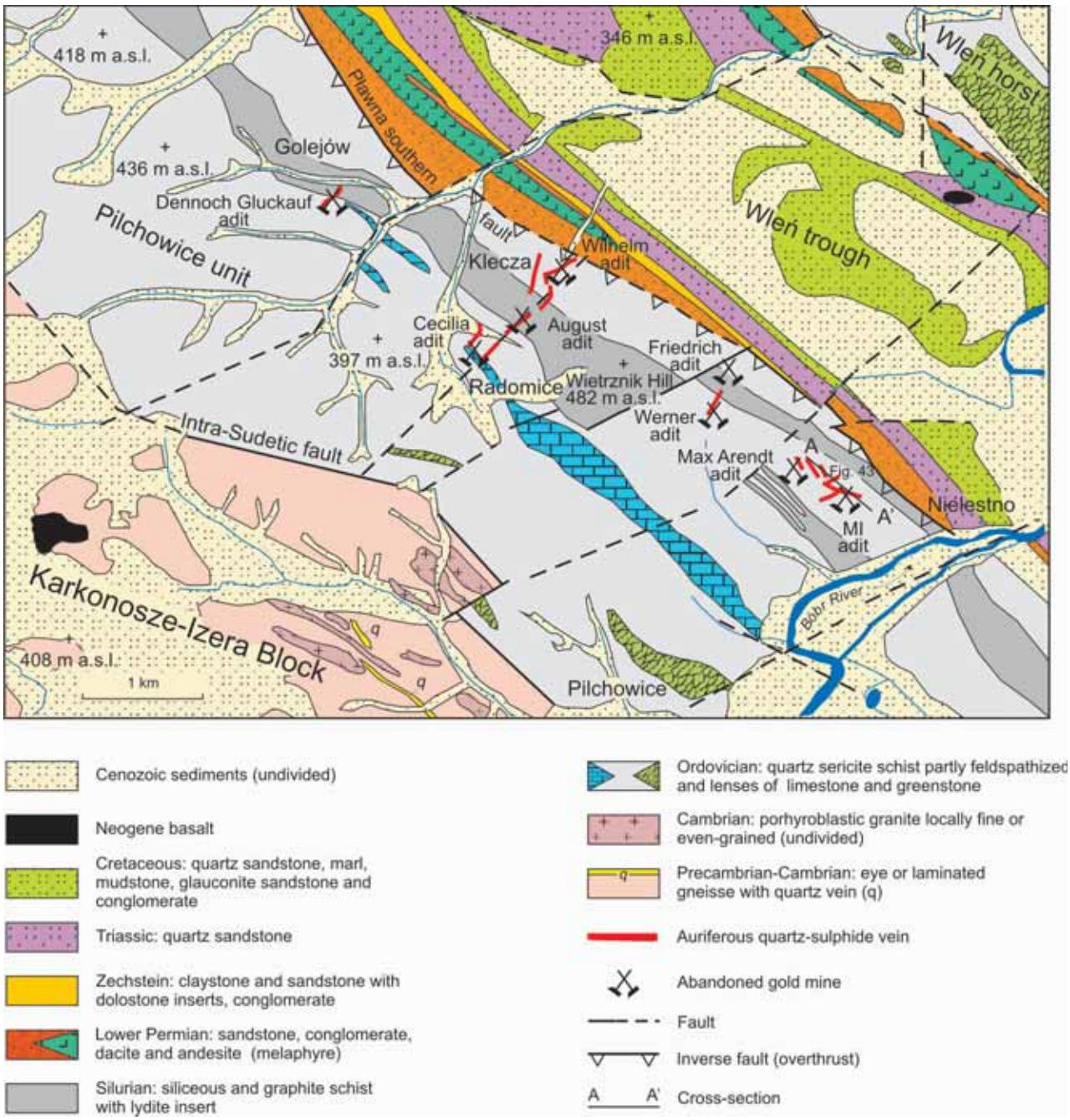

Fig. 34. Geological map of the Klecza-Radomice gold ore district (modified from Milewicz, 1962; Milewicz, Frąckiewicz, 1983; Szałamacha, 1970, 1974)

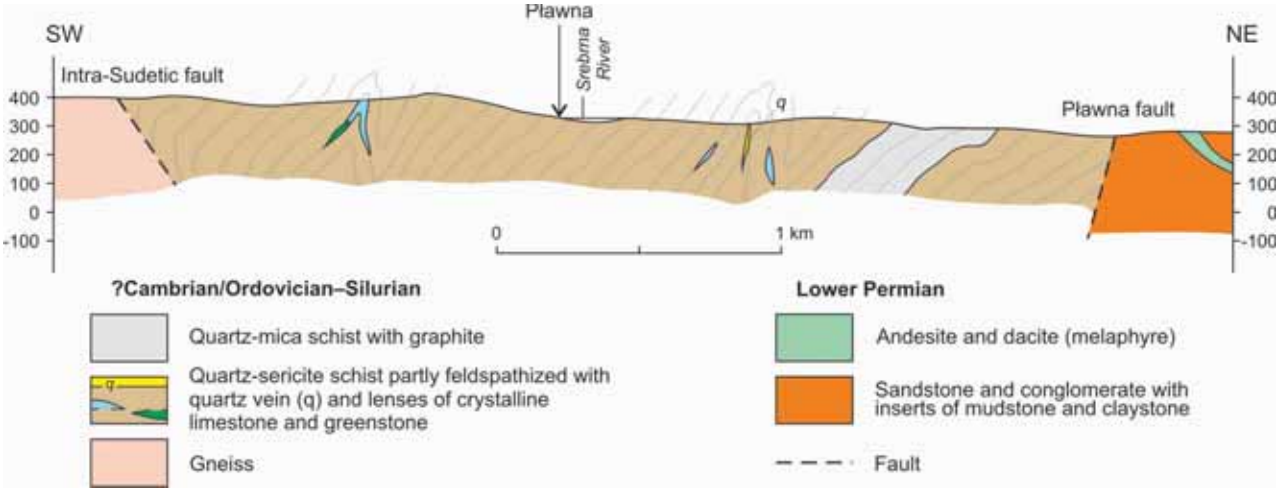

Fig. 35. Geological cross-section through the Pilchowice unit near the Pławna abandoned Au mine (modified from Milewicz, 1962)

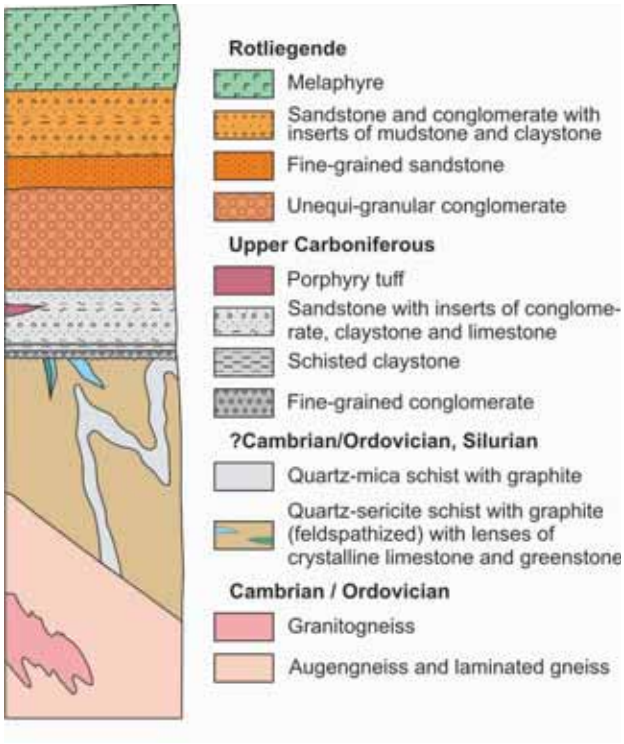

Fig. 36. Schematic geological profile of rocks of the Pilchowice unit from the Klecza–Radomice ore district (after Milewicz, 1962)

ments deformed and metamorphosed to lower greenschist facies. The main lithological rocks are representing up to a several hundred meters thick sequence of primary laminated, pelagic turbidities with intercalations of gray and black quartzites, metalydites, clay-rich graphite schists, metacherts, and basic metatuffites (Figs. 34–36). Inserts of crystalline limestones and dolostones indicate that underwater volcanic elevations became areas of calcareous sedimentation (Milewicz, 1970; Kozdrój *et al.*, 2001). These sediments are interpreted as oceanic trench-slope type depositions that took place during Ordovician–Late Devonian times (Baranowski, 1988).

Sericite and graphite schists are favourable host of sulphides mineralization. Graphite schists may contain up to 20% of TOC (total organic carbon) and graphite up 40% of rock volume. Host rocks are strongly altered due to silicification, sericitization, carbonatization, chloritization, feldspathization and sulphidization.

In the Klecza–Radomice ore district the eight main and several smaller (more than 9) quartz-sulphide veins were discovered in weakly metamorphosed Silurian argillaceous, graphite, greywacke and quartz schists (Tab. 12). Most frequently veins cut host rocks but locally may appear as saddle reefs (Nielestno area). Bigger veins are preferentially located in fractured zones discordant to the bedding and run close to, or along the axial planes of F_2 anticlines. Several veins run oblique in direct surroundings of the Pławna fault zone of inverse character (Fig. 34). This NW–SE trending zone constitute southern border of the Wleń Trough. Less commonly occurring veins of saddle reefs that are bedding-parallel. Diagonal veins were also reported from the Wilhelm adit area. It is characteristic feature of all veins that numerous transverse faults displaced (1–2 m) their bodies at different angels. Veins have major NE–SW and minor NW–SE strike directions, and are steep dipping (65–85°) to W (Fig. 37). They were examined on a length of about 90–140 m and down dip to 100 m below surface, showing different thickness from 0.1 to 1.5 m (an average thickness is about 0.2–0.3 m).

ORE MINERALIZATION IN THE RADOMICE AREA

Samples for the ore study have been collected from old mining sites located near abandoned gold workings and prospecting adits that have been located along narrow creek dewatering western slopes of Wietrznik Hill (+482 m a.s.l.) above Radomice village (Fig. 34). In this area sulphide mineralization occurs in fracture zones within rocks of the Kaczawa Metamorphic Complex represented here by sericite-muscovite-chlorite-quartz schists, quartz-sericite schists, graphite-quartz schists and quartz-feldspar schists that all belong to the Pilchowice unit (Fig. 36; Gierwielaniec, 1956; Milewicz, 1970). In this region many various folds occur. The axial plane of various folds and crenulations only partially are parallel to L_1 lineation. The most of tight to isoclinal folds (F_{1B}) and asymmetric folds (F_{2A}) is characterised by W and NW trending axes. F_{2A} folds with axial plunge to W and with vergence to the north, and F_{2A} with axial plunge to NW is characterised by vergence to SW (Cymerman, 2002). In Radomice and Klecza the shear indicators show sinistral sense of shearing, and transpressional movements top-to-the-north-west. In Golejów–Radomice the F_{2C} open folds run to NNW–SSE and have vergence to the northwest.

Schist rocks as well as quartz veins reveal evidence of strong cataclasis and mylonitization. Veins built of grey and milky-white coarse-crystalline quartz have different thicknesses, usually several centimetres (3–25 cm), however irregular quartz lodes up to several dozens of centimetres in thickness have been also found.

From 1898 to 1908 many workings were done and a several quartz-sulphide veins outcropped near Radomice, Golejów and Klecza (Grimming, 1933). The auriferous sulphide ores were explored by 4 adits (Fig. 37). In Radomice the August and Cecilia adits are situated. These adits had connection (Figs. 33, 38). In the August adit the one main vein with thickness up to 1.5 m occurs. Arsenopyrite ore with As contents up to 25% As and about 8 ppm Au was mostly subject of exploration from this adit (Grimming, 1933; Table 12).

Westward from Radomice near Golejów appear 2 bigger and 2 smaller ore veins that were explored from the Dennoch Glückauf adit. The one of the bigger vein of thickness about 0.3 m contains abundant arsenopyrite and galena and the second vein of thickness 0.12 m contains only arsenopyrite (Domaszewska, 1964). An average grade of ores from these veins according to Fedak, Lindner (1966) was about 35% As and 2.4 ppm Au. Galena contains an average admixture of silver ca. 90 ppm. Two thinner veinlets (6–8 cm) contain mostly arsenopyrite. All these veins are cut by numerous cross faults.

In schists within zones of protoclastic deformations formed under ductile-brittle and brittle conditions common ore mineral concentration occurs. Fine fissures filled by vein quartz and sulphide mineralization developed in those zones. The ore-bearing rocks were later subject of a younger extensional en-echelon fracturing (Fig. 39). The richest ore mineralization is of a massive type (Pl. VI, 1, 5–6). Angular to subangular fragments, from 0.1 to 7 cm in size of sericite-quartz schists are cemented by sulphides, very fine-grain sericite and quartz (Pl. VI, 3–6). Sulphide mineralizations appear in matrix and as veinlets. Fine-grain matrix consists of sulphide, sericite, chlorite (ripidolite), quartz, and apatite. Sulphide veinlets that healed cataclastic fractures in schists have different thicknesses from 1 mm to several cm (Pl. VI, 3, 7). This massive type sulphide mineralization was subject to later cataclasis and mylonitization (Pl. VI, 4). Cataclased sulphides were cemented and rimmed with carbonates (mainly ankerite and dolomite) and younger chalcedonic quartz, and overgrown by fine-grained quartz, sericite, muscovite, kaolinite and illite. This post-breccias mineral assemblage either forms matrix or various generations of micro-veinlets.

At least three generations of carbonates are possible to recognise. The most abundant is ankerite with chalcopyrite and galena, apparently related to the post-breccias mineralizing event. However, calcite of the first generation is probably the earliest among carbonates. Calcite I occurs as narrow rims surrounding pyrite-ankerite aggregates and as very fine remnants within ankerite pseudomorphs. Late carbonate veinlets consist of calcite II that crosscuts ankerite and associated sulphides. Calcite III veinlets contain characteristic fusiform crystals of

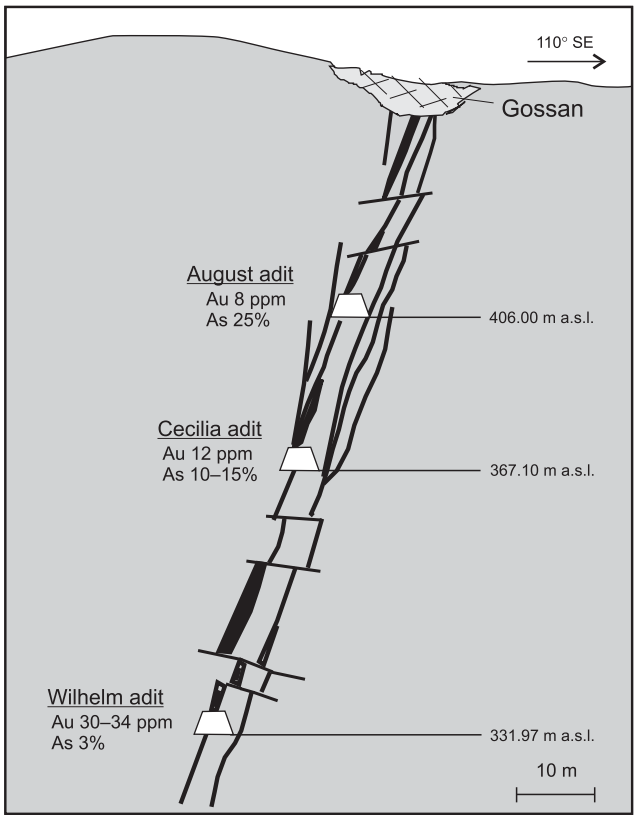

Fig. 37. Schematic cross-section through quartz-sulphide veins system in the Klecza–Radomice area

Host rocks are represented by Lower Paleozoic quartz-sericite-graphite schists with inserts of talc schist, siltstone, and minor metatuff, cherts, lydite and marble intercalation

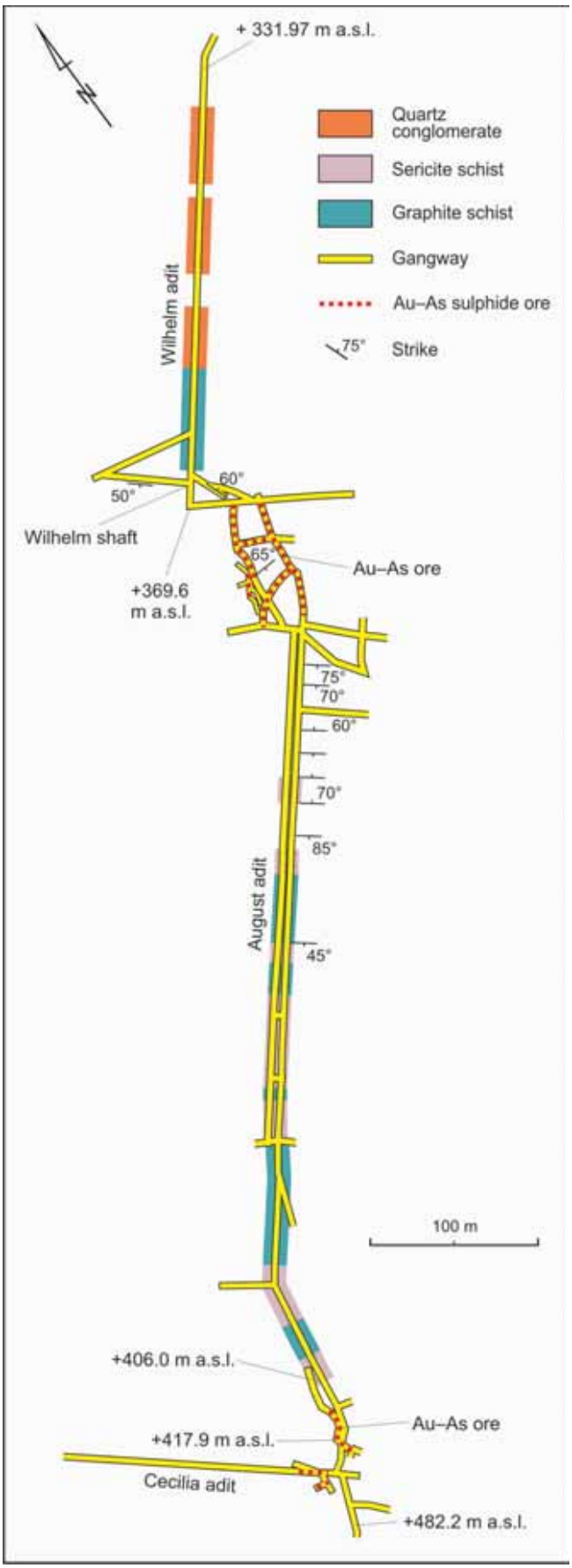

hematite. Siderite formation is probably connected with surface exposures of sulphide mineralization. Siderite form fine irregular atoll-like structures around older carbonates and red-brownish spots surrounding pyrite.

The massive-type rich in gold (27 ppm) sulphide mineralization occur in cataclased sericite-muscovite-quartz-graphite schist (Pl. VI, 4). Ore minerals occur mainly in quartzitic zones in en-echelon fissures and in micro-fractures of younger generation. The contents of sulphides in cataclasites and quartz lodes vary significantly from traces up to several dozens of volume per cent. The endogenic ore mineralization is dominated by arsenopyrite and in places by pyrite (Paulo, Salamon, 1973a).

In the quartz veins or lodes of different thickness two generations of sulphide prevail. Stage I – arsenopyrite and pyrite (Pl. VI, 1) that are cataclased and cemented by base metal sulphide (stage II). The second sulphide stage is mainly representing by chalcopyrite galena, and sphalerite associated with carbonates and chalcedony. The XRD method evidenced common presence of ankerite and siderite, with subordinate calcite and dolomite. Massive sulphide forms aggregates of variable size, up to several dozen centimetres in size. Beside that sulphide occur as veinlets and disseminations cementing fragments of sericite-quartz schists. The sulphide mineralization is associated with gangue dominated by fine crystallized sericite and quartz with carbonates.

In the massive ore mineralization two varieties of arsenopyrite occur: the first one is represented by euhedral medium-to-coarse crystals with poikilitic core up to 2–3 mm in size and the second one of euhedral fine-grained crystals from 5 up to 250 μm in size and with common cross twinning. Often medium-grained arsenopyrite sections (about 200 μm in diameter) reveal zonal internal structure. Arsenopyrite crystals are often rimed by chalcedony and/or ankerite. Both types of arsenopyrites co-exist and may form jointly aggregates up to several cm in size. Especially, bigger crystals of arsenopyrite of prismatic habit and its massive aggregates are fractured and strongly cataclased (Pl. VII, 1). Some of arsenopyrite big crystals are strongly mylonitized (so called "arsenic powder"; Pl. VI, 2). Arsenopyrite is intergrown by muscovite and quartz (Pl. VII, 2). Most of arsenopyrite samples from Radomice may contain only traces Co admixtures. Coarse- and fine-grained arsenopyrite samples have similar chemical compositions. Arsenopyrite may contain inserts and inclusions of gangue minerals and chalcopyrite, galena or electrum of sizes usually from 5 up to 500 μm in diameter (Pl. VII, 5).

Fractured arsenopyrite is cemented and overgrown by hydrothermal post-breccias mineral assemblages represented by base metal sulphides, electrum and carbonates (mainly ankerite), (Pl. VII, 3–4). The occurrences of base metal sulphides are subordinate in relation to concentrations of arsenopyrite; how-

Fig. 38. The old mining situation plans of the Wilhelm, August and Cecilia adits in the Klecza–Radomice area

ever their presence seems to be important for gold precipitation of the microscopic type. Galena, sphalerite, and pyrite occur in the base metal paragenesis beside chalcopyrite.

Chalcopyrite is most abundant among these minerals. Chalcopyrite occurs as replacement in arsenopyrite and pyrite grains, in fractures, and as disseminated anhedral blebs in interstices of the coarse-grained quartz and ankerite veins. Disseminated anhedral grains of chalcopyrite form patchy clusters aggregates that may reach up to several cm in size.

Galena occurs as single euhedral crystals from 50 μm up to several mm in size and coarse-grained aggregates as well as numerous inclusions and veinlets filling fractures in arsenopyrite or pyrite. Galena also appears as overgrowths on primary sulphides and often intergrowths with chalcopyrite or/and sphalerite. Galena locally precipitated as the last of the base metal sulphides in the deposit, and the partial replacement of the earlier sulphides by galena was typically observed. Chalcopyrite and galena appearance is commonly associated with presence of ankerite.

Sphalerite forms irregular dispersed grains up to 1 mm in size with abundant chalcopyrite linear exsolution (Pl. VII, 4). Numerous electrum-galena and/or electrum-chalcopyrite microveinlets (~20 μm) associated with amorphous silica and carbonates were observed under microscope in fractured arsenopyrite or less common in pyrite (Pl. VII, 6). Adjacent to those microveinlets numerous galena, chalcopyrite, electrum and gangue minerals inclusions (from 5 to 200 μm in size) may occur.

Pyrite occurs in various mineral generations. In massive-type mineralization pyrite is subordinate to arsenopyrite. Pyrite of this generation is intergrown with arsenopyrite and its anhedral crystals bordering host fragments that suggest pyrite early precipitation. The pyrite crystals contain rare inclusions of chalcopyrite and/or pyrrhotite, and are often fractured (Pl. VII, 3). They have different size but usually below 1 mm (20 μm–3 mm). Late pyrite is more abundant and occurs in association with base metal sulphides, carbonates as fractures filling in cataclased quartz. At least two types of this pyrite occur. The first one consists of euhedral crystals up to 3 mm in size and the second one of anhedral crystals with poikilitic texture (Pl. VII, 7). These two-generation pyrites are characterized by inhomogeneous chemical composition that is marked under the ore microscope by light (Co-, and As-rich) or dark (Ni-rich) sector within pyrites. These pyrites are associated with muscovite, carbonates (mainly ankerite), and minor quartz. Base metal sulphides are subordinate to pyrite and they replace pyrite or may form, together with magnetite, inclusions within pyrite or arsenopyrite (Mikulski *et al*., 2005c).

In ankerite veinlets the pyrite shows euhedral crystals mainly from 5 to 50 μm in size. This pyrite, beside chalcopyrite inclusions, may also contain cobaltite intergrowths. Microprobe analyses revealed the following chemical compositions of cobaltite: 36.43 wt % Co, 43.29 wt % As and 18.76 wt % S.

Detailed microprobe measurements revealed different admixtures of Ni, Co and As within pyrite of the both types. A Co/Ni ratio in anhedral pyrite is from 1:10 to 1:1 and in euhedral

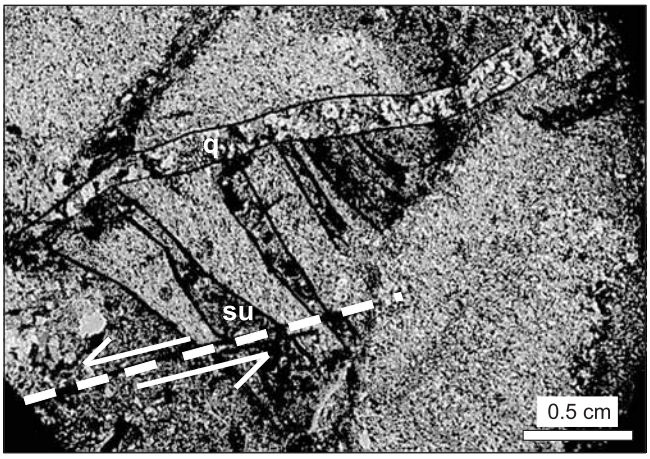

Fig. 39. The occurrence of gold-sulphide mineralization (black) in en echelon fractures within sericite-muscovite-chlorite-quartz schist from Radomice

Photo from the article by Olszyński, Mikulski (1997)

Abbreviations: su – sulphide, q – quartz veinlets

pyrites from 1:10 to 10:1 (Pl. VII, 7; Fig. 40). Among the euhedral pyrite it was also possible to recognised As-rich and As-poor types. Arsenic-rich pyrite may contain up to ca. 3 wt % As. Arsenic-rich euhedral pyrite may also contain arsenopyrite, galena or chalcopyrite inclusions. As-rich pyrite contains up to 450 ppm of gold admixture. Cobalt has correlation with Ni within both pyrite types. Arsenic distribution within pyrites has a variable correlation with Co or Ni admixtures. Pyrite bigger crystals reveal characteristic fracturing. Some of anhedral pyrite crystals show narrow rim of silica or marcasite (Pl. VII, 8).

Intergranular gold ("free gold") associated with chalcedony was also observed within strongly cataclased sericite-quartz-chlorite schists. These rocks underwent at first a pervasive silicification, sericitization and later argillization (illite-kaolinite). Primary sulphides from brecciated quartz-sericite schists have been completely leached by acid solution (pH <5) forming porous texture of the whole rock (Fig. 41). This rock contains numerous caverns and is of light beige to yellow-green colour. Some of caverns are filled with very

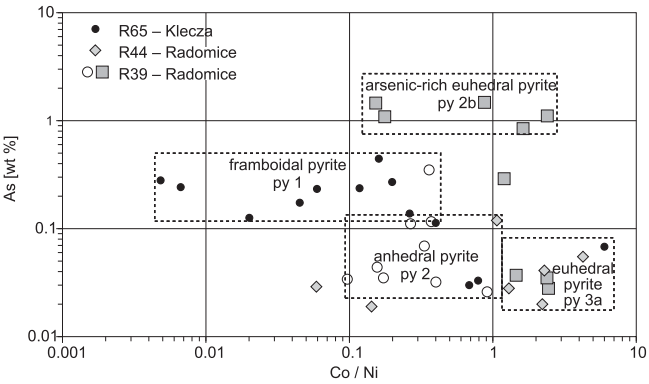

Fig. 40. Co/Ni ratio versus As content of pyrite various generations from Radomice and Klecza

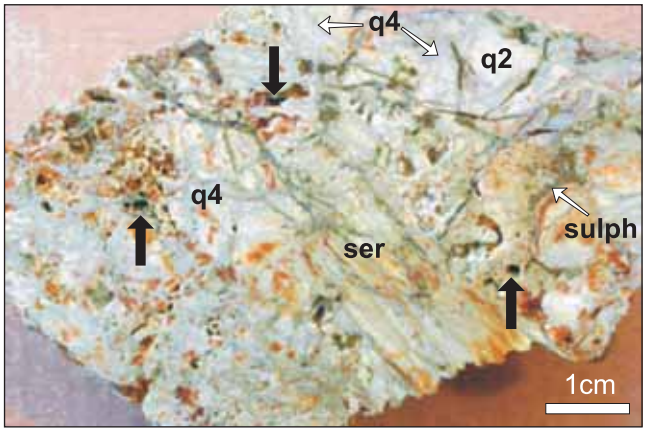

Fig. 41. The numerous empty holes within cataclased quartz-sericite schist formed after acidic dissolution of primary sulphide

Abbreviations: q2,q4 – quartz of 2nd and 4th genaration, ser – sericite, sulph. – sulphide

fine-grained silica, white illite, light green kaolinite and brownish scorodite. Scorodite of spongy-like texture may be a product of arsenopyrite replacement or low temperature crystallization within oxidative environment. Content of gold in this altered rock is up to 11.7 ppm Au. The intergranular native gold grains reach up to 100 μm in size. Gold was either remobilised from primary sulphides or/and introduced throughout the low temperature hydrothermal process. The increased Au contents occur generally in strongly cataclased rocks.

Pyrite of various generations is commonly replaced by Fe-hydroxides. Marcasite is often present in samples as the youngest sulphide mineral that replaces pyrite (marcasite II) and/or as veinlets up to 1 mm thick which cut ores and country rocks (marcasite I).

In mineralized offshoots of the main zone, pyrite selectively replaced gangue minerals. The fine- and medium-grained euhedral pyrite (5 μm to 1 mm) occurs mainly within folded foliation formed by quartz intercalating with sericite, mica and graphite. In the part of graphite-quartz-chlorite schists also very fine abundant pyrite was found. Pyrite occurs in various mineral associations. Early paragenesis of pyrite is suggested by remnants of framboidal clusters that are subject of recrystallization by pyrite of the next generation.

In quartz veins cut cataclastic sericite-quartz schists occur also younger generation veinlets with rare sulphide mineralization. Maximum gold contents found in such samples reached 0.6 ppm, however microscopically discernible gold was not observed. White and grey quartz is massive and brecciated, commonly deformed showing undulose extinction, polygonization or recrystallization and cataclasis. Sulphides filling fractures are represented mainly by pyrite, marcasite, minor chalcopyrite, and occur in paragenesis with ankerite. Fractured quartz-ankerite assemblage is cemented by transparent micro-veinlets of chalcedony with calcite rims and younger generation pyrite micro-veinlets. Locally hematite occurred (1–3 volume %) in close association with calcite. Hematite occurs as aggregates and single crystals of needle-like habit up to 1 mm in size.

Chalcedony commonly recrystallized into quartz. Frequently minerals such as hydrated iron oxides heal numerous micro-fractures yield red-brownish colour of the rock. Hydrated Fe-oxides consist mostly of goethite with minor lepidocrocite. They commonly replace pyrite, forming characteristic collomorphic textures.

Apatite occurs in two generations: older connected with metamorphic processes of primary sedimentary components and younger as a result of hydrothermal activity. Older apatite occurs in narrow laminas in quartz-sericite-graphite schists as numerous anhedral rounded grains from 10 to 50 μm in size. Sharp-edge fragments of such apatite-rich lamina cemented by amorphous silica were often observed. Younger, hydrothermal apatite occurs in association with carbonates (ankerite) as euhedral crystals about 100 μm in size (Pl. XIV, 7).

ORE MINERALIZATION IN THE KLECZA AREA

Accessible mineralization was found in the abandoned gold-mining tailings located along the narrow valley of stream that dewatered north-western slopes of Wietrznik Hill. In this area primary mineralization occurs in the contact zone of the Permian sediments with rocks of the Pilchowice unit (Fig. 34). Permian sediments together with Mesozoic rocks are overthrusted here by the Paleozoic rocks along NW–SE trending fault zone that constitute the southern border of the Wleń trough. In the Klecza area the schists of the Pilchowice unit in general have the NW–SE run and the dip from 65 to 70° to SW.

In Klecza 2 main ore fields are accessible by 2 separate adits. The Wilhelm adit was the one of the most important adit within the whole Klecza–Radomice ore district. Two ore veins of an average thickness 20–25 cm (max. 1.2 m) and one diagonal vein were found there (Tab. 12; Fig. 33, 38). These veins were recognised about 90 m along strike (Krusch, 1907; Grimming, 1933). Veins have various compositions and are tectonically disrupted. These veins revealed increased concentration of arsenic at low grade of gold at distance about 30 m above the Wilhelm adit. Deeper parts of veins revealed decreased As amount and increased concentration of auriferous

pyrite. In the upper part of vein the sulphide ores had grade ca. 10–20 ppm Au at 10–15% As, and in deeper part of the deposit from 30 to 34 ppm Au at 3% As (Domaszewska, 1965). The diagonal vein had usually less than 10 cm thicknesses, and was especially rich in gold, an average ca. 40 ppm Au, sometimes about 60 ppm Au and maximum up to 120 ppm Au (Domaszewska, 1964). The Cecilia adit is about 200 m far from the Wilhelm adit and 35 m above that, and about 20 m below the August adit (Fig. 37). In the Cecilia adit additional 2 main parallel running veins and 5 side veins, appear. During exploration works in 1925 about 100 m of the main vein of thickness at least 25 cm was outcropped (Grimming, 1933). Ore minerals were represented by arsenopyrite accompanied by minor pyrite and galena. Gold concentration in arsenopyrite ores was relatively lowers (ca. 12 ppm Au) to compare with sulphide ores from the Wilhelm adit, but instead it contains more arsenic 10–15 % (*op. cit.*).

In the Klecza area also remnants of the oxidized parts of primary sulphide ores also occur, beside the low temperature of primary oxide mineralization. The zone of rich though very fine crystalline hematite mineralization occurs in sericite-quartz schists. Hematite crystals of prismatic habit are from 20 up to 100 μm in size. Most crystals are disseminated and evenly distributed but some occur in bands within sericite laminae and fill fractures as well (Pl. X, 2). Titanium oxides are represented by fine needle-like leucoxene particles from 10 up to 50 μm in size, that suggests replacement of biotite. Rutile and/or titanite crystals up to 100 μm in size were encountered. Anhedral single grains of chalcopyrite up to 0.5 mm in size occur in calcite veinlets. In graphite-quartz-chlorite schists very fine abundant pyrite was found in places (Pl. IX, 1, 2). Pyrite occurs in various mineral associations. Early paragenesis of pyrite is suggested by framboidal clusters (from 1 up to 20 μm in size) associated with graphite (Pl. IX, 3, 4). According to microprobe investigation framboidal pyrite contains admixture of Ni (from 0.005 to 0.35 wt %) and As (from 0.03 to 0.44 wt %), (Pl. IX, 5, 6; Tab. 13). In framboidal pyrite Co/Ni ratio is much below 1:15 (usually from <1:10 to 1:500). Late pyrite occurs as anhedral crystals recrystallized from framboidal pyrite and as euhedral fractured crystals up to 200 μm in size in quartz veinlets that cut graphite schists (Pl. IX, 5). Graphite platy crystals reach up to 300 μm in length (Pls. IX, 4; X, 1). Anhedral pyrite that recrystallized after framboidal pyrite characterized by loss of Ni and As admixtures (Pl. IX, 6). Euhedral pyrite may contain chalcopyrite or galena inclusions. The euhedral pyrites from Klecza represent mostly As-poor pyrite generation (below 0.1 wt % As). Arsenic-poor euhedral pyrite is in paragenetic association with arsenopyrite and may contain small arsenopyrite inclusions (Pl. IX, 7, 8).

Chalcopyrite appears in quartz veinlets or in silicified part of lodes, and forms anhedral crystals up to 100 μm in size that are subject to covellite replacement. This pyrite-rich graphite schist contains up to 15 ppm Au. Gold mineralization of impregnation-veinlets type occurs in dark-gray to white quartz breccia veins with fragments of sericite-muscovite-quartz schists. Chalcedony cements brecciated quartz and ore frag-

Table 13

Trace element contents (in wt %) and correlation matrix in pyrite samples from Klecza and Radomice

Element	Framboidal pyrite (py1a)		Pyrite 2		As-rich pyrite (py 3b)	
	aver. cont.	range	aver. cont	range	aver. cont	range
Co	0.022	0.005–0.043	0.012	0.000–0.060	0.01	0.001–0.02
Ni	0.299	0.005–0.350	0.131	0.000–0.302	0.016	0.0–0.058
Co/Ni	~1:15	–	~1:10	–	~1:2	–
As	0.181	0.030–0.444	0.174	0.030–0.431	1.46	0.822–3.09
Au	–	b.d.l.	–	b.d.l.	–	b.d.l.– 0.045

Element	Correlation matrix								
	framboidal pyrite			pyrite 2			As-rich pyrite (py 3b)		
	Co	Ni	As	Co	Ni	As	Co	Ni	As
Co	1	0.33	0.56	1	0.14	–0.02	1	0.08	0.36
Ni	0.33	1	0.12	0.14	1	0.78	0.08	1	–0.17

b.d.l.– below detection limit

ments. Pyrite and arsenopyrite are most common sulphides, however often one of them dominate; other base metal sulphides are subordinate.

The veinlets of younger generation are filled by carbonates of different compositions and Fe-hydroxides. In pyrite-rich zones euhedral crystals of this mineral from 50 μm up to 5 mm in size form either disseminated crystals or massive aggregates. Gold mineralization was found both in sulphide rich and sulphide poor samples (Pl. VIII, 2, 3). Highest gold contents, exceeding 60 ppm, was found in cataclased gray quartz lode, rich in arsenopyrite. Gold is present as inclusions in pyrite and arsenopyrite as well as microveinlets associated with chalcopyrite and galena and as grains (Pl. XII). Free grains of gold in the cataclastic quartz cemented by chalcedony and younger ankerite are less common (Pl. XIII). Therefore it appears that gold was either remobilised or brought by low temperature hydrothermal fluids. The richest in gold samples are cataclastically deformed and contain abundant sulphides.

Arsenopyrite and pyrite forms two characteristic varieties (Fig. 42). The first one represents by big euhedral crystals (up to 3–5 mm in size) that exhibit cataclastic deformation textures accompanied by the second variety composed of very fine euhedral crystals (from 10 up to 200 μm in size; Pl. X, 3–5). These fine-grained sulphides form pyrite- or arsenopyrite-rich bands within cataclased quartz and coarse-grained ores. The sulphides are mostly rich of galena, chalcopyrite, electrum and gangue (chalcedony, sericite) inclusions, however locally they are devoid of any inclusions. At least three generations of pyrite occur within quartz veins: the first one is euhedral medium- to-coarse-grained commonly surrounded by cataclastic fine-grained particles, the second one forms poikilitic pyrite rims, and the third one - micro-veinlets which fill fractures. Pyrite is dominant among sulphides and reveals anhedral habits, and cataclastic and poikilitic textures. Anhedral pyrite crystals up to 50 μm in size border coarse-grained quartz or occur as angular fragments in chalcedony or carbonates matrix. The pyrite coarse-grains are fractured and some of them contain inclusions of galena. Fine prismatic crystals of arsenopyrite up to 100 μm in length occasionally twinned.

Cobaltite appears as overgrowths on replacement of arsenopyrite as well as fillings fractures in arsenopyrite (Pl. XII, 5). Cobaltite crystals may reach 60 μm in size. Arsenopyrite is subject to replacement by scorodite (Pl. XIII, 4).

In several samples of cataclased quartz veins and lodes in sericite-quartz schists, cemented by narrow veinlets of younger generation quartz (chalcedony) and carbonates, gold occurs in concentrations of several ppm despite a poor sulphides mineralization.

Chalcopyrite and less frequently galena occur as fillings of fractures (up to 20 μm thick) in the coarse-grained sulphides, as inclusions, and as overgrowths on these. The base metal sulphides less frequently associate with carbonates. Sphalerite is rare and may contain linear inclusions of chalcopyrite (Fig. 42E). Sphalerite is characterized by lack of internal reflexes. Galena may form locally clusters of crystals up to a several millimetres in size. Anhedral single crystals of galena have usually less than 100 μm in size. Galena that replaced pyrite may contain arsenopyrite inclusions, and also overgrowths on sphalerite.

Numerous pyrite microclasts about 20–50 μm in size and rare anhedral chalcopyrite and single electrum grains occur in chalcedony veinlets and matrix. Quartz-sulphide breccias are cemented by older generation carbonates and/or next generation chalcedony with fine-grained sulphides (marcasite-pyrite) cut by the youngest generation carbonates and finally by Fe-hydroxides (Pl. X, 7).

Alteration processes started with strong silicification and sulphidization followed by extensive sericitization yielded a beige-yellow colour of the quartz-muscovite schists hosting quartz veins and lodes. There is also evidence of a near-surface hydrothermal activity that post-dated deformation. The hydrothermal fluids migrated in a zone of intense brecciation and were characterized by a low temperature. As a result of hydrothermal low temperature precipitation formed amorphous silica, fine-fibrous quartz, and chalcedony. Chalcedony may be fractured again and cemented by the younger generation of carbonate and Fe-hydroxides.

Fig. 42. Microphotographs of ore minerals in the reflected light and table of the mineral sequence for the Klecza–Radomice ore district

A – medium-grained euhedral arsenopyrite and pyrite, fractured and cemented by galena micro-veinlets (sample no. G3); **B** – coarse-grained aggregate of arsenopyrite fractured and cemented by carbonates, chalcopyrite and electrum (sample no. G-6); **C** – euhedral arsenopyrite fractured and overgrown by chalcopyrite and sphalerite; **D** – large crystals of arsenopyrite are replaced by chalcopyrite, galena and pyrite in association with carbonates (sample no. R44); **E** – numerous inclusions of base metals sulphide hosted by arsenopyrite. Note elongated inclusion of chalcopyrite in sphalerite (sample no. D4); **F** – intergranular native gold in association with covellite and pyrrhotite. (sample no. R63); **G** – intergranular free gold (Au – 80.3 wt %; Ag – 19.4 wt %) within micro-fissures in association with clay minerals and chalcedony (sample no. D1); **H** – platy hematite with native gold grain in association with covellite (sample no. R80); **I** – mineral succession of the hydrothermal ore minerals in the main quartz-sulphide veins from the Klecza–Radomice ore district; note the range of quartz temperature crystallization according to fluid inclusion measurements

Abbreviations: asp – arsenopyrite, Au – gold, cov – covellite, chp – chalcopyrite, el – electrum, ga – galena, he – hematite, po – pyrrhotite, py – pyrite, sph – sphalerite

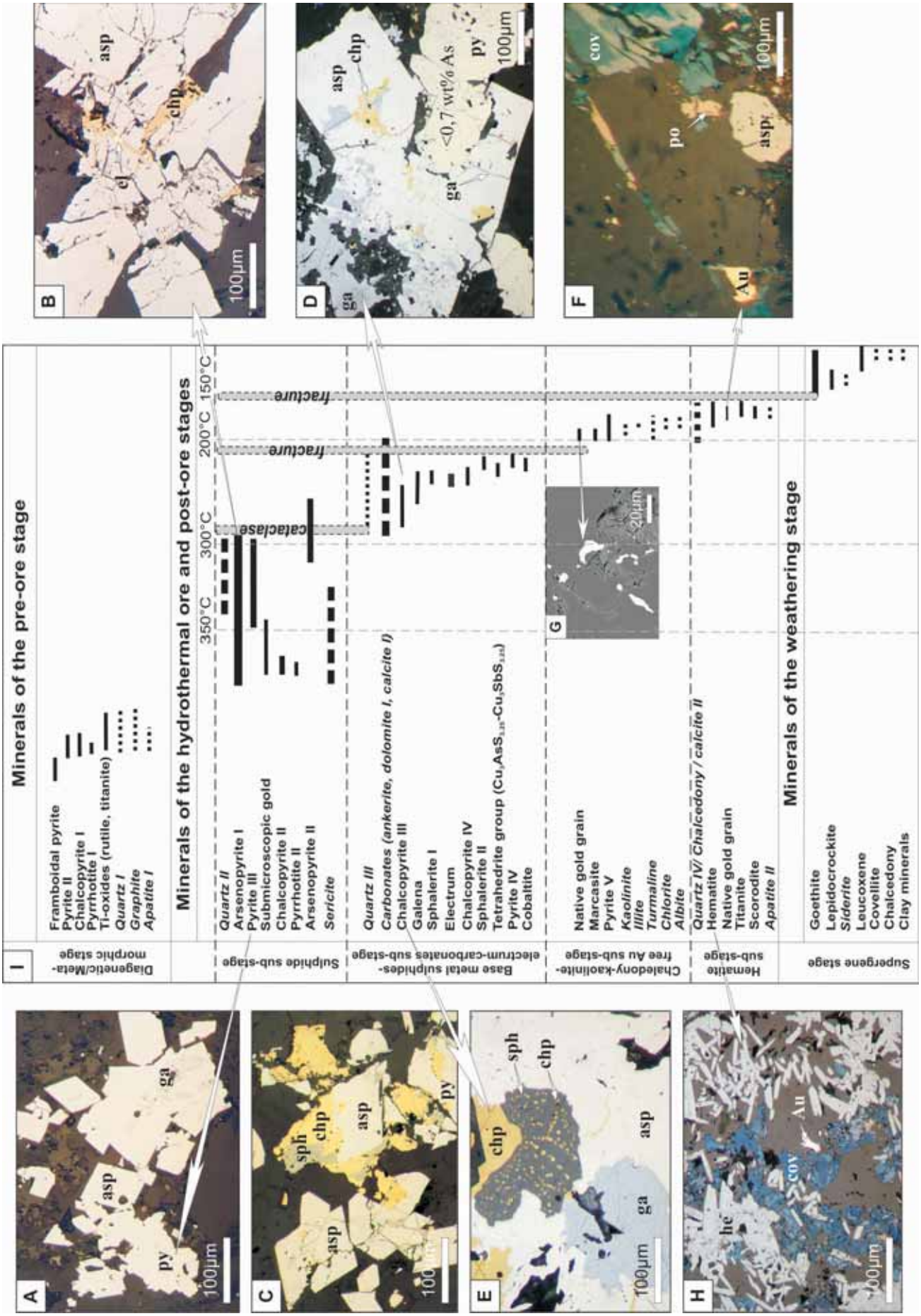
Minerals of the pre-ore stage
Framboidal pyrite
Pyrite II
Chalcopyrite I
Pyrrhotite I
Ti-oxides (rutile, titanite)
Quartz I
Graphite
Apatite I
Minerals of the hydrothermal ore and post-ore stages
350°C
300°C
200°C
150°C
cataclase
fracture
fracture
Quartz II
Arsenopyrite I
Pyrite III
Submicroscopic gold
Chalcopyrite II
Pyrrhotite II
Arsenopyrite II
Sericite
Quartz III
Carbonates (ankerite, dolomite I, calcite I)
Chalcopyrite III
Galena
Sphalerite I
Electrum
Chalcopyrite IV
Sphalerite II
Tetrahedrite group (Cu3AsS3,25-Cu3SbS3,25)
Pyrite IV
Cobaltite
Native gold grain
Marcasite
Pyrite V
Kaolinite
Illite
Turmaline
Chlorite
Albite
Quartz IV/ Chalcedony / calcite II
Hematite
Native gold grain
Titanite
Scorodite
Apatite II
Goethite
Lepidocrockite
Siderite
Leucoxene
Covellite
Chalcedony
Clay minerals
I
Diagenetic/Meta-morphic stage
Sulphide sub-stage
Base metal sulphides-electrum-carbonates sub-stage
Chalcedony-kaolinite-free Au sub-stage
Hematite sub-stage
Supergene stage
Minerals of the weathering stage
A
asp
ga
py
100µm
B
asp
chp
100µm
C
sph
chp
asp
py
asp
100
D
asp
chp
ga
<0,7 wt% As
py
100µm
E
chp
sph
chp
asp
100µm
ga
F
cov
po
Au
asp
100µm
G
20µm
H
he
cov
Au
100µm

ORE MINERALIZATION IN THE NIELESTNO AREA

Samples with ore mineralization were collected at abandoned gold mining sites and natural outcrops along small left-side tributaries of the Bóbr River near Nielestno. Geological setting here is similar to that of the Klecza area, where the rocks of the Kaczawa Metamorphic Complex are overthrusted on the Permian sediments (Milewicz, 1962; 1970; Milewicz, Frąckiewicz, 1983; 1988). This area is located only about 2.5 km to the southeast from Klecza region along the southern border of the Wleń trough. Rocks of Pilchowice unit are represented here by sericite-muscovite-chlorite-quartz schist, graphite-quartz schist and quartz-feldspar schist, epidote-albite greenstone, greenstone schist, and crystalline limestone (Szałamacha, 1974).

In this part of the district 2 adits and several ventilation shafts were excavated (Grimming, 1933). In the upper Max Arendt adit there appears the vein of thickness up to 2 m and about 120 m in length (Tab. 12). This vein has strike to NW–SE direction and dip from 48 to 74°SW (Figs. 43, 44). The ore grade from this vein was about 30 ppm Au and about 3% As.

Southwards to Nielestno, beside veins running across the lamination in schists also were recognised veinlets that occurred closely within schist's lamination. The workings distribution indicates for NW–SE and NE–SW directions of veins (Fig. 44). The host rocks are folded with axial planes of folds striking to NW–SE. Rocks such as Silurian schists are striking variable from ENE–WSW to NNW–SSE directions and steeply (60–80°) dipping to SE or SW (Szałamacha, 1974). F_{2A} folds with axial-planes almost parallel to L_1 lineation dominated and they characterised by vergence to S and SW (Pl. XI, 1). These folds reveal dispersion in the axial-planes orientation similar to L_1 lineation, as a result of the horst rotation caused by development of regional dislocation zones (Cymerman, 2002). Rare kinematics data from outcrops along the Bóbr River indicate for transtensional movement top-to-the-east. In this area occur numerous and various folds.

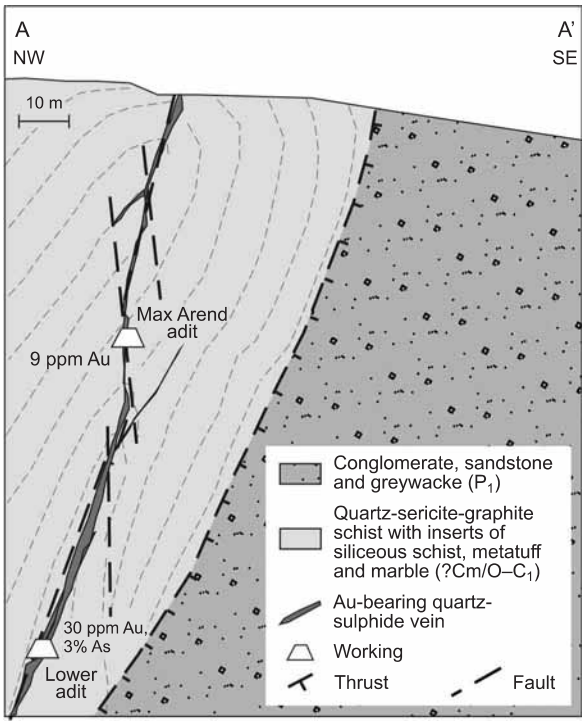

Fig. 43. Schematic cross-section through quartz-sulphide vein system at Nielestno

For the cross-section location see Fig. 34

Quartz-sulphide veins are located within the zone of the Kaczawa Metamorphic Complex overthrust on the Rotliegende sediments of the Wleń trough, along the fault zone of NW–SE direction. In the direct vicinity of veins occur transversal faults that are striking in NE–SW direction (Domaszewska, 1964). Sulphide mineralization is rare and appears mostly as fine-grained pyrite or coarse-grained arsenopyrite impregnation within thin quartz veins up to several centimetres thick that cut sericite-muscovite-graphite-quartz schists and in the surroundings (Pl. XI, 2, 3). Mineralization in veins of gray-white quartz is representing mostly by oxide and hydroxide mineralization (hematite, lepidocrocite and less frequently goethite) that filled micro-fissures in host rocks giving them characteristic brown or yellow colours (Pl. VIII, 4), Fe-hydroxides replaced also primary sulphides forming pseudomorphs with relicts of pyrite.

Hematite pseudomorphs after arsenopyrite may also have collomorphic textures (Pl. XI, 6). Single hematite euhedral crystals of tabular habit up to 150 μm in size and hematite aggregates built of very fine crystals up to 10 μm in size are common. Hematite aggregates in association with chalcedony that are filled fractures in cataclased quartz veins, contains relicts of pyrite, chalcopyrite and arsenopyrite (Pl. XI, 5). Fe-hydroxides such as goethite and lepidocrocite beside chalcedony are associated with carbonates. XRD method confirmed presence of dolomite that occurs in spotty or veinlet forms (Pl. XI, 7). Hematite as well as gangue minerals (mainly chalcedony) commonly replace fractured sulphides. Locally, in quartz veins massive intergrowths of white opal with brown hematite were observed (Pl. VIII, 4). These samples contain up to 4 ppm Au. Strongly oxidized samples of quartz veins with relicts of pyrite mineralization often contain microscopic gold. Fine-grains of inter-granular gold may reach up to 20 μm in size and occur in pseudomorphs of chalcedony and secondary ore minerals after sulphides (Pl. XI, 3). These mineral assemblages may have relicts of post-pyrite pyrrhotite, covellite and hematite (Fig. 42F). Pseudomorphs are fractured and cut by micro-veinlets of Fe-hydroxides. The euhedral pyrite crystals have from 0.5 up to 1.0 mm in size while euhedral crystals of arsenopyrite from 50 μm up to several millimetres. The coarse arsenopyrite crystals form also aggregates up to a

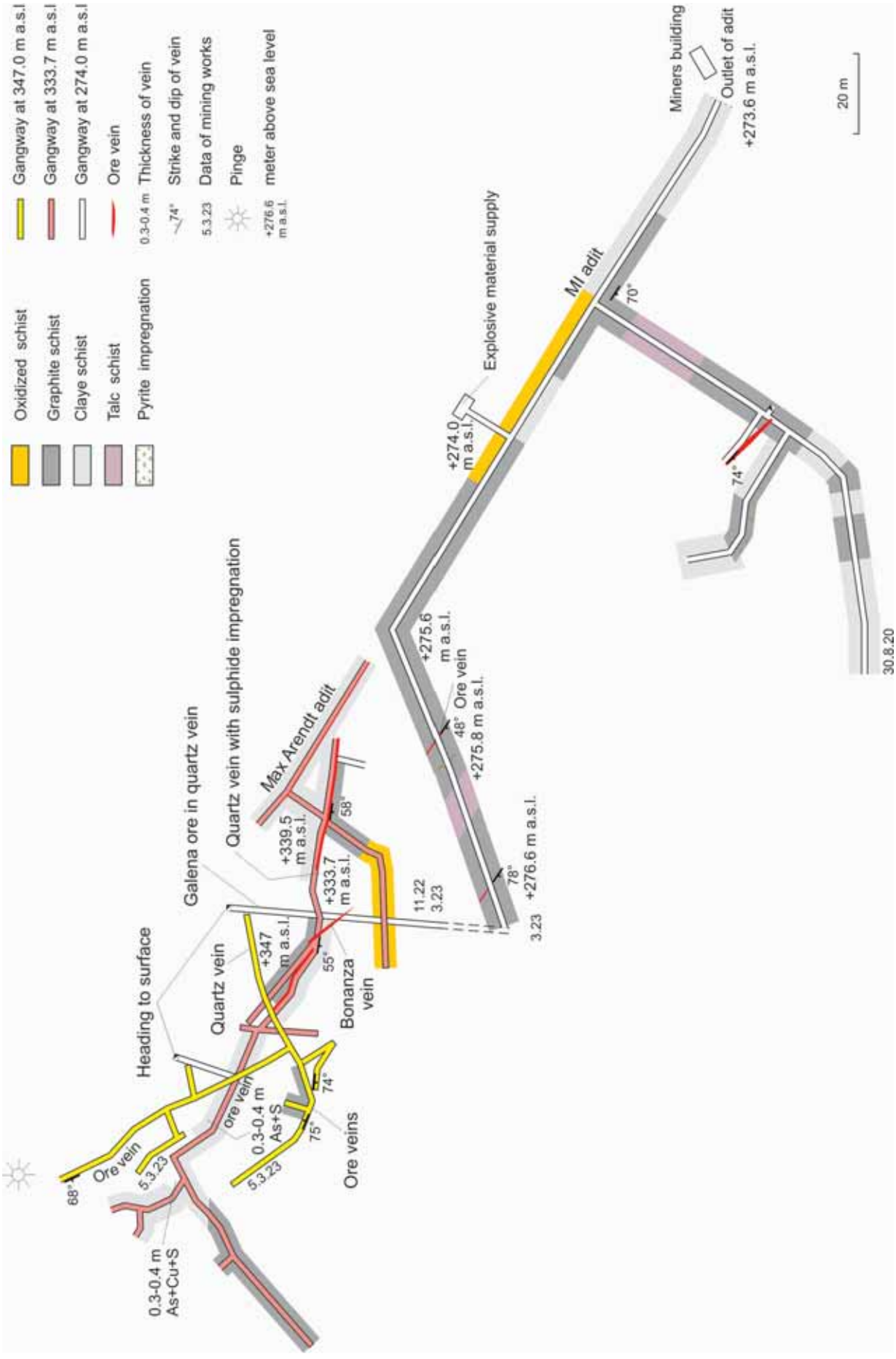

Fig. 44. The old mining situation plans of the Max Arendt adit in Nielestno

several centimetres in size. Arsenopyrite is subject to strong replacements by scorodite ($Fe^{+3}[AsO_4]$ $2H_2O$) and chalcedony (Pl. XIII, 4). Hydrated arsenates occur in oxidation zones and within zones of low-temperature hydrothermal processes with high Eh that favoured formation of the for As^{5+}-bearing ions (Savage *et al*., 2000). Covellite forms narrow rim and radial structures built of very fine-grained crystals of prismatic habits up to 20 μm in size, or aggregates up to 0.5 mm with column-like crystals.

In cataclased veins of gray-white quartz fine grains of rutile from 5 up to 20 μm in size appear. The presence of rutile grains cemented by chalcedony is also characteristic for fractured and cataclased muscovite-graphite-quartz schists from this area. Titanium oxides more commonly occur in sericite-quartz schists of yellow-green colour. They are represented by rutile, titanite and leucoxene. Ti-oxides infill fractures and occur as single crystals or mica replacements. Rutile has euhedral acicular crystals or anhedral crystals ranging from 5 up to 100 μm in size. Pyrite is most common mineral among sulphides, though rather rare in schists. Only few samples of dark gray-black muscovite-graphite-quartz schists contain abundant pyrite impregnation or veinlets. Rich pyrite impregnation occurs in quartz laminae and less frequently within graphite laminae and in micro-fractures (Pl. XI, 2). The schists with pyrite mineralization have characteristic yellow colour after sericite that appears during weathering processes. Pyrite forms mainly euhedral crystals from 10 to 250 μm in size. Some of pyrite shows texture of poikilitic core with numerous quartz inclusions and inclusion-free rims that may be subject to replacement by chalcedony. Pyrite locally occurs as coarse aggregates of variable grain to some millimetres in size. The pyrite coarse-grained crystals are fractured and cemented by chalcedony (Pl. XI, 8). Anhedral crystals of chalcopyrite (up to 200 μm in size) and sphalerite (Zn – 39.04 wt %, Fe – 17.6 wt %, S – 42.9 wt %) appear rarely. In partly oxidized samples, pyrite is readily altered to Fe-hydroxides with colloform structure. Ti-oxides appear mostly as fine grains associated with pseudomorphs of gangue minerals after micas. In quartz-graphite schists cut by quartz-dolomite veinlets scarce euhedral pyrite impregnation occur with younger Fe-hydroxides.

In red Permian conglomerates, with patchy white sandstones no sulphide mineralization was found. Only single grains of Ti- and Fe-oxides appear in these rocks. Euhedral single hematite fine grains up to 100 μm in size with poikilitic core and rounded rutile or titanite fine grains from 10 up to 50 μm in size may occur. Additionally, detritus of rutile fine grains from 10 up to 30 μm in size in association with chalcedony appears. The samples of the Permian rocks contain only gold traces from 5 to 23 ppb Au.

SULPHUR ISOTOPE DISTRIBUTION PATTERN

The sulphur isotope compositions ($\delta^{34}S_{CDT}$) have been determined in 33 separated sulphide samples from Radomice and Klecza areas (arithmetic average = 1.72, n = 33, std. = 1.42). Contents of sulphur $\delta^{34}S_{CDT}$ in medium- and fine-grained arsenopyrite from Radomice range from –2.24 to +4.88‰ (Fig. 45).

A wider range of sulphur isotope values from –1.49 to +7.8‰ $\delta^{34}S_{CDT}$ revealed arsenopyrite from Klecza. It also indicated admixtures of crustal sulphur in magmatic sulphur, especially, within brecciated sericite-graphite-quartz schists in sulphide cement.

Medium-grained pyrite from ores of the impregnation type have sulphur isotope compositions from 0.0 to +0.6‰ $\delta^{34}S_{CDT}$. Additionally, the sulphur isotopic compositions of coarse-grained galena up to 3 mm in size derived from massive arsenopyrite vein have value 0.56‰ $\delta^{34}S_{CDT}$.

The arithmetic average value of sulphur isotope compositions of the all arsenopyrite samples is 1.86‰ $\delta^{34}S_{CDT}$, for n = 28 (std. is 1.47‰).

Samples of massive arsenopyrite aggregates hosted by quartz vein cutting chlorite-sericite schists from the Klecza area revealed heavier sulphur isotope composition (up to 7.84‰). That suggest the main magmatic source of sulphur with some contribution from the host rocks into mineralizing fluids during precipitation of the sulphides.

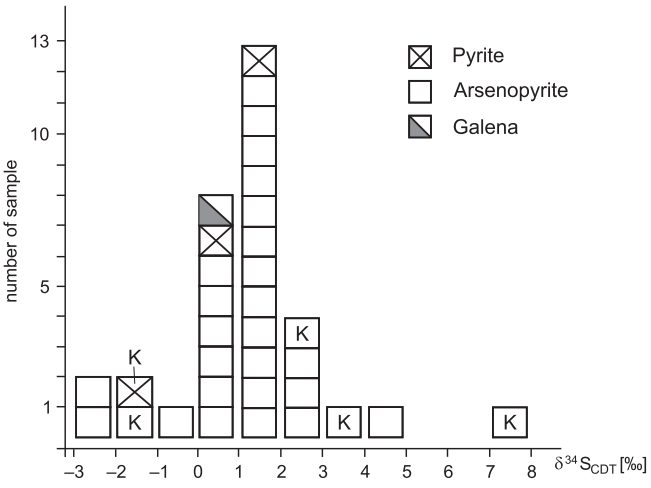

Fig. 45. Sulphur isotope composition of sulphide minerals of the gold-bearing ores from the Klecza–Radomice ore district

Abbreviation: K – Klecza; other – Radomice

ARSENOPYRITE GEOTHERMOMETER DATA

On the base of microprobe investigation of arsenopyrite, two groups of its different contents of As and Fe was possible to distinguish: the first group includes arsenopyrite samples from Radomice and Nielestno and the second group from Klecza (Fig. 46). Inside arsenopyrite grains from both groups, no inclusions of loellingite or pyrrhotite were found. However, these arsenopyrite crystals contain inserts of younger minerals such as galena, chalcopyrite and/or electrum.

Arsenopyrite samples from the whole area revealed a constant cobalt admixture from 0.12 to 0.92 atom. % with arithmetic average about 0.44 atom. % Co for n = 70 measurements. The probably source of Co could be framboidal pyrites, which according to microprobe investigation contained ca. 220 ppm (average) of Co admixtures (Tab. 13). During framboidal pyrite recrystallization Co decreases in pyrite (py2a – average 100 ppm).

Arsenopyrite from Nielestno has in general lower contents of arsenic ranging from 30.1 to 31.4 atom. % with an arithmetic average of 30.8 atom. % As (std. = ±0.5; for n = 15 measurements; Table 14).

Arsenopyrite from Radomice reveals higher content of arsenic. They have arsenic content ranging from 30.1 to 33.5 atom. % with an arithmetic average of 31.5 atom. %, (std. = ±1.0) for n = 41 measurements, however most of them have content of arsenic from 30–32 atom. %. They have content of sulphur reaching up to 1 atom. % and iron up to 3 atom. % in excess to stochiometric composition.

Arsenopyrite from Klecza characterised in general by higher arsenic and lower iron content in comparison with stochiometric composition. Their composition is ranging between 31.5 and 33.4 atom. % As. Arithmetic average of arsenic contents in arsenopyrite from this group is 32.6 atom. % As (std. = ±0.6).

To establish a temperature range for arsenopyrites from 3 areas, it should be assumed that the beginning of this crystallization took place at the arsenopyrite-pyrite buffer $f(S_2)$ due to absence of pyrrhotite appearance and lack of loellingite intergrowths. According to the isopleths of arsenopyrite composition in the log$f(S_2)$ – T from Kretschmar, Scott (1976), modified by Sharp *et al.* (1985), the temperature ranges in general between 491–390°C for Klecza, 440–315°C for Radomice and 390–315°C for Nielestno. In the same way, sulphur fugacity – log$f(S_2)$ for the range of arsenopyrite compositions (Fig. 47) varies from –4.5 to –6.5 (Klecza), from –6.5 to –10.5 (Radomice) and from –7.0 to –10.5 (Nielestno), respectively.

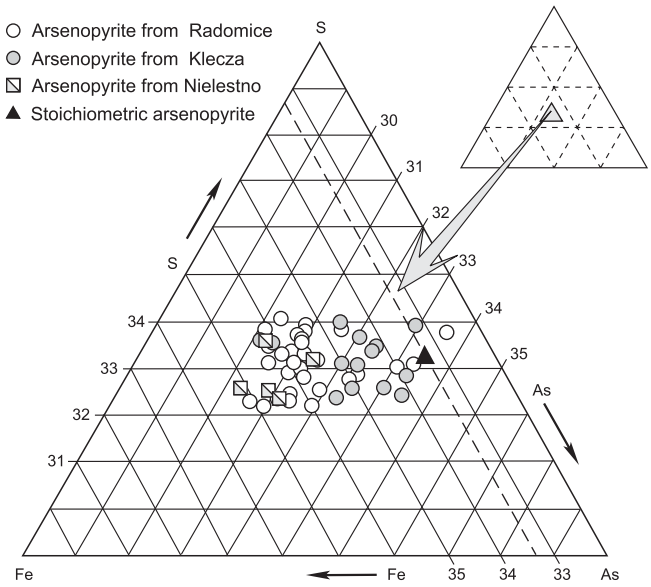

Fig. 46. Plot of the atomic percent composition of arsenopyrite samples from Radomice, Klecza and Nielestno

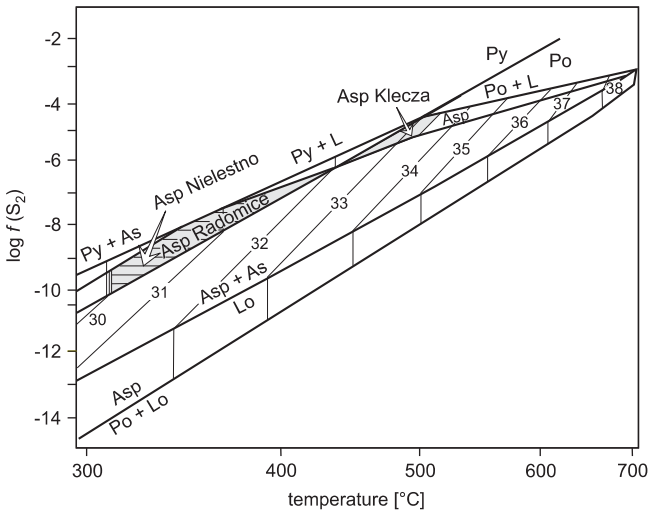

Fig. 47. Projection on log $f(S_2)$ versus temperature diagram of the arsenopyrite microprobe analyses (from Kretschmar, Scott, 1976; modified by Sharp *et al.*, 1985)

Shaded area shows range of arsenopyrite compositions for specific areas within the Klecza–Radomice ore district

Abbreviations: As – arsenic, Asp – arsenopyrite, L – liquid sulphur, Lo – loellingite, Po – pyrrhotite, Py – pyrite

Table 14

Statistic parameters of the As contents in arsenopyrite samples from the Klecza–Radomice ore district and their crystallization temperatures (acc. to arsenopyrite geothermometer by Kretschmar, Scott, 1976)

Location	Arsenopyrite type	As [atom. %]			Number of samples	Interval of arsenopyrite crystallization [°C]
		range	arithmetic mean	standard deviation		
Klecza Co<0.92 atom. %	Arsenopyrite I	31.49–33.38	32.59	0.59	14	491–390
Radomice Co<0.88 atom. %		30.06–33.48	31.53	0.98	41	440–315
Nielestno Co<0.60 atom. %		30.11–31.40	30.80	0.49	5	390–315

GOLD MINERALIZATION

Gold in the Klecza–Radomice deposits was commonly considered as submicroscopic admixture within auriferous pyrite and at a lower scale in arsenopyrite (Krusch, 1907; Grimming, 1933; Domaszewska, 1965; Fedak, Lindner, 1966). Separated pyrite contains up to 68.5 ppm of Au and arsenopyrite grains from Radomice have only ca. 15 ppm of gold (determined by use of GF-AAS methods). It indicating that pyrite hosts most of the submicroscopic gold. Gold has a high positive correlation with Cu what indicates that it is also bound by chalcopyrite. However, its strong correlation with base metal sulphides revealed most probably much more in the form of microscope than submicroscope gold. Microscopic gold was first described by Paulo, Salamon (1973a) in forms of electrum inclusions (older generation gold – I) in arsenopyrite or rarely in pyrite and of gold microveinlets (younger generation gold – II) associated with galena and hematite. Fineness of the older generation gold was about 700 and the younger gold 820–860 (Paulo, Salamon, 1973a). Later studies confirmed previous findings and additionally recognized numerous native gold-electrum aggregates up to 0.1 mm in size within cataclastic fissures in sericite-muscovite-chlorite-quartz schists from Radomice (Olszyński, Mikulski, 1997). Microprobe investigations documented very low (630) and very high fineness (920–940) of these gold aggregates.

The present studies added new data about microscopic gold mineralization in Klecza–Radomice ore district (Fig. 48; Pls. XII, XIII). Gold has been found in the following types of ore mineralization:

- breccias of sericite-muscovite-graphite-quartz schist or phyllite cemented by massive sulphides,
- sulphide impregnation of massive and/or veinlet type in quartz veins or lodes cutting mica-graphite-quartz schist or phyllite,
- strongly silicified by chalcedony sericite-quartz schist with remnants of sulphide mineralization,
- weathered sulphide ores.

The earlier known electrum associations with galena or rarely with chalcopyrite, sphalerite or cobaltite that occur as inclusions or inserts in fractured coarse-grained pyrite and arsenopyrite revealed at present microprobe studies significant amounts of silver from 15 up to 30 wt % Ag and different traces of Te, Bi, Se and Cu. These monomineral gold inclusions, microveinlets, or grains have different size (from 5 up to 120 μm in size). Fineness of monomineral gold microveinlets is from 840 to 880 and those with galena from 760 to 790 indicating for slightly higher silver admixture. This gold generation revealed admixtures of tellurium from 0.4 to 0.9 wt % and copper from 0.25 to 0.83 wt %. Similar fineness have irregular gold grains that filled fractured arsenopyrites and those that overgrowths arsenopyrites e.g. from 790 to 840 and admixtures of tellurium 0.58–0.98 wt % and copper up to 0.58 wt %. Electrum inclusions in arsenopyrite or in pyrite have lower fineness about 700 (710–730) and traces of Te and Se admixtures. Single gold grains occurring in rocks in association with base metal sulphides and ankerite have low similar fineness about 700 and small admixtures of tellurium below 0.5 wt %, bismuth below 0.4 wt % and selenium up to 0.3 wt %.

Additional inclusions of gold have been recognized within coarse-grained sphalerite. Sphalerite contains numerous linear inclusions of chalcopyrite and several elongated gold inclusions that may reach from 5 up to 25 μm in size (Pl. XII, 6). Locally not only galena-electrum micro-veinlets (Pl. XII, 7) were observed but also native bismuth-electrum-galena veinlets up to 10 μm thick. Bismuth minerals are very rare and tellurium minerals have been not found in Klecza–Radomice ore district. Only the traces of bismuth as native bismuth in association with electrum and galena in micro-veinlets cut arsenopyrites were noted. Geochemical results indicate very low concentrations of Te and Bi in those ores and may suggest a long lateral migration of hydrothermal fluids from a magmatic (granitic) source (Mikulski, 2005b).

Gold of microscopic size grains may also occur between base metal sulphides (chalcopyrite-galena-sphalerite) that fills fractures within coarse-grained arsenopyrite or pyrite. Electrum besides fractures filling in sulphides may overgrow sulphide grains (Pl. XII, 1, 4). Moreover, numerous single grains of different sizes (0.005–0.3 mm) have been found in sulphide surroundings.

Different types of microscopic gold associated with low temperature quartz (chalcedony) ± hematite ± calcite ± marcasite/pyrite ± kaolinite have been recognised in strongly altered sericite-muscovite schists of characteristic white-yellow-green colour and common selective corrosion interstices (Pl. XIII, 3–6). These gold-bearing samples of very characteristic colour and lightweight contain about a dozen ppm of Au and rare sulphides mineralization. Different in size fragments of sericite-muscovite schists are cemented by chalcedony. In chalcedony that fills vugs, cracks and fractures, there occurs fine-grained gold from 5 up to 40 μm in size (Pl. XIII, 7, 8). Chalcedony forms also very narrow rims up to 10 μm thick around caverns (Pl. XIII, 7). These caverns are a result of chemical corrosion that (pH <5) removed primary sulphide mineralization without any trace left.

Another type of microscopic gold associated with lepidocrocite-covellite aggregates have been observed in weathered sulphide samples. Rare single gold grains mostly about 30–40 μm in size (range 5–100 μm) occur in association with covellite and Fe-hydroxides replaced primary sulphides. Fe-hydroxides and covellite usually form narrow rims surrounding pyrite-pyrrhotite-chalcedony core (Fig. 42F, Pl. XI, 5).

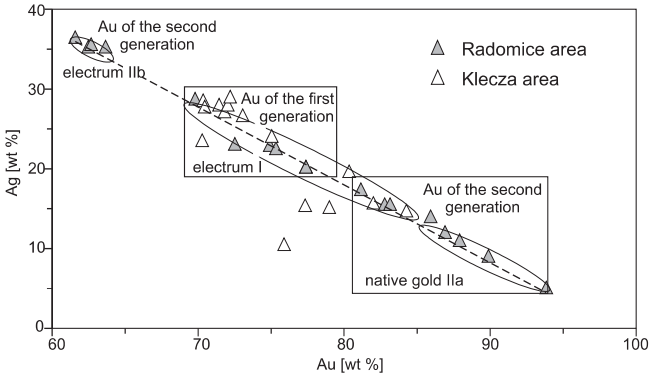

Fig. 48. Silver and gold contents in gold minerals (native gold and electrum) from the Klecza–Radomice ore district

Summarizing at least four main generations of gold is possible to distinguish: 1st generation is connected with submicroscopic gold hosts by sulphides, 2nd generation forms micro-veinlets, inclusions, inserts in fractured sulphides and intergranular gold (so called "free gold") associated with base metals sulphides, 3rd generation associated with chalcedony that may contain very fine gold grains, and 4th generation is common of oxidizing processes represented by minerals such as Fe-hydroxides and covellite.

SUMMARY OF ORE MINERALIZATION MINERAL SUCCESSION AT KLECZA–RADOMICE ORE DISTRICT

Characteristic features of the ore minerals succession at Klecza–Radomice ore district is multistage evolution followed by changes in ore mineral composition. At the Radomice deposit all recognised stages of ore minerals that are presented on Figure 42I occur. Ore minerals formed during diagenetic or/and greenschist facies metamorphic stages and weathered minerals are also present in the considered areas. Minerals of the hydrothermal stage were divided into 4 sub-stages (episodes), however at Radomice appear 4 sub-stages and in Klecza or in Nielestno only 3 sub-stages of the hydrothermal stage were recognised.

The main episode of the sulphide mineralization was recognised within the whole Klecza–Radomice ore district and is dominated by auriferous pyrite and arsenopyrite. In this study the richest grade of massive sulphide mineralization of hydrothermal breccia type occurred in quartz vein samples from Radomice. This pyrite-arsenopyrite stage represents mesothermal type of ore mineralization that crystallized within temperature range from ca. 450 do 300°C (arsenopyrite geothermometry). The formation of submicroscopic gold in sulphide was coeval with gray quartz crystallization. Submicroscopic gold is mostly bound not like at the Radzimowice within arsenopyrite but rather in pyrite with As admixture (Mikulski *et al.*, 2005c). Sporadically within these sulphides inclusions of chalcopyrite or pyrrhotite appear. Sulphide mineralization of this sub-stage is commonly associated by sericite. Sulphides are fractured and cataclased and similarly like at the Radzimowice deposit were cemented by carbonate minerals associated with base metal sulphides and electrum. To this stage was also included arsenopyrite II, which does not contain Co admixture and minerals from the tetrahedrite group and cobaltite (Radomice, Klecza). Among gangue minerals commonly appears carbonate of various compositions in veins or/and in host rocks as well as abundant tourmaline and apatite II. Base metal sulphides in comparison with the Radzimowice deposit are much less frequent and among them chalcopyrite dominate. Galena and sphalerite are rare. Electrum occurs in paragenetic association with galena and sphalerite.

The third sub-stage of hydrothermal crystallization at Klecza–Radomice ore district is represented by chalcedony and carbonates of younger generations (mainly calcite II). It is possible to distinguish in this sub-stage two different paragenetic associations: the first one was recognised at Radomice and consists of chalcedony, kaolinite and free gold that formed during reducing condition (pH <5) and the second one described from Klecza and Nielestno that consists of

chalcedony, hematite and free gold and formed during oxidizing condition. Elongated micrograins of native gold at Radomice occurs as infillings of fissures and free spaces within strongly altered rocks. Beside chalcedony and kaolinite marcasite and/or pyrite associated with chlorite and low temperature albite appear. These mineral assemblages (IVa and IVb) represent a low temperature stages (<200°C). Some problems may cause the recognition of time formation of these stages, however they could form coeval. The hematite stage is closely connected with chalcedony veinlets that are associated by calcite II.

Origin of native gold in samples from Nielestno may be also connected with the weathering processes and replacements of arsenopyrite by secondary Fe-oxides and Fe-hydroxides and chalcopyrite by covellite. Refractory gold bound by pyrite or arsenopyrite could be remobilised and then crystallized together with hematite and calcite II in oxidative environment.

ORE GEOCHEMISTRY

Geochemical data set of Klecza–Radomice ore district contains 73 samples, from which 32 samples were collected from Radomice, 23 from Nielestno and 18 from Klecza. The representative geochemical composition of several ores and mineralized rock samples from Klecza–Radomice ore district are shown in Table 15. For the further statistical elaboration samples were divided into four sample populations separately for each of areas and for the district (Tab. 16).

CORRELATIONS

In Klecza–Radomice ore district it is possible to distinguish four types of mineralized rock samples: massive or/and banded sulphide breccias in association with quartz and carbonates in cataclased quartz-sericite schists, cataclased quartz-sulphide-carbonate veins hosted by epimetamorphic rocks of flysch-like protolith, pyrite-impregnated quartz-graphite schists, and strongly weathered primary sulphide ores. Range of gold contents in the considering areas varies from traces up to 61.4 ppm. The arithmetic average of Au concentration in all samples is 3.6 (n = 73) and in samples with Au contents above 0.5 ppm is 9.6 ppm (n = 31). However, for each area arithmetic and geometric average values vary significantly.

Sulphide ores (mainly arsenopyrite or pyrite) contain high concentration of As, Fe, S, SiO_2, carbonates and low contents of base metal sulphides. The ores have variable, but generally high gold compositions with gold to silver ratios above 1. The richest As–Fe sulphide ores (20–40% As; about 10–30 ppm Au) have base metals concentration up to 2.2%, however only lead concentration may reach maximum to 1–2 wt % and the maximum Cu and Zn concentrations are only up to 1.3% and 0.5%, respectively.

Comparison of the average values for the selected metals in each area of the Klecza–Radomice ore district indicates differences in elements distribution (Fig. 49). The highest average values of Au, Ag, As, Pb, Fe (total), S and Co have been calculated for samples from Radomice. Similar values for Au and base metals have samples from Klecza. Elements concentra-

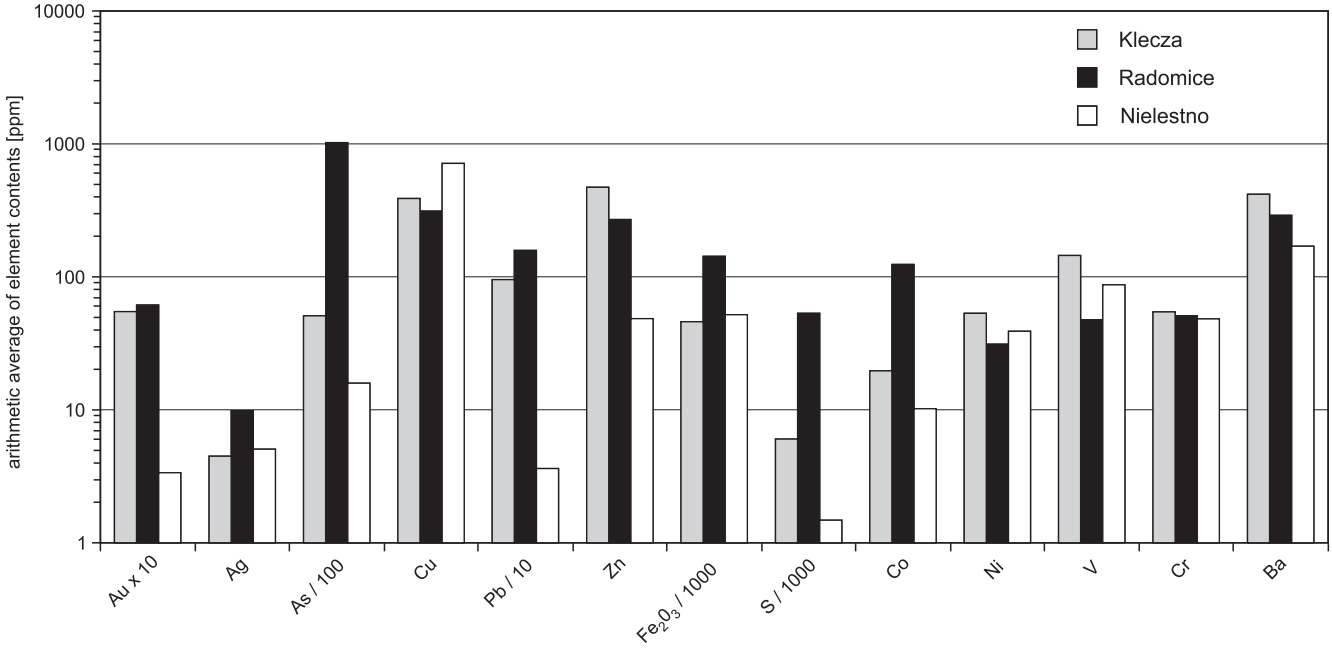

Fig. 49. Comparison of the arithmetic average of some elements and Fe_2O_3 in Klecza, Radomice and Nielestno

Table 15

Representative geochemical composition of several ore and mineralized rock samples from the Klecza–Radomice ore district

Sample	S-44	S-45	S-50	R46	R79	G2	G3-4	D1	D2	D10	MS-8	R69	R80	R67
Location	R	R	R	R	R	G	G	K	K	K	N	N	N	N
Lithology	mb	mb	mb	qs	qsv	qsv	qs	cqs+v	cqs+v	f	qgs	qw	qsb	d
Major elements [wt %]														
SiO_2	48.94	50.9	78.89	56.69	30.88	83.1	68.3	75.92	86.52	66.41	95.76	83.1	65.14	8.66
Al_2O_3	5.16	10.86	7.86	21.76	7.96	2.18	1.20	5.38	4.63	16.99	0.96	7.97	1.266	1.67
Fe_2O_3	19.71	16.17	5.01	5.93	16.79	4.79	12.75	3.42	1.76	5.36	3.45	0.57	13.2	2.52
MgO	0.68	0.83	0.75	1.63	0.34	2.03	0.90	1.73	0.43	1.00	0.005	0.13	0.147	5.25
CaO	0.61	0.36	0.61	0.14	0.03	1.07	1.21	3.2	0.37	0.08	0.12	0.15	0.022	39.91
Na_2O	0.71	–	0.95	1.14	0.39	0.05	0.026	0.2	0.21	0.46	0.02	0.05	0.02	0.17
K_2O	1.29	2.19	2.16	4.51	3.08	0.50	0.32	1.24	1.14	4.53	0.47	0.23	0.351	0.32
TiO_2	0.22	0.35	0.39	0.87	0.41	0.10	0.05	0.216	0.218	0.638	0.04	0.13	0.034	0.1
P_2O_5	0.04	–	0.06	0.105	0.07	0.013	0.016	0.038	0.033	0.1	–	0.038	0.143	0.055
MnO	0.04	–	0.016	0.102	0.003	0.12	0.073	0.294	0.053	0.042	–	0.018	0.004	0.347
S	4.58	4.14	0.98	0.005	–	0.30	3.89	0.41	<0.01	<0.01	0.87	0.005	–	0.005
Cl	–	–	–	0.009	–	–	–	0.033	0.027	0.03	–	0.014	–	0.0005
TOC	–	–	–	<0.10	0.12	–	–	<0.10	<0.10	<0.10	–	<0.10	0.86	<0.10
LOI	–	–	–	4.29	–	–	–	6.39	2.15	4.04	–	3.41	–	38.95
Cu	0.0027	0.0021	0.0014	0.0017	0.0009	0.0028	0.0613	0.0577	0.2775	0.011	0.0739	0.0009	1.3153	0.0049
Pb	0.0293	0.0015	0.0028	0.0042	0.0311	0.0071	0.445	0.1338	0.2192	0.0024	0.0091	0.0008	0.0391	0.0009
Zn	0.0279	0.0432	0.0034	0.0105	0.0013	0.0091	0.168	0.0162	0.5092	0.0069	0.0023	0.002	0.0069	0.0053
As	12.8	13.87	2.16	0.001	20.6711	0.741	7.38	0.0105	0.0891	0.0013	0.2	0.0011	2.844	0.0012
Total	94.88	99.73	99.89	97.24	80.77	95.01	96.79	99.14	99.18	100.32	101.96	95.88	85.39	98.01
Trace elements [ppm]														
Au	16.0	6.2	0.528	0.001	11.6	3.94	61.4	0.0101	9.4	2.96	0.76	0.023	2.81	0.003
Ag	6.64	6.0	0.23	4	19	0.54	20.6	4	<3	<3	2.5	3	29	4
Bi	10.3	103.0	0.611	–	–	1.88	4	9	13	< 3	6	–	–	–
Co	33	43	16	18	1.5	32	63	6	45	14	8	1.5	1.5	1.5
Cr	55	40	54	107	52	87	32	77	6	63	–	9	1.5	7
Mo	3	2	<1	–	–	5	5	<2	12.5	<2	10	–	–	–
Ni	29	32	25	38	1.5	162	127	15	161	26	–	6	27	28
V	35	40	50	145	66	17	8	28	29	81	–	8	95	21
W	<11	<10	<1	–	–	4	<8	14	33	9	–	–	–	–
Sn	1.2	1.3	1.4	–	–	<1	<1	–	–	–	–	–	–	–
Ba	340	110	590	726	309	220	81	846	838	711	–	45	78	66
Be	1.3	1.3	1.7	–	–	0.68	0.36	–	–	–	–	–	–	–
Cs	3.0	3.8	4.6	–	–	1.8	0.98	–	–	–	–	–	–	–
Cd	1.4	1.3	2.5	–	–	0.3	24.8	–	–	–	2.5	–	–	–
Ge	1.6	0.98	0.3	–	–	0.17	0.59	–	–	–	–	–	–	–
Hf	2.4	2.41	2.39	–	–	1.75	0.61	<3	4,0	<3	–	–	–	–
Li	26.04	23.22	20.65	–	–	14.08	6.77	–	–	–	–	–	–	–
Nb	4.8	5.08	7.98	–	–	2.11	1.13	5.0	6.0	12.0	1.5	–	–	–
Rb	60	84.8	102	–	–	33	20	56	55	186	25	–	–	–
Re	0.003	0.002	0.001	–	–	0.046	0.016	–	–	–	–	–	–	–
Sb	138	108	25.1	–	–	11.2	98.9	–	–	–	–	–	–	–
Se	6.1	9.3	1.7	–	–	0.7	8.4	–	–	–	–	–	–	–
Sr	45.0	57.4	61.4	–	–	15.3	12.8	39	21	30	10	–	–	–
Ta	0.37	0.39	0.65	–	–	<0.1	<0.1	7	9	5	–	–	–	–
Te	1.9	2.5	0.6	–	–	1.4	15.3	–	–	–	–	–	–	–
Tl	0.4	0.5	0.6	–	–	0.2	0.1	–	–	–	–	–	–	–
Th	6.4	7.1	8.3	–	–	4.0	1.9	6	7	15	–	–	–	–
U	2.5	2.3	2.1	–	–	26.8	4.8	2.7	4.5	2.6	–	–	–	–
Y	9.6	8.2	8.5	–	–	11.3	6.9	14	9	22	6	–	–	–
Zr	322	218	112	–	–	83	167	6	<2	138	16	–	–	–
La	19.4	21.5	26.3	–	–	15.3	6.9	12.0	10.0	35.0	–	–	–	–
Ce	41.9	46.7	53.9	–	–	30.9	13.3	214.0	950.0	85.0	–	–	–	–

Abbreviations: R – Radomice; G, K – Klecza; N – Nielestno; mb – mylonitic breccia of quartz-sericite schist with sulphide; qs – quartz-sericite schist with sulphide; qsv – quartz-sericite schist with vein; qcsv – quartz-carbonate-sulphide vein; f – fyllite; qgs – quartz-graphite schist; qw – quartz wacke; qsb – quartz-sulphide breccia; d – dolomite insert

Table 16

The statistic parameters of gold and other element contents in rock samples from the Klecza, Radomice and Nielestno areas

Element	Range				Geometric mean				Arithmetic average (number of samples)				Standard deviation			
	KROD	Radomice	Klecza	Nielestno	KROD	Radomice	Klecza	Nielestno	KROD	Radomice	Klecza	Nielestno	KROD	Radomice	Klecza	Nielestno
[ppm]																
Au	0.001–61.4	0.001–27	0.001–61.4	0.001–3.87	0.086	0.78	0.13	0.013	3.64 (73)	6.06 (32)	5.4 (18)	0.33 (23)	8.23	6.80	14.32	0.97
Ag	0.23–49.0	0.23–49	0.54–20.6	1.5–29	4.31	5.86	2.94	3.78	6.96 (73)	9.73 (32)	4.5 (18)	5.02 (23)	8.37	10.74	4.92	5.59
Cu	2.5–13153	3–1960	14–2780	9–1 3153	88	74.6	152	69.7	453 (71)	316 (32)	387 (18)	720 (21)	1601	566	644	2853
Pb	2–2 0000	2–2 0000	3–4450	4–391	58	109.5	103	13.4	962 (71)	1575 (32)	952 (18)	36 (21)	2964	4255	1383	84
Zn	13– 5092	13–2030	13– 5092	15–292	85	123.9	125	34.8	255 (71)	269 (32)	471 (18)	49 (21)	682	445	1214	59
Co	1.5–1400	1.5–1400	1.5–63	1.5–103	15.3	34.6	13.9	4.5	65.1 (70)	124.9 (32)	19.63 (18)	10.2 (20)	229	333.1	15.62	22.3
Ni	1.5–330	1.5–51	6–162.34	4–330	27	26.1	34.98	21.3	39.9 (60)	30.87 (22)	52.61 (18)	38.4 (20)	50.23	13.26	53.06	69.8
V	6–1825	6–145	7–1825	8–360	39.1	33.7	40.5	44.6	89.17 (60)	46.76 (22)	144.43 (18)	86.1(20)	235	38.45	420.85	98.3
Cr	1.5–141	22–107	1.5–110	1.5–141	38	46.1	38.3	29.4	51.32 (60)	51.13 (22)	55.19 (18)	48.03 (20)	35	25.55	32.51	37.7
Ba	11–997	25–726	11–997	14–548	164.3	193.7	227.6	103.3	291.6 (55)	287.9 (18)	420.1 (18)	169.5 (19)	274.1	238.1	359.4	155.9
Mo	0.50–101.0	0.5–5	1–101	10	1.74	1.51	1.41	–	2.37 (26)	1.8 (20)	19.16 (7)	–	18.91	1.5	40.13	–
Bi	0.6–316	1–316	1–10	6	29	52.1	5.0	–	91.4 (27)	120 (20)	7.0 (6)	–	103	108	5	–
Cd	0.1–24.8	0.5–17	0.31–24.78	2.5	2.24	2.18	–	–	4.65 (23)	3.95 (20)	12.54 (3)	–	6.03	4.58	17.3	–
Te	0.6–15.3	0.6–6.1	1.5–15.3	–	2.87	2.66	–	–	4.38 (8)	3.03 (6)	8.41 (2)	–	4.45	1.08	–	–
[wt %]																
As	0.0002–40.8	0.0004–40.8	0.0001–7.38	0.0006–2.84	0.0657	0.78	0.0141	0.0057	4.75 (71)	10.16 (32)	0.504 (18)	0.157 (21)	9.16	11.63	1.72	0.61
S	0.005–15.00	0.005–15.00	0.005–3.89	0.005–0.87	0.564	3.01	0.1245	0.012	3.31 (37)	5.28 (22)	0.604 (9)	0.149 (6)	3.66	3.59	1.24	0.353

KROD – Klecza-Radomice ore district; number of samples in brackets

tion in Nielestno is usually much lower than in other areas except Cu and Ag.

Distribution of Cr, Ni, and V reveal values that are rather characteristic for primary concentration in the host rocks of the flysch type than for hydrothermal processes. The average arsenic concentration in Radomice is almost 20 and 100 times higher than for Klecza and Nielestno, respectively. The samples of arsenopyrite-pyrite ores in cataclased quartz-carbonate veins from Klecza with arsenic concentration about 7%, and small base metals content below 0.5% are richest in gold (60-70 ppm Au).

(1) Gold has distinct positive correlation with arsenic, base metals, iron, silver and sulphur for selected areas as well as for the whole sample population (Tabs. 17, 18). The values of these correlation coefficients (r) vary between the Klecza, Radomice and Nielestno areas from weak to very significant. Gold correlation with arsenic (r = 0.56) and iron (r = 0.47), suggests the formation of submicroscopic gold in paragenetic association with arsenopyrite and pyrite. Gold correlation with silver and selected base metals in different areas is confirmed by mineralogical studies, which yield a presence of electrum in association with galena, chalcopyrite, and sphalerite. Au correlation with Cd (r = 0.41) may suggest admixture of Cd in sphalerite related to electrum and base metals association. Microprobe measurements indicated admixtures of Co in arsenopyrite and Ni in pyrite that may explain significant gold (of submicroscopic type) correlation with As (r = 0.98) and Ni (r = 0.42), in samples from Klecza. Furthermore, in this area correlation between Au and SiO_2 indicates for additional association of microscopic gold with low temperature chalcedonic quartz crystallization (r = 0.31). In Radomice, there are variable negative correlations of Au with CaO (r = –0.34), and with SiO_2 (r = –0.66). In Radomice it is also Au correlation with Bi (r = 0.65), TiO_2 (r = 0.55), and with Te. However, small number of samples limits the importance of the last observation. Figure 50 shows the variation logarithmic plots of the selected trace and metallic elements in Klecza, Radomice and Nielestno. In general gold and silver negatively correlate with alkali oxides, Al_2O_3, SiO_2, and TiO_2 and with CaO indicating for development of alteration processes such as sericitization, carbonatization, and silicification in the country rocks. Gold correlation with sulphur (Au–S, r = 0.26 for n = 37) indicates also its main crystallization during the process of the sulphidization.

(2) Silver displays correlation with Pb (r = 0.67), Fe (total), Bi and As (r = 0.54) and weaker with Cu and Zn in the whole deposit areas. Significant correlation of silver with As, Cu, and Pb (r = 0.88–0.94) occur especially in Nielestno, and with Pb and Zn (r = 0.71, 0.73) in Radomice. In Klecza Ag has a strong correlation with As (r = 0.81), Pb, Fe and Co and a weaker correlation with Ni, and Zn suggesting association of Ni-bearing pyrite and Co-bearing arsenopyrite with base metal sulphides. An arithmetic average of silver concentration is 6.96 for n = 73

Table 17

Correlation matrix of selected elements for the rock samples from Klecza–Radomice ore district and Radomice

KROD / Radomice		Au	Ag	As	Cu	Pb	Zn	Co	Fe_2O_3	Ni	V	Ba	S	Bi	SiO_2	CaO
		n=71	n=71	n=71	n=71	n=71	n=71	n=71	n=71	n=60	n=60	n=55	n=37	n=27	n=43	n=43
Au	n=32	1.000	**.4453**	**.5585**	.0218	.3883	**.4423**	–.0139	**.4672**	.2374	–.0890	–.0431	.2576	.2204	–.1560	–.1377
Ag	n=32	**.4478**	1.000	**.5439**	.3449	**.6726**	.2986	.0712	**.5989**	.0833	.0701	–.0389	.2582	**.5880**	–.4372	–.1088
As	n=32	**.8686**	**.5102**	1.000	–.0346	.3860	.1963	.0031	**.8022**	–.0118	–.0915	–.0713	**.5534**	**.8966**	–.6512	–.1964
Cu	n=32	–.1065	.2045	–.1376	1.000	.0605	.1539	.1251	.0892	.0300	.0124	–.0165	.2565	–.2090	.0769	–.0372
Pb	n=32	.3839	.7154	.3392	.2385	1.000	**.4737**	–.0149	.3620	.0745	–.0659	.2176	–.0739	**.5574**	–.1973	–.0852
Zn	n=32	**.5645**	.7314	.4508	.1070	**.8672**	1.000	.0031	.1701	.3992	–.0398	.2563	–.1083	.0819	.0650	–.0839
Co	n=32	–.1733	–.0034	–.1586	**.6454**	–.0730	–.0563	1.000	.3479	–.0376	–.0593	–.1237	**.5814**	–.1661	–.2129	.1636
Fe_2O_3	n=32	.7510	**.5801**	**.8437**	.1772	.3679	**.4901**	.3103	1.000	.4148	.0044	–.0150	**.7836**	**.7600**	–.7485	–.1477
Ni	n=22	.0177	–.0614	.0525	–.0997	–.1547	–.0070	–.1158	.1829	1.000	.3614	.1192	–.0292	–.1177	.2568	–.0831
V	n=22	–.0763	.0796	–.1364	–.1372	.1863	.1394	–.3090	–.2610	.1594	1.000	.0555	–.3805	–.0579	.0582	–.2039
Ba	n=18	.0891	.1498	–.0761	.0603	.3536	.2548	–.3552	–.1926	.1072	**.8603**	1.000	–.4759	–.0738	.1897	–.1875
S	n=22	.1476	–.0209	.2567	**.5332**	–.2718	–.2454	**.5750**	**.5688**	.0184	–.7253	–.9177	1.000	.3381	–.5572	–.0552
Bi	n=20	**.6517**	**.5701**	**.8719**	–.1414	**.6128**	**.5585**	–.3099	**.7054**	**.7357**	–.0476	.0681	.0701	1.000	–.7106	–.3468
SiO_2	n=25	–.5901	–.5467	–.7138	.0386	–.2549	–.3688	–.1373	–.8613	–.0226	.3821	**.5785**	–.4519	–.6583	1.000	–.3662
CaO	n=25	–.3351	–.1076	–.3546	**.6006**	–.1380	–.1292	**.9491**	.1649	–.2027	–.3926	–.4615	**.5817**	–.3746	–.0387	1.000

Bold written digit indicates moderate and/or strong (underline) correlation value between selected elements; n – number of samples; KROD – Klecza–Radomice ore district

Table 18

Correlation matrix of selected elements for the rock samples from Klecza and Nielestno

Klecza / Nielestno		Au	Ag	As	Cu	Pb	Zn	Co	Fe_2O_3	Ni	V	Ba	SiO_2	CaO
		n=18	n=18	n=18	n=18	n=18	n=18	n=18	n=18	n=18	n=18	n=18	n=11	n=11
Au	n=23	1.000	**.8322**	**.9814**	.2016	**.7520**	.3750	**.7894**	**.7393**	.4218	–.1202	–.2181	.3075	–.1884
Ag	n=23	**.4624**	1.000	**.8063**	.0484	**.7551**	.1239	**.5688**	**.6403**	.2247	.1510	–.2424	.1372	.1412
As	n=21	**.9789**	**.9363**	1.000	.0755	**.6549**	.2484	**.7361**	**.7643**	**.3979**	–.0955	–.2641	.2937	–.1727
Cu	n=21	**.9772**	**.9323**	**.9988**	1.000	.3803	**.9250**	**.4452**	–.1592	**.5411**	.0480	.3401	**.4466**	–.1275
Pb	n=21	**.9839**	**.8770**	**.9730**	**.9746**	1.000	**.4483**	**.6599**	.4899	.2357	–.1999	–.0380	.3115	.1767
Zn	n=21	**.0597**	.3168	.0889	.0781	.0542	1.000	**.6252**	–.0108	**.6005**	–.0935	.2016	.5533	–.3798
Co	n=20	–.0962	.0300	–.0408	–.0829	–.1183	**.4835**	1.000	**.6317**	**.7601**	.0480	–.1445	**.5652**	–.4394
Fe_2O_3	n=21	.2448	.4737	.2710	.2584	.2244	**.9647**	.1136	1.000	.2216	–.0752	.0339	.0025	–.0766
Ni	n=20	–.0295	.1711	–.0276	–.0355	–.0491	**.9739**	.0023	**.9320**	1.000	.3721	–.0863	**.7279**	–.4823
V	n=20	.0284	.2887	.0423	.0259	.0393	**.7528**	.2241	**.7131**	**.6901**	1.000	–.1010	–.7167	–.2379
Ba	n=19	–.1423	–.0440	–.1337	–.1362	–.0732	.2877	.2375	.1061	**.4118**	**.7265**	1.000	–.2385	.2111
SiO_2	n=9	–.0135	–.1627	–.0845	–.0913	–.0288	–.6492	.3711	–.1425	–.3983	.1424	.2086	1.000	–.3768
CaO	n=9	–.2211	–.1259	–.1848	–.1811	–.2214	**.3927**	–.3278	–.1403	.2385	–.2866	–.2541	–.9407	1.000

Bold written digit indicates moderate and/or strong (underline) correlation value between selected elements; n – number of samples

samples (range 0.23–49 ppm), is almost 6 times lower then for the Radzimowice deposit and is the one of the lower value among the late Variscan gold deposits in the Western Sudetes (Mikulski, 2001).

(3) At Radomice copper correlates with Co (r = 0.65), S (r = 0.53) and CaO (r = 0.60), and much weaker with Ag, base metals and iron. Some of correlation coefficients for copper and other elements are more significant in Nielestno or Klecza. In Nielestno the significant correlation of Cu with precious metals suggests also their coeval crystallization with base metal sulphides. In Radomice correlations of Cu with CaO, base metals and MgO (r = 0.2) indicate for association of chalcopyrite with various generation and composition carbonates. In general Cu have negative correlation with major oxides, except for the Klecza area where appears positive correlation of Cu with SiO_2 (r = 0.45). Arithmetic average of Cu in the all considering here ore district is very low (~0.05% for n = 71) and its concentration is from traces to 1.3%.

(4) Arsenic, beside its significant correlation with noble metals, has in the selected areas also strong affinities with Bi, (Radomice; r = 0.88), Fe, and Co (Klecza, r = 0.74) and weaker with S. Arsenic is present as arsenopyrite and as scorodite (Nielestno). Arsenic correlation with selected base metals varies in each area from weak to significant (Nielestno). Arsenic arithmetic average for samples of ore grade > 0.5 ppm Au is 2.4 % As (range from 0.001 to 40.8% As). However, the arsenic content in samples from various areas differs significantly (Figs. 50B, 51). For example at Radomice the arithmetic average value is over 100 times higher than in Nielestno (10.2% As for n = 32 samples, and 0.16% As for n = 21 samples, respectively).

(5) Bi and Te concentrations in sulphide ore samples are lower than within ores in Radzimowice. At Radomice deposit Bi contents range from 1 ppm to 316 ppm (for n = 20). An arithmetic average is 120 ppm (in Radzimowice – 133 ppm). The detailed microscopic investigation allowed recognising bismuth minerals in association with electrum. Bi appears practically only in samples from Radomice and only in traces within samples from Klecza and Nielestno (<3 to 13 ppm). At the Klecza–Radomice ore district Bi has a positive correlation with Au, in Radomice (r = 0.65, n = 20), Ag (r = 0.57; n = 23), As (r = 0.88), Pb, Fe_2O_3, TiO_2 , Y, Al_2O_3 , K_2O, Te and negative correlation with SiO_2 (r = –0.66; n = 25). Positive correlation of Bi with As and Ag indicates for Bi-minerals association with electrum and As- and Pb-sulphides (arsenopyrite and galena). Correlations with other elements are week or not exist. The range of Te in Radomice deposit is from 0.60 ppm to 15.25 ppm for n = 8. Arithmetic average is 4.4 ppm and is over 10 times lower that its average concentration at Radzimowice deposit. Geochemical concentrations of Te are very low. Te has strong positive correlation with: Au, Ag, Pb, Zn, Cd, and Bi and strong negative correlation with most of REE.

(6) Co correlation with S (r = 0.58) and Fe (r = 0.35) confirms microprobe results and indicates for Co admixtures in pyrites and in some arsenopyrites as well as for the presence of its own sulphide minerals (cobaltite). The highest Co concentration of about 0.14% has pyrite ore of breccia type from Radomice with contents of Au and As below 0.2 ppm and 0.2%, respectively. In the samples from Radomice the arithmetic average value for Co (124.9 ppm for n = 32 samples) is several times higher than in the samples from Nielestno or Klecza (Table 16). In samples of ore grade >0.5 ppm Au correlation of Co with Au (r = 0.37, As (r = 0.69) and Fe (r = 0.67) occurs. It suggests association of gold with Co-admixtures in

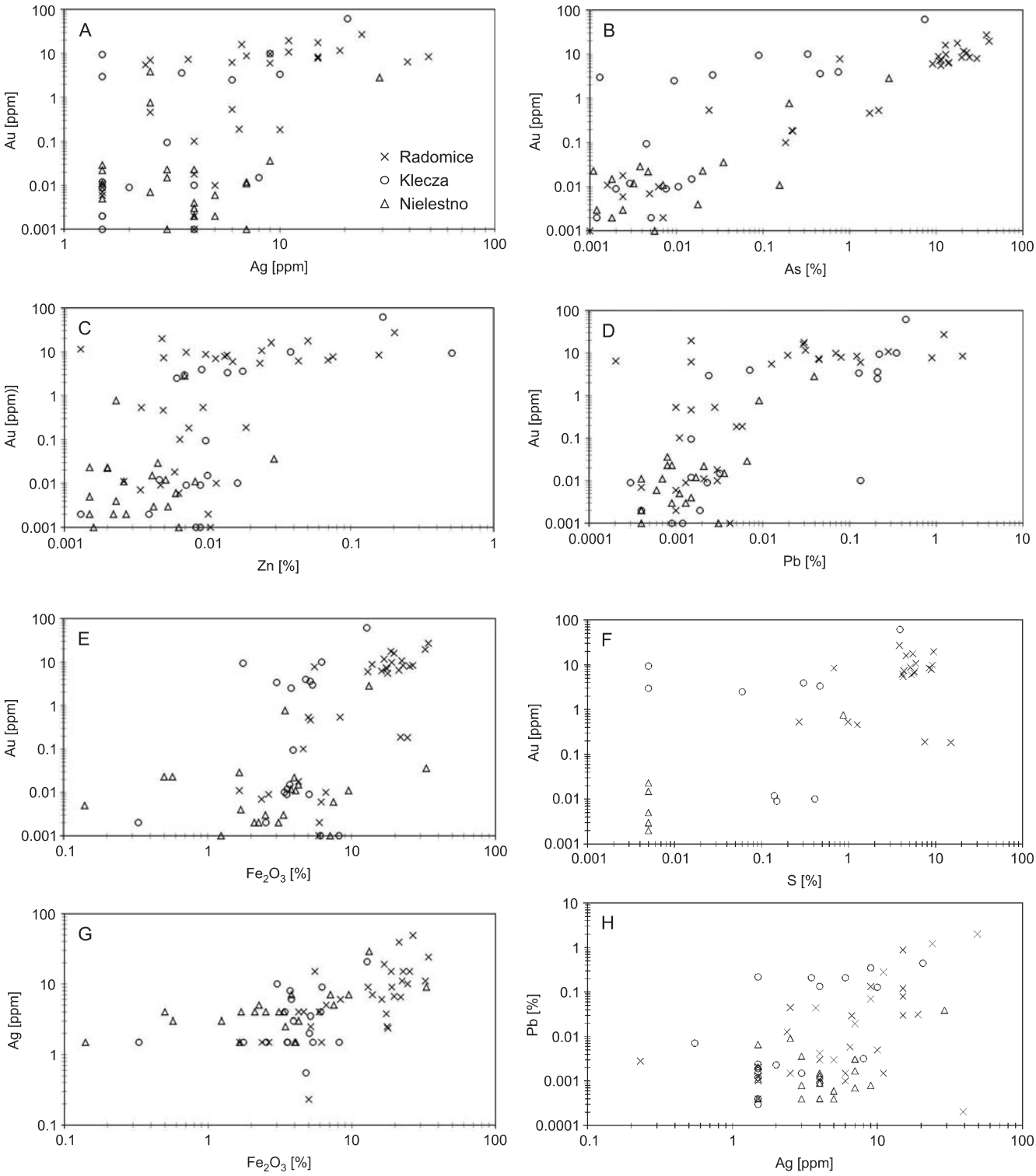

Fig. 50. The variation logarithmic plots of the selected trace and metallic elements in the Klecza–Radomice ore district

arsenopyrites or/and pyrites. High concentration of Au in sulphide samples has positive correlation with high Co concentration. Gold ores that contain over 10 ppm Au has Co concentration at the level about 100 ppm. Co–Ni–As minerals association is mainly represented by cobaltite, gersdorffite and Co-bearing arsenopyrite.

(7) Sulphur displays a strong correlation with total iron (Fe_2O_3) that confirms its strong affinity with sulphides. The sulphide ore locally may also contain small admixtures of the following elements in values: Co – 0.14%, Bi – 0.032%, Te – 15.3 ppm.

On the pseudo-ternary diagram of Au-Ag-base metals (Poulsen *et al.*, 2000) the auriferous ore samples from

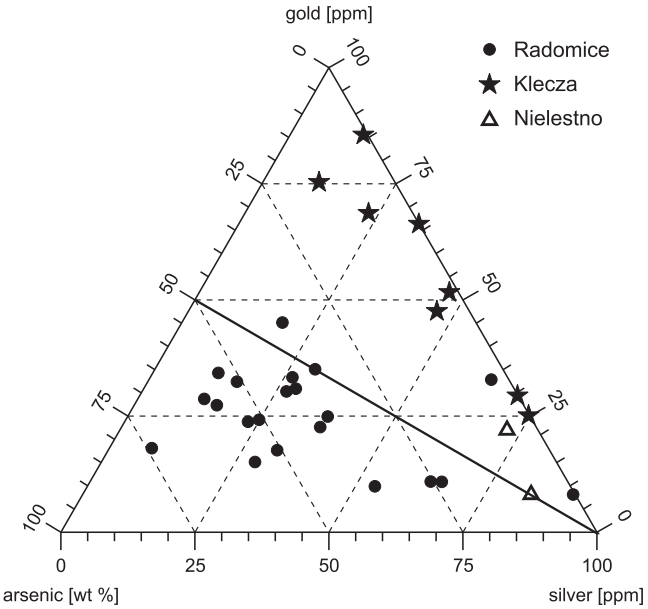

Fig. 51. Ternary of Au–As–Ag diagram illustrating the various ore compositions in the Klecza–Radomice ore district

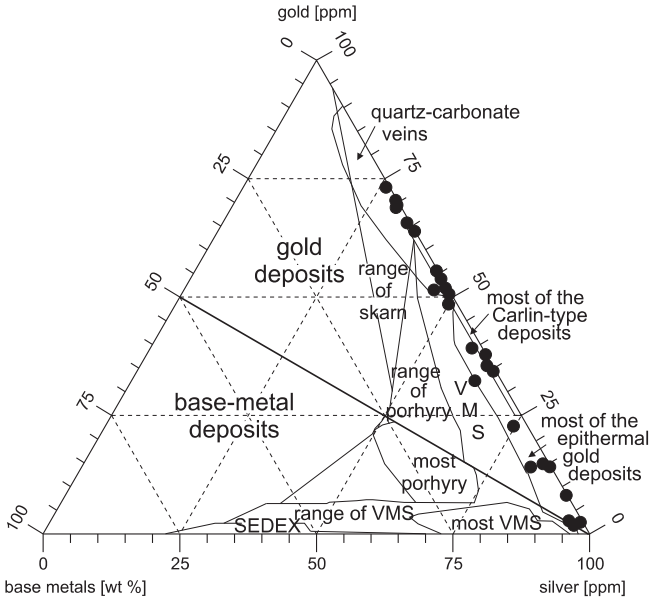

Fig. 52. Pseudo-ternary Au–Ag–base metals diagram (after Poulsen *et al.*, 2000) illustrating the estimated compositions of Au-bearing As ores from the Klecza–Radomice ore district

the Klecza-Radomice ore district are scattered, although most of them fall in the field of gold deposits in quartz-carbonate veins and some of epithermal gold and Carlin-type gold (Fig. 52).

GOLD TO SILVER RATIO

At the Klecza-Radomice ore district the gold- to-silver ratios, in samples of ore grade above 0.1 ppm Au is variable, from 7:1 to 1:10 with an average 1.8:1 (n = 67 samples; geometric average = 1.1:1). Furthermore, according to the old prospecting reports from Klecza (Krusch, 1907; Grimming, 1933) Au:Ag ratios were similar and most often from 1:1 to 4:1 (Fig. 53). An average arithmetic values of Au:Ag in Radomice is almost 1:1 (n = 24; geometric average is 1:2), in Klecza 2.4:1 (n = 40; geometric average ca. 2:1), and in Nielestno 1:0.66 (n = 3; geometric average is 1:2.5). In general gold- to-silver ratios in the Klecza-Radomice ore district changed from 2:1 (Klecza), and 1:1 in Radomice, and to 1:2 in Nielestno.

In the samples of grade >0.5 and <3 ppm Au, from the whole area an average arithmetic value is similar and about 1.9:1 (n = 6). The highest Au:Ag ratio, about 7:1 displays

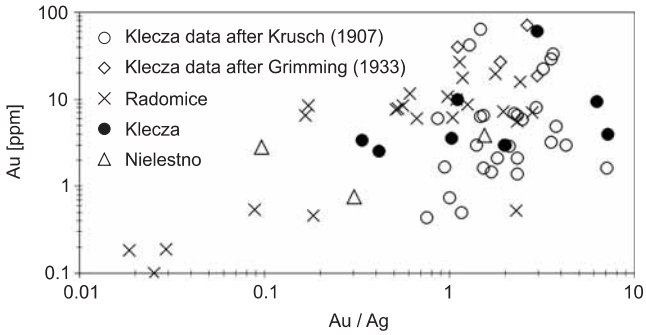

Fig. 53. Logarithmic plot of gold and silver ratio versus gold contents within the ore samples from the Klecza–Radomice ore district

cataclased quartz vein with arsenopyrite ore and carbonates overprint from Klecza. However ore grade in this sample is low about 4 ppm Au and 0.6 ppm Ag. In the samples of grade above 10 ppm Au an average Au:Ag ratio is 2:1 (n = 16; range 0.6-3.6; geometric average 1.8:1). In the richest in gold samples (60–70 ppm Au) from Klecza the ratio of Au:Ag is from 1.5–2.9 to 1.

GOLD AND BASE METALS CONCENTRATIONS IN BARREN ROCKS

Geochemical data set contains additional information concerning gold and base metals assays of 13 barren, altered and slightly mineralized rock samples of grade below 0.1 ppm Au. It comprises rocks of flysch protolith (quartz-micas-graphite schists, quartz-graphitic schists with pyrite impregnation, and carbonaceous schists). Samples have been taken from the old mining tailings of the Klecza– Radomice ore district. Gold traces in quartz-micas-graphite schists are from below 1 ppb up to 15

ppb with arithmetic average about 6 ppb (n = 13; geometric average = 4 ppb). During the prospecting for Au carried out in the railway crosscuts between Pilchowice–Nielestno the remnants of mining wastes scattered along left banks of Bóbr River were sampled. Arithmetic average of Au in schists from that area is = 4.6 ppb; n = 18 (range <1 to 29.7 ppb). In specific types of schists the average values are following: in black graphite schists – 8.0 ppb (n = 8), in gray quartz-sericite schists 2.8 ppb (n = 4), and in siliceous schists – 0.8 ppb (n = 4). The contents of metallic elements in various schists samples are low, as an example average value concentrations of Cu is ~20 ppm, Zn – 36 ppm, Pb – 26 ppm, As – 28 ppm and Cr – 30 ppm. Two quartz-sericite schists have higher content of Pt – 2 ppm. In single samples of siliceous-graphite schists an increase of Mo (~60 ppm), As (~180 ppm) and V (~600 ppm) determined.

REE DISTRIBUTION IN ORES

Samples from Radomice are represented by breccias with fragments of sericite-graphite-quartz schists cemented by fine-grained sericite, quartz and sulphide. Ore samples from Radomice contain gold from 0.18 up to 16 ppm and those from Klecza from 3.9 up to 61.4 ppm Au. The REE patterns of samples from Radomice are similar to REE patterns of mineralized quartz veins from Klecza and characterized by negative Eu anomaly and enrichment in light REE (Fig. 54). Ratios of Ce/Yb_{cn} are from 8.9 up to 11.7 for Radomice samples and from 6.6 up to 8.4 for Klecza samples (Tab. 19). Breccias sample (S-50) with arsenopyrite mineralization shows highest enrichments in light REE (Ce/Yb_{cn} = 11.7). In comparison to mineralized quartz veins from Klecza those breccias are also depleted in the heavy REE, but have strong negative Eu anomaly. Strongest negative Eu anomaly has sample of quartz vein with richest ore mineralization and gold grade. The considered samples have relatively

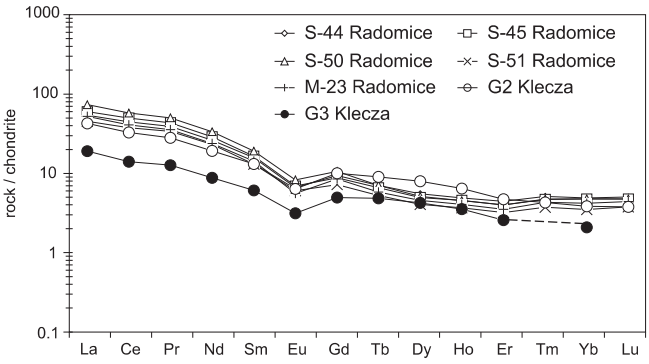

Fig. 54. Chondrite-normalized rare earth element diagram (after Taylor, McLennan, 1985) applied for the ore samples from Klecza and Radomice

Table 19

REE content in the rocks and sulphide ores from the Klecza–Radomice ore district

Element [ppm]	Radomice						Klecza	
	S-44	S-45	S-50	S-51	M-23	M-24	G2	G3
La	53.128	58.659	71.790	44.553	51.199	40.986	41.935	18.891
Ce	43.805	48.848	56.391	37.031	40.197	27.823	32.347	13.998
Pr	38.555	42.657	49.139	33.409	35.109	23.803	27.752	12.620
Nd	25.833	28.551	32.979	22.889	23.563	16.283	19.017	8.803
Sm	15.693	16.355	18.926	13.009	14.190	9.831	13.078	6.104
Eu	6.632	6.943	8.287	6.034	5.598	4.816	6.379	3.161
Gd	9.376	8.807	10.575	7.219	8.520	6.908	10.016	4.964
Tb	7.069	6.603	7.069	5.259	5.828	5.190	9.034	4.862
Dy	5.554	4.958	5.121	4.087	4.575	4.231	7.961	4.260
Ho	4.906	4.576	4.553	3.706	4.082	3.871	6.435	3.565
Er	4.438	4.024	4.020	3.225	3.542	3.161	4.727	2.594
Tm	5.140	4.691	4.747	3.764	4.326	3.174	4.298	–
Yb	4.919	4.750	4.810	3.516	4.210	2.520	3.871	2.109
Lu	5.039	4.751	4.777	3.806	4.436	–	3.806	–
Ce/Yb_{cn}	8.9	10.3	11.7	10.5	9.5	11.0	8.4	6.6

flat heavy REE (HREE) chondrite-normalized patterns with Tb/Yb_{cn} from 1.3 to 2.3. In mineralized breccias from Radomice this ratio is about 1.4 and only in one sample reached about 2. Highest value of Tb/Yb_{cn} is in Au-bearing quartz vein from Klecza (2.3). Highest content of ΣREE (190–280 ppm) have mineralized breccias from Radomice. The two samples of quartz veins from Klecza have ΣREE 190 and 85 ppm, respectively that indicate for their slight enrichment especially in LREE when compared to the ranges of ΣREE concentration in mesothermal gold-bearing quartz veins in Australian Central Victoria (Bierlein *et al.*, 1999). Correlation coefficients for REE and Ti, K, Na, P and Al oxides are strongly positive (r = 0.95; n = 8) by contrast to elements such as S, As, and Au.

HOST ROCK ALTERATION

Hydrothermal alteration is limited to the closest wallrock of veins and is dominated by intense sericitization and silicification. Several quartz generations (intergranular, veins, and veinlets) and different its forms appear as massive, coarse-grained, medium-fine-grained, recrystallized, fine-crystalline, druses, chalcedony, and opal. The wider and more significant alteration zones that are marked by light white-yellow colour occur in mylonitic schists. Fine-scale light mica (sericite) recrystallized into coarse habit (muscovite). Also, chlorite commonly appears within cataclased quartz-sericite schists with sulphide impregnation.

Carbonates are often present within cataclased barren rocks or in the association with base metal sulphides and gold that cemented fractured auriferous sulphide ore (Pl. XIV, 5, 6). According to microprobe investigation carbonates revealed various composition and structure (Tab. 20). The most common are ankerite and/or dolomite in the form of veinlets, irregular infill of intergranular porous and fractures, as well as numerous single euhedral crystals. Calcite is also locally abundant and appears in several generations and within different mineral associations. However, within samples with base metal sulphide occurrence is subordinate to ankerite or dolomite. Calcite with hematite dominated in samples from Nielestno. Some of the carbonate paragenesis characterised by successive minerals overgrowth and zone fine-structure of crystals (Figs. 55, 56). Siderite appears as spotty mineralization within weathered samples, which contained remnants of primary sulphide mineralization.

Table 20

Composition of carbonates from Klecza according to electron-microprobe analyses

Element composition	Sample									
	R68/1	R68/2	R68/3	G2/1	G2/2	G2/3	G2/4	G2/5	G2/6	G2/7
FeO	7.81	6.12	13.91	7.53	14.79	12.32	14.57	44.62	25.38	30.71
MnO	1.25	1.55	1.49	2.16	3.74	1.55	2.19	0.86	1.09	0.75
CaO	30.02	30.00	28.71	29.68	27.78	28.35	28.84	0.39	0.44	1.01
MgO	14.74	15.66	10.93	14.22	8.88	12.44	10.09	12.02	26.58	20.27
CO_2	45.22	45.36	43.91	44.78	42.83	44.33	43.94	41.29	45.60	42.19
Total	99.04	98.70	98.95	98.37	98.10	98.98	99.63	99.19	99.10	94.93
Mg (CO_3)	30.86	32.80	22.88	29.78	18.61	26.04	21.14	25.17	55.67	42.44
Ca (CO_3)	53.62	53.58	51.28	53.02	49.62	50.63	51.51	0.69	0.78	1.80
Mn (CO_3)	2.03	2.51	2.43	3.51	6.07	2.51	3.55	1.39	1.76	1.21
Fe (CO_3)	12.61	9.87	22.43	12.15	23.87	19.87	23.51	72.00	40.97	49.55
Total	99.12	98.78	99.03	98.46	98.17	99.07	99.71	99.26	99.18	95.00
(Fe+Mn) / (Fe+Mn+Mg)	25.69	21.60	44.18	27.72	53.99	38.51	48.27	67.98	35.85	46.55

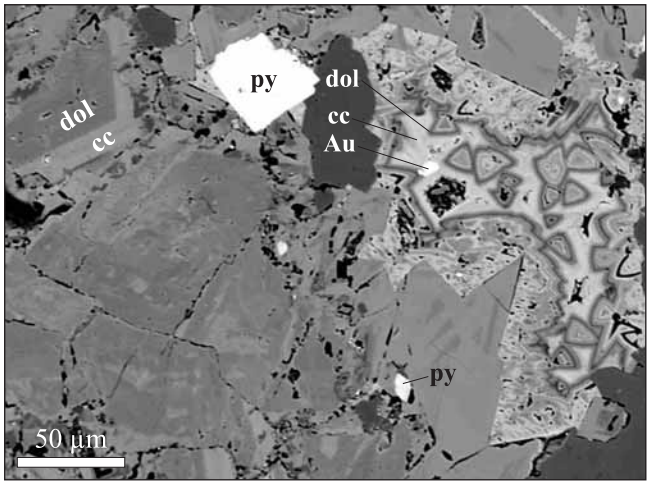

Fig. 55. Euhedral crystals of pyrite in fractured quartz vein cemented by carbonates

Sample no. G-2

Abbreviations: Au – native gold, dol – dolomite, cc – calcite, py – pyrite

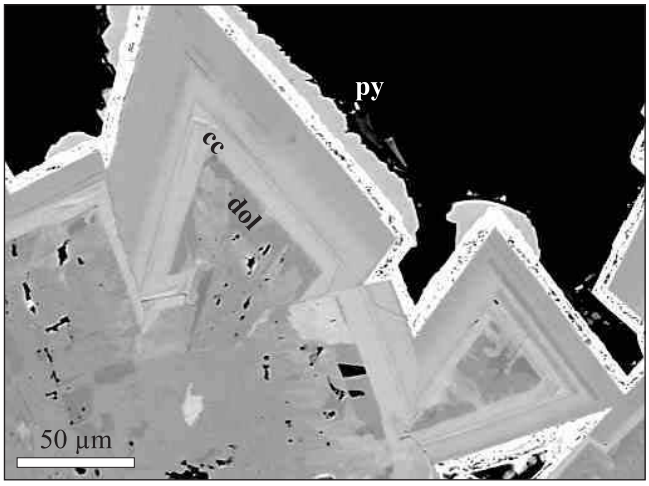

Fig. 56. Euhedral crystals with characteristic zoning structure indicating various chemical composition of carbonates

White rims are built of pure calcite and dark of dolomite

For explanations see Fig. 55

In cataclased quartz-sericite schists with sulphide mineralization within sericite and chlorite altered parts euhedral fine-coarse crystals of tourmaline were found (Pl. XIV, 4; Tab. 21).

According to the results of quantitative X-ray diffraction (XRD) kaolinite and/or illite common constituent of sulphide-bearing quartz veins as well as in the host rocks within the whole Klecza-Radomice ore district (Pl. XIV, 2, 3). These clay minerals often associate with chalcedony or opal. Chalcedony may have different textures as rosettes, fibrous or other (Pls. XI, 6, 8; XIII, 7, 8). Chalcedony in some parts is associated with albite (adularia) in Klecza or Nielestno.

Table 21

Composition of tourmaline from Radomice according to microprobe analyses (sample no. R77)

Element composition [wt %]	Sample	
	R77/1	R77/2
B_2O_3	13.072	14.061
FeO	10.036	10.189
MnO	0.000	0.056
K_2O	0.012	0.000
SnO	0.000	0.014
CaO	0.027	0.060
TiO_2	0.112	0.555
Na_2O	2.155	2.430
MgO	4.835	4.944
Al_2O_3	32.634	31.487
SiO_2	35.869	35.570
F	0.017	0.057
Total	98.770	99.424

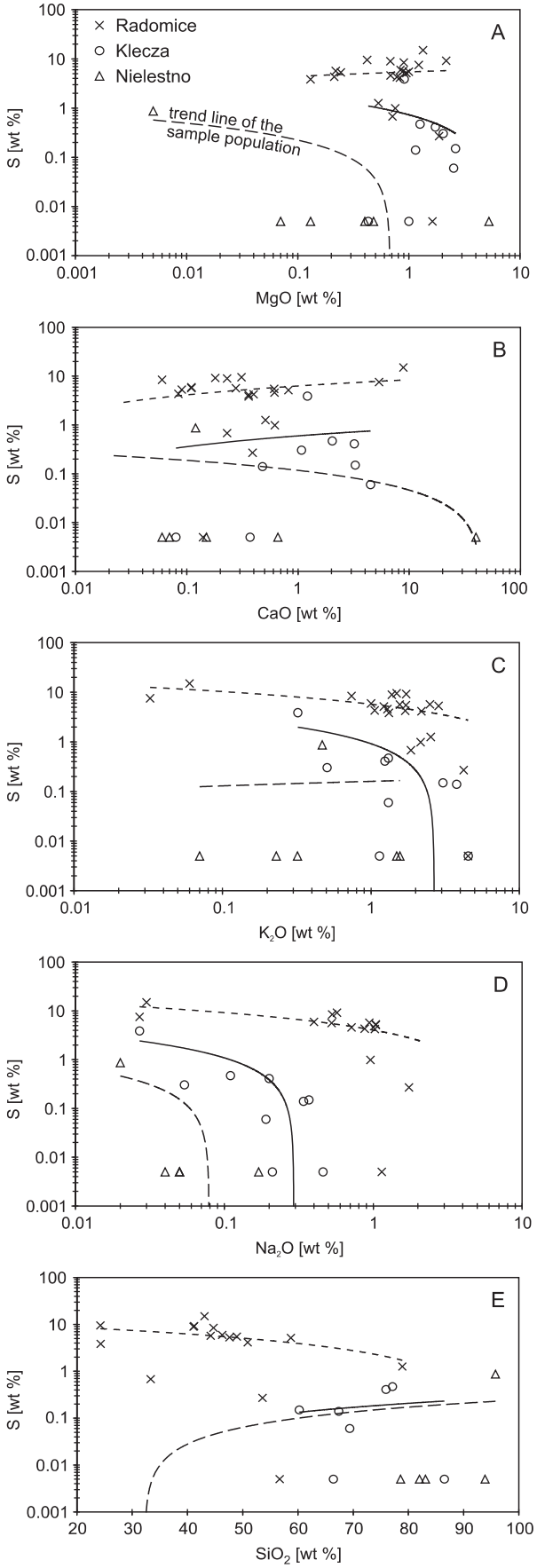

Secondary ore minerals such as Fe-hydroxides, covellite commonly replace sulphides. Veinlets of various mineral composition are marked by characteristic different colours (ankerite – yellow-brown; siderite – dark red; dolomite – light brown; kaolinite, illite – milky-white, light yellow-green and white; chalcedony – glossy-clear; goethite – black).

Some strongly altered quartz-sericite schists are characterized by light yellow-olive colour, porous texture, absence of sulphides and also some gold enrichments (up to 3 ppm) (Fig. 41). These altered rocks were oxidized by waters and as result of acidic and oxidizing solutions were capable to leach and remove metals from their sulphides. Gold leached out from these auriferous sulphides was reduced and adsorbed by chalcedony or hematite. Hematite as well as Fe-hydroxides (goethite) and scorodite are characteristic in samples from Klecza and Nielestno.

Distribution of alteration zones is variable according to host lithology. Pyritization is extensive, relatively homogeneously distributed throughout the matrix and related to quartz-sulphide veins. In banded sediments, pyritization is less extensive and produced pyrite-rich layers intercalated with quartz-rich and sericite-rich bands (Pls. IX, 2; XI, 2). In the pyrite-rich visible alteration zone, sericite is abundant, and occurs as unoriented and oriented flakes, associated with seams of leucoxene with rutile.

The element correlation between calc-alkali oxides and sulphur indicate that during processes of sulphide ore precipitation in Radomice took place significant gain of carbonates (CaO) and also MgO (dolomitization and/or ankeritization) and lose of alkalis (K_2O and Na_2O) and silica content (Fig. 57). Presence of K_2O which highly positively correlate with Al_2O_3 within ores indicates for sericitization during some early stage of hydrothermal sulphide impregnation. Strong positive correlation of K_2O with Al_2O_3 and TiO_2 suggests formation of Ti-minerals during sericitization process. Also in Klecza a gain of carbonate (calcite) during sulphidization is noted. However, for Klecza and Nielestno enrichment in silica and depletion in alkalis are more visible. Within these samples gold positively correlats with SiO_2 suggesting for its deposition with low temperature quartz (chalcedony).

Fig. 57. Lose and gain of oxides due to alteration processes in the Klecza–Radomice

Plots of sulphur versus MgO (**A**), CaO (**B**), K_2O (**C**), Na_2O (**D**) and SiO_2 (**E**)

STUDIES OF FLUID INCLUSIONS IN QUARTZ

Studied primary fluid inclusions are small, usually from 5 up to 30 μm in diameter. Typically, they are two-phase liquid-rich inclusions with a vapour bubble. They were frequently euhedral of isometric habits. Primary fluid inclusions in different quartz generations from auriferous and barren rock samples revealed the presence of low saline two-phase H_2O fluid with or without CO_2. Reported crystallization temperatures are in the ranges of 340–140°C and salinity of fluids typically below 9 wt % NaCl equivalent at pressure drop from 0.9 to 0.6 kb (Fig. 58).

Submicroscopic gold bound in coarse- and medium-grained sulphides occur in characteristic gray colour coarse grains of quartz. This quartz generation crystallized when temperature decreased from 340 to 290°C, from fluids with variable salinity from 1 to 3 wt % NaCl equivalents, and at pressure 1.0 ±0.2 kb (Au_2 – at Fig. 58A, D). Hence, at least some of these fluid inclusions are probably related to sulphide mineralization.

Microscopic gold which appears as inclusions or infilling-fracture microveinlets in arsenopyrite and pyrite is associated with carbonate and base metal sulphides (chalcopyrite, galena and minor sphalerite). Electrum occurrence may correspond with crystallization of younger fine-grained quartz or/and carbonates (Au_3 – at Fig. 58A–C) at wider temperature range from 280–220°C fluids with salinity from 4 to 8 wt % NaCl equivalent.

Younger generation barren quartz of milky-white colour crystallized at temperatures 220–180°C from fluids of low salinity (1–5 wt % NaCl equivalent) and pressure at 0.7 – 0.6 kb (Ba_1 at Fig. 58E).

Next generation of quartz is represented by chalcedony that often recrystallized into fine-crystalline chalcedonic quartz or microcrystalline glossy quartz and is associated with appearance of kaolinite.

Intergranular gold micro-grains are connected with chalcedony occurrence (Au_4 – at Fig. 58A, F) especially in samples from Klecza and rarely from Radomice areas. Chalcedonic quartz crystallized within the temperature ranges from 200 to 150°C, from fluids of low salinity 3–1.5 wt % NaCl equivalent, and pressure about 0.5–0.6 kb.

Summarizing, two types of fluid evolution, however both from the common source, responsible for ore-precipitation is possible to recognition (Fig. 58): 1st characterised by decreasing salinity during drop of temperature, and 2nd by slight increased salinity (up to 8 wt % NaCl equivalent) followed by drop of salinities. It is possible to explain as fluid-rock interaction and CO_2 sorption from country rocks by fluids of 2nd type and/or as water mixing. During this stage base metal sulphides associated with carbonates crystallized from fluids.

As examples: in Radomice carbonates crystallized at temperature range from 240 to 230°C and from 199 to 174°C from fluids with low salinity (4.2–6.0 wt % NaCl equivalent) and pressure 0.6 kbar and in Nielestno at temperature range from 194 to 186°C and similar low salinity (4.9 ±0.2 wt. % NaCl equivalent) and pressure.

THE SALT COMPOSITION

Preliminary results are presented for the Klecza area by Mikulski *et al.* (2005c). It is possible to distinct 5 basic groups of salts composition of fluid inclusions in quartz from Klecza–Radomice ore district (Fig. 59). The gray quartz of the first generation that is cataclased and rich in brecciated sulphide is characterized by presence of NaCl, KCl and $CaCl_2$. The composition of salts indicates the presence of NaCl from 65 to 80% of total salts (in brackets – Klecza 60–76%), KCl from 5 to 25% (11–23%), $CaCl_2$ from 5 to 20 % (4–15%) and $AlCl_3$ up to 15% (5%) and $FeCl_2$ <10% (5%).

Two-phase aqueous inclusions in addition to CO_2 may contain up to 10% N_2 and less frequently CH_4 (5%). The presence of $AlCl_3$ is common, especially within the gold-bearing samples from Klecza and Radomice in inclusions crystallized in temperature range from 340–270°C from fluids of moderate salinity (10 ±3 wt % NaCl equivalent) suggesting a high mobility of Al probably during sericitization. Barren samples from Nielestno do not contain any or only traces of $AlCl_3$.

The early event of gray quartz crystallization corresponds to auriferous arsenopyrite and pyrite precipitation. The second generation of white ("milky") quartz that forms veinlets and rock matrix seems to be related to pyrite and base-metal sulphide precipitation associated with crystallization of carbonates of various compositions (mainly ankerite and dolomite). The content of salts in comparison to the inclusion solution composition in gray quartz are characterised here by higher NaCl contents 70–85% and lower content of KCl (2–16%), $CaCl_2$ (2–18%) and very often presence of $MgCl_2$ (up to 10%) and lower of $FeCl_2$ (5%) and only traces of $AlCl_3$. During drop of fluid temperature (<180°C) concentration of $CaCl_2$ and $MgCl_2$ increased (up to 30% and 10%, respectively) and NaCl slightly decreased and KCl disappeared.

In the sample from Klecza that contains high-grade gold (>60 ppm Au) $FeCl_2$ appears in the amount up to 5% of total salts and within two-phase aqueous fluid inclusions beside CO_2 appears commonly CH_4 (up to 10%) and in some inclusions also N_2 (<10%) (Mikulski *et al.*, 2005c).

In Radomice and Nielestno quartz occurs, which is mostly barren and crystallised within a range of temperature <194–143°C with salinity of fluids <5 wt % NaCl equivalent and pressure at 0.6–0.5 kb. The salts in inclusion fluids are dominated by NaCl (55–75% of total salts) and $CaCl_2$ (25–45% of total salts) and very low contents of KCl (0–5%).

The lowest crystallization temperatures 170–143°C are measured in transparent microcrystaline and/or chalcedony veinlets of the next generation. Fluid inclusions in that quartz homogenized into the liquid phase and are characterised by presence of NaCl dissolved in water almost exclusively (83–100%; KCl – 0%; $CaCl_2$ – 0–17%) or moderately (55–65%; KCl – 0; $CaCl_2$ – 25–35%; $FeCl_2$ – 1–5%). The first compositions of salts are characteristic for rather barren transparent quartz and the second composition is typical for chalce

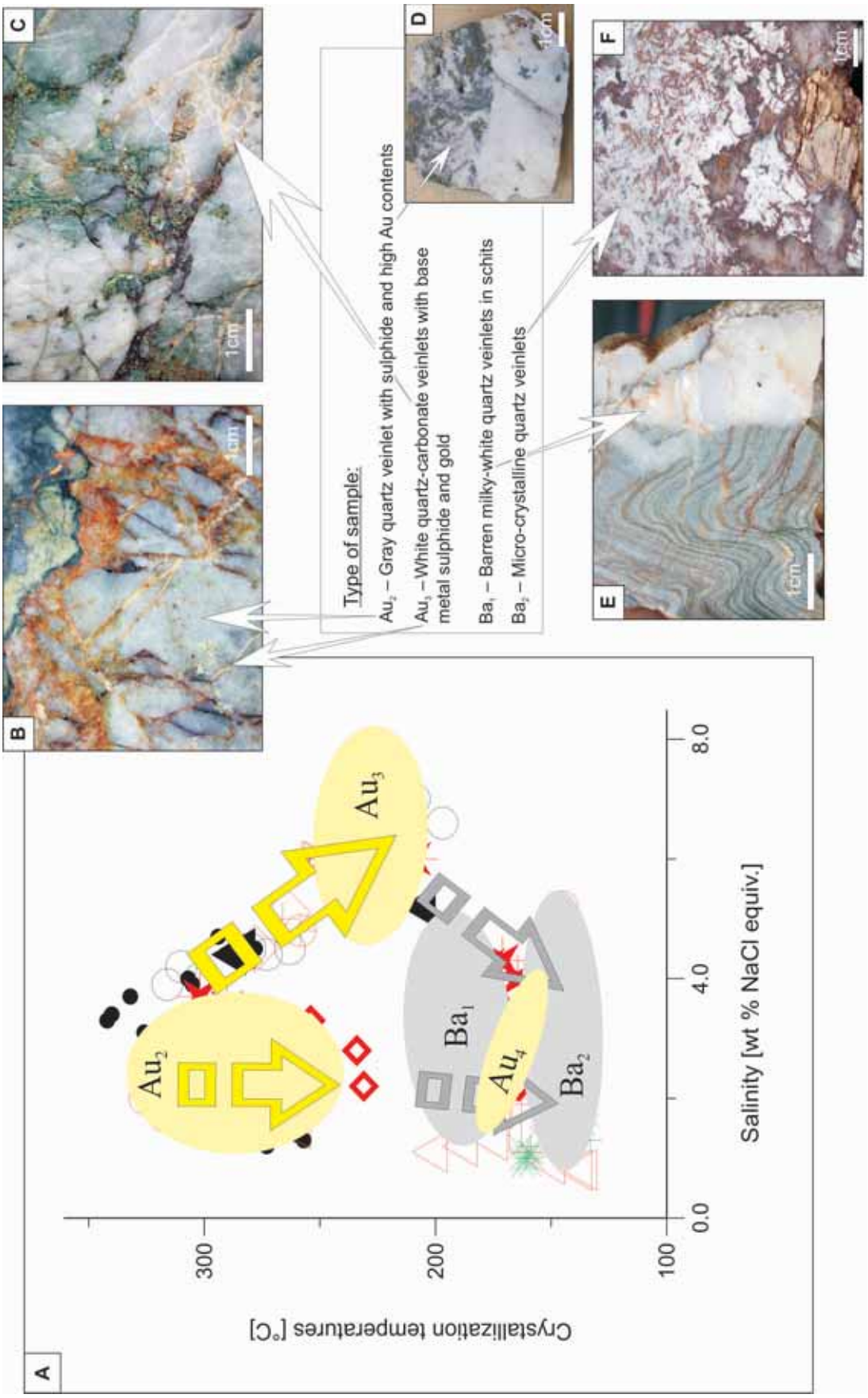

Fig. 58. Fluid inclusions studies of various quartz veinlets generation at the Klecza–Radomice ore district

The microphotographs in the reflected light of various generations of quartz veinlets with sulphide. **A** – plot of crystallization temperatures versus salinity of fluid inclusions hosted by auriferous (Au_2 and Au_3) and barren (Ba_1 and Ba_2) quartz from the Klecza-Radomice ore district; **B** – fractured coarse-grained gray quartz cemented by fine-crystalline white quartz and carbonates, quartz vein hosted by chlorite-sericite schists (sample no. G2); **C** – Fractured and cataclased coarse-grained white-gray quartz cemented by fine-crystalline quartz-carbonates and Fe-hydroxides, quartz vein hosted by chlorite-sericite schists (sample no. R64); **D** – massive vein of gray quartz with abundant gold-bearing sulphide (sample no. G4); **E** – barren milky-white quartz veinlets cutting almost perpendicular the L_1 lamination in folded quartz-sericite-chlorite schist (sample no. S49); **F** – opal with Fe-hydroxides infill fractured coarse-grained quartz (sample no. S60)
Au_2, Au_3, Au_4 – auriferous stages in European Variscan Belt (see Fig. 83)

dony-hematite-gold association recognised in samples from Nielestno (R80). Additionally, fluid inclusion of the younger generation quartz occur in Nielestno and Radomice, that beside major presence of NaCl (73–95%) contains KCl (5–27%).

In general barren quartz from Klecza–Radomice ore district characterised by drop of crystallization temperatures from <280°C (usually <220°C) to 170–150°C and of low salinities (<5 wt % NaCl equivalent) and at pressure 0.7–0.5 kbar. The composition of salts indicates the presence of NaCl (60–100% of total salts), KCl (0 – 30%) and $CaCl_2$ (0 –35%) and only traces of other salts. Beside CO_2, fluid inclusions in quartz of various generations may contain N_2 (up to 20%) and variable values of CH_4. In the opposite of these the fluid inclusions in quartz from gold-bearing samples may have different proportion of NaCl, KCl, and $CaCl_2$, however they always contain additional other salts such as $FeCl_2$, $AlCl_3$ or $MgCl_2$ and much often a higher concentration of CH_4 (5–10%) and also the presence of N_2 (≤10%)

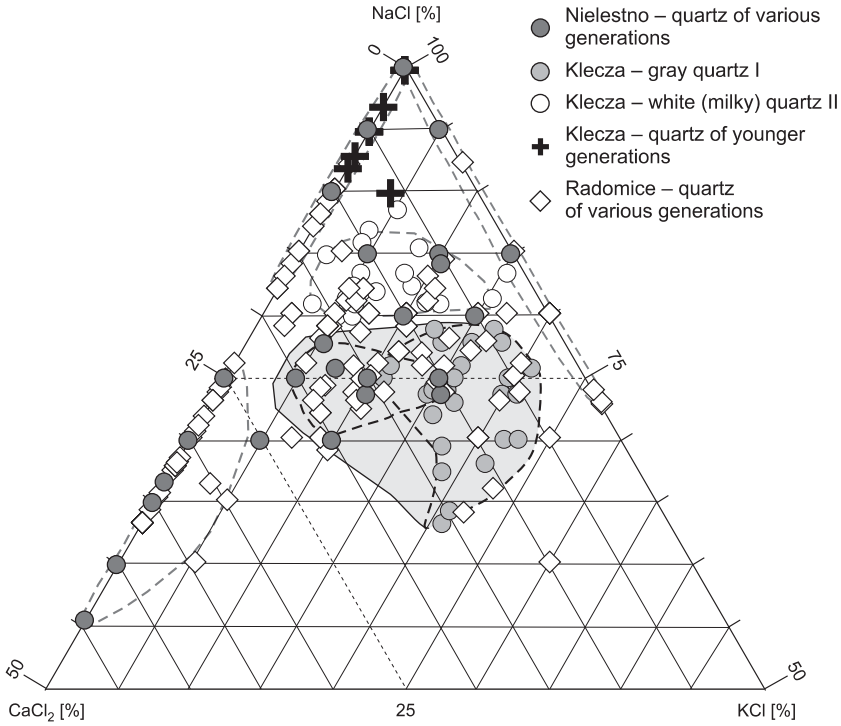

Fig. 59. Salt compositions in the fluid inclusion in quartz of various generations from Klecza, Radomice and Nielestno

THE Re–Os AGE VALUES OF GOLD-BEARING SULPHIDE FROM THE KLECZA DEPOSIT

Rock samples of the quartz vein with pyrite and arsenopyrite mineralization from the north-eastern and south-western part of the Klecza-Radomice ore district were subject of Re–Os study (Mikulski *et al*., 2005a). The several non-fractured crystals of euhedral pyrite from 0.5 to 3 mm in size and with a high gold admixture (80 ppm) were selected for Re–Os measurement (Tab. 22). Most of the analysed auriferous sulphides from Klecza-Radomice ore district was characterised by extremely low concentration of Re at blank level, so those samples were rejected, except for two ones from Klecza. The first sample was ar-

Table 22

Description of sulphides from the Klecza-Radomice ore district selected for Re-Os measurements

Sample symbols	Location	Rock description	Ore minerals description	
			major minerals	minor minerals
G4	Klecza – northern ore field	quartz vein	aggregate of fine- and medium-grained euhedral crystals of arsenopyrite (0.1-0.4 mm)	base metal sulphides
G-8		quartz-pyrite-arsenopyrite vein, cataclased and overprinted by carbonate and rare base metal sulphides	coarse-grained euhedral crystals of pyrite up to several mm in size; massive arsenopyrite aggregate, and its single crystals from 50 μm to 3 mm in size	rare base metal sulphides with electrum associated with carbonate in fractures occur
S-43	Radomice – southern ore field	cataclased quartz-sericite schists with sulphide cement	massive arsenopyrite aggregate and its single crystals from 10 μm to 3 mm in size	marcasite cutting or replacing arsenopyrite
Ra 11			massive arsenopyrite aggregate and its single coarse- and medium grained crystals from 50 μm to 3 mm in size	fine inclusions of base metal sulphide and electrum in arsenopyrite
Ra 15		zone of the quartz-vein with pyrite impregnation in quartz-chlorite schist	euhedral coarse- and medium grained pyrite, some of grains with poikilitic core fractured and cemented by chalcopyrite	acicular hematite up to 0.5 mm, calcite, rare cobaltite and base metal sulphides, arsenopyrite

senopyrite which represents the first stage of ore precipitation and the second sample – pyrite which belongs to the younger member of the mineral succession (Fig. 42I).

Arsenopyrite from Klecza has arsenic content between 31.5 and 33.4 atom. % As and a constant cobalt admixture from 0.1 to 0.9 atom. %. The G-4 sample of Co-arsenopyrite from Klecza analysed as LLHR (low level highly radiogenic, for explanation see Stein *et al.*, 2000) gave an age value of 316.6 ±0.4 Ma with the assumption of the ratio $^{187}Os/^{188}Os$ equal 0.2.

The second sample treated also as LLHR was pyrite. This pyrite of younger generation gave a Re–Os age value at 278 ±2 Ma with the assumption of ratio $^{187}Os/^{188}Os$ of 0.2 (Tab. 23).

Table 23

Low level highly radiogenic (LLHR) Re-Os data for pyrite and Co-arsenopyrite from the quartz veins in Klecza

Sample	Location	Mineral	Re, ppb (±2s)	^{187}Os, ppb (±2s)	Model age [Ma]
G-8	Klecza – northern ore field	py[2, 4]	58.11(1)	0.169(1)	278 ±2
G-4		Co-asp[1, 3, 4]	310.0(2)	1.030(1)	316.6 ±0.4

Abbreviations: py – pyrite; Co-asp – Co-bearing arsenopyrite

Notes: **1** – LLHR; Os is almost entirely radiogenic ^{187}Os; **2** – Analytical blanks: Re = 1.97 (2) pg; Os = 4.68 (5) pg with $^{187}Os/^{188}Os = 0.182$ (4); **3** – Analytical blanks: Re =2.5 (1) pg; Os = 0.635 (6) pg with $^{187}Os/^{188}Os = 0.190$ (8); **4** – Re–Os data are blank corrected with assumed initial ratio of $^{187}Os/^{188}Os$ of 0.2

DISCUSSION OF THE GENESIS OF THE KLECZA–RADOMICE ORE DISTRICT

Mineralizations in the Klecza-Radomice ore district have been formed during several stages. The oldest stage of late-diagenetic type is mostly represented by framboidal pyrite which occurs often in black siliceous and quartz-graphite schists of the Pilchowice unit. Especially rich in framboidal pyrite are samples of black graphite schist from Klecza. Black schist hosting quartz-sulphide veinlets commonly reveal the framboidal pyrite recrystallization into the younger pyrite generation similar to such feature described from the Radzimowice schists (Sawłowicz, 1987). Presence of well-preserved pyrite framboids indicates rather weak regional metamorphism.

According to various authors (e.g. Kryza *et al.*, 1990) metamorphic processes within the SE part of the Kaczawa Metamorphic Complex reached first blueschist facies (ca. 1 GPa, 300–400°C) and subsequently were overprinted by greenschist facies (600–800 MPa, 350–450°C). Ore mineralization that originated during regional metamorphism is represented mostly by Ti-oxide minerals and pyrite of the 2nd generation associated with rare chalcopyrite and pyrrhotite.

Next stages of the ore minerals crystallization are related to hydrothermal processes from which auriferous arsenopyrite crystallized ca. 317 Ma ago according to Re–Os method. This age of hydrothermal auriferous sulphide event indicates for a late Variscan stage characterised by emplacement of granite intrusion in the Western Sudetes. It followed regional metamorphism of the greenschist facies. Durable tectonic processes in the Intra-Sudetic fault zone (Aleksandrowski, 1995, 2003) were very important for the formation of ore mineralization. Deep fractures within the Intra-Sudetic fault allowed fluid penetration in the folded, metamorphosed and fractured rocks. Multiple movements were responsible for cataclasis of the oldest auriferous pyrite-arsenopyrite mineralization and new fluid migration that caused overprint of younger generation minerals. The first strike-slip movements in the zone of the Intra-Sudetic fault were directed from NW to SE, and caused transposition between the Izera and Kaczawa terranes (e.g. Cymerman, 1998b, 2000; Cymerman *et al.*, 1997). Tectonic strains of strike-slip movements to SE were responsible for fracturing in the rocks of the Pilchowice unit, especially in hinge of folds with vergence to NE, which allowed the hydrothermal fluids migration and mineral formation in opened F_2 fold hinges in schist rock series. Due to such tectonics the characteristic "saddle reef" mineralization formed in Klecza.

Folded and metamorphosed rocks of the Pilchowice unit with regard to their rheological specifications were favourable for fluid migration, however, layers of graphite schists were impermeable and were a seal of geochemical traps for mineralised hydrothermal fluids. The heat-flow connected with late Variscan granitic pluton was very important for fluid migration within fracture zones.

The type of ores, admixture of trace elements in sulphide ores, sulphur isotopic composition of sulphides, fluid inclusions composition (C–O–H–N) as well as the rocks alteration suggests a common magmatic-metamorphic origin of hydrothermal fluids. Hydrothermal processes responsible for auriferous sulphide mineralization caused strong alteration of the host rocks. Especially, graphite and quartz-graphite schists

were first cataclased and further strongly silicified, sericitized, carbonatized, turmalinized and albitized.

Mineralization zones are hosted in quartz-sericite-graphite schists. Graphite schist with their layer anisotropy favoured fluid circulation as these schists host numerous quartz veins. Common presence of organic matter and graphite has been recognised in the studied samples from Klecza– Radomice ore district. Contents of TOC range from traces up to 20%. Most probably graphite formed either by metamorphism of organic matter from clay and mud beds and later by hydrothermal fluids that caused carbon recrystallization and redistribution (Pls. IX, 4; X, 1). Carbon presence in country rocks reacted with water from fluids to produce carbon dioxide and methane according to reaction: $2C+2H_2O = CO_2+CH_4$.

Presence of methane decreases the oxygen fugacity and destabilizes gold complex causing gold precipitation (Cox *et al.*, 1991; Dubè, Lauzière, 1997). Methane was always recognized in fluid inclusions (up to 10%) in the gray quartz within most of the auriferous samples from Klecza–Radomice ore district. Graphite schists with their reducing character, acted as preferential site for gold precipitation. Additionally, in graphite schist framboidal pyrite occurs that could supply iron, which reacted with sulphur transported by the hydrothermal fluid to produce new generation of Au-bearing pyrite. Pyritization always cause reduction of sulphur activity and destabilization of gold complexes that induce gold precipitation paragenetically with pyrite (Dubè, Lauzière, 1997).

The correlation between gold and sulphur as well as common occurrence of gold inclusions in pyrite and arsenopyrite of the first ore stage mineralization, suggests that gold was transported as reduced bisulphide complexes $Au(HS)_2^-$. However, the composition of fluid inclusions indicates for chloride complexes as gold transporting during next stages of Au precipitation. The loss of H_2S from fluid resulted in the decrease of sulphur activity in the residual hydrothermal fluid inducing gold precipitation.

Primary fluid inclusions in different generations of auriferous quartz from rock samples from the Klecza–Radomice ore district revealed the presence of moderate to low saline two-phase aqueous fluids with CO_2, N_2 and CH_4.

Reported crystallization temperatures for the refractory sulphide-bearing gray quartz ranges from 340 to 270°C with the salinity of fluids of about 10 ±3 wt % NaCl equivalent and pressure of 1.0 ±0.2 kbar. The spatial geometry of the primary mineralized zones in quartz veins and lodes has been disrupted by late brittle deformation events. Multistage brecciation and silicification can be evidenced. They resulted in post-mineralization faulting with fracturing and base metal mineralization associated with carbonates and electrum as fracture filling followed by a low temperature hydrothermal acidic fluid circulation responsible for chalcedony, kaolinite, marcasite/pyrite and intergranular gold crystallization.

Minor base metal sulphides represent the second stage of hydrothermal ore mineralization. This stage of base metals overprint and microscopic gold precipitation is connected with raising the whole mineralized zone to shallow depth coeval with formation of intramountain basins and movements to NW in the Intra-Sudetic fault (Aleksandrowski, 1995; 2003; Aleksandrowski *et al.* 1997). Sphalerite crystallization indicated deposition from reduced, near-neutral hydrothermal solution with chloride (Cl^-) as the principal metal ligand (Henley, Brown, 1985). Electrum is associated with galena, chalcopyrite and sphalerite as well. At Klecza–Radomice ore district there is a very low content of base metal sulphides in ore. According to McCuaig, Kerrich (1998) the low concentration of base metals in majority of lode gold deposits is mostly connected with the low-salinity mineralizing fluids which caused complexing of Au, Ag, As and other associated elements by sulphur. White quartz associated with microscopic gold, base metal sulphides, and carbonates crystallized at temperatures from ca. 280 to 240°C from fluids of salinity of 7 ±2 wt % NaCl equivalent and at pressure 0.8 ±0.1 kb.

The Re–Os age of pyrite from Klecza ca. 280 Ma indicates for possible correlation of the epithermal ore stage crystallization with volcanic activity during Autunian. The volcanic environment is also suggested by presence of gold in paragenetic association with chalcedony, kaolinite and opal recognized as 3rd stage of low temperature mineralization in Radomice. In the subsurface level the reduced, near-seven pH solution containing NaCl, CO_2 and H_2S underwent boiling due to rapid decompression related to the hydrothermal brecciation. Boiling caused separation of H_2S gases from the mineralizing solution (White, Hedenquist, 1995). H_2S-rich vapour may condense in the vadose zone to form steam-heated, slightly acidic water with a pH of 2–3. Evidence of such strong acidic alteration is best visible in sample R-79 shown on Fig. 41. Presence of SO_4^{-2} explains the formation of kaolinite and illite minerals in acid-sulphate environment during chalcedony precipitation in Radomice. Degassing decreased the solubility of gold in the solution in the form of $Au(HS)_2^-$, which resulted in gold precipitation (Cooke, Simmons, 2000). Evidence of boiling in Klecza–Radomice ore district may be suggested by bladed textures of carbonates, intense hydrothermal brecciation, and common presence of kaolinite and illite minerals.

In Nielestno and Klecza an oxidation environment was recognised instead of strong reducing environment. Hematite appears commonly as well-developed platy crystals in paragenetic association with chalcedony and calcite.

The areas along the Pławna fault contact directly with Lower Permian sediments. It is difficult to estimate definitely the relative age correlation between formation of chalcedony paragenetic association with free gold and hematite and chalcedony associated with free gold, kaolinite and marcasite. Probably, formation of these paragenetic associations could be even coeval, however in various pH conditions. Oxidative conditions prevailed in the rocks directly contacting with the Pławna fault zone (e.g. Klecza, Nielestno) that constitute the southern edge margin of the Wleń trough.

At Klecza–Radomice ore district the appearance of weathered zones of the primary sulphide mineralization is a peculiar problem not considered in this work. According to mining reports, the gossan was also an exploited gold source. Especially, in the Nielestno area specimens of such weathered rock have been collected.

THE GOLD-BEARING QUARTZ-SULPHIDE OCCURRENCES IN THE KACZAWA MOUNTAINS

In the Kaczawa Mountains beside the earlier described deposits in the Radzimowice and Klecza–Radomice ore districts, there occur several sites with auriferous quartz-sulphide mineralization. Some of them were shortly but intensive exploited, other have only mineralogical importance.

THE WIELISŁAW ZŁOTORYJSKI ORE DISTRICT

The Wielisław Złotoryjski settlement lies near Sędziszowa village, about 10 km SSW from Złotoryja; on the northern and the western slopes of Wielisławka Hill (+375 m a.s.l.), which belongs to the Kaczawa Mountains. The Wielisław Złotoryjski deposit occurs in the tectonic structure called the Świerzawa horst that on the north is separated from the Jerzmanice trough by the ENE–WSW oriented fault and on the south from the Świerzawa trough by NE–SW trending Sędziszowa fault (Milewicz, Kozdrój, 1994a).

This deposit comprised few small-size quartz veins with gold-bearing sulphides in the contact zone between the Paleozoic metasedimentary rocks and quartz rhyolite porphyry of the Lower Permian age (Fig. 60). The complex of the Paleozoic schist unit is interpreted as mélanges from Janówek and Różana (Haydukiewicz, 1987a). These mélanges are built of chaotic blocks of Silurian and Devonian rocks of black, gray or green metamudstones and metaclaystones surrounding by Lower Carboniferous slates.

The primary gold-bearing mineralization at Wielisław Złotoryjski was considered to be one of the main sources of gold in alluvial sediments of the Złotoryja gold placer deposits, from which only during the years 1175–1240 about 6 t of gold was recovered (Domaszewska, 1965). The oldest known information concerning mining operation in the Wielisław Złotoryjski area is from 1556, when the concession for gold exploitation was granted to Duke Ferdinand and about 15 kg of gold was recovered (Zöller, 1923). The mining operation was kept until 1711, when the next concession was issued for gold prospecting and exploration. However, in the following few years mining activities collapsed (Quiring, 1948). Fedak, Lindner (1966) mentioned production of gold-bearing sulphide and silver-bearing galena, and limonite ore in the 19th century.

Gold exploration began on the northern slopes of the Wielisławka Hill, at about 135 m above the level of Kaczawa River valley (Figs. 61, 62). The western part of the gold-bearing veins was explored by three adits. These adits are oriented oblique to the run of Silurian siliceous schists and along the vein's strike of NW–SE direction. The metamorphic rock unit dips at the angle of about 50° to NW. Sulphide mineralization forms disseminated impregnations and nests in veins of NW–SE strike and of dip to NE at the angle 50–60° and also impregnation in their surroundings (Zimmermann, 1918). The veins were recognized down their dip to 70 m below surface. The host rocks found in the adits are represented by argilla-

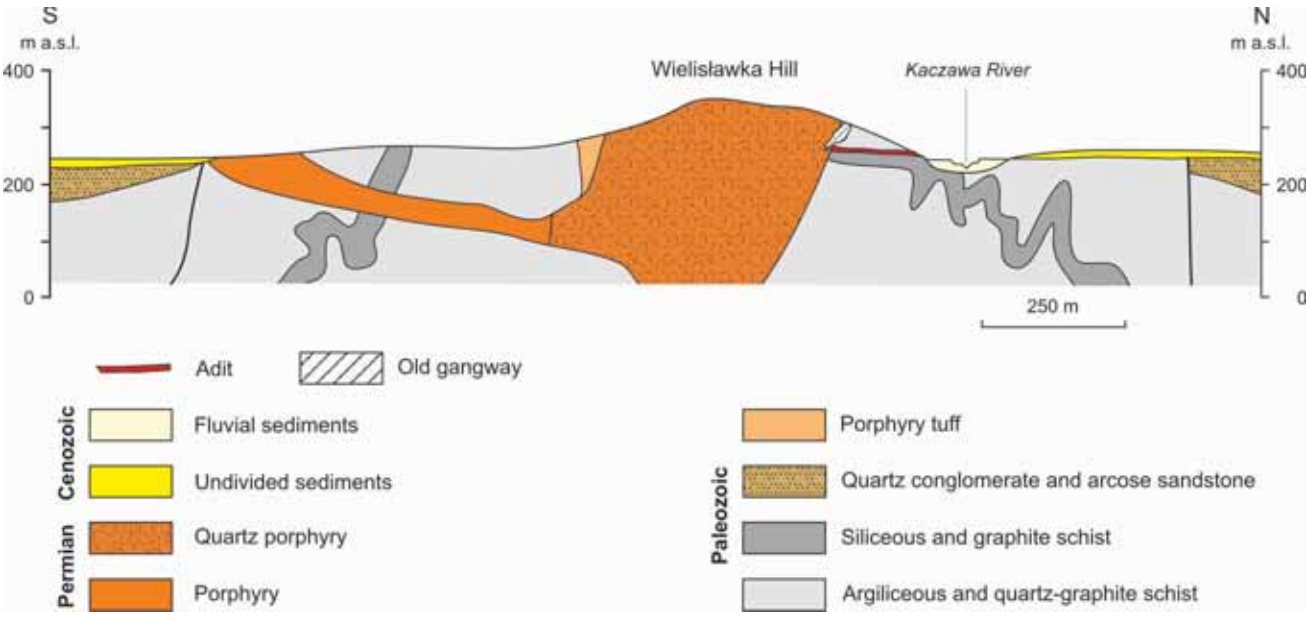

Fig. 60. Geological cross section through the Wielisławka Hill in Wielisław Złotoryjski (after Zimmermann, Kühn, 1929)

The location of the workings modified from Zöller (1936)

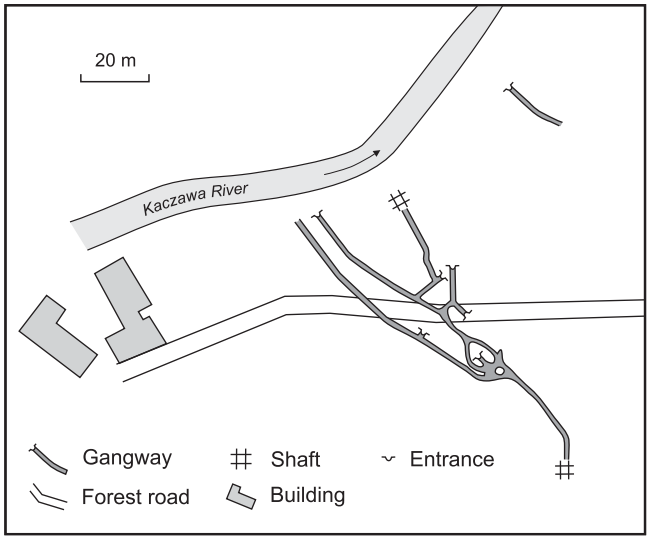

Fig. 61. The sketch plan of the underground workings in the Wielisławka Hill near Wielisław Złotoryjski (after Zöller, 1936)

ceous and graphite schists. The argillaceous schist is soft, finebedded, light gray, with silky lustre. It often contains red iron-oxide injections and fine granules within fissures. The siliceous schists are black, locally light red and cut by white quartz veinlets (up to a few cm in thickness) that contain fine sulphide grains (up to a few millimetres in diameter).

Permian rhyolites are best outcropped in the Organy Wielisławskie abandoned quarry located on the south-western slope of the Wielisławka Hill (Jerzmański, 1956; Fig. 63). Rhyolites are massive or porous and have well developed vertical jointings. They have porphyritic texture with spherolitic matrix composed of allotriomorphic matrix of quartz and potassic feldspar. In matrix occur phenocrysts of quartz, K-feldspar, plagioclases, biotite and also fine-crystalline hematite. Kaolinite pseudomorphs after plagioclases occur commonly. Biotite and K-feldspars are weathered. Sulphides are absent. On the diagram of the total alkali-silica after Le Maitre *et al.* (1989) 4 rock samples from Wielisławka Hill are located within the field of rhyolite and 2 samples in tephrite, basanite field (lamprophyre; Fig. 9A).

In the Wielisław Złotoryjski abandoned Au mine the main sulphide mineral was pyrite. At least three generations of pyrite mineralization is possible to recognise here. The oldest one occurred in graphite schists as very fine framboids from 2 to 10 μm in size. The pyrite framboids recrystallized into medium-grained anhedral pyrite of the second generation. Beside pyrites in graphite schist appear pyrrhotite (as single and very fine crystals) and chalcopyrite (as single grains up to 30 μm in size). These sulphides are commonly replaced by Fe-hydroxides. The processes were especially well developed in the western side of the Wielisławka Hill. Often chalcopyrite core is surrounded by covellite rim. Zimmermann, Kühn (1938) reported from here also turquoise ($CuAl_6[(OH)_2/PO_4]_4 \times 4H_2O$) and cacoxenite ($Fe^{3+}_4[OH/PO_4]_3 \times 12H_2O$). In graphite schists Ti-oxides and graphite commonly occur. Ti-oxides form elongate aggregates up to 2–3 mm in length. Such Ti-mineral aggregates were observed along a quartz vein that cut siliceous schist. In quartz-sericite schists commonly occurs very narrow veinlets of Fe-hydroxides that cut laminas or even coarse crystalline quartz veins. Black schists are built of quartz, sericite, chlorite, albite, organic matter, Fe- and Ti-oxides and pyrite (locally up to a 15% of 5 cm thick lamina; Milewicz, Kozdrój, 1994b).

In the quartz veins appears coarse-grained euhedral pyrite in association with rare arsenopyrite and base metal sulphides. Arsenopyrite and pyrite are cataclased and cemented by the younger generation base metal sulphides such as chalcopyrite, galena and sphalerite. The occurrence of gold formation appears to be additive mixture in pyrite. Pyrite occurs in quartz veins and as impregnations in the schist. The reported pyrite ore had an average about 18 ppm Au. Galena has about 64 ppm Ag. The sulphide ore were crushed and treated by amalgamation process (Zöller, 1923). Host rocks represented by siliceous and quartz-graphite schists contained also gold from traces up to 0.5 ppm. Single fine-grain of gold was found in fractured quartz-graphite schists. This confirmed the informa-

Fig. 62. The old entrance to the abandoned mining adit on the Kaczawa River bank at Wielisław Złotoryjski

Fig. 63. The outcrop of the Permian subvolcanic rocks of the Organy Wielisławskie near Wielisław Złotoryjski

tion given by Zöller (1923) about the findings of native gold flake in the cataclased black siliceous schist.

The surface rock sampling for gold was also carried out in the southern metamorphic cover of the Permian porphyries from Różana to Świerzawa. Range of Au contents in black graphite schists is from <1 to 67.6 ppb (Tab. 24). An arithmetic average of Au in graphite schist is 9.2 ppb (std. = 16.8; n = 15). Average value of Au in quartz-sericite (muscovite) schist is 6.7 (std.= 5.5; n = 7; range from 2 to 15.7 ppb). Au contents in rhyolite porphyry from Wielisławka Hill range from 1 to 2 ppb and in lamprophyre samples was below 1 ppb.

The detailed studies of sulphide mineralization at Wielisław Złotoryjski deposit were not made till present, but its genesis was considered as hydrothermal mineralization connected with post-magmatic activities of Variscan epoch (Fedak, Lindner, 1966). During the 2nd cycle of the Rotliegende formed deep regional fractures that allowed for the emplacement of rhyolite magma and andesite lavas from the Wielisław Złotoryjski area. The next stage of the faulting was connected with the Saal phase of the late Variscan orogeny that underwent between the 2nd and 3rd cycle of the Rotliegende (Milewicz, 1987). In the mining waste also lamprophyre dykes were found, but its geologic position is unclear. The geologic and tectonic positions of the quartz veins, suggests that auriferous pyrite and silver-bearing galena mineralization are related to the one or two Rotliegende magmatic-volcanic events. The formation of native gold grains in association with chalcedony and hematite rarely observed in Wielisław Złotoryjski may form during development of volcanic processes in upper Rotliegende or even later.

Table 24

Arithmetic average of gold contents in barren rocks from various tectonic units in the Kaczawa Metamorphic Complex

Tectonic unit	Lithology	Range	Arithmetic average of Au contents	Number of samples
Rzeszówek–Jakuszowa	Greenstone	2–4.3 ppb	3.3 ppb	5
	Quartz schist	2–6 ppb	4 ppb	2
Che³miec unit:				
Che³miec–Mêcinka region	Quartz-siderite vein with sulphide	<1–1010 ppb	51.3 ppb	32
	Host rocks	<1–2 ppb	1 ppb	9
Wilcza area	Hematite veins	<1–3 ppb	1.3 ppb	4
Stanis³awów area	Barite veins	<1–9 ppb	2.2 ppb	6
	Metapelite, metaclay	2–14 ppb	4.3 ppb	9
	Diabase, greenstone	0.5–11 ppb	4.2 ppb	6
Mélange:	Graphite schist	1–67.5 ppb	9.2 ppb	15
Lipa–Grudno area				
	Hematite ores	0.6 ppm	0.6 ppm	2
	Porphyry	0.01–0.02 ppm	–	1
Œwierzawa area	Diabase	2.3–3.7 ppb	3 ppb	2
	Graphite schist	<1–67.6 ppb	20.1 ppb	6
	Quartz schist	2–15.7 ppb	8.9 ppb	3
Ró¿ana area	Graphite schist	0.5–66.5 ppb	20.1 ppb	6
Z³otoryja area	Quartz-sericite schist	2–6 ppb	3.6 ppb	4
Konradów area	Graphite±quartz schist	3.7–5 ppb	4.7 ppb	4
Radzimowice schists:				
Wojcieszów area	Greenstone	<1–6.4 ppb	3.1 ppb	4
	Quartz-sericite schist	<1–8 ppb	3.1 ppb	12
Radzimowice deposit	Barren rock	<0.5–49.3 ppb	12.9 ppb	10
Bolków unit:				
P³awna area	Sericite schist	<1–27.6 ppb	5.5 ppb	9
Wleñ–Bystrzyca area	Siliceous schist	<1–20.2 ppb	6.9 ppb	5
	Quartz-sericite schist	<1–7.6 ppb	3.2 ppb	6
Radomice area	Barren rock	0.185–0.76 ppm	0.5 ppm	3
Nielestno–Pilchowice area	Black graphite schist	1.1–29.7 ppb	4.6 ppb	10
	Quartz-sericite schist	<1–7.9ppb	2.8 ppb	4
	Siliceous schist	<1 – 1.7 ppb	0.8 ppb	4
Radomierz area	Graphite-siliceous schist	< 1 –59.9 ppb	28.9 ppb	4
Mys³ów–Grochowice area	Quartz schist	2–3 ppb	2.7 ppb	7
	Greenstone	0.8–5.1 ppb	2.3 ppb	3
Dobromierz unit:				
Dobromierz area	Greenstone	1.7–5.3 ppb	3.2 ppb	6

THE LIPA–GRUDNO PROSPECTS

Several quartz-sulphide veins and sulphide impregnations within vein salbands occur in the region located about 3 km north-eastwards from the Radzimowice deposit (Zimmermann, Haack, 1935; Paulo, 1962). Ore mineralization in the Lipa–Grudno vicinities formed due to hydrothermal processes connected with Karkonosze granitic pluton emplaced somewhere at depth (Petrascheck, 1933; Manecki, 1965; Zimnoch, 1965; Fedak, Lindner, 1966) or regional metamorphism (Manecki, 1965). Paulo, Salamon (1974b) compared minerals composition and tectonic positions of ore veins from here with other quartz-sulphide veins from Klecza–Radomice and from Chełmiec–Stanisławów and concluded that ore veins from Grudno and Lipa are younger than Żeleźniak porphyry. Abandoned mining workings are recognizable e.g. at Lipa and on the Hill +423.7 m a.s.l. near Grudno. The surface prospecting works in these areas allowed recognising associations of minerals similar to those of the Radzimowice deposit with additional hematite veins (Paulo, 1962; Fedak, Lindner, 1966; Paulo, Salamon, 1973b).

The archive materials suggest that at Lipa at least two different types of ore veins, having variable minerals composition, strike and depth occur. The first one probably older has strike of W–E direction and consists of quartz sulphide mineralization (Zimmermann, Haack, 1935; Teisseyre, 1974, 1977). The second one is situated along N–S direction, and is built of hematite (thickness from 1.5 to 4 m and length about 100 m; Fedak, Lindner, 1966). Near Grudno on the unnamed hill the quartz-sulphide vein of W–E direction also occurs (Paulo, Salamon, 1973b; 1974b). All these veins are small (ca. 100–200 m long and several cm thick) and hosted by the Paleozoic rocks of the Bolków unit that consists there of the Radzimowice schists, greenstone, and the Wojcieszów limestones (Fig. 64). Among the ore minerals from the W–E trending veins dominate strongly cataclased arsenopyrite and pyrite cemented by base metal sulphides (Paulo, Salamon, 1974b). Moreover, in Grudno mineralization of sulphosalts of Ag, Cu, and Sb and As and stibnite also appears (Paulo, Salamon, 1973b).

According to the microscopic investigation in cataclased euhedral arsenopyrite crystals (up to 2 mm in size) and in quartz from Grudno, a single inclusion (insert) and fine-grain of electrum (<5 μm in diameter; from 25 to 30 wt % Ag.) appeared. Beside electrum, the native bismuth and bismuthinite form also inclusions in arsenopyrite. Gold content in these rocks is ca. 3 ppm. Much lower contents of Au were determined in quartz veins from Lipa. These samples with poor sulphide impregnation contained <100 ppb Au and microscopic gold was not recognised. Relatively, high gold concentration (0.6 ppm) appeared within samples of hematite veins collected on the fields along the Lipa–Mysłów main road. These hematite samples contained also Ag (from 12 to 17 ppm) and metallic elements (Cu, Zn, Pb and As from 0.1 to 0.4 wt %) and a constant Co admixture (~300 ppm) and traces of Bi (<20 ppb).

According to the present study the auriferous sulphide mineralization in veins from Grudno and Lipa is classified to the 1st stage of the hydrothermal mineralization (similar to Radzimowice deposit). In regard to mineral composition and tectonic position the hematite mineralization in veins from Lipa is classified to the younger low temperature hydrothermal processes probably connected with Autunian volcanism.

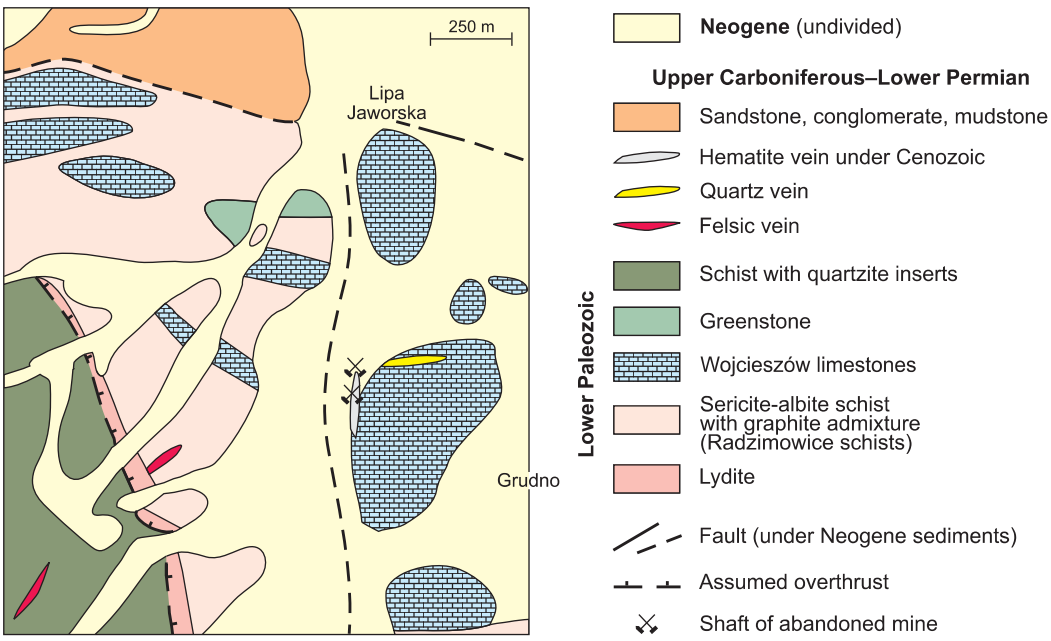

Fig. 64. The simplified geological map of the Lipa–Grudno area (after Teisseyre, 1974)

THE PŁAWNA PROSPECT

In the Pławna area numerous quartz veins with gold-bearing sulphide are hosted by Silurian schists of the Kaczawa Metamorphic Complex, which contacting on the north with Rotliegende sediments and on the south with Izera granite-gneiss. The occurrences of auriferous mineralization in the vicinities of the Pławna village are most probably the north-westward extension of the gold mineralization known from Klecza–Radomice ore district. The Silurian fine-laminated schists belong to the Pilchowice unit that consists here of quartz-sericite schists, partly feldspatized, quartz-muscovite schists with graphite, and inserts of crystalline limestones, calcareous shales, greenstone-chlorite shales and quartz veins (Fig. 36). Thick bed of black graphite schists with arenaceous shales are mapped in the northern part of the unit, however numerous thin intercalations of graphite schists are recognized in the whole unit (Gierwielaniec, 1956). These rocks are intensely folded with major NW–SE direction of fold axes. Folds are of the thrust-sheets character with vertical overthrust (*op. cit.*).

The mining operation began in 1893 when gold was found during the train rail construction between Pławna and Lubomierz (Rosenberg, Lipinsky, 1896, 1897). Gold occurred in association with sulphide in quartz veins (*op. cit.*). The Pławna deposit consisted of three ore fields. The Otilia field was located in the vicinity of Pławna Dolna village. The small fields Eureka and Kätchen were nearby, but closer to Milęcice. The prospecting and exploitation works were carried out in all the ore fields until 1898, except for the Eureka mine, which operated until 1906 (Domaszewska, 1964). The exploitation was carried out from the open pit, then by shallow shafts and short underground workings. The Eureka field was mined by use of the exploration shaft down to 18 m. The host rocks are represented by fine-bedded argillaceous schists, greenstone slates, quartz-phyllites, coarse-grained sandstones and dark graphite schists. These rocks strike in NW–SE direction and dip almost vertically. The quartz veins also had almost vertical dip and in general N–S strike. They had various thicknesses and were recognised only at shallow levels, mostly due to a high quantity of water inflows into workings.

Sulphide mineralization appeared as nests or impregnation in quartz veins, in their surroundings and in fractured zones filled by gray-blue tectonic clays. Moreover, from the Otilia mine the massive arsenopyrite body (with content of Au up to 8 ppm and As up to 26 wt %) close to quartz vein was reported. In the considered deposits quartz and carbonates were gangue minerals. The compositions of the gold-bearing ore minerals varied between mines. In the Eureka mine pyrite prevailed, while arsenopyrite was a major source of gold in the Otilia and Minna mines (Morsey-Pickard, 1898). In the Marcus mine arsenopyrite and galena were exploited. Beside that chalcopyrite, sphalerite and chalcocite occurred (Fedak, Lindner, 1966). The main vein in the Otilia field was almost vertical with N–S strike and had thickness from 0.15 to 0.66 m. It was explored 8 m below its surface (Morsey-Pickard, 1898). Eureka field was richest in gold (Au – 139 ppm; Ag – 20 ppm; Sb – 0.1 wt %; As – 0.1 wt %; S – 4.0 wt %; Morsey-Pickard, 1898). Gold concentration in quartz veins from the Otilia mine varied from 6 to 75 ppm, silver from 6 to 16 ppm and arsenic from 20 to 32 wt %. Gold concentration in sulphide-bearing veins at the Kätchen field were in samples from the surface outcrops from 4 to 9 ppm, and increased in samples from the deeper sites (Fedak, Lindner, 1966). Gold was only found by chemical analyses not in native form. It was believed to occur as submicroscopic admixture mostly in pyrite, and arsenopyrite. In the Otilia mine the gold to silver ratios in ore varied from 7:1 to 1:3 and an arithmetic average of the ratio was 2:1 (Fig. 65).

During limited surface-prospecting works several samples were collected within outcrops of the railway crosscut near Pławna Górna. Quartz-sericite and graphite schists contained only traces of sulphide mineralization and accessory oxide mineralization (e.g. hematite and titanite). An arithmetic average of Au contents in these barren schists is 5.5 ppb (n = 9; Tab. 24). On the geological map after Gierwielaniec (1956) about 2 km north-westward from Pławna there occurs a quartz vein of NW–SE strike, hosted by Silurian schists. In this quartz vein only rare and very fine disseminated pyrite was found, however without detectable gold.

Genesis of gold-bearing ore mineralization at Pławna was considered as of hydrothermal, similar to other gold-bearing quartz-sulphide vein type deposits from the Klecza–Radomice ore district (Fedak, Lindner, 1966). These small mines in the Pławna area were closed just after few years of exploitation. The main reasons for production cease were probably the difficult conditions of ore exploitation due to its vertical dip, possible small thickness of ore zone and difficult condition of the subsurface water. However, geologic position of veins allowed considering this area as a very promising target for modern gold prospecting. Moreover, recent alluvial sediments revealed increased concentration of placer gold at Lubomierz and Pławna vicinities (Jęczmyk *et al.*, 1977).

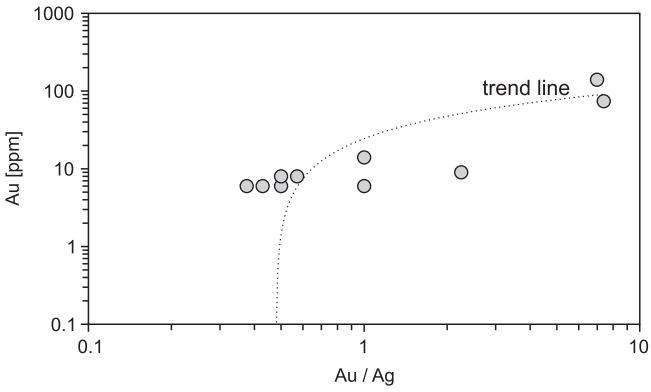

Fig. 65. Gold to silver ratio in the Otilia gold mine from the Pławna area (data after Morsey-Pickard, 1898)

THE CHEŁMIEC, MĘCINKA, WILCZA AND STANISŁAWÓW DEPOSITS

In the NE part of the Kaczawa Mountains in the Chełmiec unit at least 14 veins are well known (Fig. 66). Mineral compositions of veins within considering deposits are different and even changeable in specific veins along run and strike (siderite, hematite, barite and fluorite, quartz, carbonate, sulphide).

The area between Chełmiec and Sichów gave small Cu, Ag and Pb production since 16th to 18th century, Fe ore (hematite, and siderite) was exploited in the second half of the 19th century, and barite after the II World War (e.g. Petrascheck, 1933; Neuhaus, 1936; Paulo, 1970, 1973, 1994). These veins have different thickness (0.3–8 m) and length (0.3–1 km). They strike in general to NW–SE and dip from 50 to 80° to SW (Jerzmański, Kura, 1965; Jerzmański, 1965; 1976b; Paulo, 1972; 1973). Host rocks are represented mainly by Ordovician light-grey sericite ± chlorite ± quartz schists and Silurian dark-grey graphite schists with pyrite impregnation and by inserts of lydite, greenstone and diabase rocks (Ordovician–?Devonian).

Several samples from each abandoned mine dumps at Chełmiec, Męcinka, Wilcza and Stanisławów were collected for gold determination (Mikulski, 2000c; Dąbrowski, 2002; Proniewicz, 2002). A gold content in 70 samples (siderite, quartz, sulphide, carbonate and hematite veins, and poor in sulphide mineralization rocks) is low from 0.5 ppb to ca. 1 ppm (Tab. 25). Arithmetic average for Au is 24.8 ppb (n = 70; Fig. 67). Gold has a high positive correlation with arsenic, cobalt and nickel (r = 0.95).

Similar positive correlation of Au with As, Co and Ni occurred in veins from Męcinka–Chełmiec (veins: Dębowa, Olejna and Główna) and for diabase from Stanisławów. In the Olejna vein in two samples is relatively high Au content: 120 ppb and 1.01 ppm (Fig. 68). The Olejna vein cuts quartz-sericite schist, phyllite and epidiabase. This vein has strike ca. 135° and dip at 70° to SW. Its length is from 0.8 to 0.9 km and thickness about 0.6 m (Jerzmański, 1969). The vein is composed by siderite and goethite (limonite) with quartz and pockets of chalcopyrite, chalcocite, and rose-colour calcite associated with galena, sphalerite and marcasite (Jerzmański, 1969; Paulo, 1970). The Olejna vein also contained high concentrations of As (up to 11. 4%), Ni (to 4.9%) and Pb (even up to 21.4%). Microscopic observations moreover evidenced abundant gersdorffite and cobaltite with arsenopyrite and pyrite in this vein. Appearance of gersdorffite correlates with increasing concentration of Au (~1 ppm). Gersdorffite forms aggregates of anhedral crystals up to few centimetres in diam-

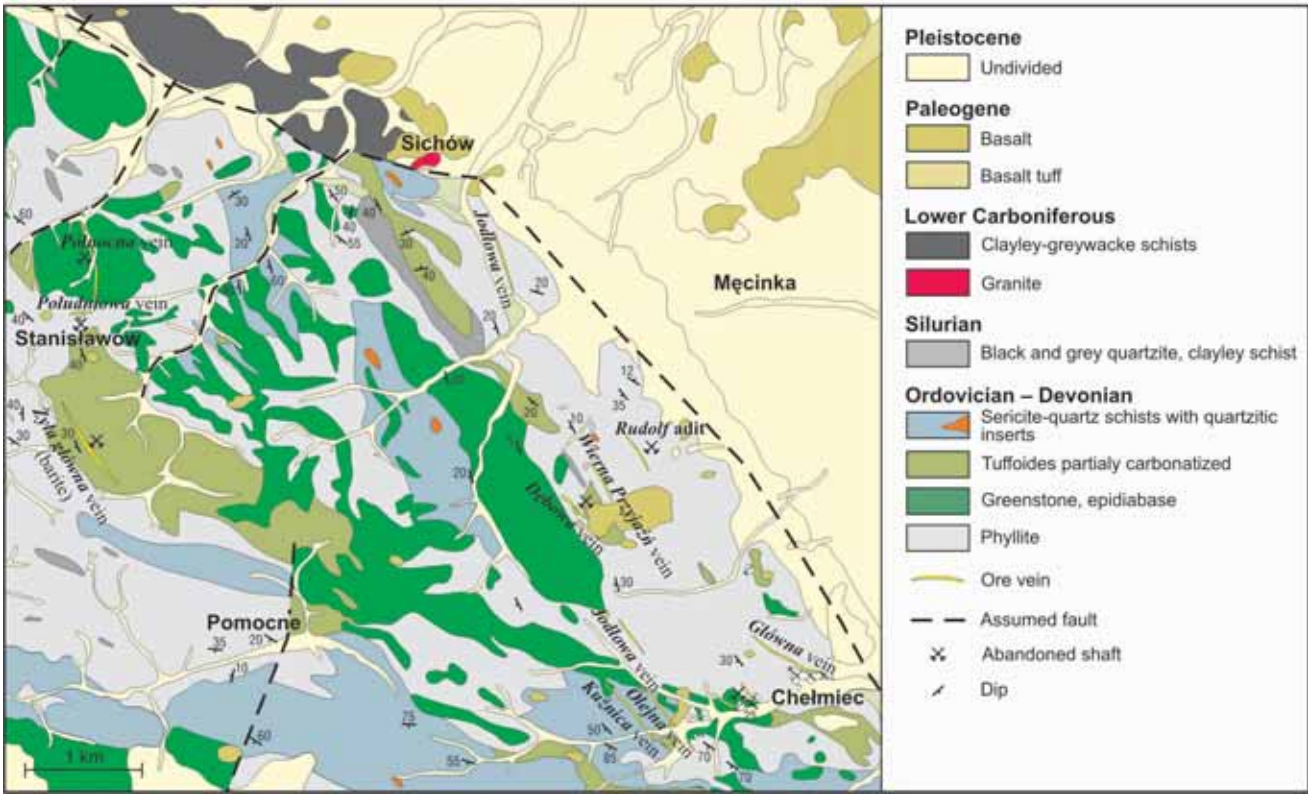

Fig. 66. Location of veins in the Chełmiec unit (after Paulo, 1973) on the geological map (after Jerzmański 1955; Jerzmański, Walczak-Augustyniak, 1993)

Table 25

Arithmetic average concentrations of the selected elements in veins from the Męcinka, Chełmiec, Stanisławów and Wilcza deposits

Location		Mêcinka	Che³miec			Stanis³awów	Wilcza
Vein name (number of samples)		Dêbowa vein (20)	G³ówna vein (3)	Olejna vein (8)	KuŸnica vein (5)	Barite vein (6)	Hematite vein (4)
Au [ppb]	range	0.5–344	0.7–1	0.5–1010	0.5–1	0.5–9	0.5–3
	arithmetic average	23.60	0.9	145.9	0.7	2.2	1.3
Ag [ppm]	range	2.5–99	1.5–10	3–80	1.5–6	1.5	1.5–10
	arithmetic average	15.8	6.2	22.6	3.6	1.5	6.9
Pb [ppm]	range	1.5–3221	55–1764	115–214519	9–51	2–6684	20–40
	arithmetic average	346.7	944	36384.4	20.6	3821.3	33.5
Cu [ppm]	range	43–12317	87–1638	2.5–4726	20–1608	9–553	2.5–45
	arithmetic average	2055.7	730.1	796.1	406	210.3	21.4
As [ppm]	range	5–8700	1.5–71	26–113903	3–35	99–1548	160–1607
	arithmetic average	1743.3	15.1	15811.6	22.6	384.8	826.5
Ba [ppm]	range	5–214	46–187	78–1886	13–202	122880–279543	35–9660
	arithmetic average	68.50	95.3	376.3	92	206933.7	2598
Fe_2O_3 [%]	range	12.6–80.8	0.7–77.7	0.6–8.6	1.8–20.7	0.2–17	75.6–92.8
	arithmetic average	38.7	27.2	3.5	9.3	5.8	82.5

eter in quartz vein and much smaller impregnations in its wall rock. Pyrite crystals are strongly cataclased and cemented by quartz. Gersdorffite forms intercalations with cobaltite. Cobaltite also appears with pyrite that may overgrow cataclased gersdorffite. Arsenopyrite occurs sporadically as fine inserts within chalcopyrite associated with pyrite and in Męcinka as fine crystals (<0.5 mm) of prismatic habit. Gold concentration in the Olejna vein wall rock is from <1 ppb to 27 ppb. In metamudstone there occurs abundant framboidal pyrite impregnation especially in laminas richer in organic matter.

Northward from Chełmiec near Górzec Hill of Męcinka, three veins with similar strike, dip and length (up to 0.5 km) and with variable thickness from 1 to 4 m occur. They are quartz-siderite veins with sulphide mineralization hosted by sericite-chlorite schists. Gold concentration ranged there from <1 ppb to almost 350 ppb. The highest Au contents, however still low, occur in the Dębowa vein (arithmetic average = 23.6 ppb; n = 20). Gold has positive correlation with Co (r = 0.86), Ni (r = 0.81) and As (r = 0.56). Microscope studies of quartz-siderite veins allowed to identify mainly base metal sulphides and microscopic gold was not found.

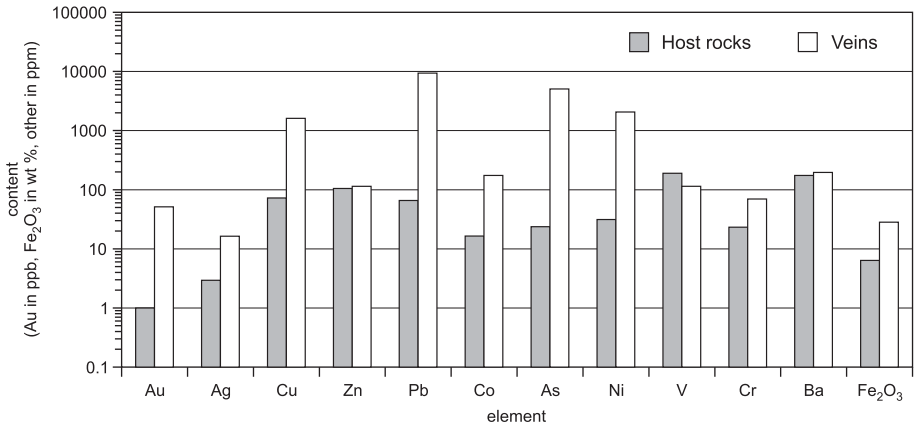

Fig. 67. Comparison of the average arithmetic values of selected elements distribution in host rocks and veins from the Męcinka, Chełmiec, Stanisławów and Wilcza areas

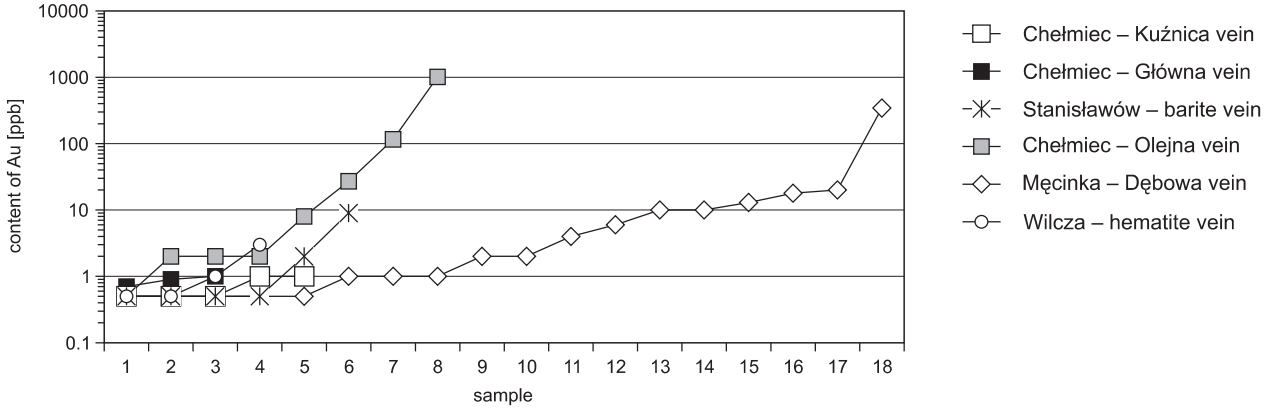

Fig. 68. Comparison of the gold distribution in samples from the veins in the Męcinka, Chełmiec, Stanisławów and Wilcza areas

Concentrations of gold in veins and rocks that belong to the Chełmiec unit are low. Gold has variable correlations with other elements that indicate its relative accumulation during formation of As–Co–Ni sulphide (mainly arsenopyrite-gersdorffite-cobaltite system – similar like from Przecznica in the Kamienica Range described by Piestrzyński *et al*., 1992) and complete lack of Au precipitation during formation of low temperature barite and/or hematite association.

POLYMETALIC DEPOSITS IN THE INTRA-SUDETIC FAULT ZONE

In the SE part of the Kaczawa Mountains northwards from the Intra-Sudetic fault between Radomierz and Świdnik, exploitation of base metal sulphides was carried out from 16th to the beginning of the 19th century, (Dziekoński, 1972). As an example, in the years 1791–1911 in the Dorothea mine located about 0.5 km northwards from the Miedzianka deposit Pb exploitation were carried out. Near Radomierz in 1794–1806 produced ca. 25 t of lead and small amount of refined copper and silver (*op. cit.*).

In the vein quartz samples collected on the old tailings of the Dorothea mine gold contents was from traces up to 134 ppb. In microscope beside galena, chalcopyrite, sphalerite, pyrite, bornite, Bi-sulphosalts and secondary minerals were also found (Kłosiewicz, 1987). Greenstone schists of the Dobromierz unit (Baranowski *et al.*, 1990) and rhyodacite porphyry vein are host rocks of these ores.

Greenstone from the vicinities of Kaczorów and Radomierz revealed slight enrichments in gold up to 50 ppb. Usually, range of Au contents in greenstone is from 1.7 to 5.3 ppb (arithmetic average is 3.2 ppb; n = 16). Greenstone with disseminated pyrite mineralization revealed traces of gold from 4 to 5 ppb. Gold contents in black graphite schist from the Radomierz adit were from 1.9 to 59.9 ppb, and in one lydite sample 45 ppb, respectively. Black schist also has increased contents of As up to 0.2%.

An increased gold concentration in black shales and lydites from Radomierz confirmed observation from other areas of the Kaczawa Mountains that black schists occurring within regional shear-zones are preferable trap for gold mineralization. In the considering area the regional shear-zone occurs which is interpreted by Cymerman (2002) as the overthrust zone called as the Kaczawa line or according to Seston et al. (2000) as a regional shear zone (so called the Kaczorów shear-zone).

In the nearest southern vicinity of the Intra-Sudetic fault the Miedzianka–Ciechanowice Cu mining district occurs (Fig. 69). Polymetallic sulphide mineralization is dominated there by copper ores occurring in numerous, small quartz veins cutting Lower Paleozoic volcanic-metasedimentary rocks in the eastern surroundings of the Karkonosze Granite Massif (Szałamacha, 1969; Teisseyre, 1968). Genesis of Cu sulphide-bearing quartz veins was connected with the post-magmatic hydrothermal activities around the Karkonosze granites (Schneiderhöhn, 1941; Zimnoch 1978; Mochnacka, 1982) and with the tectonic activity of the Intra-Sudetic fault (Berg, 1912).

Chalcopyrite is the main ore mineral. Recently gold was found in sulphide ore with high As concentration. An arithmetic average of gold contents in the considered sulphide ores and their host rocks is 0.25 ppm (n = 30, range from <1 ppb to 5.5 ppm) and of silver is 17.4 ppm (range 0.5–230 ppm). Gold has a strong correlation with Co (r = 0.96), As and CaO (r = 0.50 and 0.26, respectively). In ore samples (Au >0.5 ppm) the Au:Ag ratios is from 2:1 to 1:25. Native gold and electrum inclusions in arsenopyrite were found during microscope studies in reflected light. Electrum inclusions are rare and have sizes below 5 μm. Most characteristic feature of arsenopyrite is its strong cataclasis and base metal sulphides overprint, which are similar to observed in arsenopyrite from the Kaczawa Mountains. Additionally, the presence of lamprophyre dykes and rhyolite porphyries in the Intra-Sudetic fault zone are comparable to geological situation at the Radzimowice deposit. Arsenopyrite from Miedzianka deposit has As contents from 32.5 to 34.8 atom. % (n = 10) and also constant Co admixture (from 0.16 to 0.7 atom. %). Porphyres and lamprophyres contain only traces of gold (up to 5 ppb).

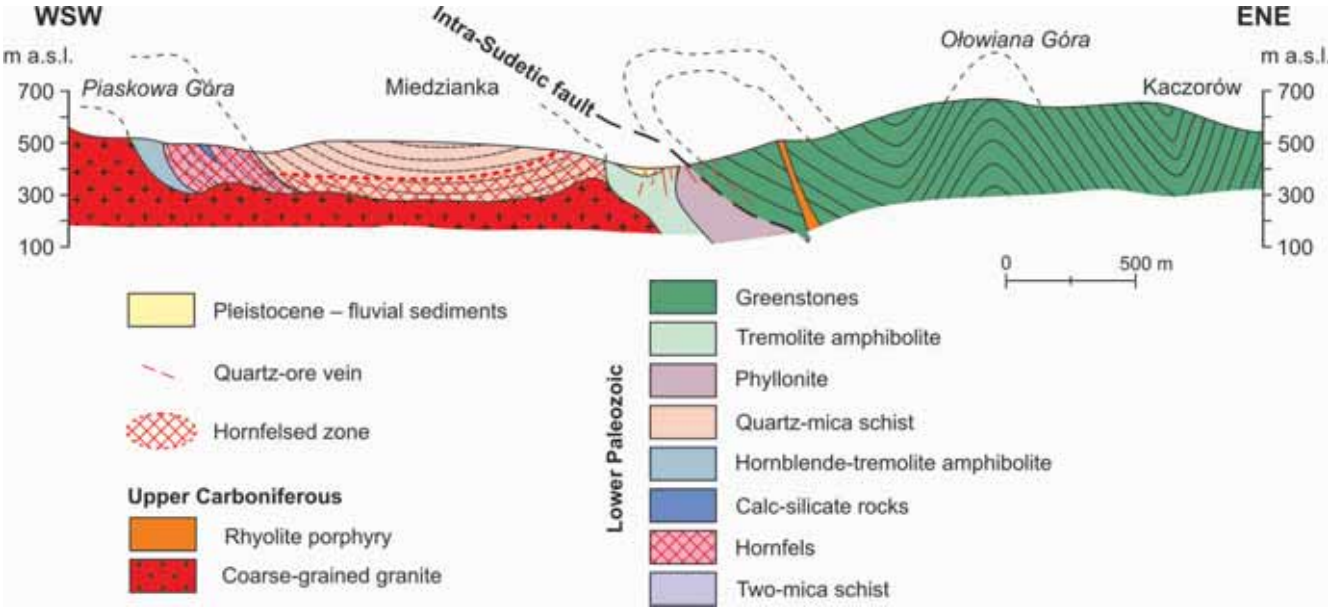

Fig. 69. Geological cross-section through the abandoned mines in Miedzianka–Ciechanowice and Ołowiane Góry ore districts (modified from Szałamacha, 1956)

MECHANISM OF GOLD TRANSPORT AND PRECIPITATION

According to Seward, Barnes (1997) the chemical behaviour of gold in ore-depositing hydrothermal environments is dominated by the formation of hydrosulphide complexes, $AuHS^0$ and $Au(HS)_2^-$. These complexes, together with cyanide complex $(AuCN)_2^-$, are the most stable inorganic complexes of Au and are many orders of magnitude more stable than the equivalent chloride complex, $Au(Cl)_2^-$ (e.g. Seward, 1973, 1989, 1991). If metals were carried in bisulphide complexes, oxidation may cause the precipitation of the sulphides and also release acid digest carbonates (Seward, Barnes, 1997). In the case of gold precipitation from chloride complexes probably decreasing temperature is particularly effective for depositing metals. Most of base and ferrous metals are transported as chloride complexes, especially above 250°C (Seward, Barnes, 1997). The experimental and theoretical data presented by Helgeson, Garrels (1968); Boyle (1979); Kerrich (1983) and others, have demonstrated that gold is mobilized by the medium-temperature chloride solutions with elevated concentrations of H_2S and especially CO_2. The increase of CO_2 activity causes better Au solubility (Kolonin, Polyanova, 1993). Thus, the loss of CO_2 by degassing or fixation in carbonates may create the favourable conditions for gold deposition.

The features of fluid inclusions in gold-bearing quartz were also considered by Kozłowski, Metz (1989). They are: temperatures 250–350°C, pressure 0.4–1 kbar, abundance of CO_2, especially heterogenisation of aqueous and carbon dioxide fluids (Popivnyak, 1975), methane in the ore-forming fluids (Kalyuzhnyi *et al.*, 1975) and presence of other than sodium cations in fluids, especially high contents of K and occurrence of Al, Ca, and Fe in gold-precipitating solutions, and strong domination of Na in pre- and post-ore fluids. These features were recognized in fluid inclusions in quartz of the studied deposits from the Kaczawa Mountains. The changes of the ore-forming solution like separation of carbon dioxide and aqueous fluids, replacement of sodium by potassium and other ions and presence of methane influencing the oxygen fugacity may cause the instability of the gold-transporting chloride, carbonate or bisulphide complexes, leading to precipitation of native gold.

Gold mineralization zones in the Kaczawa Mountains usually are hosted in quartz ± sericite ± graphite schists. Common presence of organic matter and graphite have been recognised in the studied samples from Klecza and from Radzimowice and other places with gold mineralization in the Kaczawa Mountains. Contents of TOC (total organic carbon) range from traces up to ~20%. Graphite schist horizons are common in the Pilchowice unit at the Klecza–Radomice ore district and originated during recrystallization and redistribution of carbon in metamorphosed black argillites. Carbon present in the country rocks reacted with water from fluids to produce carbon dioxide and methane according to reaction: $2C + 2H_2O = CO_2 + CH_4$. Mikulski *et al.* (2005b) reported that methane was always measured in fluid inclusions (up to 10%) in the most auriferous samples from Klecza. Presence of methane causes reduction of the oxygen fugacity and destabilizes gold complex inducing gold precipitation (Cox *et al.*, 1991; Springer, 1986). Graphitic schist with their reducing environment, acted as preferential site for gold precipitation (Fig. 70). The presence of methane or carbon

dioxide in fluid inclusions of quartz veins may change the equilibrium in the solution bearing gold complexes causing the precipitation of gold and nitrogen. Methane may be other indicator of the approaching formation of gold ore (Mikulski *et al.*, 2005b).

According to Noronha *et al.* (2000) gold ores in the northern Portugal appear as the result of successive fluid circulation stages during Variscan orogeny. Deeply penetrating water in uplifting basement was driven up by heat flow linked to the late granite intrusions. Gold was remobilised from metamorphic series and deposited in structural and geochemical traps. Gold deposition was related to progressive dilution and cooling of the crustal fluids by oxidising solutions penetrating the basement from the surface (Noronha *et al.*, 2000).

In the Kaczawa Mountains the correlation between gold and sulphur as well as common occurrence of gold inclusions in pyrite and arsenopyrite of the first stage mineralization suggest that gold was transported as reduced bisulphide complexes [$Au(HS)_2^-$] during this stage. The bisulphide complex could also be the source of sulphur and gold and thus gold coprecipitated with pyrite (Romberger, 1986): $Au(HS)_2^- + Fe_2 + 1/4O_2 = Fe(Au)S_2 + 1/2H_2O + H^+$. According to Nekrasov (1996) the mechanism of the extraction of gold complexes and their reduction to Au^0 occurred during reaction of hydrothermal solutions with ores and vein gangue minerals.

Beside the formation of the complex compounds of Au with As and S also the adsorption on the surface of the deposited sulphide minerals plays an important role in the migration and concentration of gold in sulphide-arsenic minerals. Gold content in acicular arsenopyrite is usually higher than gold in the coarse crystalline one even of an order magnitude. Similar observation was made by Nekrasov (1996) within finely crystalline arsenic-bearing pyrite of dodecahedral habit, which was richer in gold than large cubic crystals. At the Klecza–Radomice ore district arsenopyrite is locally associated with As-bearing pyrite and content of gold in FeS_2 is much higher than in FeAsS. This indicates that arsenic participates in migration and deposition of gold in sulphide-arsenic mineralization. Here it precipitated during sulphide crystalization. As-bearing pyrite that was recognised in Radomice is especially rich in gold. According to Hofstra, Cline (2000) most gold in the Carlin-type gold deposits in Nevada resides in arsenic-bearing pyrite, arsenic-bearing marcasite or arsenopyrite, where it occurs as sub-micrometer inclusions of native gold and/or as structurally bound ionic Au^I (e.g. $Fe(S,As)_2 + 2Au(HS)^0 = Fe(S,As)_2^- + Au_2S + H_2S$; Simon *et al.*, 1999). Adsorption or coprecipitation of As and other trace elements (Au) in pyrite in the North American Cordillera took place at temperature <250°C (Hofstra, Cline, 2000). However, in the Kaczawa Mountains formation of auriferous As-bearing pyrite formed probably at higher temperature. According to arsenopyrite geothermometer, the first generation of the auriferous arsenopyrite at Klecza crystallized from <491 to 390°C, and at from Radomice and Nielestno from 440 to 315 and from 390 to 315°C, respectively.

In the Kaczawa Mountains microscopic gold as inclusions in ore minerals is the oldest one and represents "chemically bound gold" (the 1st generation of microscopic/visible Au; Fig. 21). Younger generations of Au represent gold, remobilised from sulphides (mostly from Co-arsenopyrite) and new gold brought into fractured rocks by next inflow of hydrothermal fluids. Gold redistribution from sulphides was recognized in the gold-bearing sulphide ores from the Kaczawa Mountains. Usually, the release of gold from arsenopyrite and loellingite started immediately after they formed (Möller, Kersten, 1994). According to Mumin *et al.* (1994) the gold remobilization is several stage processes. Primary deposition of invisible Au as structural admixture in sulphide and arsenic minerals is followed by its redistribution and concentration to form colloidal and microscopic gold particles in fractures and voids. Further migration of Au took place from host minerals and interstices to gangue minerals probably have had a long residence time (Heinhorst, Lehmann, 1994; Mumin *et al.*, 1994).

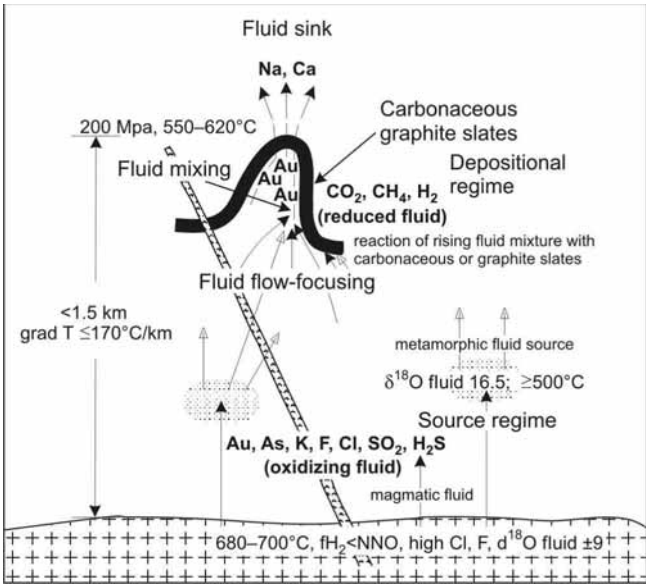

Fig. 70. The ore-forming hydrothermal system within the reducing environment (acc. to the model presented by Matthäi *et al.*, 1995)

Younger microscopic gold (the 2nd and 3rd generation) occurs in microveinlets, cutting ore and gangue minerals, or as cavity- and void fillings in rocks or quartz veins and as "free gold" in rocks. Commonly this gold (mainly as electrum) is associated with base metal sulphides. Precious metals are preferentially transported in chloride complexes which are typical species in chloride-rich but sulphide-poor solutions (e.g. Romberger, 1988). Beside, the composition of fluid inclusions indicates also for chloride complexes as gold transporting during next stages of Au precipitation. Especially at the Radzimowice, when the second stage of electrum precipitation was associated with carbonate minerals crystallization. As indicated, mineral formation was close to neutral conditions at temperatures <371°C (maldonite melting point) and probably <250°C (Cabri 1965; Afifi *et al.*, 1988). This temperature range is characteristic for low sulphidation epithermal mineralization (Hedenquist *et al.*,

1998). Bi and Te played a significant role as scavengers of non-refractory gold in the arsenic–polymetallic gold deposits in the Western Sudetes (Mikulski, 2005b).

At Radomice microscopic gold associated with chalcedony, kaolinite, illite and marcasite as mineral paragenesis typical of subvolcanic environment. In the subsurface level the reduced, near-neutral solution containing NaCl, CO_2 and H_2S boiled due to rapid decompression related to the hydrothermal brecciation. Boiling caused separation of the H_2S from the mineralizing solution (White, Hedenquist, 1995). H_2S-rich vapour might concentrate in the vadose zone to form steam-heated, distinctly acidic solution with pH of 2–3. Evidence of such strong acidic alteration is best visible in sample shown in Fig. 41. Presence of H_2SO_4 explains the acid-sulphate environment favourable for kaolinite and illite formation during chalcedony precipitation at Radomice. Degassing destroyed the mobile $Au(HS)_2^-$ complex resulting in gold precipitation (Cooke, Simmons, 2000). Evidence of boiling in Klecza–Radomice ore district may be suggested by bladed textures of carbonates, intense hydrothermal brecciation, and common presence of kaolinite and illite.

Another mechanism caused gold precipitation in association with hematite, chalcedony and calcite, recognised at Nielestno and Klecza. The characteristic paragenetic association of hematite and gold locally abundantly appears on the Fore-Sudetic Monocline in oxidized Rote Fäule facies and the overlying reduced Permian Kupferschiefer horizon (Piestrzyński *et al.*, 1996; Speczik *et al.*, 1997). The mechanism of these minerals precipitation were considered in details (Piestrzyński, Wodzicki 2000; Oszczepalski *et al.*, 2002). At Klecza and Nielestno with hematite and the youngest generation of gold is associated calcite which indicates oxidative and near-neutral conditions. Experimental data suggests that fluids in equilibrium with hematite are capable to transport significant quantities of Au (Jaireth, 1992). According to fluid inclusion data these fluids are typically chloride-rich but sulphide-poor solutions. Gold migrated in a chloride complex ($AuCl_2^-$) and becomes increasingly stable at low pH and under oxidizing conditions and high chloride activity (Hayashi, Ohmoto, 1991). The chloride complexes might have been decomposed and silica, organic matter or iron-oxides adsorbed of the precipitating gold (e.g. Machesky *et al.*, 1991). The fluid inclusion data from chalcedony from Klecza indicates its precipitation at 165 to 154°C from solution of low salinity (ca. 1.2 ±0.1 wt % NaCl equivalent) and at pressure 0.6 kbar. In chalcedony and hematite-rich gold-bearing sample from Nielestno (2.81 ppm Au) fluid inclusion study shows similar range of chalcedony precipitation (164–153°C) from fluids of salinities ca. 1.9 ±0.1 wt % NaCl equivalent, under pressure 0.6 kbar. The dissolved salts consist of NaCl (65–75% of total salts), $CaCl_2$ (25–35%). $FeCl_2$ also appears up to a several % of total salts. Gold released from sulphides during oxidation was bound in the presence of Cl^- to a gold chloride complex transported as $AuCl_2^-$. Eventually, further oxidation would accompany the change of the gold into $AuCl_4^-$ and Au^{3+} especially during surface weathering. Fluid inclusion measurements in Klecza also revealed the next generation of low temperature quartz, which crystallized at temperature from 135 to 126°C from fluids of salinities ca. 2.5 ±0.2 wt % NaCl equivalent, at pressure 0.5 kbar. The dissolved salts contained NaCl (95–100% of total salts) and KCl (<5%), moreover CO_2 and CH_4 (up to 10%) were present. Methane may be the important cause of gold precipitation in veinlets without boiling. Upon complete oxidation, the only resulting minerals are hematite and native gold (Reed, Spycher, 1985). The mineral assemblage of chalcedony, hematite and gold occurs in low temperature hydrothermal environment that may be mistaken for that one formed by weathering. At lower temperatures (<65°C) an assemblage of goethite and gold would probably prevail. However, at Klecza and Nielestno Fe-hydroxides post-dated chalcedony and hematite crystallization and formed by weathering.

THE SOURCE OF GOLD AND OTHER METALS

In the Kaczawa Mountains the major source of metals and gold accumulated in the gold-bearing As-polymetallic deposits may be found in thick Paleozoic flysch suites of the Kaczawa Metamorphic Complex. These rocks underwent numerous tectonic processes that caused formation of deep-seated fractures. The regional deep fractures became conduits of hydrothermal fluids after the Variscan granite emplacement. During a long migration hydrothermal fluids penetrated various rocks and leached metals from the lower structural unit of the Kaczawa Mountains. In the volcanic-sedimentary rock complex especially interesting are Silurian quartz graphite schists as well as volcanic basal rocks that occur mainly in the SE part of the Kaczawa Mountains. Leaching of metals from black schists should cause a decreased metal concentration in wall-rocks of the ore-bearing quartz veins. In the Kaczawa Mountains the gold deposits are enriched in arsenic only when they occur in the black schists. Increase of arsenic contents in FeS_2 occurred during recrystallization of framboidal pyrite. Constant Co admixture in high-temperature arsenopyrite may also indicate common source of As and Co in black shales. The mobilization of S and other metals (Cu) from the sedimentary pyrite-bearing units was caused by hydrothermal fluids of metamorphic and post-magmatic origin.

The second possible source of metals may be found in the Variscan magmatic rocks. They comprise rock varieties from granite to lamprophyre and from sub-volcanic (rhyodacite, rhyolite) to volcanic ones (andesite). Granites were mainly consid-

ered by some geologists as a source of metals in the sulphide deposits in the Sudetes (Petrascheck, 1933; Neuhaus, 1936; Manecki 1965; Zimnoch, 1965; Fedak, Lindner, 1966; Paulo, Salamon 1973b). In the Central Massif the probable source of gold is correlated with leucocratic granite (Bouchot *et al.*, 2000). In the Iberian Peninsula granite intrusions are not considered as a probable source of gold despite numerous gold lodes hosted by granites (Murphy, Roberts, 1997; Noronha *et al.*, 2000).

The $\delta^{34}S_{CDT}$ values of auriferous sulphide from various deposits in the Western Sudetes range from –5 to +8‰, indicating a magmatic origin with local significant crustal contribution (Kajiwra, Krouse, 1971; Ohmoto, 1986; Ohmoto, Goldhaber, 1997). Moravék (1995, 1996) considered the source of Au–As mineralization in the Bohemian Massif within primary preconcentrations in the volcanogenic-sedimentary suite and their later mobilization by Variscan granitoid intrusions. In the Kaczawa Mountains mobilization of metals was also attributed to heat flow around the Upper Carboniferous post-orogenic intrusions and hydrothermal activities along regional and second-order faults and fractures.

GOLD DISTRIBUTION IN SCHISTS

The present works were focused on gold concentration in the various lithotectonic units of the Kaczawa Mountains (Tab. 26). Arithmetic average of Au contents is in: greenstone –3.0 ppb (n = 18; range of arithmetic average concentration in the specific units is from 2.3 to 3.3), quartz-sericite schists –3.5 ppb (n = 40, range from 2.7 to 5.5 ppb), graphite and siliceous-graphite schists –10.1 ppb (n = 38, range from 0.8 to 28.9 ppb). The highest arithmetic average value of gold (28.9 ppb) has graphite schist from the Mysłów–Grochowice area (Fig. 71). Arithmetic average of Au in barren rocks represented mainly by graphite, siliceous and quartz-sericite schists from areas beyond the polymetallic deposits is 6.5 ppb (n = 60; Table 26) and from the ore deposits is 8.7 ppb (n = 72). Gold has positive correlation with V (r = 0.36), Cu (r = 0.29), and Pb (r = 0.25). Beside, Au has a weak correlation with As and Ag (Tab. 27). Characteristic is positive correlation of V with Au, Ag, As, Ni and base metals within black schists.

Much higher gold concentrations occurred in sulphide ores and rocks from vein selvages, especially in the Klecza–Radomice and Radzimowice deposits. Gold concentrations are over 1000 higher than its average geochemical clark values for specific rocks (Fig. 72). As an example in the massive sulphide ore from the level –70 m of the Wilhelm shaft in Radzimowice the arithmetic average of gold concentration is 62.27 ppm (from 18.3 to 135 ppm) and in mineralized porphyries is 1.64 ppm (from 0.124 to 6.6 ppm). Host rocks from the ore zones also have higher average gold concentration. In the Radzimowice deposit the host rocks represented mainly by the Radzimowice schists contain from 50 to 493 ppb Au. These concentrations are much higher in comparison with Au contents in primary volcanic-sedimentary rocks from the lower struc-

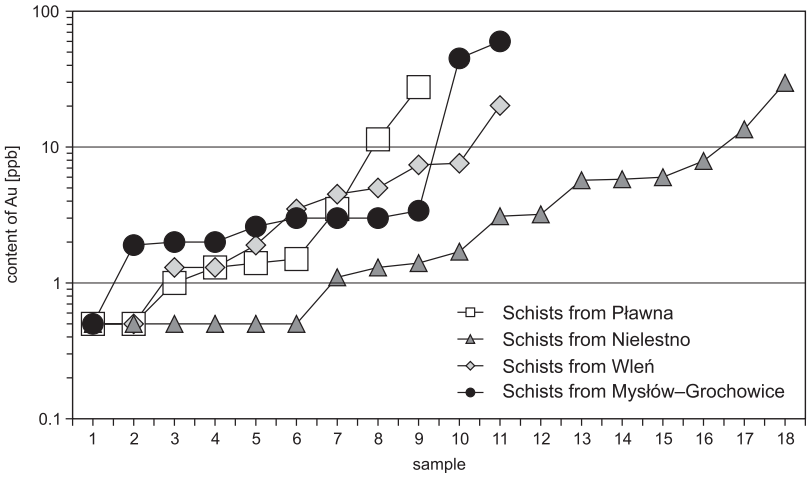

Fig. 71. Comparison of gold contents in quartz-sericite-graphite schists from the various locations in the Kaczawa Mountains

Table 26

Statistics parameters of the metal concentrations in black schists in the Kaczawa Mountains

Element	Minimum [ppm]	Maximum [ppm]	Arithmetic average [ppm]	Standard deviation [ppm]
Au	0.5	67.6	6.5	10.4
Ag	0.5	8	1.9	1.9
As	1.5	215	34	44.9
Cu	3.0	565	66.2	99.2
Pb	2.5	100	23.3	22.3
Zn	6.0	357	60.4	58.3
V	7.0	1825	163.4	278.9
Co	0.5	37	10	8.6
Ni	6.0	137	30.9	22.6
Cr	1.5	141	48.4	35.1

Table 27

Correlation matrix of selected elements for the barren black schists in the Kaczawa Mountains without the Radzimowice and Klecza–Radomice ore districts

Element		Au	Ag	As	Cu	Pb	Zn	V	Co	Ni	Cr
		n=60	n=60	n=60	n=60	n=60	n=60	n=60	n=42	n=42	n=42
Au	n=60	1.00	.07	.12	.29	.25	–.13	.36	–.21	.08	.14
Ag	n=60	.07	1.00	.39	.34	–.08	–.11	.37	–.08	.23	–.01
As	n=60	.12	.39	1.00	.37	.15	.07	.32	.28	.40	.10
Cu	n=60	.29	.34	.37	1.00	–.01	.17	.49	.33	.58	–.18
Pb	n=60	.25	–.08	.15	–.01	1.00	–.06	.10	–.13	.09	.06
Zn	n=60	–.13	–.11	.07	.17	–.06	1.00	–.03	.31	.30	–.05
V	n=60	.36	.37	.32	.49	.10	–.03	1.00	.13	.68	.01
Co	n=42	–.21	–.08	.28	.33	–.13	.31	.13	1.00	.47	–.02
Ni	n=42	.08	.23	.40	.58	.09	.30	.68	.47	1.00	.05
Cr	n=42	.14	–.01	.10	–.18	.06	–.05	.01	–.02	.05	1.00

n – number of samples

tural units located beyond the mining districts in the Kaczawa Mountains.

Gold and base metals content in flysch-like rocks cut by barren quartz veinlets are several times lower than in similar rocks without quartz veinlets. It indicates metal leaching from fractured rocks by hydrothermal fluids. Instead, they contain high concentrations of sulphur and organic matter. Sulphur is present as Fe-sulphide, i.e. pyrite of various generations. The abundant appearance of framboidal pyrite in graphite schist from the Kaczawa Mountains is very characteristic phenomena. However, in the places with ore mineralization the framboidal pyrite is commonly subject of further recrystallization into the younger generation pyrite. Graphite that is also common in schists most probably derived from recrystallization and redistribution of carbon in deformed black argillites.

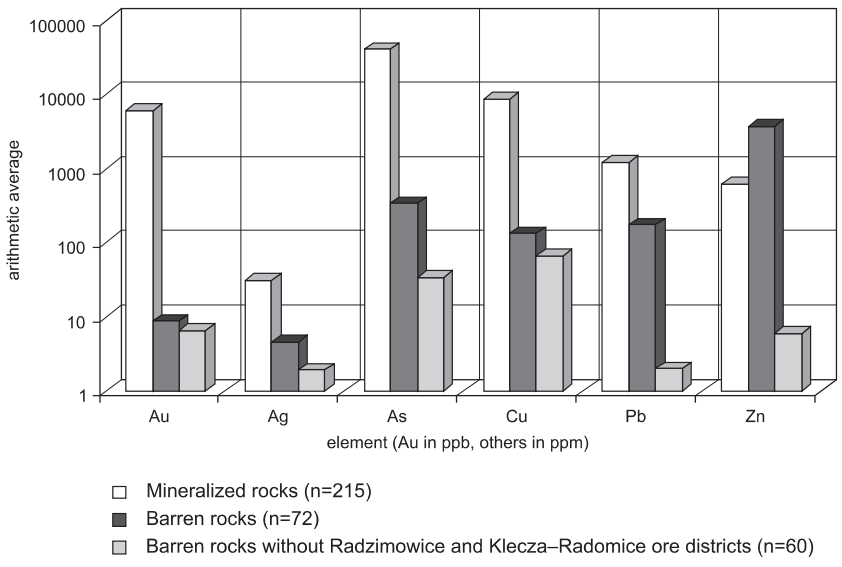

Fig. 72. Comparison of the arithmetic average values of metals in mineralized and barren rocks in Radzimowice and Klecza–Radomice ore districts

Metasedimentary and volcanic rocks in the Kaczawa Metamorphic Complex have average metal contents higher than average crustal values. For example the average Au concentration in the Kaczawa Metamorphic Complex is 6.5 ppb while the crustal average is 3.2 ppb (Taylor, McLennan, 1985). In general there is enrichment in metallic elements (Co, Ni, Cr and V) derived from basic sources. Shales with higher contents of these elements have a higher Au background (ca. 9 ppb). Graphite schist from the various units of the Kaczawa Mountains have average concentration of Au at 14.6 ppb (n = 30). Greenstones contained ca. 3.1 ppb Au. The acid volcanic rocks have usually lower concentration of gold (<5 ppb).

GOLD AND OTHER METALS POTENTIAL OF THE VARISCAN GRANITES

A part of the modern gold genetic models included calc-alkaline and alkaline magmas as a source of gold in numerous gold deposits (Richards, 1995; Spiridonov, 1996; Sillitoe, 1991, 2000; Sillitoe, Thompson, 1998; Thompson *et al.*, 1999; Jensen, Barton, 2000; Müller, Groves, 2000; Thompson, Newberry, 2000). These genetic models for gold formation indicate for significant zone distribution of deposits in relation to the source acidic (granitic) magmas.

In the Western Sudetes such specific distribution of the ore deposits around the Karkonosze granite were also noted (Petrascheck, 1933; 1937; Neuhaus, 1936; Mochnacka, 1982). In the close neighbourhoods of granite massifs small vein type sulphide deposits with various Au contents occur (e.g. Czarnów, Miedzianka–Ciechanowice, Radzimowice and also Au deposits in the Czech Republic; Fig. 73). Genesis of these sulphide polymetallic deposits was connected with the post-magmatic activities of the Karkonosze granite intrusion (e.g. Zimnoch, 1965; 1978; Mochnacka, 1982; 2000; Mochnacka, Banaś, 2000). Detailed petrographic and geochemic characteristics of the Karkonosze granite, Strzegom–Sobótka granite and granite from the Radzimowice area are presented elsewhere (e.g. Borkowska, 1966; Duthou *et al.*, 1991; Kural, Morawski, 1968; Machowiak, Muszyński, 2000; Majerowicz, 1972; Maciejewski, Morawski, 1975; Majerowicz, Skurzewski, 1987; Mierzejewski *et al.*, 1994; Oberc-Dziedzic *et al.*, 1999; Pin *et al.*, 1989; Puziewicz, 1985, 1990; Wilamowski, 1998). The interpretation of geochemical data in the aspect of ore metals potential of granites from the Kaczawa Mountains (Bukowinka granite) and adjacent areas (granites from the Karkonosze Massif and from the western part of the Strzegom–Sobótka Massif) are presented in this monograph.

The changeable ways of magmas fractionation, degree of compositional evolution and further tectonic processes caused different types of ore mineralization that reflected transition from magmatic to hydrothermal environments. Cu and Au deposits are connected with more maphic granites; W mineralization correlates with granitic magmas of transition character and Mo–W–Sn with felsic and fractionated granite (Blevin, Chappell, 1995). Oxidation state of magmas is of paramount importance in controlling nature of many ore elements and allowed

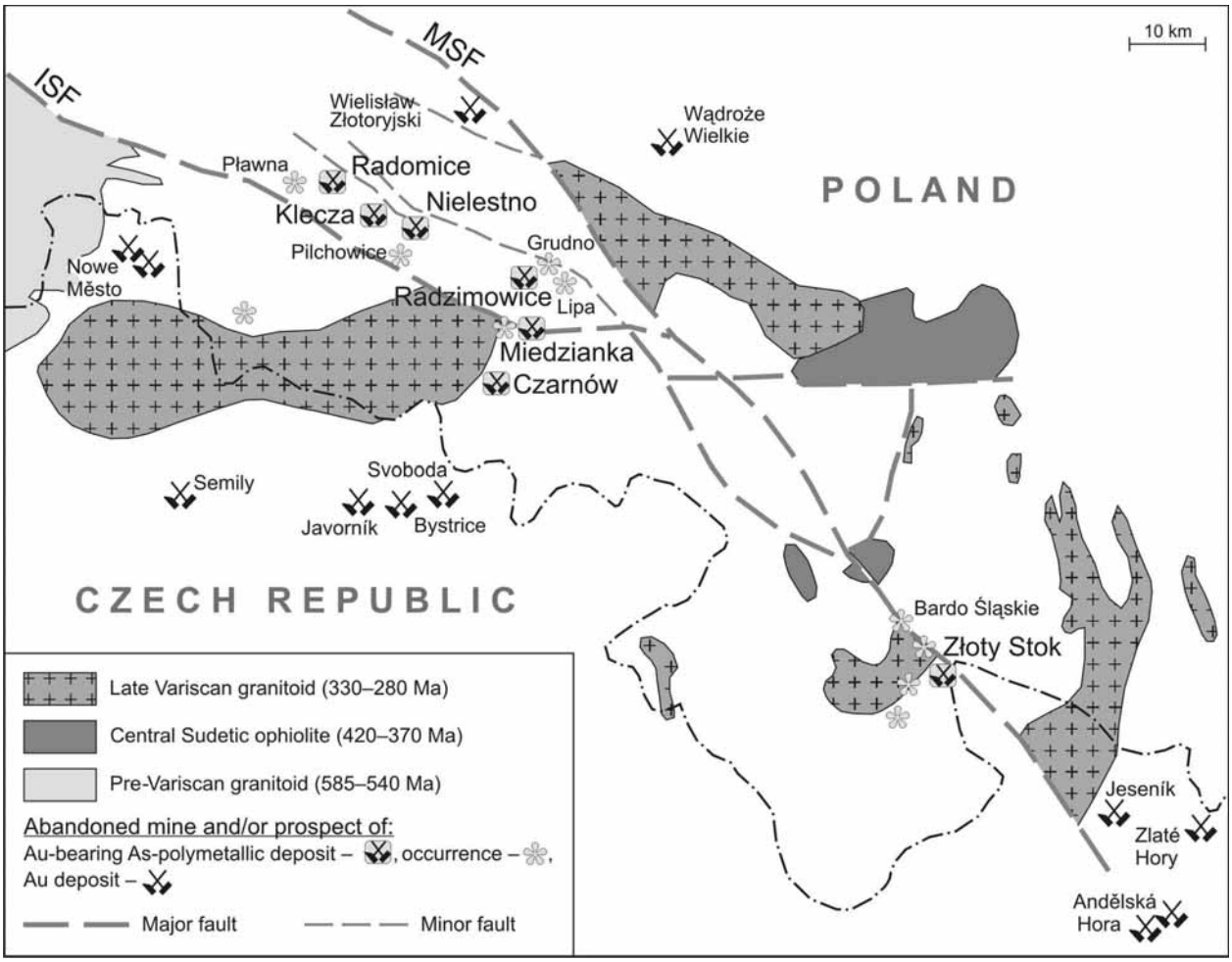

Fig. 73. The schematic location of gold deposits around the Variscan granites in the Western Sudetes

Abbreviations: ISF – Intra-Sudetic fault, MSF – Marginal Sudetic fault

for division of granites into ilmenite- and magnetite series (Ishihara, 1981). Cu, Mo and Au deposits are typically related to magnetite-bearing (oxidised) granite and Sn (±W) deposits to ilmenite-bearing (reduced) granite (Ishihara, 1981). The oxidation state of the igneous system controlled the process of hydrothermal redistribution of elements (Lehmann, 1994).

According to Blevin (2003) the K/Rb ratio versus silica contents is very useful for definition of strongly fractionated granite most characteristic for Sn and W mineralization. The position of granite samples in the considered diagram (Fig. 74) indicate that the Strzegom–Sobótka granite together with Bukowinka granite is moderately evolved. Such granite formed in continental arc environment with direct derivation from the mantle material (I-type granites). The Karkonosze granites are classified to the group of the strongly evolved and fractionated granite. Strongly evolved granite formed by contamination of oceanic material with crust rocks (Blevin, 2003).

The specific Karkonosze granite formed from magmas of different degree of fractionation. The central granite formed from magma of the relatively most primitive composition and crystallized as the earliest among the all three types of the Karkonosze granites (Mierzejewski *et al.*, 1994). Higher degree of fractionation-characterized magma from which crystallized the ridge granite. More advanced was magma differentiation responsible for granophyre granite crystallization and next for aplite and pegmatite formation. This magma was enriched in volatile compounds, water and silica (Gajda, 1960; Janeczek, 1985). Beginning phases of the ore mineralization were connected with the final stage of pneumatolytic processes, and further ore mineralization processes increased during a high temperature hydrothermal stage. At this stage wolframite and molybdenite mineralization followed by scheelite crystallization formed in quartz veins cut aplogranite mainly in the western parts of the massif (Karwowski *et al.*, 1973; Kozłowski *et al.*, 1975). The aplogranite magma often hidden beneath porphyry-like (central granite) and equigranular (ridge) granites was already considered by Mierzejewski, Grodzicki (1982) as the tin-bearing type. Recognised within these granites W–Mo mineralization is very characteristic and belongs to the S-type granite. Granophyre granite seems to be the most favourable for presence of reduced-lithophile elements (W, Sn) and Au association with W.

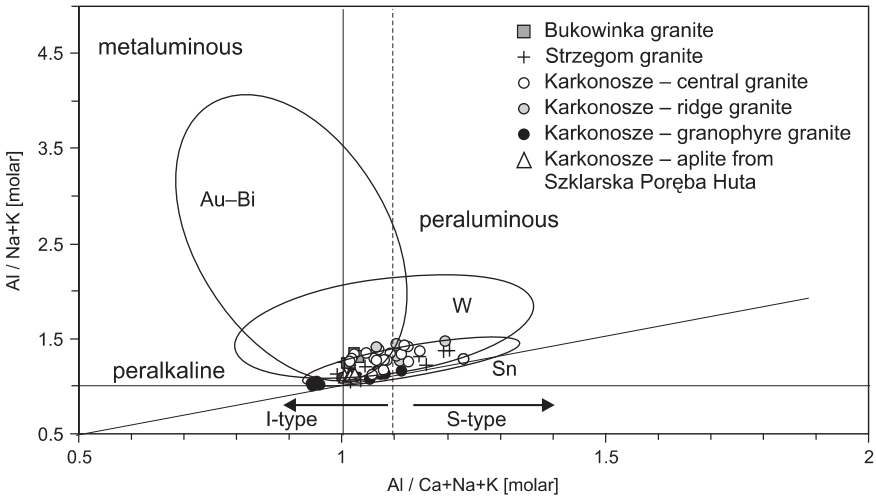

Fig. 74. Blevin's plot (2003) of K/Rb versus SiO_2 applied for samples from this study

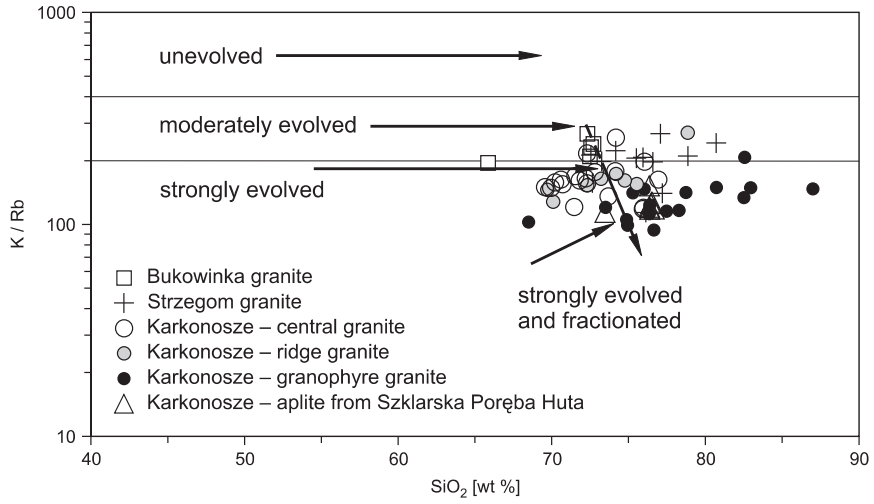

Fig. 75. A/NK versus A/CNK classification of selected granites from the Lower Silesia

Abbreviation of ellipsoids (after Baker *et al.*, 2005): Au–Bi – dominants granites; W – dominant granites; Sn – dominant granites

Variation in oxidation state may be consistent with a change in metallogeny from tin-rich to tungsten gold-rich systems (Thompson *et al.*, 1999). In Figure 75 it is well visible the position of granophyre granite samples in peraluminous and metaluminous fields. Beside, macroscopic studies indicate for the presence of magnetite and ilmenite in granite samples suggesting transition state of magma oxidation. If it is a case, in the Karkonosze Massif may formed various type of W–Sn–Mo–Cu ore mineralization (sheeted veins, breccias, disseminated and veins) with local enrichments in Au and Bi.

In region where appears granite with high silica contents preferably formed Sn, Mo, U and Au deposits, while those skewed to intermediate or lower SiO_2 values are more typically associated with

Cu mineralization (Blevin, 2003). Among samples located in the VAG field high concentration of SiO_2 were determined (from 72 to >80 wt %.). These samples with high silica concentrations were collected in places with the Mo-W-Sn mineralization (Paszowice and Szklarska Poręba Huta). The wolframite-molybdenite-cassiterite mineralization was also found in Radzimowice (Sylwestrzak, Wołkowicz, 1985).

The presence of quartz veins with gold were noted in the Karkonosze Massif (e.g. Domaszewska, 1965; Kozłowski, Metz, 1989). In the time period from 1175 to 1492 ca. 3 t of gold was extracted from the alluvial sediments on the Karkonosze Massif (Quiring, 1948; Grodzicki, 1967). The pH evolution of the moderate and low temperature hydrothermal fluids into more oxidized is evidenced by the common occurrence of hematite and quartz hematite veins, which dominate and are widely distributed in the whole Karkonosze Massif. However, gold concentration within these veins is still unknown.

Chemical analyses of the granite composition from the western part of the Strzegom–Sobótka Massif as well as the position of samples on the Harker's diagrams suggest the intensive development of differentiation process during magma intrusion (Mikulski, 2005d). Similar to the Karkonosze granite the main factor of the magma differentiation was fractional crystallization. Locally, magma was enriched in volatile compound, water and silica, which caused formation of miarolitic pegmatite, aplite dyke and quartz vein (Janeczek, 1985). This magma characterized by high potential for generation of post-magmatic fluids from which precipitated ore minerals (Sałaciński, 1978). Mineral assemblages, present here, reveal domination of molybdenite and chalcopyrite over the other metal components that is characteristic feature of the I-type granite.

In the zone of the occurrence of the I-type granite more probably formed Mo–Cu±Au mineralization, especially within the occurrence of the high temperature and oxidised granite (magnetite series; Blevin, 2003). The most variable composition of ore minerals were found in the Paszowice quarry located on the western margin of the Strzegom–Sobótka Massif and in the shear zones of the marginal Sudetic fault. Ore minerals are represented mostly by molybdenite, and chalcopyrite, and rarely by pyrite, sphalerite, and native bismuth. They appear in quartz veinlets infilling fractures of NNW–SSE direction in aplogranite (Pendias, Walenczak, 1956; Sałaciński 1973, Kanasiewicz, Mikulski, 1989). Beside, in the other places (e.g. the Rogoźnica quarry) the ore mineralization (pyrite, chalcopyrite, sphalerite, molybdenite, bismuth minerals, hematite and magnetite) in quartz veinlets were found (Sałaciński, 1978). Around such core of the high temperature oxidised granite (magnetite series) and with moderate degree of differentiation may formed the following zones of ore mineralization: (1) Pb, Cu, Zn and outward from the core (2) Au, Bi, Ag (3) and (Au, As, Sb) (Blevin, 2003). According to this scheme it is possible to connect genesis of the some polymetallic mineralization in the northern part of the Kaczawa Mountains (e.g. Chełmiec, Męcinka) and in the Fore-Sudetic Block (e.g. the quartz veins near Wądroże Wielkie) with tectonic-magmatic activities of the Strzegom–Sobótka massif and/or with its probably extension (Bolesławiec granite; Fig. 76), recognised by geophysics methods at the depth. Some information about auriferous veins and placer gold deposits in

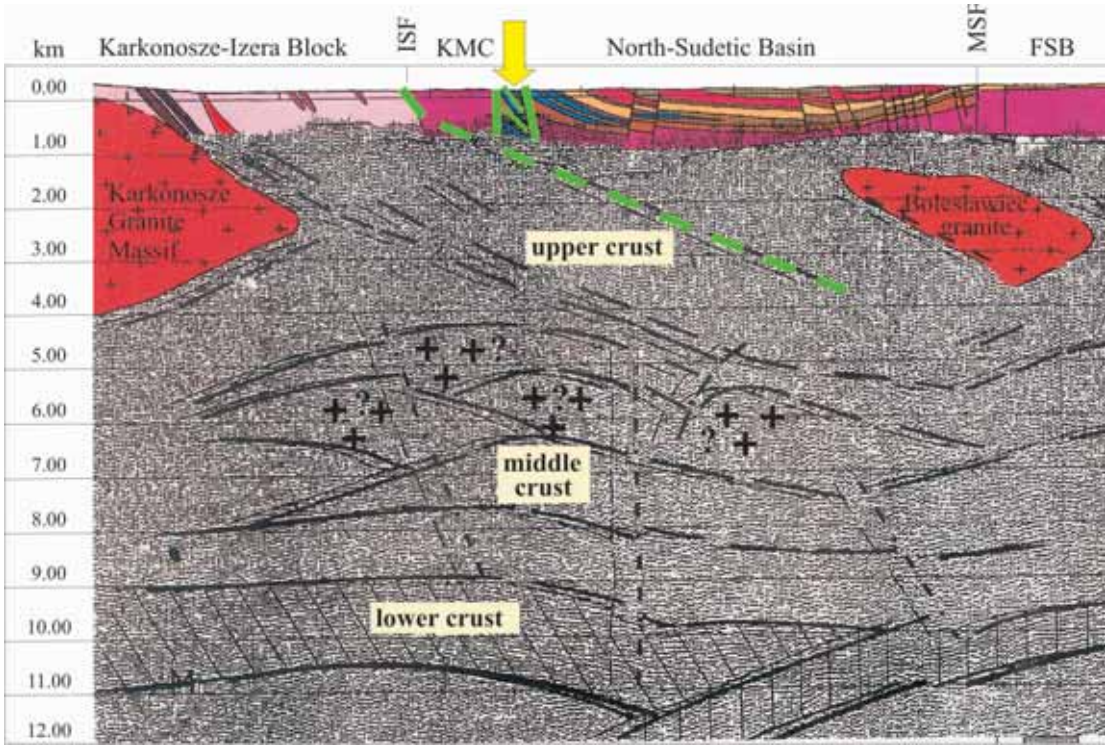

Fig. 76. Depth migrated section with interpretation of a deep-crustal structure (modified from Żelaźniewicz *et al.*, 1997)

Abbreviation: ISF – Intra-Sudetic fault; MSF – Marginal Sudetic fault; KMC – Kaczawa Metamorphic Complex; FSB – Fore-Sudetic Block

Wądroże Wielkie were given by Zöller (1932; 1938), Uberna (1959), Grodzicki (1960; 1972), Grocholski (1982) and Grocholski, Sawicki (1982).

Acidic (granitic) magma from the western part of the Strzegom–Sobótka Massif with regard to its geochemical characteristic may formed porphyry mineralization of Mo–Cu type.

The reconstruction of a spatial mineral zonation and fluid plumbing systems connected with the occurrence of a complex igneous rock suite in the less eroded areas like the Variscan molasse basins (e.g. Intra-Sudetic Basin or North Sudetic Basin) and Fore-Sudetic Block may point also towards the porphyry type mineralization of the Cu–Au mineralising systems that survived under thick rock covers.

HYPOTHETICAL GRANITE UNDER THE KACZAWA MOUNTAINS

Beneath the Kaczawa Mountains in the crust (from ~3 to ~15 km) the crystalline basement was recognized by geophysical methods (Cwojdziński *et al.*, 1995; Cwojdziński, Żelaźniewicz, 1995; Żelaźniewicz *et al.*, 1997). It was found to be built of gneiss-granitoid rocks and of single granitic plutons out of which the biggest is located below the town of Bolesławiec (hypothetical extension of the Strzegom granite) in the basement of the Fore-Sudetic Block and the Kaczawa unit (*op. cit.*). The gneiss complex of the Karkonosze-Izera Block is underlain by the Karkonosze granitoid to the line of the main Intra-Sudetic fault (Fig. 77). The Intra-Sudetic fault is not visible in the Griffin's anomaly and negative gravimetric anomaly shifted from

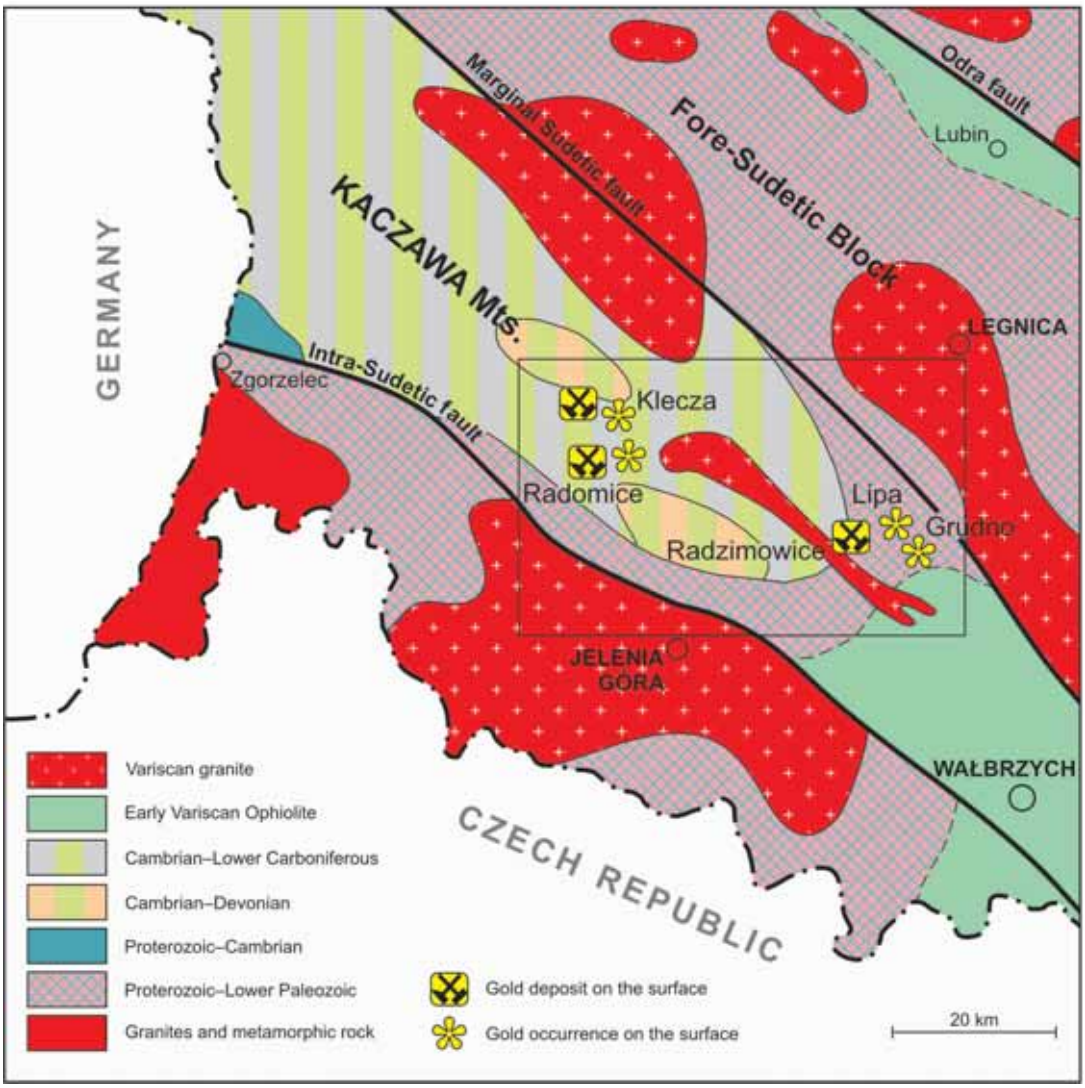

Fig. 77. Geological map of horizontal cutting on the plane of 5 km b.s.l. (after Kotański, 1997) with the relation of the Radzimowice and Klecza–Radomice gold ore districts to the hypothetical granite located beneath

the outcrops of the Karkonosze granites to the west direction under the Izera gneisses block suggesting the presence of big granitoids bodies (*op. cit.*).

The presence of granites in the Kaczawa Mountains basement was also interpreted from the maps of the horizontal cut by Kotański (1997). At the depth of 2 km b.s.l. occur granitoid-like bodies. These hypothetical granitoids form a strongly elongated massive body (apophyse?) extending in the WNW–ESE direction (contrary to the NE–SW trend postulated by Petrascheck, 1933, and others). This hypothetical granite body extends at the distance of over 20 km from the north of the Wojcieszów vicinities to Wleń. At the depth of 5 km b.s.l. this granitoid body is located more to the southwards both in the Wojcieszów and Wleń areas (Fig. 77). These granitoids underly most probably auriferous ore mineralization not only at Radzimowice, Grudno and Lipa but also in Klecza–Radomice and further north-westwards. Granites from the Żeleźniak and Bukowinka massifs could be the outcrops of this deep-seated granitoid pluton. In the Klecza–Radomice gold ore district granite outcrops are absent, however the hypothetic granite (or Karkonosze granite) that underlying Klecza-Radomice ore district at depth may cause circulation of the fluids that distributed metals along regional deep fractures and shear zones. These hydrothermal fluids of variable origins were also able to leach metals from the country rocks (e.g. Lower Paleozoic schists).

THE RELATION OF THE AURIFEROUS QUARTZ-SULPHIDE MINERALIZATION TO DEEP FRACTURES IN THE KACZAWA MOUNTAINS AND BEYOND

In this part of the Western Sudetes it is possible to group metalifferous deposits along linear zones of various directions (NE–SW, NW–SE, ENE–WSW), which run parallel to deep fracture zones of similarly different directions.

Some of the quartz-sulphide vein type arsenic-polymetallic deposits occurring in Rudawy Janowickie and Kaczawa Mountains are located along the one structural line, which extend from the eastern margin of the Karkonosze massif to the northeast. In the about 5 km wide and over 90 km long zone occur several deposits (e.g. Kowary, Podgórze, Czarnów, Miedzianka–Ciechanowice and Radzimowice) and occurrences (Lipa and Grudno). Petrascheck (1933, 1937) first and later Neuhaus (1936) connected the origin of porphyry intrusions, granite apophyses and contact metasomatic phenomena in the Kaczawa Mountains with extension to the north of the Karkonosze granite pluton from which along a deep fracture (of NE–SW direction) magma rose into the upper parts of crust.

A similar concept about granitic magma generation below the considered polymetallic sulphide deposits and its extrusion along the NE–SW oriented deep regional fractures was later formulated by Kanasiewicz, Sylwestrzak (1970) and Michniewicz (1981, 2003), (Fig. 78). This idea was also supported by Mroczkowski (1992) who on the basis of the Thematic Mapper satellite image reported N-trending double photolineament roughly following Rudawy Janowickie. He interpreted such double photo-

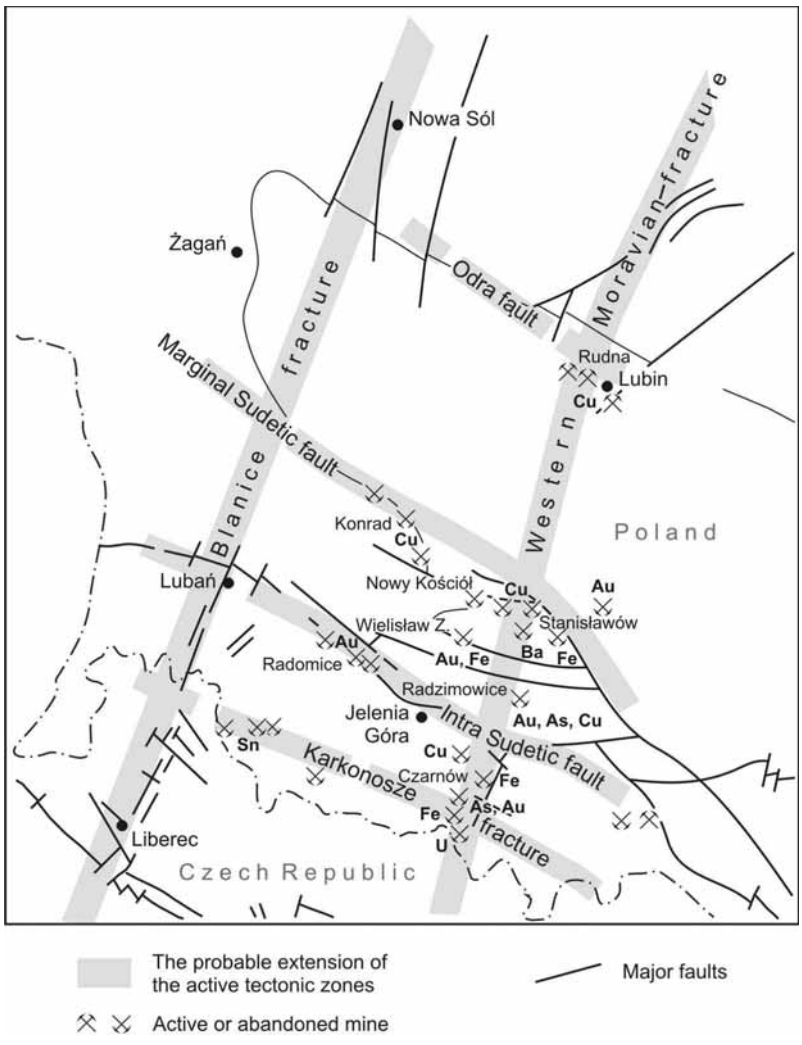

Fig. 78. The deep fracture zones in the Lower Silesia region with location of the ore deposits (after Kanasiewicz, Sylwestrzak, 1970; Michniewicz, 2003)

lineament as an important fracture zone active from Early Carboniferous through recent. However, on the map of the photolineaments in the considered area of the Sudetes such photolineaments have not been recognised (Doktór, Graniczny, 1983). Instead, numerous photolineaments of NW–SE and ENE–WSW directions have been documented.

Beside photolineaments, on the satellite photos in several regions of the Sudetes, the ring-like structures related to intrusions of the central type were identified (Doktór, Graniczny, 1983). In the areas here considered the cross-section of photolineaments with ring-like structures in the vicinity of Jawor were recognized and interpreted as very favourable for the emplacement of various metal deposits (e.g. Kanasiewicz, Mikulski, 1989).

According to Michniewicz (2003) in the area of the Karkonosze–Izera Block the most important was the Western Moravian fracture zone (of NE–SW direction) recognized earlier by Chrt *et al.* (1968). This zone was also considered as a source of magmatic association and direct channels for the mineral-forming solutions. One of the arguments against such simple connection is the fact that these sulphide deposits are small in size and mainly of arsenic and base metal sulphide composition typical for a granite environment. In the described here deposits no significant enrichment an PGE was found. In the orogenic type of gold deposits, where Au mineralization originated close to the deep fractures, concentration of base metal sulphides is low and much less than a few per cent (Groves *et al.*, 1998b; Goldfarb *et al.*, 2001). Nevertheless, contents of the base metal sulphides in some of the polymetallic deposits located within the zone of the Western Moravian fracture may reach up to several dozen per cent by volume (e.g. at Czarnów or at Miedzianka). Moreover, deposits located along a deep fracture are always marked by long linear anomalies of metals in soil (*e.g.* As and Au anomalies in the French Massif Central – Roig *et al.*, 2000). Such regional metal anomalies indicate the hydrothermal linear paleofields responsible for the formation of ore mineralization along preferable fracture direction. However, until now regional linear metal anomalies of NE–SW orientation within the zone of the Western Moravian fracture have not been recognised. Instead, numerous As and Au anomalies have been recognised in alluvial sediments located on faults of NW–SE direction (Kanasiewicz, 1990, 1992; Mikulski, 2001). The Western Moravian deep fracture was supposed to be active from Paleozoic till the present time (Michniewicz, 2003). This concept is also contrary to the Aleksandrowski (1995, 2003) idea of multiple regional movements on the Intra-Sudetic fault that separates different tectonostratigraphic terranes.

Seismic data indicated that ISF and MSF really are not deep-seated, subvertical crustal boundaries but rather they are listric faults (Żelaźniewicz *et al.*, 1997). Prolongation of the Intra-Sudetic fault at depth changed from the steep at the subsurface levels to subhorizontal at depth and with dip to NE (Figs. 76, 79).

Multiple stages of different movements within Intra-Sudetic fault postulated by Aleksandrowski (1995; 2003) and Aleksandrowski *et al.* (1997) and formation of the regional shear-zones between Sudetic terranes (Fig. 80) (Cymerman, Piasecki, 1994; Cymerman *et al.*, 1997; Cymerman 2000, 2002, 2004) resulted from geotectonic and magmatic processes on the western margin of the Baltic platform at the end of the Carboniferous (Seston *et al.*, 2000). The younger, sinistral displacements of Intra-Sudetic fault occurred at semi-brittle to brittle regime during Late Carboniferous to Early Permian (Aleksandrowski, 1995; 2003) and were coeval with Au mineralization. It is important that considering the presence of the deep fractures and their probable connection with the formation of ore mineralization in the Kaczawa Mountains the discussion should be limited only to the Upper Carboniferous–Permian.

Considering the origin of auriferous mineralization at the Radzimowice deposit Mikulski (2003a) pointed to a late injection of mafic alkaline magma manifested by lamprophyre dykes that are spatially related to quartz-sulphide veins. Alkaline magma that rose into the upper part of the lithosphere had to use very deep fractures. The Western Moravian deep fracture has a NE–SW direction that is oblique to the direction of strike (W–E) of the most known auriferous quartz-sulphide veins in the Radzimowice area. It seems that in this case deep fluid migration was rather along fractures of the NW–SE direction and in the shallower parts of the crust along fracture zones with W–E and NW–SE directions. Only at the Czarnów deposit the main quartz-ore vein has an extension coherent with the NE–SW direction. Auriferous mineralization in the Klecza–Radomice ore district is located almost half distance between two postulated (e.g. Chrt *et al.*, 1968; Kanasiewicz, Sylwestrzak, 1970; Michniewicz, 2003) deep fractures of

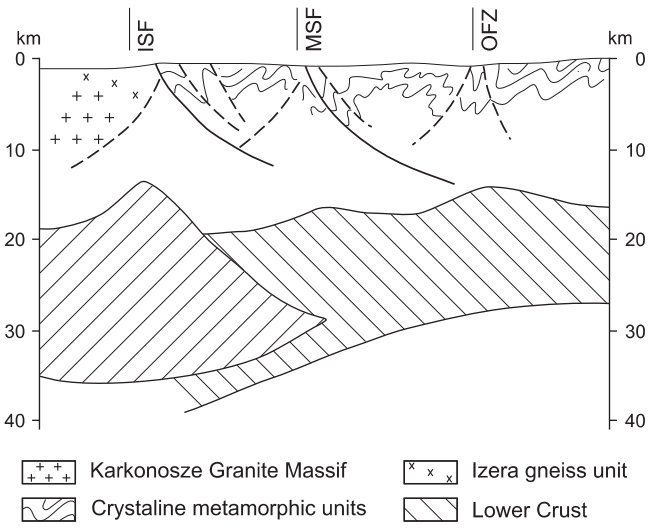

Fig. 79. The "crocodile" model of the crust construction (after Żelaźniewicz *et al.*, 1997)

Abbreviation: ISF – Intra-Sudetic fault; MSF – marginal Sudetic fault; OFZ – Odra fault zone

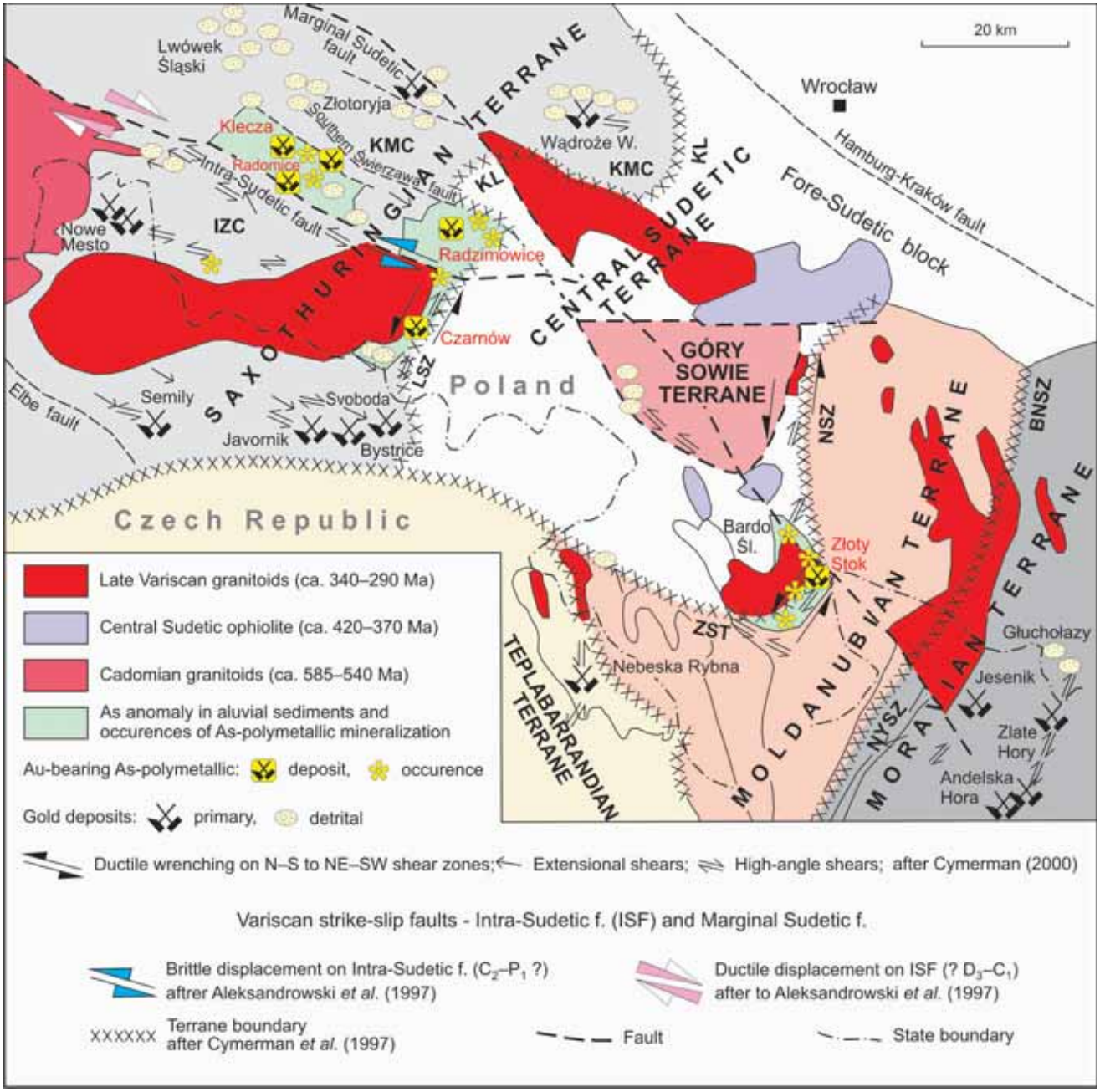

Fig. 80. Location of deposits and occurrences of Au-bearing As-polymetallic association and generalized tectonic-structural features in the Polish Sudetes (Aleksandrowski *et al.*, 1997; Cymerman *et al.*, 1997; Cymerman, 2000)

Abbreviation: KAC – Kaczawa Metamorphic Complex; KL – Kaczawa tectonic line; BNSZ – Brzeg–Nysa shear zone; LSZ – Leszczyniec shear zone; NSZ – Niemcza shear zone; NYSZ – Nyznerov shear zone; ZST – Złoty Stok – Trzebieszowice shear zone

NE–SW direction. However, Mikulski (2001) suggested the possible connection of this gold mineralization with deep fractures of NW–SE direction (e.g. Intra-Sudetic fault).

The hypothesis about the connection of the origin of the ore mineralization with deep fractures in the Western Sudetes required more detailed geophysical work especially of the seismic-reflective types. The postulated presence of the deep fractures with NE–SW directions was not confirmed by photolineament studies and even by seismic-reflective work, completed for the deep parts of crust under the Kaczawa Mountains (Cwojdziński *et al.*, 1995; Żelaźniewicz *et al.*, 1997).

THE RELATION OF THE AURIFEROUS QUARTZ-SULPHIDE MINERALIZATION TO TECTONIC STRUCTURES IN THE KACZAWA MOUNTAINS

In the Radzimowice deposit the quartz-sulphide veins strike E–W, which is similar to the axial plane direction of the Radzimowice (F_2) fold (WNW–ESE) or the Bolków–Wojcieszów saddle. Similar strikes have been noted also in quartz-sulphide veins in Lipa and Grudno hosted by the same fold structure. Appearances of the calcareous rocks and greenstone on the both sides of the Radzimowice schists were primary interpreted as synclinal fold with normal southern flank and locally reversed northern flank (Kryza, Muszyński, 1992). However, in the light of new relative age determination which dated Wojcieszów limestones at not older than Silurian (Kozdrój, 1995) the Radzimowice schists should be considered as younger and this fold structure should be reinterpreted as rather an anticlinal than synclinal form. Nevertheless, the axial surfaces of these mesoscopic F_2 folds were favorable for post-magmatic fluid migration and the occurrence of the graphitic schist played a significant role as structural traps for hydrothermal fluids.

At the Wielisław Złotoryjski deposit the strike of quartz veins (NNW–SSE) is also similar to the axial direction of the narrow folds. Moreover, in Radzimowice the vein strike is concordant with S_1 foliation and lithological boundaries of the host rocks. These veins are strongly structurally controlled. The run of veins is also concordant with direction of the Chmielarz schists thrust over the Radzimowice schists. Here numerous mylonitic and cataclastic structures were found. However, low-angle thrusting between thrust sheets dominated and is not comparable with a high-angle dip of ore veins. The strike and vertical dip of veins indicate rather their connection with the development of the fault zones. The veins orientation is in conformity with the WNW–ESE direction of the Southern Świerzawa fault, which is located only ~2 km northwards (Fig. 80). This fault is classified to the group of the regional frame faults of the Sudetic extensional troughs, which started to form in the Viséan/Stefanian and begun the formation of the Sudetic basins (Teisseyre, 1967; Kozdrój, 1995; Cymerman, 2002). These faults strike almost E–W and are responsible for the division of the Kaczawa Metamorphic Complex into elongated blocks and tectonic troughs. In the Bolków unit these faults are almost vertical or very steep and in most cases of a dextral strike-slip type (Cymerman, 2002). The quartz-ore veins are vertical or steeply dipping from about 60 to 85° to the N or S. The coincidence of the direction of fault surfaces and their steep or vertical dip with the similar distribution of auriferous vein suggests that post-magmatic hydrothermal fluids in the Radzimowice deposit used fractures of such orientation. Furthermore, the strike of the ore veins in Lipa and Grudno is also in conformity with the orientation of the Southern Świerzawa fault. The direction of the vein strike in Wielisław Złotoryjski deposit is similar to the orientation of the fault, which bordered from the west the Świerzawa horst (NNW–SSE). The orientation of these extensional faults seems to be the main factor controlling distribution of auriferous veins in this part of the Kaczawa Mountains. Also the lamprophyre dyke found in the zone of the Miner consolation vein has similar orientation suggesting that this fault is a deep seated, multiple active and suitable way for magma and fluid migration.

In the Klecza–Radomice ore district the vein type ore mineralization is also structurally controlled. In Radomice and Nielestno the surface distribution of the mining waste materials strongly indicate the NE–SW and WNW–ESE strike of quartz-sulphide veins. The NE–SW vein strike is similar to F_2 folds axial-planes with vergence from 5 to 20° to NW. Strike and dip of sedimentary bedding of the feldspathized Ordovician quartz-sericite schists are concordant with limestone lenses emplacements. Moreover, the Silurian quartz-sericite schists with graphite have similar strike and steep dip from 70 to 85° to NE. In Radomice the extension of quartz-sulphide veins is mainly limited to the F_2 fold axial-plane and usually concordant with the bedding. If we accept the newest interpretation that the limestone cropping out near the Radomice deposit is of Silurian or younger age (by correlation with the Wojcieszów limestones), so they constitute the cores of the asymmetric and tight synclines with very steep dip (80°) to SW. Furthermore, the folded Silurian black graphite schist formed asymmetric anticline with steep dip of bedding (75–85°) to NE.

In Pilchowice the mining sites are located along the NW–SE and NE–SW directions suggesting veins distribution along these two directions. Additionally in Klecza occur diagonal veins. The various strike of the quartz-sulphide veins in Klecza–Radomice ore district indicate a more complementary tectonic regime than in the Radzimowice area and not simple shearing. The distribution of veins is irregular and indicates a changeable strength field in the regional shear zone developed between variable terranes along the active Intra-Sudetic fault. Additionally, the veins in Nielestno and Klecza occur directly in the zone of the Kaczawa Metamorphic Complex overthrust along the Pławna fault zone (of NW–SE direction) on the Lower Permian sediments of the Wleń trough. However, this overthrust postdated the formation of auriferous veins.

THE AGE CONSTRAINS OF GOLD AND METALLIC ORE FORMATION OF THE VEIN TYPE IN THE KACZAWA MOUNTAINS

According to $^{40}Ar/^{39}Ar$ data presented by Marheine *et al.* (2002), in the Western Sudetes the host rock schists unit of Ordovician–Lower Carboniferous shaly flysch-type sediments recrystallized during regional uplift-related greenschist metamorphism in the Viséan at 344–333 Ma (Fig. 81). The auriferous mineralization post-dated regional metamorphism of host rocks, orogenic deformation, and the oldest stage of late Variscan magmatism (ca. 330 Ma). The upper limit of the Variscan tectonometamorphic and magmatic activity was dated at 314-312 Ma (Namurian/Westphalian boundary) by $^{40}Ar/^{39}Ar$ method (Marheine *et al.*, 2002). SHRIMP age of zircon from the fine-grained rhyolite is similar to the zircon age from the medium-grained microgranites and indicate that the main magmatic event in the Żeleźniak intrusion at the Radzimowice deposit was restricted to the late Namurian (weighted average $^{206}Pb/^{238}U$ at 316.7 ± 1.2 Ma; Muszyński *et al.*, 2002). According to the Re–Os data presented here and earlier by Mikulski *et al.* (2005a) the age of ca. 317 Ma for auriferous Co-arsenopyrite from the Radzimowice deposit is coeval with SHRIMP ages of igneous rocks from Żeleźniak intrusion. This age of arsenopyrite despite its close correlation with magmatic evolution in the Żeleźniak intrusion is also close to Re–Os age of auriferous arsenopyrite from Klecza.

In the light of the precise Re–Os data for the auriferous Co-arsenopyrite from Klecza (316.6 ±0.4 Ma), its age is younger than the semi-brittle and brittle left-lateral displacements along the Intra-Sudetic fault described by Aleksandrowski (2003). The first stage of refractory gold mineralization at Klecza may be slightly younger than the porphyritic granite of the Karkonosze Massif dated at 325–330 Ma by the Rb–Sr method (Duthou *et al.*, 1991) or dated at 320 ±2 Ma by $^{40}Ar/^{39}Ar$ on biotite (Marheine *et al.*, 2002). Au mineralization is most likely timely associated with lamprophyre dyke dated at 314 ±6 Ma $^{40}Ar/^{39}Ar$ that occur in the Southern Karkonosze Complex (Marheine *et al.*, 2002) and probably predate or are coeval with aplitic granite formation date at 310 ±5 Ma by Rb–Sr (Duthou *et al.*, 1991) or at 312 ±2 Ma by $^{40}Ar/^{39}Ar$ on white mica (Marheine *et al.*, 2002). The Re–Os age of auriferous arsenopyrite from Klecza is somewhere between these magmatic events. In the Radzimowice deposit lamprophyre dykes also occur, however without absolute age determination until now.

The Re–Os result indicates that the one of the major late Namurian post-orogenic extension movement, regional uplift and tectonic displacement along the regional Intra-Sudetic fault took place after emplacement of porphyritic granite (ca. 317 Ma) and was responsible for opening deep-seated fractures that triggered upwelling of lamprophyric magma and opened channel ways for the further migration of post-magmatic mineralizing fluids from various magmatic-metamorphic sources. Shear movements in the Intra-Sudetic fault during Namurian (325–315 Ma) recognised by kinematics and analytical $^{40}Ar/^{39}Ar$ works (Aleksandrowski *et al.*, 1997; Oliver, Kelley, 1993; Marheine *et al.*, 2002) complicated spatial geometry of veins at Klecza–Radomice ore district.

Microscopic gold mineralization of the second and third Au generations described from the Radzimowice and Klecza–Radomice ore district deposits are younger and followed the submicroscopic gold precipitation. The Re–Os measurement of the younger generation pyrite from Klecza and Radzimowice yealded ages of ca. 294 and 280 Ma, respectively. This Lower Permian (Autunian) age indicates the next stage of sulphide (base metal) precipitation before the Triassic. Additionally, even younger mineralization of base metal sulphides are indicated by the results of lead isotope measurements on galena from the Radzimowice deposit (Legierski, 1973). These very questionable data yielded an age of 240–210 Ma (Middle to Late Triassic).

Szałamacha (1976) connected the origin of the barite ± polymetallic deposits from the Kaczawa Mountains with tectonic activities of the Intra-Sudetic fault in Triassic and/or Cretaceous. Jerzmański (1976b) concluded that if ages of galena (240–210 Ma by Pb/Pb method; Legierski, 1973) from Sudetes are reliable the Sudetic barite and fluorite mineralization should be regarded jointly with the polymetallic formation as possibly formed in the same mineralization cycle of regional extent in the early Cimmerian stage (Permian–Triassic) as a result of the reactivation of deep seated regional fault-zones. Also, Pawłowska (1973) postulated the early Cimmerian age for barite and polymetallic ore formation.

Paulo (1973) on the basis of the comprehensive work belived that direction of the successive tectonic structures in the Kaczawa Mountains supposed that quartz-sulphide veins from Klecza–Radomice, Radzimowice and Grudno and barite veins from Stanisławów, and hematite veins from the northern part of the Kaczawa Mountains formed most probably in the Upper Carboniferous and/or Lower Permian. Wajsprych (1974) studied the veins with sulphide in the northern part of the Kaczawa Mountains and concluded that they formed in the Upper Permian within fissures of NW–SE direction. Two-stages of the ore mineralization (older – sulphide, younger – barite ± siderite ± hematite) in the vicinities of Chełmiec, Męcinka and Stanisławów were also connected with two-stages of the magmatic activities (from ca. 310 to 280 Ma) in the Strzegom–Sobótka Granitoid Massif on the Fore-Sudetic Block (Mikulski, Stein, 2005).

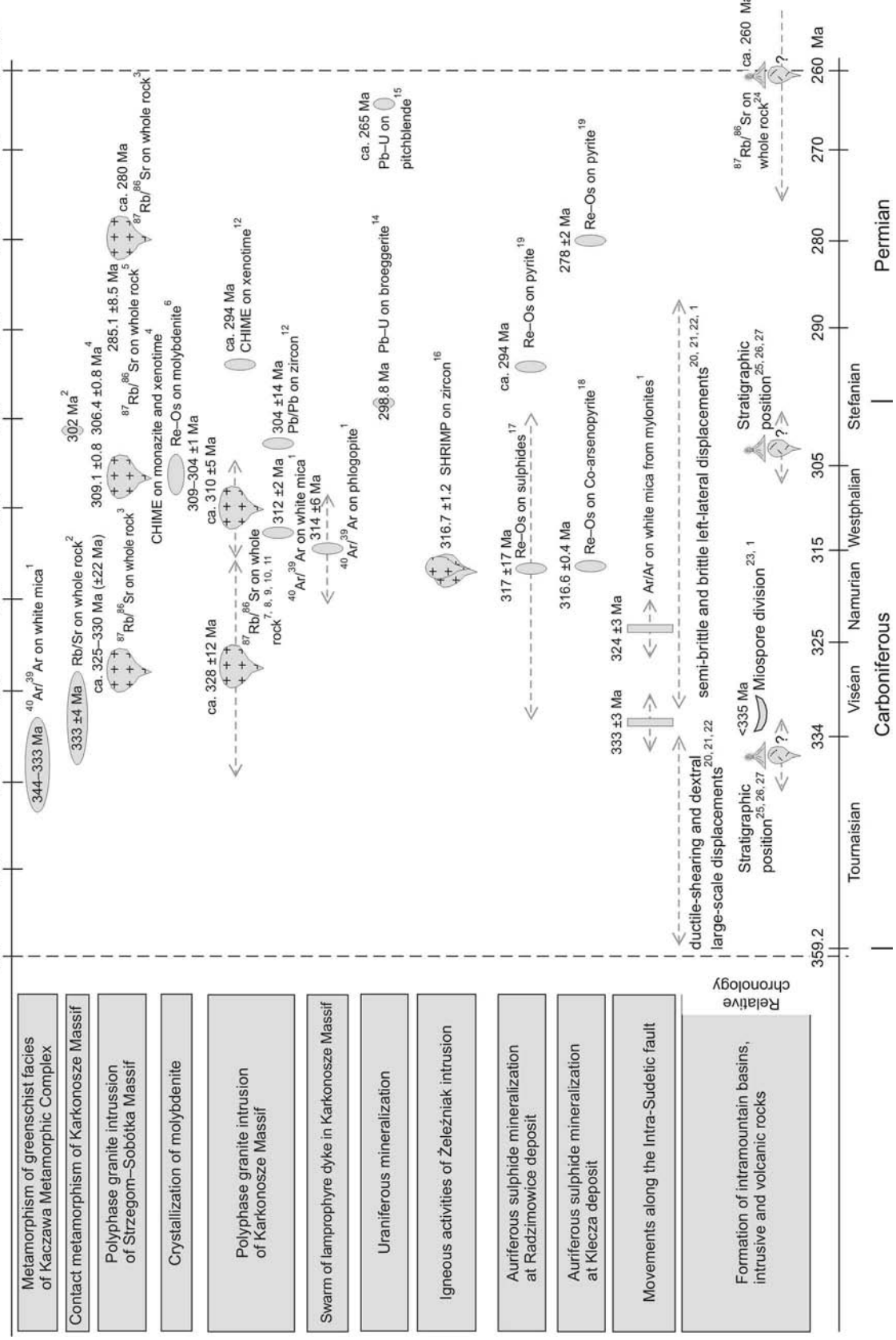

Fig. 81. The age constrains of tectonometamorphic and magmatic activities in the Kaczawa Mountains and beyond in the time period 360–260 Ma

1 – Marheine et al. (2002); **2** – Fila-Wójcicka (2004); **3** – Pin *et al.* (1989); **4** – Turniak, Bröcker (2002); **5** – Domańska-Siuda *et al.* (2004); **6** – Mikulski, Stein (2005); **7** – Depciuch, Lis (1971); **8** – Duthou *et al.* (1991); **9** – Pin *et al.* (1987); **10** – Mierzejewski *et al.* (1994); **11** – Kennan *et al.* (1999); **12** – Mikulski *et al.* (2004); **13** – Kröner *et al.* (1994); **14** – Kucha *et al.* (1986); **15** – Lis *et al.* (1971); **16** – Muszyński *et al.* (2002); **17** – Mikulski *et al.* (2005a); **18** – Mikulski *et al.* (2005d); **19** – this study; **20** – Aleksandrowski (1995); **21** – Aleksandrowski *et al.* (1997); **22** – Aleksandrowski (2003); **23** – Turnau *et al.* (2002); **24** – Pańczyk, Bachliński (2004); **25** – Awdankiewicz (1999); **26** – Mastalerz, Prouza (1995); **27** – Kozłowski, Parachoniak (1967)

THE RELATION OF AGE OF THE GOLD MINERALIZATION IN THE KACZAWA MOUNTAINS WITH OTHER AREAS IN THE LOWER SILESIA

According to Mikulski *et al.* (1999) in the Western Sudetes five main genetic types of gold mineralization can be distinguished:

1. Contact-metasomatic,
2. Hydrothermal connected with developments of the regional shear zones,
3. Hydrothermal related to final sub-volcanic events,
4. Listvenite within ophiolite complexes,
5. Stratabound in Lower Permian sediments.

Gold-bearing ores occur in different forms (skarn, lode, stockwork, vein, rock impregnation and strata-controlled horizon). Paleozoic volcanic-sedimentary rock complexes metamorphosed to greenschist or amphibolite facies, which have been further intruded by Variscan granite, host the first four types of gold mineralization. The fifth type of gold mineralization occurrs within the unconformity between Rotliegende and Zechstein sediments.

At Złoty Stok the loellingite-arsenopyrite or pyrrhotite and magnetite mineralization are believe to formed coeval with the Kłodzo–Złoty Stok granite emplacement ca. 330–320 Ma. Traces of gold recognized in listvenite rocks post-date the formation of the central Sudetic ophiolite (ca. 420–370 Ma) and to be formed simultaneously with one of the tectonic-magmatic stages during Variscan orogeny.

The auriferous mineralization in the Kaczawa Mountains is considered as younger than contact-metasomatic or skarn-like gold mineralization recognized in the Western Sudetes. The gold mineralization in Kaczawa Mountains formed during at least three separate stages. According to Re–Os method auriferous sulphide stages precipitated since ca. 317 Ma to 280 Ma (Namurian–Autunian).

Gold mineralization discovered in the transitional Rotliegende/Zechstein sediments of the North Sudetic Basin near the Nowy Kościół Cu deposit is younger than 280 Ma. This mineralization of unclear origin (Speczik, Wojciechowski, 1997; Wojciechowski, 2001) may be comparable with gold-PGE mineralization in intimate association with red-coloured rocks described as the "Rote-Fäule" facies which mostly underlins the Kupferschiefer horizon in the area of the KGHiM mining district on the Fore-Sudetic Monocline (e.g. Piestrzyński *et al.*, 1997; Speczik *et al.*, 1997; Oszczepalski *et al.*, 1999; Piestrzyński, Sawłowicz, 1999). This gold mineralization was formed as a result of Au leaching by brine from underlying rocks within the Permian–Triassic basins (Piestrzyński, Wodzicki, 2000; Blundell *et al.*, 2003; Shepherd *et al.*, 2005). Gold associated with PGE and organic matter was also reported from the Kupferschiefer by Kucha (1974, 1982). The age of sulphide precipitation within Kupferschiefer varies between ca. 250–180 Ma based on the lead isotopic composition (Wedephol, 1994) and from 256 to 239 Ma according to K–Ar on illite (Oszczepalski, 1999). According to K–Ar illite ages the formation of copper and associated gold within Kupferschiefer deposition took place between 258 and 190 Ma (Mid-Triassic–Lower Jurassic; Bechtel *et al.*, 2000).

COMPARISON OF THE AGE OF THE GOLD EVENTS IN THE KACZAWA MOUNTAINS WITH OTHER AREAS OF THE EUROPEAN VARISCIDES

The European Variscan orogenic gold deposits formed ca. 350–280 Ma in uplifting massifs along the active western edge of the Paleo-Thetys Ocean (Fig. 82; Goldfarb *et al.*, 2001; Groves *et al*., 2005). Those deposits are now exposed in southern and central Europe. Processes of gold mineralization recognized in the Kaczawa Mountains are quite similar to gold-mineralization processes described from the other areas of the European Variscan Belt. However, the age of the gold ore formation is variable. The similar features are mostly caused by geotectonic evolution, two- or three-stage evolution of fluid compositions and mineral precipitation, characteristic mineral paragenesis and texture (e.g. Morávek *et al.*, 1996; Zachariáš *et al.*, 1997; Noronha *et al.*, 2000; Cathelineau *et al.*, 2003). Gold formation, exhumation of host rocks, extensional tectonic setting and lamprophyre dyke appear coeval in the Massif Central, Central Bohemian Province (Bouchot *et al.*, 1989, 2000, 2003) and in the Kaczawa Mountains as well (Mikulski, 2003a).

In the Western Sudetes granite emplaced in the post-collisional continental arc setting is followed by a new continental break in Late Carboniferous. The age of auriferous sulphide mineralization (ca. 317 Ma; Namurian) recognised in the Kaczawa Mountains formed during post-orogenic extension is coeval with uplift of orogen. However, mineralization is not simultaneous with gold events described from the Central Bohemian province ca. 338 Ma (Bouchot *et al.*, 2003) or at 344 ±2.8 Ma by Re–Os method on molybdenite (Zachariáš *et al.*, 2001; Zachariáš, Stein, 2001; Fig. 83). Stein *et al.* (1997) indicate the emplacement of gold lodes in the Proterozoic and Lower Paleozoic high-grade metamorphic rocks of the Bohemian Massif even earlier at 349–342 Ma. This age of gold mineralization is indicated either by the Re–Os method on molybdenite that is paragenetic with gold or by the $^{40}Ar/^{39}Ar$ method on mica from alteration zones.

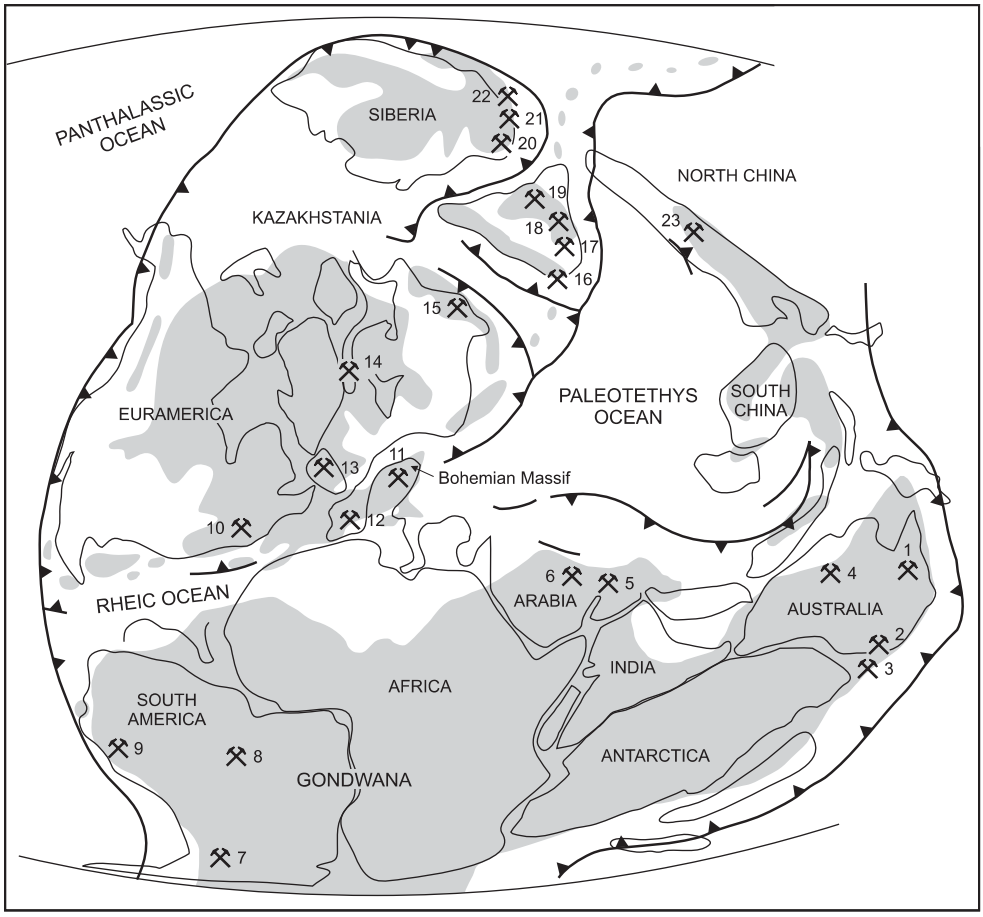

Fig. 82. The distribution of major Paleozoic gold provinces (after Goldfarb *et al.*, 2001)

1 – Thomson Fold Belt; **2** – Lachlan Fold Belt; **3** – Westland, South Island, New Zeland; **4** – Telfer; **5** – Arabian–Nubian shield; **6** – Hoggar shield; **7** – Sierra Pampeanas; **8** – Brasilia Fold Belt; **9** – Eastern Cordillera; **10** – Southern Appalachians; **11**– Bohemian Massif; **12** – Iberian Massif; **13** – Meguma; **14** – Caldonides; **15** – Central Ural Mts., **16** – Western Tian Shan; **17** – Eastern Tian Shan; **18** – Altaids; **19** – Northern Kazakhstan; **20** – Eastern Sayan; **21** – Mongol–Zabaikal Belt; **22** – Baikal; **23** – Northern China Craton

In the Massif Central auriferous lodes were deposited between 330 and 285 Ma (Bouchot *et al.* 1989; Guean *et al.* 1992; Marcoux *et al.*, 2004) with a distinct peak at 310–305 Ma (Bouchot *et al*., 2000). According to Cuney *et al.* (2002) it is possible to define two stages of gold mineralization in the Massif Central. The first stage of gold formed in the early extensional syn-convergence setting during high temperature condition in the period of 330–315 Ma and the second stage of low temperature gold deposits formed at 315–300 Ma. Gold-bearing lodes of the Iberian Massif in Spain and Portugal were also formed during at least two separate periods of time ca. 347 ±10 Ma, <292 ±11 Ma, and 286 ±3.6 Ma (Murphy, Roberts, 1997).

The auriferous mineralization in the Kaczawa Mountains lacks molybdenite and is not spatially associated with granite. But, it was possible to make the Re–Os determinations of molybdenite from the Paszowice quarry in the Strzegom–Sobótka Massif. Molybdenite yields ages from 309 to 304 Ma (Mikulski, Stein, 2005). This molybdenite is younger than the auriferous Co-arsenopyrite (ca. 317 Ma) from Klecza or Radzimowice. Molybdenum mineralization of similar type and age (307 ±3 Ma) has been reported from the southern margin of the Variscan orogen from the Austrian Alps (Langthaler *et al.*, 2004) and similarly, but slightly younger Re–Os ages from Sardinia are also latest Variscan (289 ±1 Ma; Boni *et al.*, 2003). The narrow range of molybdenite age from Paszowice is coeval with the second episode of gold mineralization recognized in the Massif Central and also coincides with a sharp increase in the rate of uplift (310–305 Ma; Bouchot *et al.*, 2000) within the western part of the European Variscides. It seems that molybdenite mineralization at Paszowice postdates the first stage of auriferous sulphide precipitation at Radzimowice and Klecza deposits and possibly is older than the microscopic gold and base metal sulphide mineralization recognised in the Kaczawa Mountains that formed in the within-plate setting. This age range is coeval with the age of gold formation described from the Massif Central (ca. 310–305 Ma) by Bouchot *et al.* (2000). Also, a cross-cutting relationship from the lodes in northern Portugal indicates gold formation first subsequent to emplacement of ca. 320–305 Ma granitoid and later mineralization being coeval with post-tectonic 290–280 Ma granitoid (Noronha *et al.*, 2000).

In the Autunian sandstone in the Massif Central auriferous epithermal sinter that formed ca. 295 Ma was recognised (Marcoux *et al.*, 2004). The Re–Os pyrite ages ca. 294 and 280 Ma from the Radzimowice and Klecza gold deposit respectively are evidently younger and strongly correlated with volcanic activities during rifting in a late Autunian. The formation of gold associated with hematite in Lower Silesia is connected with oxidized fluid migration during the basin formation in a wide range of time from Upper Permian to Cretaceous.

According to Re–Os studies of auriferous sulphide, the 3 separate gold events in the Kaczawa Mountains took place from ca. 320 to 280 Ma. The comparison of gold formation within European Variscan Belt with the Kaczawa Mountains indicates the lack of the oldest Variscan gold-stage ca. 350–330

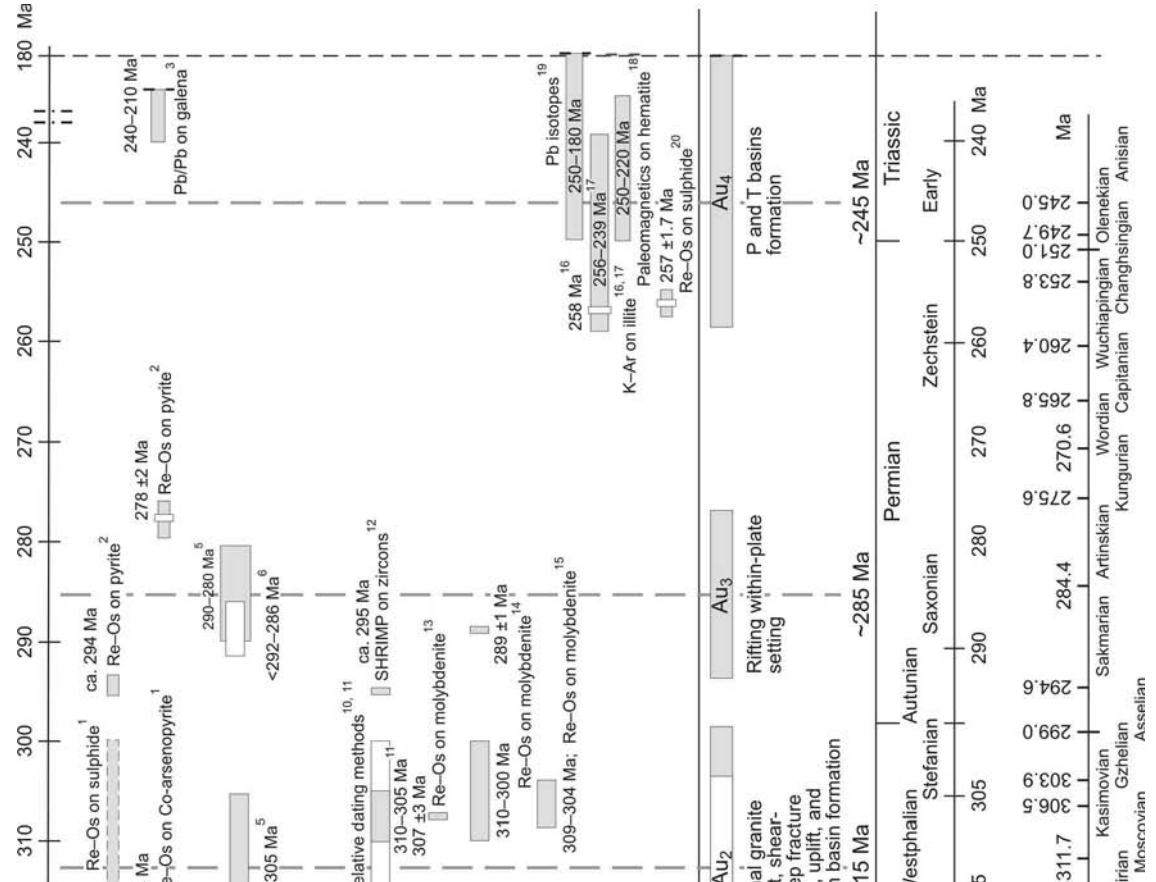

Fig. 83. The comparison of the isotope age determination of ore mineralization associated with gold deposits recognised in the European Variscan Belt and in the Lower Silesia

References to figure: **1** – Mikulski *et al.* (2005a); **2** – this study; **3** – Legierski (1973); **4** – Naden, Shepherd (1991) in Murphy, Roberts (1997); **5** – Noronha *et al.* (2000); **6** – Roberts *et al.* (1991) in Murphy, Roberts (1997); Cotela Neiva, Neiva in Murphy, Roberts (1997); **7** – Stein *et al.* (1997); **8** – Zachariáš *et al.* (2001); **9** – Zachariáš, Stein (2001); **10** – Cuney *et al.* (2002); **11** – Bouchot *et al.* (2000); **12** – Marcoux *et al.* (2004); *13* – Langthaler *et al.* (2004); **14** – Boni *et al.* (2003); **15** – Mikulski, Stein (2005); **16** – Bechtel *et al.* (2000); **17** – Oszczepalski (1999); **18** – Jowett *et al.* (1987); **19** – Wedepohl (1994); **20** – Brauns *et al.* (2003)

Note the stages of the gold formation (Au1-Au4) in the European Variscan belt are recognised by the author

Ma in the Kaczawa Mountains, which elsewhere was connected with the first episode of the syn-collisional granite emplacement (Fig. 83).

In general, within the European Variscan Belt it is possible to distinguished four main stages of gold deposit formation:

1. Stage Au_1 connected with emplacements of syn-collisional granite,
2. Stage Au_2 originated during orogenic uplift, emplacement (where occurs) post-collisional granite, development of regional shearing and/or regional deep fracture (so called submicroscopic gold – auriferous sulphide),
3. Stage Au_3 connected with subvolcanic and volcanic activities in the post-collisional continental arc or within-plate setting (microscopic gold with base metal sulphide),
4. Stage Au_4 originated during the basin formation (native gold-hematite-chalcedony association).

The gap of age between the considered above gold formation stages is ca. 30–40 Ma.

COMPARISON OF THE LATE VARISCAN GOLD-BEARING ARSENIC-POLYMETALLIC MINERALIZATION IN THE KACZAWA MOUNTAINS TO OTHER AREAS IN THE WESTERN SUDETES

In the Western Sudetes the gold-bearing sulphide mineralization occurs in different forms within quartz veins, lodes, and stockworks, or as replacement ore bodies, skarn and host rock impregnations (Tab. 28). These gold-bearing arsenic-polymetallic deposits and occurrences are located within regional shear zones around the syn, late- and post-tectonic Variscan granitoid (Złoty Stok, Czarnów, Bardo Śląskie, Ptasznik, Radzimowice) typically near large-scale transcrustal faults such as the Marginal Sudetic fault (Złoty Stok and Bardo Śląskie) or are located distal from granitoid and are sited in the second-order tectonic structures (Klecza–Radomice ore district; Fig. 80).

The degree of the metamorphism of the rocks hosting gold mineralization varies in different deposits in the Sudetes. In Kaczawa Mountains the host rocks comprise various components of the Paleozoic sedimentary-volcanic succession which were metamorphosed to greenschist facies. In the other areas of the Western Sudetes (e.g. Czarnów, Miedzianka deposits in the Rudawy Janowickie; Złoty Stok deposit and Ptasznik prospect in the Złote Mountains; and Bardo Śląskie prospect in the Bardo Mountains) of Au deposits are hosted by rocks that underwent regional amphibolite facies metamorphism, and additionally were thermally overprinted along the contact with the Variscan granitoid massifs.

Some occurences of gold ore mineralization are accompanied by lamprophyre dykes (Radzimowice, Złoty Stok, Czarnów, Ptasznik and Bardo Śląskie).

In the Złoty Stok As–Au deposit, Au-bearing loellingite-arsenopyrite mineralization of skarn-type is related to elongated lenses of dolomitic marbles and black and green serpentinite along the contact with granitogneisse and Variscan granitoid (Muszer, 1997; Mikulski, 1996). In the Czarnów As-deposit the ore bodies are concordant with a late stage high-angle NE–SW Leszczyniec shear zone within the eastern metamorphic cover of the Karkonosze granite intrusion. In the Kaczawa Mountains gold mineralization occurs almost exclusively in quartz-sulphide veins, which are preferentially located close to or along the fractured axial plane of F_2 anticlines.

In the Western Sudetes the Au-bearing As-polymetallic mineralization followed a contact-metasomatic stage of oxide mineralization (Złoty Stok and Czarnów deposits) and preceded vein-type mesothermal and epithermal hydrothermal mineralization with auriferous sulphides, base metal sulphides associated with Au, Ag, Bi, Te and sulphosalts minerals associated with quartz and carbonates (Fig. 84).

In the Złoty Stok deposit the metasomatic and the oldest stage of ore precipitation with gold-bearing sulphide mineralization was related to processes in the exocontact zone of the I-type Variscan Kłodzko–Złoty Stok granodiorite massif. The younger gold-bearing stages revealed cycles of brittle deformation and hydrothermal infill by mineralising fluids, connected with the development of the regional Skrzynka shear zone (Mikulski, 1996). This stage of mineralization was probably coeval with the first episode of auriferous sulphide mineralization in the Kaczawa Mountains. Gold mineralization of the contact metasomatic type (Złoty Stok) is considered as older (ca. 340–330 Ma) in comparison with the auriferous sulphide mineralization of the vein type character from the Ptasznik macroenclave (Mikulski, 2000b) as well as that described from the Kaczawa Mountains (ca. 317 Ma).

In the Western Sudetes it is possible to separate at least three stages of auriferous sulphide ore mineralization. The two older ones are of the mesothermal types and are overprinted by the younger epithermal sulphide ore mineralization.

The typical alterations of country rocks surrounding gold-sulphide ores are: silicification, feldspathization, sericitization, sulphidization, carbonatization and chloritization. However, in the deposits here described occurs also a very specific mineral assemblages reflecting alteration processes characteristic only of the specific deposit. For example serpentinization strongly developed at Złoty Stok deposit, argillization at Radzimowice deposit and tourmalinization at Klecza deposit.

Arsenopyrite is the principal component of the most gold-bearing ores in the Western Sudetes. However, at Złoty Stok and Czarnów deposits loellingite, pyrrhotite, or magnetite

Table 28

Main features of the gold-bearing As-polymetallic mineralization in the Western Sudetes

Deposit	Type of occurrence	Host rock	Orientation of the ore zone	Ore minerals	Au:Ag ratio	Alteration	Relative timing	Age
Radzimowice	7 quartz veins with sulphides	Radzimowice schists: quartz-graphite-sericite schist, chlorite schist, Chmielarz schists unit: quartz-sericite schist; Igneous rocks of the Żeleźniak massif: ryodacite porphyry, dacite porphyry, lamprophyre	W–E veins steeply dipping south or north (70–85°)	Trace to 20 % sulphides; arsenopyrite, pyrite, followed by chalcopyrite and minor sphalerite, galena, electrum, tellurides and fahlore	in samples with Au contents >0.5 ppm 1:2 to 1:80 Average 1:8 for n=80	Extensive argilitization in dacite porphyry; pyritization, carbonatization, chalcedonitization and local chloritization in metasediments	Post- D_2 deformation; post-metamorphic (post D_3–C_1); post-tonalie and rhyolite emplacement of Żeleźniak intrusion	317 ±17 Ma (Re–Os on sulphides) and ca. 294 Ma on pyrite
Radomice–Golejów	Quartz veins/ lodes, saddle reefs,	Pilchowice unit: quartz-graphite-sericite schists, siliceous schist, lydites,	2 bigger and 2 smaller veins/ lodes up to several dozens cm thick of major NE–SW and minor NW–SE strike directions, and steeply dipping (65–85°) to W; saddle reefs; Examined on a length of about 90–140 m and down dip to 100 m below surface,	In veins: trace to 30 % sulphides; abundant arsenopyrite, As-pyrite with minor galena, sphalerite, chalcopyrite and electrum. In host rocks: framboidal pyrite and Ti-oxides	>0.5 ppm Au 7:1 to 1:10; average 1:1 for n=24	Intensive silicification, and sericitization in vein salbands, moderate carbonatization, illitization, kaolinitization, chalcedonitization, tourmalinization, and extensive pyritization, minor albitization and hematitization	Post-D_2 deformation; post-metamorphic (post D_3–C_1)	No data
Klecza	Quartz veins, saddle reefs, diagonal veins	Pilchowice unit: Quartz-graphite-sericite schists	2 main ore veins of an average thickness 20–25 cm (max. 1.2 m) and 5 side veins and one diagonal vein. These veins were recognised about 90 m along strike. NE–SW and minor NW–SE strike directions, and steeply dipping (65–85°) to W; saddle reefs; diagonal veins	Trace to 25 % sulphides arsenopyrite and As-pyrite and lesser amounts of galena, electrum and sphalerite; remnants of the oxidized parts of primary sulphide ores (covelite, and Fe-hydroxides)	>0.1 ppm Au 8:1 to 1:4; average 2.4:1 for n=40.	Intensive silicification and sulphidization followed by extensive sericitization and later by moderate carbonatization, chalcedonitization, Fe-hydroxidation	Post-D_2 deformation; post-metamorphic (post D_3–C_1)	316 ±0.4 Ma (Re–Os on Co-arsenopyrite) and 278 ±2 Ma (on pyrite)
Złoty Stok	Skarn-type: a) in a contact between four major elongated lenses of dolomitic marbles; b) quartz veins with sulphides	Stronie Śląskie formation: dolomitic marbles; calc-silicate rocks; black- and green serpentinites, amphibolite; granito-gneisses, quartz-mica schist, leptynite	Ore bands of various length (up to 300) and thickness (20–30 m) of NE–SW strike. Several massive nest of As-ore up to 2 m in thickness exploited down to 300 m. Beside, As ore disseminated and in quartz veins	Major loellingite and, As-pyrite replacements bodies and dissemination; Locally rich magnetite-pyrrhotite lenses; minor pyrite, titanite, base metal sulphides, scheelite, Bi-minerals, electrum; In quartz veins U-mineral	>1 ppm Au ~5:1 to 1:9; average 2:1 for n=21	Dolomitization, diopsidization, sulphidization, serpentinitization, silicification, feldspatization, carbonatization, prehnitization, chloritization, epidotization	Post-metamorphic (post D_3–C_1) and post- Kłodzko-Złoty Stok granite emplacements	Post 298 Ma (K–Ar); syn- formation of leucocratic veins ca. 280–262 Ma (K–Ar)
Czarnów	Quartz- -sulphide vein	Eastern metamorphic cover of the Variscan Karkonosze granite; Czarnów schist formation: calc-silicate rocks, marbles, quartz- mica schist, amphibolite, gneiss	NE–SW main quartz vein/lode splits in 2 or 3 parts; Lode has length *ca*. 0.6 km and average thickness 0.4 m, steeply dipping (80°) to SE. Pyrrhotite and magnetite formed isolated lenses or nests up to 3 m thick	Major arsenopyrite, magnetite, pyrrhotite, moderate pyrite, galena, chalcopyrite, minor cassiterite, scheelite, electrum, Bi-minerals	>1 ppm Au ~1:4 to 1:100; average 1:10 for n=18	Silicification, feldspatization, carbonatization, chloritization, epidotization	Post-metamorphic (post D_3–C_1) and post-Karkonosze granite emplacements	Post-: a) porphyritic biotite granite emplacements 329 ±19 Ma (Rb–Sr) and b) equigranular granite and leucogranite 309 ±3 Ma

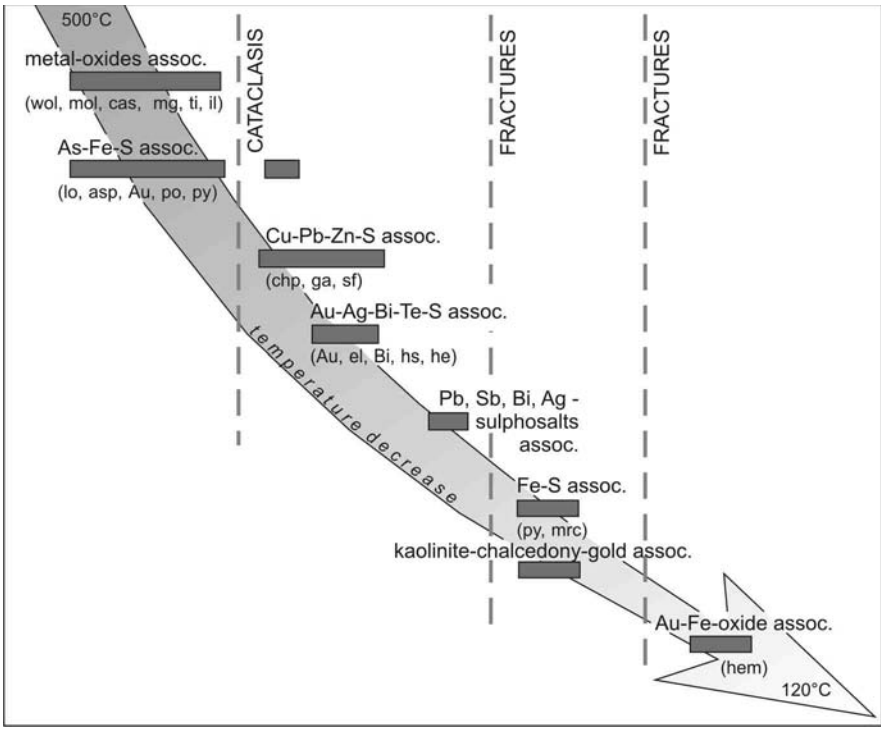

Fig. 84. Schematic mineral succession in Au-bearing As-polymetallic deposits in the Western Sudetes

Abbreviation: q – quartz; wol – wolframite; mo – molibdenite; cas – cassiterite; sch – scheelite; mg – magnetite; ti – titanite; il – ilmenite; py – pyrite; lo – loellingite; asp – arsenopyrite; po – pyrrhotite; mrc – marcasite; chp – chacopyrite; Au – native gold; el – electrum; Bi – native bismuth; hs – hessite; he – hedleyite; ga – galena; sf – sphalerite; hem – hematite

are in places the principal component of ores. Arsenopyrite occurs in three generations with the oldest most characteristic Co-bearing generation that shows massive brecciated textures. Arsenopyrite has a variable chemical composition (Fig. 85). Arsenopyrite geothermometry applied to the samples from the Western Sudetes indicates that arsenopyrite crystallized in wide range from ca. <540 to <300°C (Mikulski, 2005c).

Most gold occurs as fine-dispersed submicroscopic particles in arsenopyrite with high Co-admixture (1–7 at %). Other sulphides, except As-bearing pyrite from Klecza, contain less submicroscopic gold (Fig. 86).

As a rule microscopic native gold and electrum, in association with Bi (±Te) minerals, are representing younger stages of Au precipitation. The measured Ag concentrations in gold ranged from 5 to 45 wt % (Fig. 87). The high-grade gold (850–950) from microveinlets, inclusions, and as "free" gold occurs in the Klecza–Radomice ore district and as inclusions in arsenopyrite ores from the Bardo Śląskie prospect (Mikulski, 1998). The lowest grade (550–620) was revealed by electrum from the Czarnów deposit (Mikulski, 1997). Gold of purity from 650 to 800 is dominant in the deposits here considered.

In the Western Sudetes the $\delta^{34}S_{CDT}$ values of auriferous and base metal sulphides are in the range from ca. –3 to +8‰. These values are different and vary for the specific deposits and between sulphides (Fig. 88). In general these results of $\delta^{34}S_{CDT}$, indicate a postmagmatic hydrothermal origin with local crustal contribution of sulphur. The presence of Au in association with Bi (±Te) is characteristic feature of deposits located close to acidic magmas (Złoty Stok, Bardo Śląskie, Radzimowice).

Geothermobarometric studies in quartz from rocks hosting impregnated arsenopyrite mineralization revealed crystallisation temperatures at about 400°C and in quartz from Au-bearing arsenopyrite/pyrite quartz veins at 320–230°C, from fluids with salinity from 1 to 14 wt % equivalent NaCl (Fig. 89). Increased salinities were recognised in deposits with higher contents of base metals (Czarnów) or only copper (Radzimowice).

Geochemical studies indicate that the Au/Ag ratio varies within wide limits for deposits of Western Sudetes (Fig. 90). In ore grade material (>1 ppm) it averages: 2:1 (Złoty Stok), 1:1 (Radomice), 1:6 (Radzimowice) and 1:10 (Czarnów). In Radzimowice, Au shows a positive correlation with Ag, S, Bi, Fe, Co, Cd, Cu and CaO in Złoty Stok with Bi, As, and poorer with SiO_2 in Czarnów with Co, Fe, S,

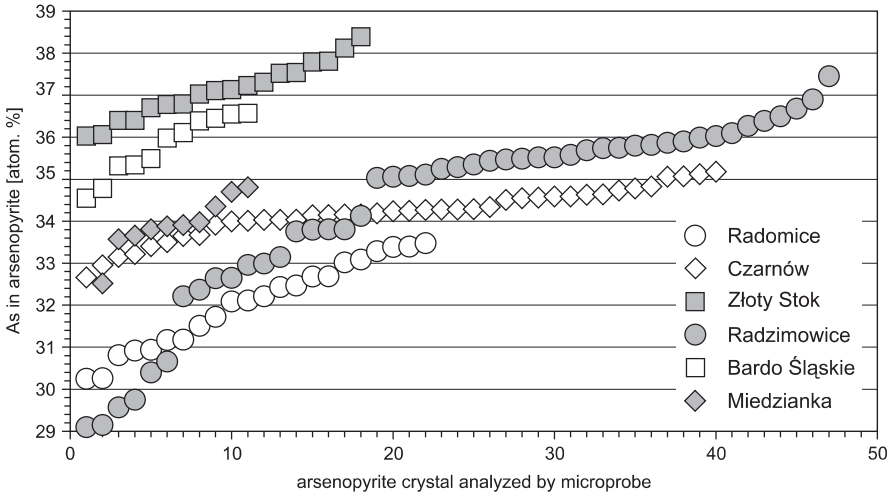

Fig. 85. Plot of the comparison of arsenic contents in arsenopyrite from various gold-bearing arsenic-polymetallic deposits in the Western Sudetes

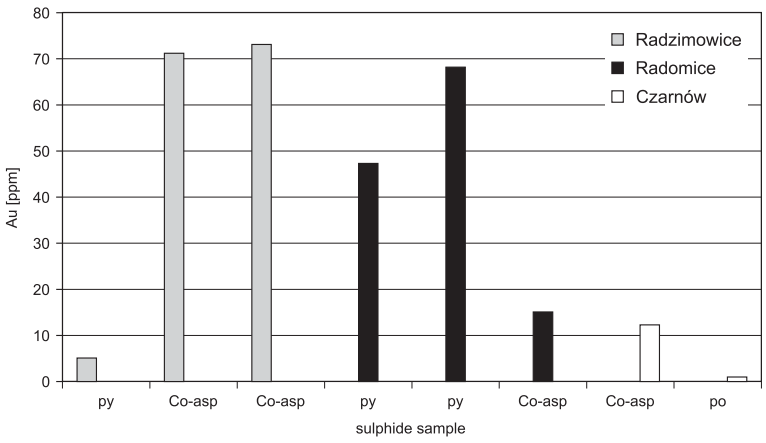

Fig. 86. Histogram of submicroscopic gold contents in the selected sulphides from the gold-bearing As-polymetallic deposits in the Western Sudetes

Abbreviations: Co-asp – Co-bearing arsenopyrite, po – pyrrhotite, py – pyrite

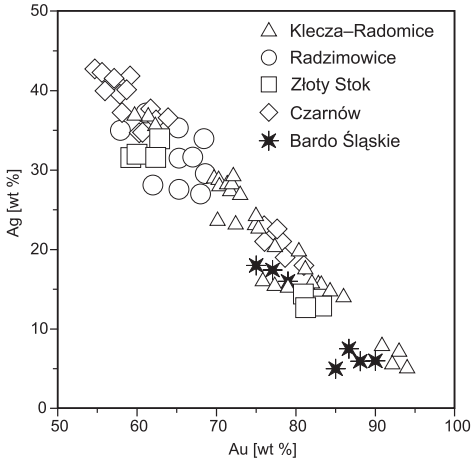

Fig. 87. Silver and gold contents of native Au and electrum in arsenic-polymetallic ores from the Au-bearing arsenic-polymetallic ores in the Western Sudetes

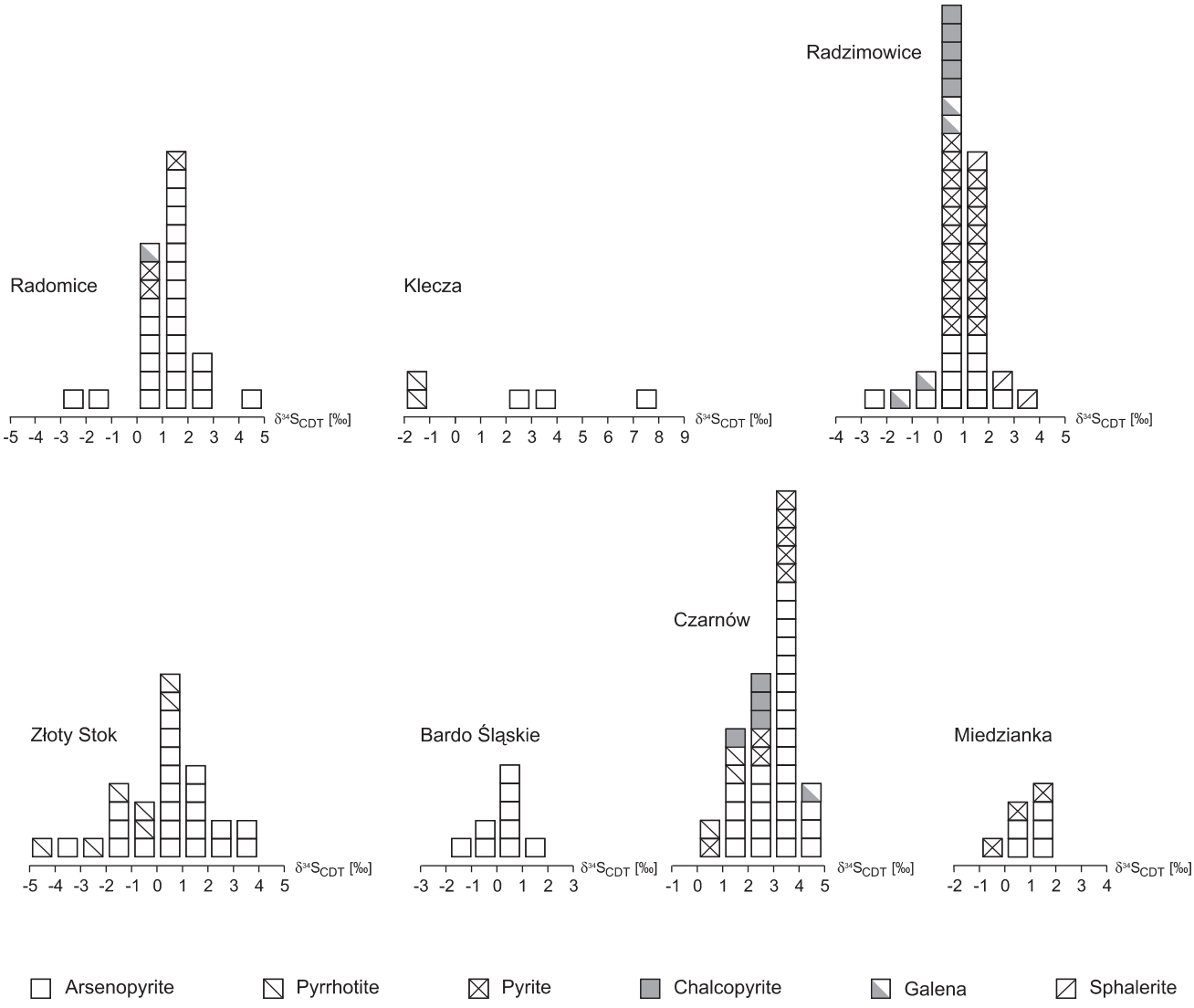

Fig. 88. The $\delta^{34}S_{CDT}$ value histograms for sulphides from gold-bearing arsenic polymetallic ores in the Western Sudetes

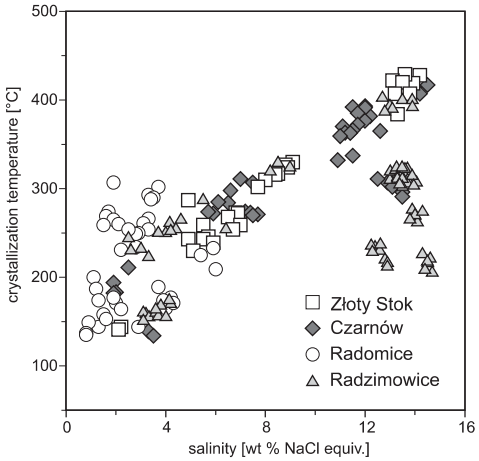

Fig. 89. Crystallisation temperature versus salinity for primary fluid inclusions in quartz from Au-bearing mineralization in quartz-veins and host rocks in the Western Sudetes (Mikulski, 2001)

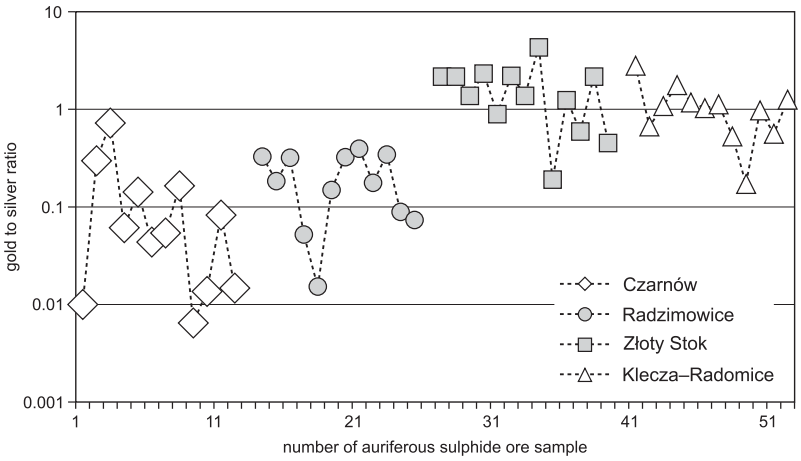

Fig. 90. Gold to silver ratio in gold-bearing arsenic ores of grade higher than 1 ppm Au

Fe, Bi, Cu, Ag and Pb in Klecza–Radomice ore district with As, Fe, Ag, Zn, S and Bi (Tabs. 29, 30). The above confirms a strong affinity of Au to sulphides in all deposits. The average concentration of gold in ore samples of grade >1 ppm Au is 14.9 ppm (n = 52), (Fig. 91; Tab. 31).

Geological setting and ore structures of the 1st stage of ore mineralization in the Złoty Stok deposit and the low Au/Ag ratios and significant base-metal and Sn contents in the Czarnów deposit suggest gold crystallization from intrusion related systems to Lower Paleozoic VMS deposits (Fig. 92).

The most characteristic of the auriferous mineralization in the Kaczawa Mountains are: geological setting in accreted metamorphic terranes and the strong structural control of the quartz-sulphide veins which are distal from the granites systems.

Table 29

Correlation of Au with other metals in Au-bearing As-polymetallic Radzimowice and Klecza–Radomice deposits

Klecza–Radomice ore district / Radzimowice		Au	Ag	As	Cu	Pb	Zn	Co	Fe_2O_3	Ni	V	Bi	SiO_2	CaO
		n=71	n=71	n=71	n=71	n=71	n=71	n=71	n=71	n=60	n=60	n=27	n=43	n=43
Au	n=178	1.00	.45	**.56**	.02	.39	**.44**	–.014	**.47**	.24	–.09	.22	–.16	–.14
Ag	n=178	**.89**	1.00	**.54**	.35	**.67**	.30	.07	**.60**	.08	.07	**.59**	–.44	–.11
As	n=178	.07	.19	1.00	–.04	.39	.20	.01	**.80**	–.01	–.09	**.90**	–.65	–.20
Cu	n=178	**.44**	**.62**	.24	1.00	.06	.15	.13	.090	.03	.01	–.21	.08	–.04
Pb	n=178	–.05	.10	.29	–	1.00	**.47**	–.02	**.36**	.07	–.07	.56	–.20	–.09
Zn	n=57	**.44**	**.53**	.18	**.68**	.25	1.00	.00	.17	**.40**	–.04	.08	.07	–.08
Co	n=57	.57	.53	.23	**.64**	–.18	**.59**	1.00	.35	–.04	–.06	–.17	–.21	.16
Fe_2O_3	n=57	**.63**	**.67**	.33	**.46**	–.07	**.45**	.61	1.00	**.41**	.00	**.76**	–.75	–.15
Ni	n=41	–.09	–.14	–.07	–.04	–.19	–.16	–.04	.01	1.00	.36	–.12	.23	–.08
V	n=41	–.24	–.33	–.34	–.33	–.12	–.40	–.33	–.37	.62	1.00	–.058	.06	–.20
Bi	n=132	**.79**	**.76**	.15	**.40**	–.10	.16	.32	**.53**	.15	–.02	1.00	–.71	–.35
SiO_2	n=49	–.61	–.63	–.36	–.54	.11	–.39	–.63	–.93	–.26	.10	–.59	1.00	–.37
CaO	n=25	.20	.11	–.21	.08	–.12	.11	.09	.08	**.85**	**.59**	**.41**	–.32	1.00

Bold written digit indicates moderate and/or strong (underline) correlation value between selected elements; n – number of samples

Table 30

Correlation of Au with other metals in Au-bearing As-polymetallic Złoty Stok and Czarnów deposits

Czarnów / Złoty Stok		Au	Ag	As	Cu	Pb	Zn	Co	Fe_2O_3	Ni	V	Bi	SiO_2	CaO	MgO
		n=37	n=37	n=37	n=37	n=37	n=37	n=37	n=37	n=26	n=26	n=28	n=37	n=37	n=37
Au	n=65	1.00	**.41**	.22	**.43**	.34	.07	.32	**.65**	–.09	–.26	**.44**	–.33	–.48	.03
Ag	n=65	–.12	1.00	.25	**.92**	**.98**	**.65**	–.04	–.01	–.13	–.12	**.96**	.24	–.18	–.31
As	n=65	**.67**	.01	1.00	.27	.20	.22	.18	.17	–.28	–.20	.19	–.03	–.20	–.25
Cu	n=65	–.21	.09	–.18	1.00	**.90**	**.67**	.06	.02	–.14	–.13	**.93**	.27	–.21	–.25
Pb	n=65	–.14	–.27	–.017	–.01	1.00	**.66**	–.12	–.11	.02	.08	**.94**	.34	–.18	–.38
Zn	n=65	.00	–.09	.09	.13	.22	1.00	.12	.04	–.22	–.08	.57	.29	–.11	–.31
Co	n=65	.03	**.37**	.27	.26	–.30	–.08	1.00	**.61**	–.19	–.16	–.11	–.29	–.37	.25
Fe_2O_3	n=65	–.29	.18	–.21	**.50**	–.157	–.02	**.68**	1.00	–.18	–.27	–.21	–.81	–.57	.32
Ni	n=0	–	–	–	–	–	–	–	–	1.00	**.84**	–.13	–.08	–.05	–.11
V	n=67	.04	–.10	.20	–.09		.03	.07	–.15	–	1.00	–.45	–.05	–.08	–.19
Bi	n=21	**.92**	–.40	**.89**	–.41	–.12	.17	–.20	–.41	–	–.18	1.00	.13	–.13	–.39
SiO_2	n=65	.35	–.13	.28	–.21	.05	.02	–.23	–.59	–	.30	.17	1.00	.08	–.41
CaO	n=65	–.16	.01	–.21	–.38	.04	–.10	–.44	–.54	–	–.12	.06	–.09	1.00	.05
MgO	n=65	–.07	–.01	–.22	–.31	–.13	–.02	–.38	–.18	–	–.45	**.37**	–.19	.10	1.00

Bold written digit indicates moderate and/or strong (underline) correlation value between selected elements; n – number of samples

The present data suggest that the gold-bearing arsenic-polymetallic deposits in the Western Sudetes formed during geotectonic transition from post-collisional continental arc to within-plate settings.

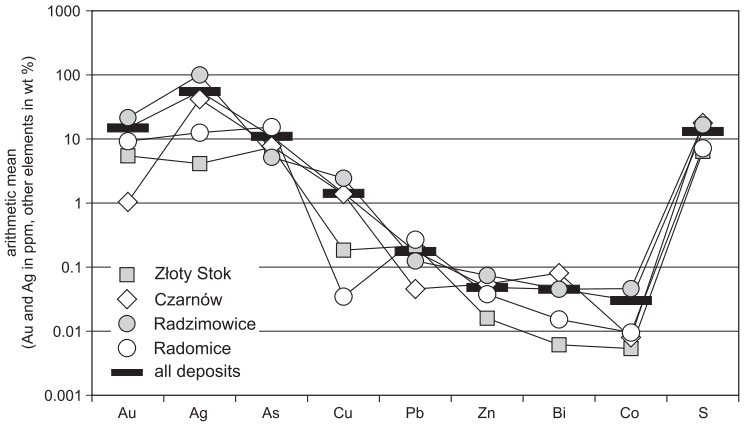

Fig. 91. Arithmetic mean for selected elements in ore of grade higher than 1 ppm Au (after Mikulski, 2001)

Table 31

Arithmetic average concentrations of Au, Ag, Bi, and Te in gold-bearing As-polymetallic deposits in the Western Sudetes

Element [in ppm]	Złoty Stok			Radzimowice			Radomice-Klecza			Czarnów		
	a	n	max	a	n	max	a	n	max	a	n	max
Au	3.90	88	40.0	6.57	131	135	10.1	99	100	1.05	47	12.6
Ag	4.68	73	14	38.63	131	436	7.17	69	49	31.93	39	380
Bi	61.4	21	251	147.6	127	1860	105	23	320	77.9	28	5520
Te	5.8	10	26.8	48.7	9	149	4.3	8	15.3	4.03	10	13.65

a – aritmetic average, n – number of samples, max – maximum contents

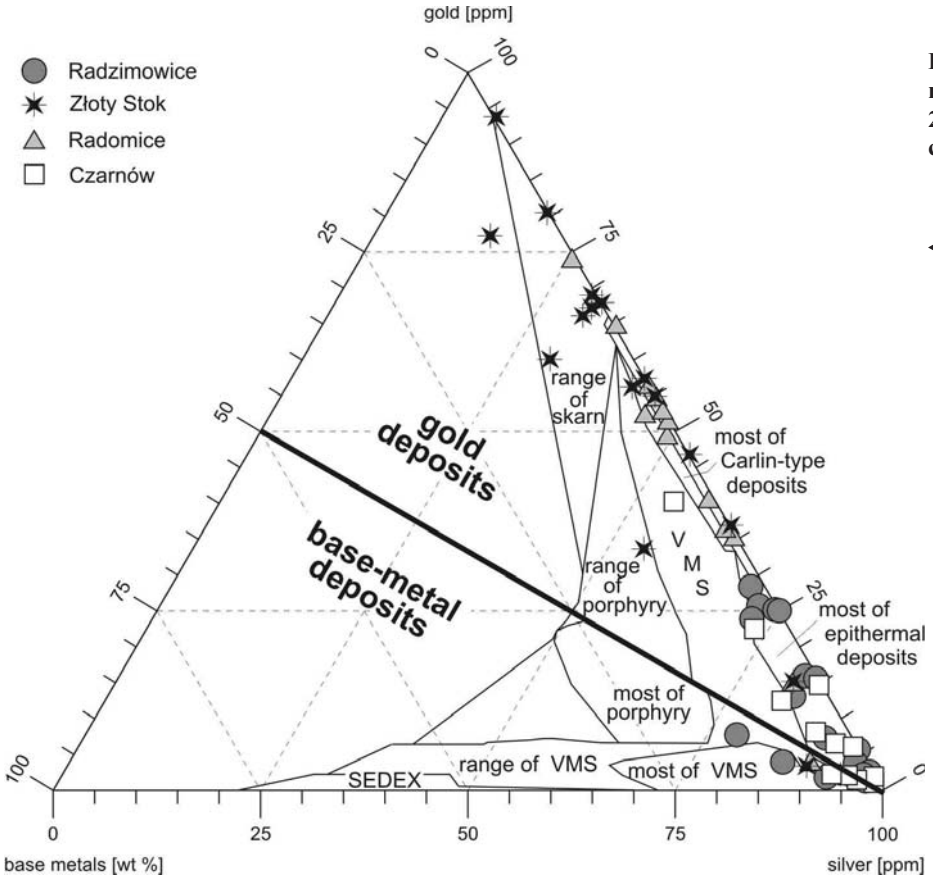

Fig. 92. Pseudo-ternary Au–Ag-base metals diagram (after Poulsen *et al.*, 2000) illustrating the estimated compositions of Au-bearing As ores from the Western Sudetes

GEOTECTONIC SETTING OF THE GOLD MINERALIZATION IN THE KACZAWA MOUNTAINS DURING CARBONIFEROUS–PERMIAN

The terrane collision in front of the closing Rheic Ocean between Euamerica and Gondwana, during the period of 360–280 Ma, led to the formation of a series of European Variscan gold provinces in Bohemian and Iberian massifs (Fig. 82; Goldfarb *et al.*, 2001). Various geotectonic settings of gold ore formation after Groves *et al*. (1998a) are shown on the Figure 93.

In the Kaczawa Mountains, which constitute the NE part of the Bohemian Massif, the rocks hosting gold mineralization consists mostly of volcanic-sedimentary series that represent Paleozoic geological evolution of the Western Sudetes characterized first by rifting during Ordovician to Devonian times, and further by subduction-collision setting during Late Devonian to Early Carboniferous (Franke, Żelaźniewicz, 2000; Kozdrój *et al.*, 2001; Matte, 2001). The geotectonic setting of the Kaczawa Mountains during Early Carboniferous is characterised by tectonic regime of compression/transpression characters on the convergent margin within orogen first of an accretionary character followed by collisional setting (*op. cit.*). After the first stage of granite emplacement in the Western Sudetes during Namurian the late collisional setting changed into post-collisional. In Carboniferous the major NW–SE trending dextral strike-slip faults were developed as a result of the oblique convergence between the amalgamated Bohemian Massif and the blocks already accreted to the East European Craton (Aleksandrowski, 1997, 2003; Seston *et al.*, 2000). The Kaczawa Metamorphic Complex was rapidly uplifted during Namurian/Westphalian. In the Western Sudetes several volcanic centres were controlled by NNW–SSE to NW–SE aligned fault zones which also bound the Variscan depressions such as the North Sudetic Basin, Intra-Sudetic Basin and the Świerzawa graben, (Dziedzic, 1996). These intramountain-basins formed during Westphalian and are filled with flysch-like sediments associated by volcanic rocks.

According to the Re–Os data the first stage of mesothermal auriferous sulphide mineralization (ca. 317 Ma; Namurian) slightly postdates the emplacement of porphyritic granites of the Karkonosze Granite Massif and multiple magmatic events of the Żeleźniak intrusion in Radzimowice. The first stage of granite emplacement was during the Sudetian phase of the Variscan orogeny ca. 330–325 Ma (Viséan–Namurian) according to Rb–Sr data (Pin *et al.*, 1989; Duthou *et al.*, 1991; Oberc-Dziedzic *et al.*, 1999) or 320 ±2 Ma (Ar/Ar on biotite after Marheine *et al.*, 2002). According to SHRIMP data (Muszyński *et al.*, 2002) the age values of Żeleźniak granite and rhyolite porphyry formation are almost identical (ca. 317–316 Ma).

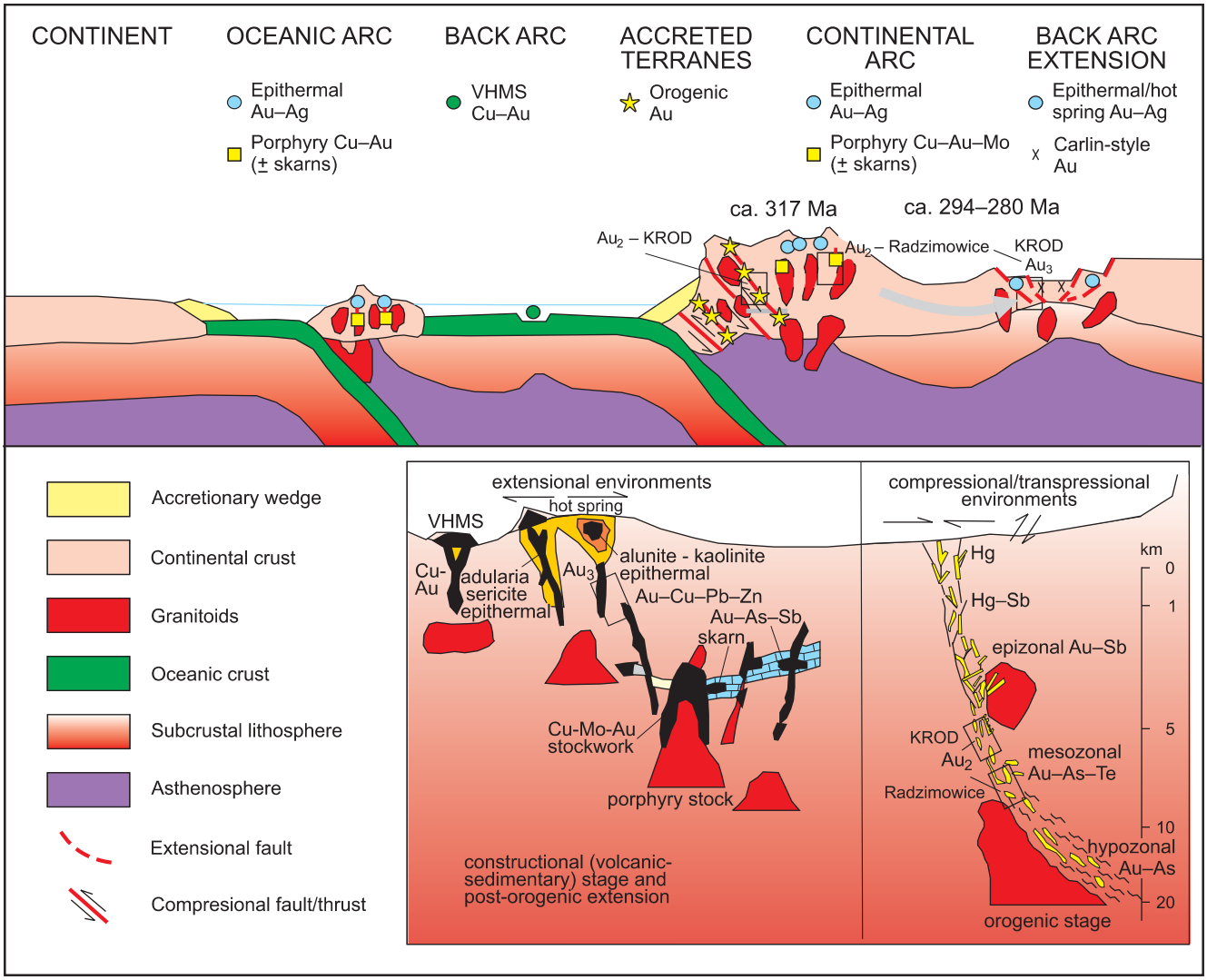

Fig. 93. The tectonic settings of the gold-rich epigenetic mineral deposits (after Groves *et al.*, 1998a)

Gold mineralization stages (see Fig. 83): Au_2 – mezothermal quartz with submicroscopic gold; Au_3 – epithermal quartz with microscopic gold – recognised by author within the quartz-sulphide deposits in the Kaczawa Mountains, which formed in Upper Carboniferous–Permian;

KROD – Klecza–Radomice ore district; for more explanation see text

Granite characteristics suggest a syn-collisional I-type (porphyry granites of the Karkonosze Granite Massif and the oldest generation granite of the Strzegom–Sobótka Massif). However, the location of most Karkonosze granite samples in the field of syn-COLG on the Rb/Y + Nb diagram (Fig. 94) after Pearce *et al.* (1984) suggest that they should be regarded rather as S-type granites according to White, Chappell (1977) classification. The Strzegom–Sobótka granites from the western part of the massif are situated in the VAG field, far enough from the limit of the collisional granite field, suggesting that these granites formed within a subduction regime in magmatic oceanic arcs. Furthermore, several granite samples of younger generation are located in the field of the within-plate granites (WPG). Such conclusions are supported by values of the A/CNK coefficient. Granite from the eastern part of the Strzegom–Sobótka Massif represented mostly by biotite granodiorite reveals even a more metaluminous character, whereas the two-mica granite is peraluminous (Puziewicz, 1985, 1990).

The granitoid and other igneous rocks of Żeleźniak and Bukowinka intrusions plot in the volcanic arc granites field on the Y + Nb versus Rb diagram after Pearce *et al.* (1984) close to a triple boundary point that is characteristic of post-collisional granites. On a Ti *vs*. Zr diagram (after Pearce, 1983) the samples plot in the volcanic arc lavas, out of within-plate lavas. On diagrams of Müller, Groves (2000) also based on simple ratios of "immobile" elements Zr/Al_2O_3 versus TiO_2/Al_2O_3 it is possible to discriminate potassic igneous rocks from continental (CAP) and post-collisional areas (PAP) from the within-plate

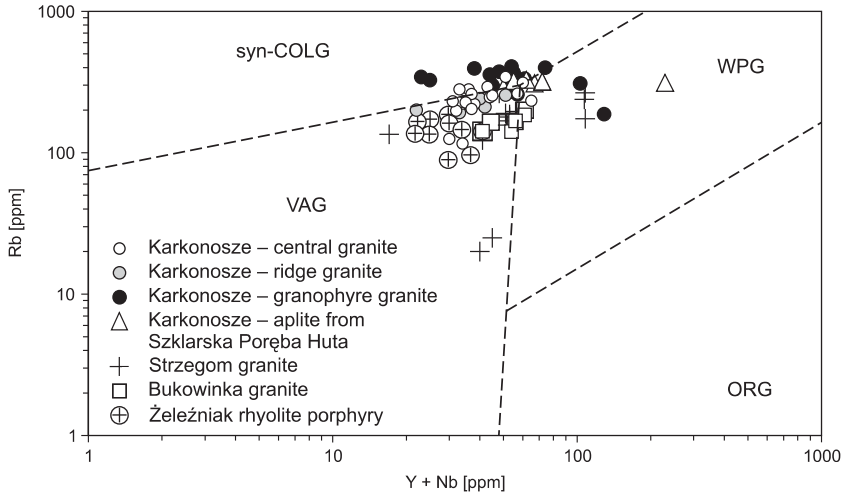

Fig. 94. Rb versus Y+Nb (after Pearce *et al.*, 1984) applied for samples from this study

Abbreviations: syn-COLG –syn-collisional granite, VAG – volcanic arc granite, WPG – within-plate granite, ORG – oceanic ridge granite

setting. Samples from Radzimowice fall into the continental and post-collisional fields. The above is confirmed on the next figures that discriminates oceanic from continental and post-collisional arc settings, based on the lower La and Hf contents of the former.

Based on geochemical results, during the processes of rhyodacitic magma generation, a significant role was played by continental crust with contributions from maphic alkaline magmas (lamprophyre). This model is consistent with tectonic interpretations of the area presented by Awdankiewicz (1999) for the older calc-alkaline volcanic suite of Upper Carboniferous age from the Intra-Sudetic Basin formed in a post-collisional tectonic setting.

Probably one of the major processes of post-orogenic extension, rapid regional uplift and tectonic displacement along the regional Intra-Sudetic fault occured ca. 317 Ma (late Namurian–early Westphalian) and were responsible for opening deep-seated fractures that triggered upwelling of alkaline lamprophyric magma and opened channel ways for the migration of post-magmatic mineralizing fluids related to acidic magmas (granites of the post-collisional characteristic: the ridge granite of the Karkonosze Granite Massif, Bukowinka granite and two-mica granite of the Strzegom–Sobótka Massif). Lamprophyre dykes predates auriferous sulphide mineralization.

On the diagram of Rb/30-Hf-Tax3 after Harris *et al.* (1986) the Karkonosze and Bukowinka granite fall within the late- and post-collisional granite fields and most of the Strzegom–Sobótka granite in the within-plate granite field (Fig. 95).

The transition from the post-collisional to within-plate settings was favorable for the formation of gold mineralization of epithermal type in upraised areas of the Kaczawa Mountains.

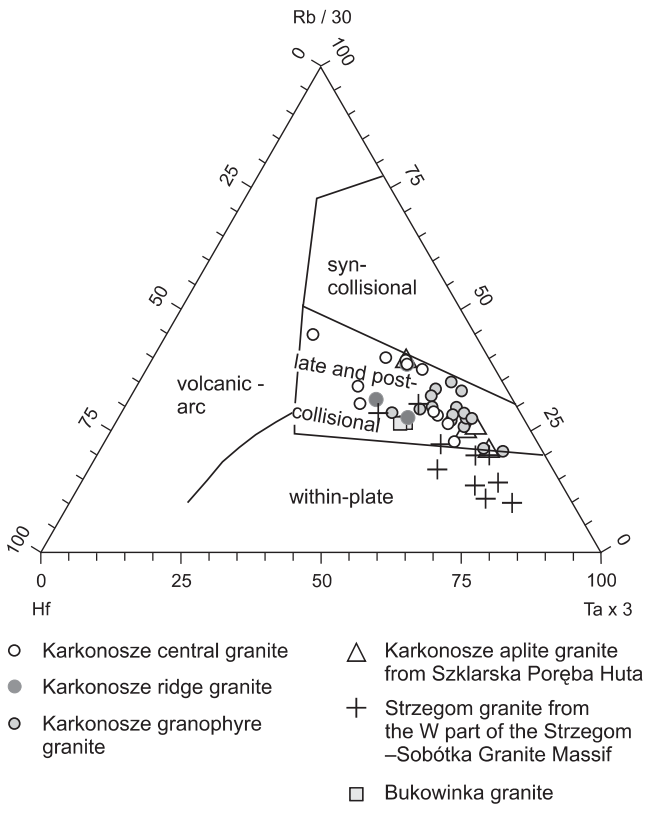

Fig. 95. Rb/30-Hf versus Ta x 3 (after Harris *et al.*, 1986) applied for samples from this study

CLASSIFICATION AND TECTONIC MODELS OF GOLD MINERALIZATION IN THE KACZAWA MOUNTAINS

There are several modern gold deposits classifications and numerous genetic models of gold deposits formation published elsewhere (e.g. Richards, 1995; Goldfarb *et al.*, 1997, 2001; Robert *et al.*, 1997; Groves *et al.*, 1998a, b, 2005; Hedenquist *et al.*, 1998, 2000; Bierlein, Crowe, 2000; Bouchot *et al.*, 2000, 2003; Jensen, Barton, 2000; Müller, Groves, 2000; Poulsen *et al.*, 2000; Sillitoe, 2000; Thompson, Newberry, 2000; Baker *et al.*, 2005). Recently, Kerrich *et al*. (2000) presented the summary of the modern gold formation models. They also distinguished six distinct world-class gold deposits: orogenic gold, Carlin and Carlin-like gold deposits, epithermal gold-silver deposits, copper-gold porphyry deposits, iron-oxide copper-gold deposits, and gold-rich volcanic hosted massive sulphide to sedimentary-exhalative (SEDEX) deposits. This classification reflects distinct geodynamic settings. However, it embraces only world-class deposits with resources of gold >300 ton. For that reason the classification of gold deposits from the Kaczawa Mountains should be related also to other genetic models that take into consideration small and medium-size Au deposits (e.g. Richards, 1995; Groves *et al.*, 1998a; Bouchot *et al.*, 2000; Poulsen *et al.*, 2000; Thompson, Newberry, 2000; Cathelineau *et al*., 2003).

Until now the genesis of gold deposits in the Kaczawa Mountains has been mostly connected with the Karkonosze granitoid parent magma or with the rhyolite magma in the Żeleźniak Massif (e.g. Manecki, 1965; Zimnoch, 1965; Fedak, Lindner, 1966). Gold deposits in Klecza–Radomice and in Radzimowice and the other small occurrences were also linked to volcanic-epithermal processes (Paulo, Salamon, 1973a) and to metamorphic processes (Manecki, 1965). Two main genetic models of gold deposit mineralization in the Kaczawa Mountains are presented below.

The geological setting and ore structures, type of alteration, physical-chemical characteristics of mineralized fluids, high contents of silver and base metals in Radzimowice indicates gold mineralization in the magmatic systems. Furthermore, geotectonic setting of igneous rocks of the Żeleźniak intrusion on the discrimination diagrams, ore textures, low Au/Ag ratios, and significant Cu content point to a formation within magmatic environment of a post-collisional continental arc setting. Strong alteration processes at first of acidic and than of alkalic nature produced mineral assemblages that are characteristic of alkaline-related gold deposits. According to the characteristics of alkaline gold deposits presented by Richards (1995), and Jensen, Barton (2000), it is possible to regard the early mineralization at the Radzimowice deposit as transitional between porphyry and epithermal, and the late mineralization as epithermal type (Mikulski, 2005a). The transition from mesothermal to epithermal mineralization may be interpreted either as a result of continuous syn-mineralization uplift of the Żeleźniak igneous complex in relation to post-orogenic regional uplift started in Upper Carboniferous or as simple cooling of the high-temperature hydrothermal system. Telescoping is a characteristic feature of magmatic-hydrothermal systems in a high-level setting (Jensen, Barton, 2000). The common presence of breccia textures of the early sulphides testifies to rapid and perhaps explosive ascent of late fluids from the depth. The shift from mesothermal to epithermal conditions of the gold mineralization in quartz-lode type deposits in the European Variscan Belt is recently recognised as a common feature driven by changes in the uplift rates, tectonic regimes and heat production (Cathelineau *et al.*, 2003). The latter authors recognised that the series of Late Carboniferous orogenic gold deposits shows identical patterns of P-T-X-t fluid evolution that strongly differ from the commonly accepted models for orogenic Au deposits, allowing the definition of a Variscan-type.

According to Thompson, Newberry (2000) model the mineralization a the Radzimowice deposit may be classified as the shallow level expression of the intrusion-related low sulphidation mineralization. The predominant sulphide assemblage (pyrite-pyrrhotite-arsenopyrite) in reduced intrusion-related gold deposits differs from porphyry copper deposits, but is similar to that of the W–Sn–Mo systems (Thompson, Newberry, 2000). At Radzimowice the granitic rocks are also present as small stocks with cogenetic volcanic rocks, and dyke swarms. The mineral assemblage of greisens association (cassiterite-wolframite-molibdenite-fluorite) was found only in samples from mining waste in Radzimowice (Sylwestrzak, Wołkowicz, 1985). This type of mineralization is of minor significance and was never reported by miners or other geologists. However, the ore composition indicates granite intrusion of the S-type. In the Bohemian massif porphyry –type mineralization was described from the Petráčkova Hora on the Czech side (Zachariáš *et al.*, 2001). However, ores at Petráčkova Hora deposit are characterised by gold-rich, and copper-poor porphyry mineralization. At the Radzimowice deposit copper in association with other base metals is one of the major elements during the second stage of ore precipitation.

The pyrite-pyrrhotite-arsenopyrite assemblage is also comparable to minerals described from deposits of orogenic areas (Groves *et al.* 1998a; Goldfarb *et al.* 2001). However, intrusion related-gold deposits also contain a suite of trace minerals characterised by low-f below the pyrite-pyrrhotite buffer (loellingite, maldonite, gold-bismuthinite inclusions in arsenopyrite, native Bi, and Te–Bi minerals,) and elemental associations (Au, Bi, As, W, Mo, Te and Sb) that to a large degree define the class (Thompson, Newberry, 2000). Especially, characteristic is high positive correlation of Au and Bi and Au with As with correlation coefficients commonly >0.9 and 0.6 to 0.85, respectively (McCoy *et al*., 1997). According to Thompson, Newberry (2000), a strong correlation between Bi associations and Au is a very characteristic feature of various magmatic-hydrothermal deposits (Sn–Ag greisens, Sn skarn, pegmatites, and intrusion-related gold deposits). In contrast, a Bi–Au association is not well documented from orogenic gold deposits. In the type of intrusion-related gold deposits such as

the Vasilkovskoe deposit in Kazakhstan fluid inclusions recorded moderate homogenization temperatures 280–370°C and salinities <11 wt % NaCl equivalent and elevated CO_2 in early paragenetic stages (Spiridonov, 1996). At the Radzimowice deposit conditions recognized by fluid inclusion studies indicate a very similar mesothermal character of the first generation auriferous sulphide-bearing quartz veins. The oxygen isotopic results indicate mixing of meteoric water and magmatic and/or metamorphic water. A gradual increase in the proportion of meteoric water recorded by later vein stages also suggests uplift. According to Hedenquist *et al.* (1998), injections of low- to moderate-salinity, metal-rich, oxidized magmatic fluids into groundwater during the late stages of magma crystallization may lead to the formation of relatively base-metal and silver-rich low sulphidation deposits within distal parts of high-sulphidation deposits.

Another model of gold mineralization within the European Variscan Belt was proposed by Bouchot *et al.* (2000; 2003). These authors presented models for gold mineralization in the Bohemian Massif and in the Massif Central that associate with W and Mo and coincide with regional detachments and with a sharp increase in the rate of uplift in the Bohemian Massif during Viséan and in the Massif Central in Westphalian. According to Żelaźniewicz *et al.* (1997) no detachment has been found in the upper crust at the base of the Paleozoic succession of the Kaczawa Mountains. Thus its contact with light, granite-gneiss basement are sedimentary disconformities, rather than a flat-lying, major tectonic discontinuity.

The genesis of gold mineralization at the Klecza–Radomice ore district was commonly assumed to be a hydrothermal (epithermal?) type connected with the Variscan Karkonosze Granite Massif (Petrascheck, 1933; Neuhaus, 1936; Fedak, Lindner, 1966). However, there is not direct evidence for close magmatic source of hydrothermal fluids. The geological setting in accreted metamorphic terranes and the strong structural control of the ore bodies is characteristic for the Klecza–Radomice ore district. Besides, a low Au/Ag ratios, unsignificant base-metal contents, and low salinity of mineralizing fluids allowed to regard the ore mineralization from the Klecza–Radomice ore district as an orogenic gold type mineralization according to the classification proposed by Groves *et al*. (1998a). Most of Au mineralization occurs within schists with no direct relation with any magmatic body. Furthermore, a causative pluton has not been identified, and the direction of fluid flow, system geometry, and probably distance to a pluton are unconstrained. However, auriferous-sulphide mineralization has been dated at ca. 317 Ma what may indicate a close association with the regional late Variscan magmatism (Fig. 96).

On the Poulsen *et al.* (2000) diagram some of the samples from Radomice are situated within the field of the gold Carlin-type deposits. Furthermore, mineralization in Radomice is hosted by schists that contain CaO up to ca. 3.5 % wt., which is a characteristic feature of Carlin type mineralization in addition to other phenomena such as ore textures, gangue mineral composition (auriferous As-bearing pyrite) and alterations (low temperature silification and carbonatization) characteristic of this type. Hence, it is possible to regard auriferous mineralization of the Klecza deposit as Carlin-type; however, detailed isotope studies are necessary. At Klecza–Radomice ore district lower temperature base metal sulphides mineralization and alteration followed brecciation and was superimposed on the early pyrite-arsenopyrite mineralization. The composition of fluids at Klecza–Radomice ore district indicates a common presence of CO_2, N, and CH_4. Methane could be derived from fluids in equi-

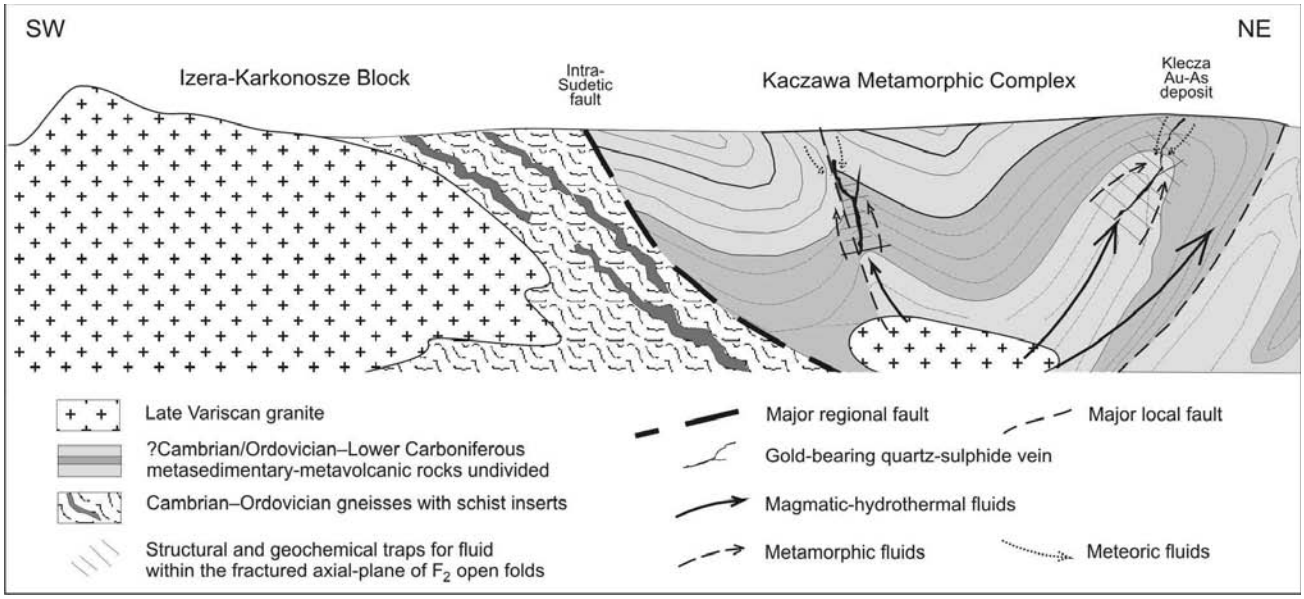

Fig. 96. Schematic diagram illustrating the post-magmatic-metamorphic hydrothermal systems in the Klecza–Radomice ore district in Upper Carboniferous

librium with carbonaceous wall rocks or by reduction of carbon compounds in the magmatic fluid during wall-rock interaction (Baker, Lang, 1999; Lang *et al.*, 2000). Methane is similarly reported from fluid inclusions in intrusive rocks, further supporting low magmatic f (Thompson, Newberry, 2000). The presence of CO_2-rich fluid inclusions does not define only the magmatic association of gold deposits (Roedder, 1984; Thompson *et al.*, 1999; Jia *et al.*, 2003) because it has also been used as evidence for a metamorphic origin for orogenic gold deposits (Goldfarb *et al.*, 1997; Groves *et al.*, 1998b).

Summarizing the above the gold mineralization of the Radzimowice deposit is classified as transitional from porphyry to epithermal type and from Klecza–Radomice as the orogenic gold type. However, the most characteristic feature of Au mineralizations in the Kaczawa Mountains is their multiple characters of hydrothermal fluids responsible for successive stages of Au precipitation. These auriferous deposits contain strong evidence of mesozonal and epizonal mineralizations according to the classification proposed by Groves *et al.* (1998a; Fig. 93). The schift from mesothermal to epithermal conditions of Au mineralization recognised in European Variscan Belt allowed to defined a new class of the Variscan-type of Au-deposit (Cathelineau *et al.*, 2003). Furthermore, according to the classification of the gold deposits proposed by Groves *et al.* (1998a), Kerrich *et al.* (2000), and Poulsen *et al.* (2000) it was possible to distinguish four types of the successive gold mineralization in the Kaczawa Mountains. The first type was connected with a magmatic source of hydrothermal fluids; the second type has no direct evidence of magmatic activity in the close surroundings. However, migration of hydrothermal fluids of variable origin along deep fractures was responsible for gold transportation and precipitation in favourable places. The third type was connected with subvolcanic and volcanic processes during Autunian. The fourth type of gold formation characterized by strong oxidation condition (hematite crystallization) was connected with basins formation in Upper Permian and/or Triassic.

SUMMARY OF GOLD MINERALIZATION IN THE KACZAWA MOUNTAINS

In the Kaczawa Mountains, there are several gold-bearing sulphide deposits and occurrences that were subject to exploitation and operation since the medieval time till the beginning of the 20th century. The most important of them were described in this study i.e. Radzimowice, Klecza, Radomice, Nielestno, Pławna, and Wielisław Złotoryjski. These deposits are small and medium in size with limited gold, silver, arsenic and minor base metals reserves. However, no modern gold prospecting or evaluations of gold reserves have been made yet. Some of them still have a high potential for gold exploration.

The most characteristic feature of these deposits is that gold and silver are intimately associated with sheeted quartz-sulphide veins and vein arrays hosted by various compositions Paleozoic schists and late Variscan magmatic rocks (rhyolite, lamprophyre). These schists belong to flysch-like sediments represented by the ?Cambrian/Ordovician–Lower Carboniferous sequence of primary laminated, pelagic turbidities with intercalations of gray and black quartzite, metalydite, clay-rich graphite slate, metachert, and minor basic metatuffites with inserts of crystalline limestone and dolostone. This clastic rock sequence, up to several hundred meters thick, was folded, deformed and metamorphosed in lower greenschist facies during Upper Devonian–Lower Carboniferous.

Auriferous sulphide mineralization in the quartz vein postdates regional metamorphism of greenschist facies, and regional-scale ductile thrusting of Late Devonian–Early Carboniferous age. Emplacement of Sudetian granite started in Viséan and was followed by new continental break up in late Namurian–early Westphalian accompanied by regional uplift of the orogen. Post-magmatic fluids migration originated in acidic magma (granitoid) triggered by maphic (lamprophyric) magma took place along deep-seated regional faults and secondary dislocations. Deep-seated regional faults and ductile-brittle and brittle deformation in thickened crust formed during extensional regime. The the first stage of the gold mineralization in the Kaczawa Mountains (ca. 317 Ma) took place during the Sudetic phase of the orogenic deformations. This age indicates the connection with late Variscan tectonic-magmatic processes within post-collisional continental arc setting associated with regional uplift and extension after granitoid emplacements in this part of the Western Sudetes.

The formation of the intramountain basins was accompanied by sub- and volcanic processes as a result of gradual transition from the collisional through post-collisional into the within-plate settings (Fig. 97).

Au mineralization is strongly structurally controlled and occurrs mostly in quartz±carbonate veins, minor lodes, sheeted veins, vein-arrays, and stockworks. The gold-quartz veins are preferentially located close to or along the axial plane of mesoscopic fold (F_2) structures. Usually, major auriferous quartz-sulphide veins have an average thickness of 0.2–0.3 m (from 0.05 to 1.5 m), general strike of W–E or NE–SW, and steep dip at about 70° (60–85°). In the most cases they were examined in length at least of about 100 m, and 100 m down the dip. However, the major veins may reach over 2 km in length (Miner consolation vein at the Radzimowice deposit) and were recognized almost 250 m down the dip. All the mineralized structures have small post-mineralization displacement (less than 1 m) at different angles.

Limited resources of these deposits had high gold ore grade. Especially, high-grade ores were extracted from the oxidation zone at Klecza (up to 190 ppm Au) and Radzimowice

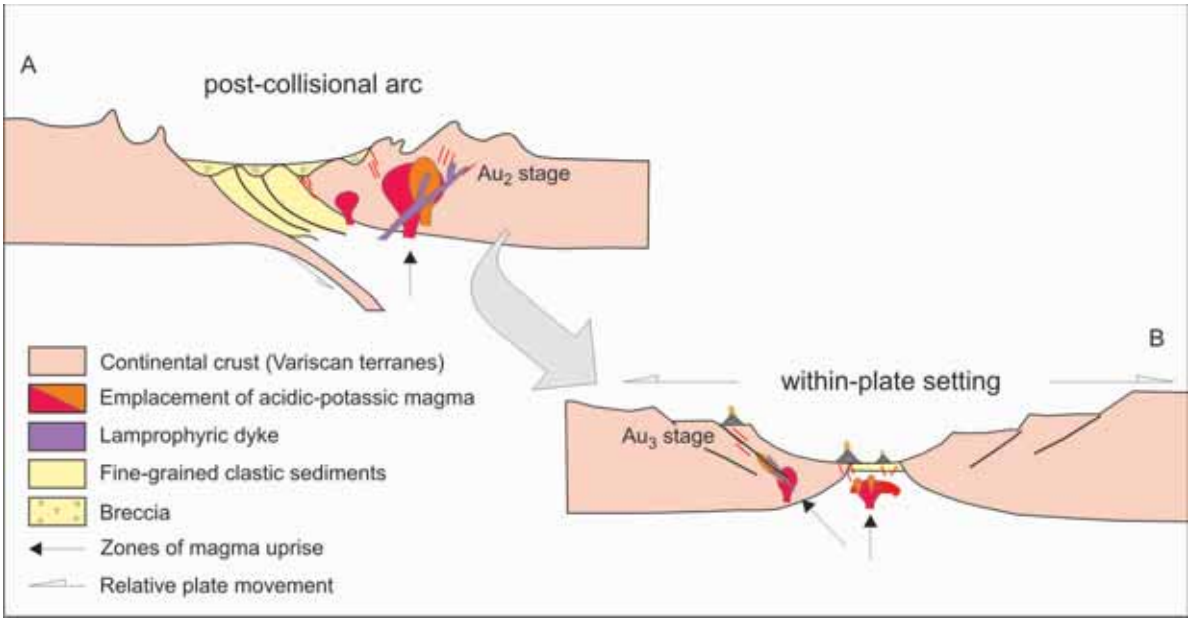

Fig. 97. Schematic diagrams of gold formation in the Kaczawa Mountains during the late Variscan orogeny (with modification of general model after Müller, Groves, 2000).

A. Kaczawa Metamorphic Complex formed accretionary prism as a result of terrane collision. In the uplifted orogen underwent emplacement of post-collisional granitic magmas. In late Viséan the D_2 deformation tectonic movements became extensional and ended with development of deep fracturing and formation of grabens (334–315 Ma). Within the shallow crust parts intruded rhyolite composite bosses, laccoliths and apophyses and from the remnant melts crystallized veins of andesite, lamprophyre and from hydrothermal fluids mesothermal quartz-auriferous sulphide-bearing veins (Au_2 stage ca. 317 Ma recognised in Radzimowice and Klecza–Radomice deposits). **B**. During Upper Carboniferous–Lower Permian underwent transition from the post-collisional continental into the within-plate setting (Autunian). It was accompanied by volcanic processes which were responsible for epithermal gold mineralization in the Radzimowice and Klecza– Radomice ore districts (Au_3 stage; ca. 294 and 280 Ma respectively).

(up to 120 ppm Au). Typically with increased depth the content of gold and silver in sulphide ores decreased and arsenic concentration increased (e.g. to 35 wt. % at Radomice deposit).

These gold deposits were located within tectonic zones of the lower order, which are usually situated within regional shear zones and in the vicinities of deep fractures. Additionally, these deposits could be located in variable distance of the Variscan magmatic bodies. Locally, a spatial co-association of auriferous quartz-sulphide veins with lamprophyre dykes (e.g. Radzimowice) was observed. The formation of these dykes directly pre-dated the formation of the auriferous quartz-sulphide veins in the Kaczawa Mountains.

Submicroscopic gold-bearing Co-arsenopyrite and As-pyrite were the main source of gold from these deposits. Gold mineralization generally depends directly on the abundance of these sulphides in quartz veins. However, recent studies recognized also rich concentration of native gold in extensional fractures within quartz sericite schists (e.g. at Radomice). The proportions of sulphide in deposits were highly variable, from traces to over 40 volume percent of the quartz veins. Sulphide may occur either disseminated or massive, in band aggregates or as breccias reaching concentration up to 30–40 wt % of the rock volume. At Radzimowice the gold to silver ratios in gold-bearing sulphide ores are variable and usually from 1:2 to 1:80; however, the geometric average for ore samples grading >3 ppm Au is about 1:5. The Au/Ag ratio varies within wide limits but in the ore grade material (>1 ppm) averages: 1.1:1 (Radomice), 1:5 (Radzimowice), 2.5:1 (Klecza) and 1:2 (Nielestno). In Radzimowice, Au shows a positive correlation with Ag, S, Bi, Co, Cd, Cu and CaO and in Radomice with As, Bi, Fe, Ag and S. These correlations with gold confirm its strong affinity to sulphides. In the Kaczawa Mountains the average concentration of gold in ore samples of grade higher than 1 ppm Au is 14.9 ppm (n = 52). Additionally, abundant of As, constant admixtures of Co and Bi, variable concentrations of base metals, similar mineral succession, and almost identical mineral textures are characteristic feature of these deposits.

Two- or three stages of the successive gold mineralization are very typical (Fig. 84). Auriferous sulphide mineralization in the Kaczawa Mountains represents crystallization temperatures typical of mesothermal and epithermal zones. Application of arsenopyrite geothermometry (Kretschmar, Scott, 1976; modified by Sharp *et al.* 1985) to the samples from the Kaczawa Mountains indicated that the first and second generation arsenopyrite crystallized at temperature from 535 to 345°C (Radzimowice), 491–315°C (Klecza–Radomice ore district), and the third generation at <370°C (Radzimowice) or <300°C (Radomice).

The first stage of mesozonal character represented by submicroscopic gold associated with Co-arsenopyrite and As-bearing pyrite crystallized ca. 317 Ma from hydrothermal fluids of post-magmatic origins. The sulphide ore paragenetic

with coarse-grained quartz of the first stage of hydrothermal ore mineralization underwent strong cataclasis and was later overprinted by next generation minerals of minor importance represented by base metal sulphide, and submicroscopic gold associated with medium- and fine-grained quartz and carbonates of various composition. They overgrew and selectively replaced previous As- and Fe-sulphide or filled fractures in them. The early event of gray quartz crystallization corresponds to auriferous arsenopyrite and pyrite precipitation. The results indicate that crystallization of gray massive quartz fragments, rich in brecciated sulphide, was at temperatures from 350 to 290°C with the salinity of fluids of 10 ± 3 wt % NaCl equivalent and of pressure of 1.0 ±0.2 kbar. The second generation of white quartz forms veinlets and rock matrix, is related to pyrite and base-metals sulphide precipitation also associated with crystallization of carbonates of various compositions at Klecza–Radomice ore district (mainly ankerite and dolomite). This quartz crystallized within the temperature ranges from 280 to 220°C with the salinity of fluids of 7 ±2 wt % NaCl equivalent and at pressure of 0.7 ±0.1 kbar. This stage of epithermal type of gold mineralization was connected with sub-volcanic and volcanic activity ca. 294 and 280 Ma ago (late Autunian) during rifting within-plate environment. This base metal sulphide mineralization is overprinted by third stage of Au mineralization represented by chalcedony-kaolinite-pyrite / marcasite-native gold association (Radomice). The third generation of quartz comprises clear quartz forming eu-, to anhedral crystals inside the veinlets crystallized at 200 to 180°C with salinity of fluids about 3 ±1 of wt % NaCl equivalent and at pressure of 0.6 ±0.1 kbar. In association of chalcedony with hematite, calcite and native gold grains is known from Klecza and Nielestno. Probably this Au–Fe oxide mineralization was connected with strong oxidation during the formation of basins in Upper Permian and/or Triassic. The lowest crystallization temperatures from <170 to 140°C are measured in quartz veinlets of the next generation.

The oxygen isotopic studies reveal mixing of meteoric waters with magmatic fluids especially during the crystallization of quartz of younger generations in Radzimowice deposit. The highest values are estimated for quartz of the earliest vein stages, and the lower ones are recorded by later vein stages, indicating a gradual increase in the proportion of meteoric water that may also suggest uplift.

Most gold occurs as fine-dispersed submicroscopic particles in arsenopyrite with high Co-admixture (1–6 wt %) and As-bearing pyrite (up to ca. 3 wt %). Microscopic gold is represented by native gold and electrum in association with Bi and Te minerals in variable forms as inclusions in Co-arsenopyrite or pyrite of the earliest generation, in association with galena, chalcopyrite, sphalerite, pyrrhotite as micro-veinlets within these sulphides, or as native free gold in host rocks, and in the oxidized zone with hematite and chalcedony. The chemical composition of native gold varies between deposits and may contain different quantities of admixtures of Ag, Bi, Cu, Te and Se. Maldonite (Au_2Bi) was recognised only at Radzimowice. The presence of Bi minerals in paragenetic association with Te and Au suggests a post-magmatic source of these metals connected with acid magma. The measured Ag concentrations in native gold and electrum ranged from 5 to 45 wt %. The high-grade gold (850–950) from microveinlets, inclusions, and as a free gold occurs in the Klecza–Radomice ore district. Gold of 650–800 purity is most common in the deposits discussed here.

In the Radzimowice and Klecza–Radomice ore district deposits the $\delta^{34}S_{CDT}$ values of sulphides from the first stage of the ore precipitation (Co-arsenopyrite, arsenopyrite and As-pyrite) range from –2.24 to +7.84 ‰ (at Radzimowice from –2.13 to +2.76). Especially, samples of massive arsenopyrite aggregates hosted by a quartz vein in chlorite-sericite schists have heavier sulphur isotope compositions (up to 7.84‰) that indicate sulphur contribution from the host rocks. The sulphur isotope compositions ($\delta^{34}S_{CDT}$) have been also determined in several pure sulphide samples from the second stage of the ore precipitation. Contents of sulphur $\delta^{34}S_{CDT}$ in base metal sulphides (galena, pyrite, chalcopyrite) from Klecza–Radomice ore district and Radzimowice range from –1.62 to +0.60‰ and from –1.13 to 2.76, respectively. The source of gold and other metals is assumed to be in pre-Variscan rocks (mostly Silurian quartz-sericite-graphite schists) with a magmatic (acid melt) contribution. Besides, the late Variscan magmatic sources supplied not only fluids and heat but also sulphur and other metals, which were deposited during later post-magmatic hydrothermal processes. Thus, the organic matter mobilized from graphitic schists during the mineral-forming process served as a geochemical buffer, which provided the Au concentration within fractures, which for example in the Klecza deposit formed in axial planes of the F_2 folds with vergence to the WNW–ESE direction.

In the zone of gold ore mineralization in the Kaczawa Mountains the following alterations can be recognised: feldspathization, silicification, sericitization, pyritization, carbonatization, tourmalinization, kaolinitization, illitization, chloritization, and low-temperature silicification. In the Radzimowice deposit the hydrothermal alteration started with feldspathization and silicification and than was followed by strong acidic (sericitization, pyritization, and kaolinitization) and propylitic alteration (illitization, chloritization) with albitization and carbonatization. At the Klecza–Radomice ore district hydrothermal alteration is limited to the nearest surroundings of veins and is marked by characteristic light white-yellow colours indicating a strong sericitization and silicification. Sericite is commonly replaced by muscovite. Carbonates such as ankerite calcite, and dolomite are often present. Also abundant tourmaline is present in altered zones. Siderite occurs as late generation veinlets. Besides, those zones of low temperature quartz (chalcedony), albite and Fe-oxide appearances are recognized. The alterations within these two gold regions have numerous common elements such as carbonatization, silification, kaolinitization, and sericitization as well as evidently different elements. For example tourmalinization was recognized only in the Klecza–Radomice ore district.

The pseudo-ternary diagram of Au–Ag-base metals after Poulsen *et al.* (2000) illustrates the composition of the repre-

sentative gold-bearing arsenic-polymetallic sulphide ores from the Kaczawa Mountains within different fields for genetic types. The samples from the discussed here deposits are located in the following fields (Fig. 92): epithermal type of ore mineralization (Radzimowice; Radomice), porphyry mineralization (Radzimowice), mineralization of the Carlin-type (Klecza, Radomice) and the quartz-carbonate veins (Radomice). Most probably, the same position would occupy the gold ores from the orogenic type of gold deposits described by Groves *et al.* (1998a) but not included into the ternary diagram classification by Poulsen *et al.* (2000).

If we consider the almost identical Re–Os age of the auriferous Co-arsenopyrite from Radzimowice and Klecza and spatially connect these two important gold areas in the Kaczawa Mountains with WNW–ESE direction which is similar to the direction of hypothetic granitoid body underlying these deposits already at 2 km b.s.l. that is presented on maps by Kotański (1997; Fig. 77). Thus, the connection of gold deposits in the Klecza–Radomice district with underlying hypothetic Variscan granitoid has some reasonable explanations. Especially, that in the Radomice area besides bismuth the ore also contains traces of tellurium which strongly indicates a genetic relation with hydrothermal processes sourced in acid magma. Migration of fluid was along deep fractures; however according to seismic-reflective data these NW-trending faults dip at low-angle (Fig. 80) (Żelaźniewicz *et al.*, 1997). Furthermore, most probably small and second order faults and fractures with major NW–SE and WNW–ESE directions, which occur in the folded black schists (e.g. hinge breaks and axial planes of the F_2 open folds) were traps for these mineralized fluids. However, close spatial relation to fault zones of major NW–SE and NE–SW directions suggest that these high-angle faults may have acted as fluid conduits. The spatial correlation of the metalliferous deposits occurrence indicates that they group along linear zones, which run parallel to deep fracture zones within the schist belt belonging to Pilchowice and Bolków units. Deep fractures of NW–SE directions seem to be important because they have a late Variscan setting and are marked by zones of regional faults, which are parallel to the direction of lithological boundaries within the Kaczawa Metamorphic Complex.

The geological setting in accreted metamorphic terranes and the strong structural control of the ore bodies distal from the granites is characteristic of the Klecza–Radomice ore district allowed to classify them into the orogenic gold type deposits. The geological setting and ore structures, low Au/Ag ratios, and significant Cu contents in the Radzimowice deposit indicate their formation within a continental arc. This mineralization is of transition type from porphyry to epithermal low sulphidation type.

CONCLUSIONS

The gold deposits in the Kaczawa Mountains are classified as strongly structurally controlled, hosted by schist belt, and of variable (proximal – e.g. Radzimowice or distal – e.g. Klecza– Radomice) positions to late Variscan magmatic source of hydrothermal fluids. The economic ore mineralizations in quartz-sulphide veins are the result of the two main hydrothermal stages of ore precipitation, with early mesothermal quartz – arsenopyrite (pyrite) and submicroscopic gold, cataclased and followed by epithermal base-metal sulphide-microscopic gold and carbonates and of minor importance late association of chalcedony with native gold grains and with kaolinite–pyrite/marcasite or hematite–calcite. The most favorable hosts for auriferous-sulphide quartz veins are the fractured axial planes of F_2 folds in quartz-sericite-graphite schists from the Pilchowice and Bolków (Radzimowice schists) units, which are located within shear-zones near regional deep faults and/or late Variscan igneous rocks.

The auriferous sulphides from the Kaczawa Mountains are indicative of submicroscopic mesothermal Au mineralization (acc. to the present author the Au_2 stage in the European Variscan Belt) ca. 317 Ma (late Namurian–early Westphalian) during post-orogenic extension and regional uplift in post-collisional continental arc setting and the younger epithermal and microscopic gold mineralization (Au_3 stage) of sub-volcanic and volcanic origin of geodynamic transition from post-collisional to within-plate settings (ca. 294–280 Ma). The Au_4 stage (chalcedony-hematite-calcite-gold) recognised only in the Klecza and Nielestno deposits is of minor importance. It is the result of oxidative low temperature hydrothermal processes connected with post-Variscan basin formations in Upper Permian–Triassic and even in Cretaceous.

The presented results allow to regard the Kaczawa Mountains as a good target for successful gold exploration in the abandoned mining areas as well as in their surroundings.

Acknowledgements. I am extremely grateful for the valuable comments from the scientific editor, Prof. Andrzej Kozłowski, which have greatly improved this publication and also for his stimulating discussions, and co-operation during fluid inclusion studies of gold-bearing quartz from the Western Sudetes.

I particularly wish to thank Prof. Stanisław Speczik for his support, constructive discussion and suggestions considering this manuscript.

The analytical work was supported by National Committee for Scientific Research Grants nos. 9 T12B 002 17 and 5 T12B 001 22.

REFERENCES

AFIFI A.M., KELLY W.C., ESSENE E.J., 1988 — Phase relations among tellurides, sulphides, and oxides: I. Thermochemical data and calculated equilibrium. II. Applications to telluride-bearing ore deposits. *Econ. Geol.*, **83**: 377–404.

ALDERTON D.H.M., PEARCE J.A., POTTS P.J., 1980 — Rare earth element mobility during granite alteration: evidence from south-east England. *Earth Planet. Sci. Lett.*, **49**: 149–165.

ALEKSANDROWSKI P., 1995 — Rola wielkoskalowych przemieszczeń przesuwczych w ukształtowaniu waryscyjskiej struktury Sudetów. *Prz. Geol.*, **43**, 9: 745–754.

ALEKSANDROWSKI P., 2003 — Śródsudecka strefa uskokowa – przykład przesuwczej granicy terranów. *In*: Sudety Zachodnie od wendu do czwartorzędu (eds. A. Ciężkowski *et al.*): 155–168. WIND, Wrocław.

ALEKSANDROWSKI P., KRYZA R., MAZUR S., ŻABA J., 1997 — Kinematics data on major Variscan strike-slip faults and shear zones in Sudetes. *Geol. Mag.*, **134**: 727–739.

AUGUSTITHIS S.P., 1995 — Atlas of the textural patterns of ore minerals and metallogenic processes: 44–48. Walter de Gruyter & Co., Berlin.

AWDANKIEWICZ M., 1999 — Volcanism in a late Variscan intramontane trough: the petrology and geochemistry of the Carboniferous and Permian volcanic rocks of the Intra-Sudetic Basin, SW Poland. *Geol. Sudet.*, **32**: 83–111.

BAKER T., LANG J.R., 1999 — Geochemistry of hydrothermal fluids associated with intrusion-hosted gold mineralization, Yukon Territory. *In*: Mineral Deposits: processes to processing (eds. Stanley *et al*.): 17–20. Proceedings of the 5th Biennial meeting SGA and 10th Quadrennial IAGOD, London, 22–25 August, 1999. A.A.Balkema, Rotterdam/Brookfield.

BAKER T., POLLARD P.J., MUSTARD R., MARK G., GRAHAM J.L., 2005 — A comparison of granite-related Tin, Tungsten, and Gold-Bismuth deposits: Implications for exploration. *SGA Newsletter*, **61**: 5–17.

BANAŚ M., MOCHNACKA K., 1997 — Mineralizacja Au i Ag na tle paragenez mineralnych w wybranych regionach polskich Sudetów. *In*: Metale szlachetne w NE części Masywu Czeskiego i w obszarach przyległych – geneza, występowanie, perspektywy (ed. A. Muszer): 24–28. Jarnołtówek, 19–21.06.1997 r. Konf. Nauk., Wrocław.

BARANOWSKI Z., 1975 — Zmetamorfizowane osady fliszowe północnej części Gór Kaczawskich (jednostka Rzeszówek–Jakuszowa). *Geol. Sudet.*, **10**, 1: 119–151.

BARANOWSKI Z., 1988 — Lithofacies characteristics of trench-fill metasediments in the Radzimowice Slate (Palaeozoic, Sudetes, SW Poland). *Ann. Soc. Geol. Pol*., **58**: 325–383.

BARANOWSKI Z., HAYDUKIEWICZ A., KRYZA R., LORENC S., MUSZYŃSKI A., URBANEK Z., 1987 — Rozwój struktury wschodniej części Gór Kaczawskich na podstawie dotychczasowego rozpoznania stratygrafii, warunków sedymentacji i wulkanizmu. *In*: Przewodnik 58 Zjazdu PTG, Wałbrzych, 17–19 września 1987: 61–73. Wyd. AGH, Kraków.

BARANOWSKI Z., HAYDUKIEWICZ A., KRYZA R., LORENC S., MUSZYŃSKI A., SOLECKI A., URBANEK Z., 1990 — Outline of the Geology of the Góry Kaczawskie (Sudetes, Poland). *N. Jb. Geol. Pal. Abh*., **179**: 223–257.

BARANOWSKI Z., HAYDUKIEWICZ A., KRYZA R., LORENC S., MUSZYŃSKI A., URBANEK Z., 1998 — Litologia i geneza zmetamorfizowanych skał osadowych i wulkanicznych jednostki Chełmca (Góry Kaczawskie). *Geol. Sudet.*, **31**: 33–59.

BARTON Jr. P.B., 1973 — Solid solutions in the system Cu–Fe–S. Part I: the Cu–S and CuFe–S joins. *Econ. Geol.*, **68**: 455–465.

BARTON P.B., SKINNER B.J., 1979 — Sulphide mineral stabilities. *In*: Geochemistry of hydrothermal ore deposits (ed. H.L. Barnes): 278–403. J. Wiley & Sons Inc., New York.

BAU M., 1991 — Rare-earth element mobility during hydrothermal and metamorphic fluid-rock interaction and the significance of the oxidation state of europium. *Chem. Geol*., **93**: 219–230.

BECHTEL A., SHIEH Y.N., ELLIOT W.C., OSZCZEPALSKI S., HOERNES S., 2000 — Mineralogy, crystallinity and stable isotopic composition of illitic clays within the Polish Zechstein basin: implication for the genesis of Kupferschiefer mineralization. *Chem. Geol*., **163**: 189–205.

BERG G., 1912 — Erläuterungen zu Blatt Kupferberg. Geol. Karte von Preussen 1:25 000. Geol. Landesanst., Berlin.

BEYSCHLAG F., KRUSCH P., VOGT J.H.L., 1921 — Die Lagerstätten der nutzbaren Mineralien und Gesteine. **2.** Bd. *Erzlagerstätten*: 363–365. Stuttgart.

BIERLEIN F.P., CROWE D.E., 2000 — Phanerozoic Orogenic Lode Gold Deposits. *SEG Reviews*, **13**: 103–139.

BIERLEIN F.P., WALDRON H.M., ARNE D.C., 1999 — Behavior of rare earth and high field strength elements during hydrothermal alteration of meta-turbidities associated with mesothermal gold mineralization in central Victoria, Australia. *J. Geochem. Explor.*, **67**: 109–125.

BLEVIN P., 2003 — Metallogeny of granitic rocks. *In*: Magmas to mineralization. The Ishihara symposium (eds. P. Blevin *et al.*): 1–4. GEMOC MacQuarie University, 22–24 July 2003. Geoscience Australia, record 2003/14.

BLEVIN P., CHAPPELL B.W., 1995 — Chemistry, origin and evolution of mineralized granites in the Lachlan Fold Belt, Australia; the metallogeny of I-type and S-type granites. *Econ. Geol*., **90**: 1604–1619.

BLUNDEL D.J., KARNKOWSKI P.H., ALDERTON D.H.M., OSZCZEPALSKI S., KUCHA H., 2003 — Copper mineralization of the Polish Kupferschiefer: A proposed basement fault-fracture system of fluid flow. *Econ. Geol*., **98**: 1487–1495.

BONI M., STEIN H.J, ZIMMERMAN A., VILLA I.M., 2003 — Re–Os age for molybdenite from SW Sardinia (Italy): A comparison with Ar/Ar dating of Variscan granitoids. *In*: Mineral exploration and sustainable development (eds. Eliopoulos *et al*.): 247–250. Millpress, Rotterdam.

BORKOWSKA M., 1966 — Petrografia granitu Karkonoszy. *Geol. Sudet.*, **2**: 107pp.

BOUCHOT V., GROS Y., BONNEMAISON M., 1989 — Structural controls on the auriferous shear zones of the Saint Yrieix district, Massif Central, France – evidence from the Le Bourneix and Laurieras gold deposits. *Econ. Geol*., **84**: 1315–1327.

BOUCHOT V., MILESI J.P., LEDRU P., 2000 — Crustal scale hydrothermal Paleofield and related Au, Sb, W orogenic deposits at 310–305 Ma (Massif Central). *SGA News Letters*, **10**, 1: 6–10.

BOUCHOT V., FAURE M., FEYBESSE J.L., CORREIRA P., ZACHARIAS J., 2003 — Variscan orogenic gold district related to a regional scale Viséan detachment in the Central Bohemian metallogenic province (Czech Republic): a geodynamic reas-

sessment. *In*: Mineral exploration and sustainable development (eds. D.G. Eliopoulos *et al.*): 747–750. Proc. of the 7th Biennial SGA Meeting Athens, Greece. 24–28, August 2003. Millpress, Rotterdam.

BOYLE R.W., 1979 — The geochemistry of gold and its deposits (together with a chapter on geochemical prospecting for the element). *Geol. Surv.Can.*, **280**: *Energy, Mines and Resources of Canada*, 584pp.

BRAUNS C.M., PÄTZOLD T., HAACK U., 2003 — A Re-Os study bearing on the age of the Kupferschiefer black shale at Sangerhausen (Germany). Abstr. XVth Int. Congr. Carbonif. Perm. Stratigr. in Universitet Utrecht: p. 66, Utrecht.

BÜRG G.H., 1930 — Die Sichtbarmachung des feinverteilen Goldes in göldhoffingen Erzen und ihre wirtschaftliche Bedeutung. *Metall. Erz.*, **27**: 333–338.

CABRI L.J., 1965 — Phase relations in the Au–Ag–Te system and their mineralogical significance. *Econ. Geol.*, **60**: 1569–1606.

CABRI L.J., CHRYSSOULIS S.L., de VILLIERS J.P.R, LAFLAMME J.H.G., BUSECK P.R., 1989 — The nature of "invisible" gold in arsenopyrite. *Can. Mineral*., **27**, 353–362.

CATHELINEAU M., BOIRON M.C., HOLLIEGER P., MARION P., DENIS M., 1989 — Gold in arsenopyrites: crystal chemistry, location and state, physical and chemical conditions of deposition. *Econ. Geol.*, *Monogr.*, **6**: 328–341.

CATHELINEAU M., BOIRON M.C., FOURCADE S., MARIGNAC C., 2003 — The shift from "mesothermal" to "epithermal" conditions in orogenic gold: definition of a Variscan-type of quartz lode gold deposits. *In*: Mineral exploration and sustainable development (eds. D.G. Eliopoulos *et al*.): 751–753. Proc. of the 7th Biennial SGA Meeting Athens (Greece), 24–28, August 2003. Millpress, Rotterdam.

CHAPPELL B.W., 2003 — Causes of variation in granite suites. The Ishihara symposium (eds. P. Blevin *et al.*): 27–34. GEMOC MacQuarie University, 22–24 July 2003. Geoscience Australia, record 2003/14.

CHOROWSKA M., 1978 — Wizeńskie wapienie w epimetamorficznym kompleksie Gór Kaczawskich (Sudety). *Rocznik PTG*, **48**, 2: 245–261.

CHOROWSKA M., 1982 — Badania stratygraficzne formacji metamorficznych Sudetów. *Biul. Inst. Geol.*, **341**: 117–139.

CHOROWSKA M., RADLICZ K., TOMCZYK H., 1981 — Utwory ordowiku, syluru i dewonu w Lubaniu (Sudety, Góry Kaczawskie). *Kwart. Geol*., **25**, 2: 243–264.

CHRT J., BOLDUAN H., BERNSTEIN H., LEGIERSKI J., 1968 — Räumliche und Zeitliche beziehungen der Bömischen Masse zu Magmatismus und Bruchtektonik. *Zeitschr. für angewande. Geologie*, **14**, 7: 362–376.

COOK N.J., CHRYSSOULIS S.L., 1990 — Concentrations of "invisible gold" in the common sulphides. *The Canadian Mineralogist*, **28**: 1–16.

COOK N.J., CIOBANU C., 2004 — Bismuth tellurides and sulphosalts from the Larga hydrothermal system, Metaliferi Mountains, Romania: Paragenesis and genetic significance. *Miner. Mag.*, **68**: 301–321.

COOKE D.R., SIMMONS S., 2000 — Characteristics and genesis of epithermal gold deposits. *SEG Rev.*, **13**: 221–244.

CONNORS K.A., NOBLE D.C., BUSSEY S.D., WEISS S.I., 1993 — Initial gold contents of silicic volcanic rocks: Bearing on the behavior of gold in magmatic systems. *Geology*, **21**: 937–940.

CORBETT G.J., LEACH T.M., 1998 — Southwest Pacific Rim Gold-Copper Systems: Structure, alteration, and mineralization. *Soc. Econ. Geol. Sp. Publ.*, **6**: 237pp.

COX S.F., WALL V.J., ETHERIDGE M.A., POTTER T.F., 1991 — Deformational and metamorphic processes in the formation of mesothermal vein-hosted gold deposits: examples from the Lachlan fold belt in central Victoria, Australia. *Ore Geology Reviews*, **6**: 391–432.

CUNEY M., ALEXANDROV P., LE CARLIER de VESLUD C., CHEILLETZ A., RAIMBAULT L., RUFFET G., SCAILLET S., 2002 — The timing of W–Sn-rare metals mineral deposit formation in the Western Variscan chain in their orogenic setting: the case of the Limousin area (Massif Central, France). *In*: The timing and location major ore deposits in an evolving orogen. (eds. D.J. Blundell *et al.*). *J. Geol. Soc. London, Sp. Publ.*, **204**: 213–228.

CWOJDZIŃSKI S., KOZDRÓJ W., 1994 — Szczegółowa mapa geologiczna Sudetów w skali 1:25 000 – arkusz Wojcieszów. Polska Agencja Ekologiczna, Warszawa.

CWOJDZIŃSKI S., ŻELAŻNIEWICZ A., 1995 — Podłoże krystaliczne bloku przedsudeckiego. Rocznik PTG, Przewodnik LXVI Zjazdu PTG: 11–27. Wrocławska Drukarnia Naukowa, Wrocław.

CWOJDZIŃSKI S., MŁYNARSKI S., DZIEWIŃSKA L., JÓŹWIAK W., ZIENTARA P., BAZIUK T., 1995 — GB-2A – pierwszy sejsmiczny profil głębokich badań refleksyjnych (GBS) na Dolnym Śląsku. *Prz. Geol.*, **43**, 9: 727–737.

CYMERMAN Z., 1998a — The Góry Sowie terrane: a key to understanding the Palaeozoic evolution of the Sudetes area and beyond. *Geol. Quart.*, **42**, 4: 379–400.

CYMERMAN Z., 1998b — Uskok śródsudecki a regionalne strefy ścinań podatnych w Sudetach. *Prz. Geol.*, **46**, 7: 609–616.

CYMERMAN Z., 2000 — Palaeozoic orogeneses in the Sudetes: a geodynamic model. *Geol. Quart.*, **44**, 1: 59–80.

CYMERMAN Z., 2002 — Analiza strukturalno-kinematyczna i waryscyjska ewolucja tektoniczna kompleksu kaczawskiego. *Pr. Państw. Inst. Geol*., **175**: 147pp.

CYMERMAN Z., 2004 — Tectonic map of the Sudetes and Fore-Sudetic Block 1:200 000. Państw. Inst. Geol., Min. Środowiska, Warszawa.

CYMERMAN Z., PIASECKI M., 1994 — Terrane concept in the Sudetes, Bohemian Massif. *Geol. Quart.*, **38**, 2: 191–210.

CYMERMAN Z., PIASECKI M.A.J., SESTON R., 1997 — Terranes and terrane boundaries in the Sudetes, northeast Bohemian Massif. *Geol. Mag.*, **134**: 717–725.

DĄBROWSKI R., 2002 — Mineralizacja kruszcowa w strefie sudeckiego uskoku brzeżnego między Chełmcem a Męcinką. M.Sc. Thesis. UW, Warszawa.

DEPCIUCH T., LIS J., 1971 — Wiek bezwzględny K–Ar granitoidów masywu Karkonoszy. *Kwart. Geol*., **15**, 4: 855–861.

DOKTÓR S., GRANICZNY M., 1983 — Struktury koliste i pierścieniowe na zdjęciach satelitarnych – ich geneza i znaczenie. *Prz. Geol.*, **31**, 1: 30–37.

DOMAŃSKA-SIUDA J., BACHLIŃSKI R., SŁABY E., 2004 — Studium izotopowe Rb–Sr i Sm–Nd granitu hornblendowo-biotytowego z masywu Strzegom–Sobótka i jego enklaw. *In*: VIII Ogólnopolska Sesja Naukowa. Datowanie minerałów i skał (eds. M. Michalik *et al.*): 14–18. Kraków, 18–19 listopada 2004 r.

DOMASZEWSKA T., 1964 — Występowanie złota w Polsce: 101–138. Centr. Arch. Geol. PIG, Warszawa.

DOMASZEWSKA T., 1965 — Występowanie i eksploatacja złota na Dolnym Śląsku. *Prz. Geol.*, **13**, 4: 180–184.

DON J., 1995 — Problem hercynidów i waryscydów w Sudetach. *Prz. Geol.*, **43**, 9: 738–744.

DUBÈ B., LAUZIÈRE K., 1997— Gold metallogeny of the Cape Ray fault zone, Southwest Newfoundland. *Geol. Sur. Can. Bull*., **508**: 90pp.

DUTHOU J.L., COUTURIE J.P., MIERZEJEWSKI M.P., PIN C., 1991 — Oznaczenia wieku granitu Karkonoszy metodą izochronową rubidowo-strontową, na podstawie całych próbek skalnych. *Prz. Geol.*, **39**, 1: 75–79.

DZIEDZIC K., 1996 — Two-stages origin of the Hercynian volcanics in the Sudetes, SW Poland. *N. Jb. Geol. Paläont. Abh*., **199**, 1: 65–87.

DZIEKOŃSKI T., 1972 — Wydobywanie i metalurgia kruszców na Dolnym Śląsku od XIII do XX w. [Eng. Sum.]. *PAN Instytut Historii Kultury Materialnej*, **4**: 249–258. Ossolineum, Wrocław.

EBY G.N., 1992 — Chemical subdivision of the A-type granitoids: petrogenetic and tectonic implications. *Geology*, **20**: 641–644.

FEDAK J., LINDNER M., 1966 — Metalogeneza Sudetów. *Instytut Geologiczny Prace*: 100–113. Wyd. Geol., Warszawa.

FILA-WÓJCICKA E., 2004 — Rb–Sr isotope studies in the Garby Izerskie zone – evidence for the Karkonosze intrusion activity. *Miner. Soc. Pol. Sp. Papers*, **24**: 153–155.

FLEET M.E., MUMIN H., 1997 — Gold-bearing arsenian pyrite and marcasite from Carlin Trend gold deposits and laboratory synthesis. *Amer. Miner.*, **82**: 182–193.

FLEET M.E., MacLEAN P.J., BARBIER R.K., 1989 — Oscillatory-zoned As-bearing pyrite from stratabound and stratiform gold deposits: an indicator of ore-fluid evolution. *Econ. Geol.*, Monogr., **6**: 356–362.

FLOYD P.A., WINCHESTER J.A., SESTON R., KRYZA R., CROWLEY Q.G., 2000 — Rewiev of geochemical variation in lower Palaeozoic metabasites from NE Bohemian Massif: intracratonic rifting and plume-ridge interaction. *In*: Orogenic processes: quantification and modeling in the Variscan Belt of Central Europe (eds. W. Franke *et al.*). *J. Geol. Soc. London, Spec. Publ.*, **179**: 155–175.

FOUILLAC A.C., GIRARD J.P., 1996. Laser oxygen isotope analysis of silicate/oxide grain separates: evidence for a grain size effect. *Chem. Geol*., **130**: 31–54.

FRANKE W., ŻELAŻNIEWICZ A., 2000 — The eastern termination of the Variscides: terranes correlation and kinematics evolution. *In*: Orogenic processes: quantification and modeling in the Variscan Belt of Central Europe (eds. W. Franke *et al.*). *J. Geol. Soc. London, Spec. Publ.*, **179**: 63–89.

GAJDA E., 1960 — Żyły pegmatytowe okolic Szklarskiej Poręby (Karkonosze). *Kwart. Geol*., **4**, 3: 546–562.

GASPARRINI C., 1983 — The mineralogy of gold and its significance in metal extraction. *Can. Inst. Min. Metall. Bull.*, **76**: 144–153.

GIERWIELANIEC J., 1956 — Budowa geologiczna północnej okolicy Lubomierza. *Biul. Inst. Geol.*, **106**: 61–118.

GOLDFARB R.J., GROVES D.I., GARDOLL S., 1997 — Gold deposits in metamorphic rocks of Alaska. *Econ. Geol. Monog.*, **9**: 151–190.

GOLDFARB R.J., GROVES D.I., GARDOLL S., 2001 — Orogenic gold and geologic time: a global synthesis. *Ore Geol. Rev*., **18**: 1–75.

GRADSTEIN F.M., OGG J.G., SMITH A. *et al.*, 2004 — A Geologic Time Scale 2004. Cambridge University Press, Cambridge.

GRIMMING H., 1933 — Das Gold und Arsenerzvorkommen von Hüsdorf-Wünschendorf. Centr. Arch. Geol. PIG, Warszawa.

GROCHOLSKI A., 1982 — Serie krystaliczne bloku przedsudeckiego i związane z nimi perspektywy surowcowe. *Biul. Inst. Geol*., **341**: 97–116.

GROCHOLSKI A., 1986 — The Proterozoic and Palaeozoic in the south-western Poland in a light of a new data. *Biul. Inst. Geol*., **355**: 7–29.

GROCHOLSKI A., SAWICKI L. (eds.), 1982 — Stan rozpoznania strukturalnego i kierunki badań Dolnego Śląska. Inst. Geol., Oddz. Dolnośl., Wrocław.

GRODZICKI A., 1960 — Piaski złotonośne okolic Złotoryi. *Achiw. Mineral.*, **24**, 1/2: 239–289.

GRODZICKI A., 1967 — O występowaniu piasków złotonośnych w okolicach Jeleniej Góry. *Prz. Geol*., **15**, 6: 285–289.

GRODZICKI A., 1971 — Okruchowe złoża złotonośne bloku karkonosko-izerskiego. *Arch. Miner.*, **29**, 1/2: 305–343.

GRODZICKI A., 1972 — Petrografia i mineralogia piasków złotonośnych Dolnego Śląska. *Geol. Sudetica*, **6**: 233–291.

GROVES D.I., GOLDFARB R.J., GEBRE-MARIAM M., HAGEMANN S.G., ROBERT F., 1998a — Orogenic gold deposits: A proposed classification in the context of their crustal distribution on relationship to other gold deposit types. *Ore Geol. Rev.*, **13**: 7–27.

GROVES D.I., GOLDFARB R.J., ROBERT F., HART C.J.R., 1998b — Gold deposits in metamorphic belts: overview of current understanding, outstanding problems, future research and exploration significance. *Econ. Geol*., **98**: 1–29.

GROVES D.I., CONDIE K.C., GOLDFARB R.J., HRONSKY J.M.A., VIELREICHER R.M., 2005 — Secular changes in global tectonic processes and their influence on the temporal distribution of gold-bearing mineral deposits. *Econ. Geol*., **100**: 203–224.

GUEN M.L., LESCUYER J.L., MARCOUX E., 1992 — Lead-isotope evidence for a Hercynian origin of the Salsigne gold deposits (Southern massif Central, France). *Miner. Depos.*, **27**: 129–136.

HARRIS N.B.W., PEARCE J.A., TINDLE A.G., 1986 — Geochemical characteristics of collision-zone magmatism. *In*: Collision tectonics (eds. M.P. Coward, A.C. Reis). *Sp. Publ. Geol. Soc.*, **19**: 67–81.

HASKIN M.A., HASKIN L.A., 1966 — Rare earths in European shales: a redetermination. *Science*, **154**: 203–219.

HAYASHI K., OHMOTO H., 1991 — Solubility of gold in NaCl- and H_2S-bearing solutions at 250–350°C. *Geochemi. Cosmochim. Acta*, **55**: 2111–2126.

HAYDUKIEWICZ A., 1977 — Litostratygrafia i rozwój strukturalny kompleksu kaczawskiego w zachodniej części jednostki Jakuszowej i w jednostce Rzeszówka (Góry Kaczawskie). *Geol. Sudet.*, **12**, 1: 7–68.

HAYDUKIEWICZ A., 1987a — Sekwencja stratygraficzna w kompleksie kaczawskim. Przew. 48 Zjazdu Pol. Tow. Geol., 17–19.09.1987, Wałbrzych: 95–102. Wyd. AGH, Kraków.

HAYDUKIEWICZ A., 1987b — Melanże Gór Kaczawskich. Przew. 48 Zjazdu Pol. Tow. Geol., 17–19.09.1987, Wałbrzych: 106–112. Wyd. AGH, Kraków.

HAYDUKIEWICZ A., URBANEK Z., 1986 — Zmetamorfizowane skały dewońskie we wschodniej części Bolkowa (Góry Kaczawskie). *Geol. Sudet.*, **20**, 1: 185–196.

HEDENQUIST J.W., ARRIBAS A. Jr., REYNOLDS T.J., 1998 — Evolution of an-intrusion-centered hydrothermal system: Far Southeast-lepanto porphyry and epithermal Cu–Au deposits, Philippines: *Econ. Geol.*, **93**: 374–404.

HEDENQUIST J.W., ARRIBAS A. Jr., GONZALES-URIEN E., 2000 — Exploration for epithermal gold deposits. *Rev. Econ. Geol.*, **13**: 245–277.

HEINHORST J.P., LEHMANN B., 1994 — A radiotracer study on the kinetics of gold sorption by mineral surfaces. *Miner. Deposita*, **29**: 399–403.

HENLEY R.W., BROWN K.L., 1985 — A practical guide to the thermodynamics of geothermal fluids and hydrothermal ore deposits. *In*: Geology and geochemistry of epithermal systems (eds. B.R. Berger, P.M. Bethke) *Rev. Econ. Geol*., **2**: 25–44.

HEINRICH C.A., GÜNTHER D., ANDÉTAT D., ULRICH T., FRISCHNECHT R., 1999 — Metal fractionation between magmatic brine and vapor determined by microanalysis of fluid inclusions. *Geology*, **27**: 755–758.

HELGESON H.C., GARRELS R.M., 1968 — Hydrothermal transport and deposition of gold. *Econ. Geol*., **63**: 622–635.

HOEHNE K., 1935 — Quantitativ chemische und erzmikroskopische Bestimmung von Arsen, Antimon, Zinn und Wismut in vorwiegend schlesischen Bleiglanzes. *Chemie der Erde*, **9**. Jena.

HOFSTRA A.H., CLINE J.S., 2000 — Characteristics and models for Carlin-type Gold deposits. *Rev. Econ. Geol.*, **13**: 163–220.

IRVINE T.N., BARAGAR W.R.A., 1971 — A guide to the chemical classification of the common volcanic rocks. *Canad. J. Earth Sc.*, **8**: 523–548.

ISHIHARA S., 1981 — The granitoid sereies and mineralization. *Econ. Geol.,* 75th Ann. Vol.: 459–484.

JANECZEK J., 1985 — Typomorficzne minerały pegmatytów masywu Strzegom–Sobótka. *Geol. Sudet.*, **21**, 2: 62pp.

JAEGER H., 1964 — *Monograptus hercynicus* in den Westsudeten und das Alter der Westsudeten-auptfahltung. *Berlin Geol. Ges. DDR*, **8**, 5/6: 649–652.

JAIRETH S., 1992 — The calculated solubility of platinium and gold in oxygen-saturated fluids and the genesis of platinium-palladium and gold mineralization in the unconformity-related uranium deposits. *Miner. Deposita*, **27**: 42–54.

JĘCZMYK M., KANASIEWICZ J., LOMOZOVA V., TENCIK I., 1977 — Mapa rozmieszczenia kasyterytu i złota w aluwiach na obszarze metamorfiku izerskiego. Inst. Geol., Warszawa.

JĘDRYSEK M.O., 1990 — Isotope effects in geological systems. *In*: Course-book of isotope geology. Third School on Physics of Minerals. Part I – Isotopes (ed. M.O. Jędrysek): 19–41. Wrocław University and Com. Miner. Sc., Wrocław.

JENSEN E.R., BARTON M.D., 2000 — Gold deposits related to alkaline magmatism. *SEG Rev. Econ. Geol.*, **13**: 279–314.

JERZMAŃSKI J., 1955 — Szczegółowa mapa geologiczna Sudetów w skali 1:25 000, ark. Chełmiec. Inst. Geol., Warszawa.

JERZMAŃSKI J., 1956 — Porfir wzgórza Wielisławka w Górach Kaczawskich. *Prz. Geol*., **6**, 4: 174–175.

JERZMAŃSKI J., 1958 — Okruszcowanie północno-wschodniej części Gór Kaczawskich i ich wschodniego przedłużenia na tle budowy geologicznej. *Prz. Geol*., **6**, 8–9: 345–348.

JERZMAŃSKI J., 1965 — Geologia północno-wschodniej części Gór Kaczawskich i ich wschodniego przedłużenia. *Biul. Inst. Geol.*, **185**: 109–168.

JERZMAŃSKI J., 1969 — Objaśnienia do Szczegółowej mapy geologicznej Sudetów w skali 1:25 000, ark. Chełmiec. Inst. Geol., Warszawa.

JERZMAŃSKI J., 1976a — Główne uskoki sudeckie i ich znaczenie dla metalogenii Dolnego Śląska. *Kwart. Geol.*, **18**, 4: 684–689.

JERZMAŃSKI J., 1976b — Barite and fluorite mineralization and its position in the metallogenic development of the Lower Silesia area. *In*: The current metallogenic problems of Central Europe (ed. J. Fedak): 227–250. Wyd. Geol., Warszawa.

JERZMAŃSKI J., KURA J., 1965 — Charakterystyka geologiczno-mineralogiczna żył kwarcowych w rejonie Sichowa Góry Kaczawskie. *Kwart. Geol*., **9**, 2: 432–433.

JERZMAŃSKI J., WALCZAK-AUGUSTYNIAK M., 1993 — Szczegółowa mapa geologiczna Sudetów w skali 1:25 000, ark. Krotoszyce. Państw. Inst. Geol., Warszawa.

JIA Y., KERRICH R., GOLDFARB R., 2003 — Metamorphic origin of ore-forming fluids for orogenic gold-bearing quartz vein systems in the North American Cordillera: Constraints from a reconnaissance study of $\delta^{15}N$, δD, and $\delta^{18}O$. *Econ. Geol*., **98**: 109–123.

JOHAN Z., MARCOUX E., BONNEMAISON M., 1989 — Comptes Rend II. **308**, 185pp. BRGM, Orléans.

JOHN D.A., 2001 — Miocene and Early Pliocene epithermal gold-silver deposits in the Northern Great Basin, Western United States: Characteristic, distribution, and relationship to magmatism. *Econ. Geol.*, **96**: 1827–1853.

JOWETT E.C., PEARCE G.W., RYDZEWSKI A., 1987 — A Mid-Triassic paleomagnetic age of the Kupferschiefer mineralization in Poland, based on a revised apparent polar wander path for Europe and Russia. *J. Geoph. Res*., **92**: 581–598.

KALISZUK R., 2000 — Zróżnicowanie śladowych zawartości złota w skałach należących do kompleksu kaczawskiego. *Prz. Geol.*, **48**, 2: 166–170.

KALYUZHNYI V.A., DAVIDENKO N.M., ZINCHUK I.N., SVOREN J.M., PISOTSKIY B.J., 1975 — Role of carbon dioxide-aqueous and methane-aqueous fluids in formation of the gold ore deposits in Chukotka. Carbon and its compounds in endogene processes of mineral formation, Lviv: 80–81.

KANASIEWICZ J., 1990 — Structure and mineralization of the ENE part of the Ohře continental rift. *Geotectonica et Metallogenia*, **14**, 2: 141–147.

KANASIEWICZ J., 1992 — Perspektywy wykrycia mineralizacji arsenowo-złotonośnej związanej z granitoidowym masywem kłodzko-złotostockim w świetle wyników zdjęcia geochemicznego. *Prz. Geol*., **40**, 2: 108–113.

KANASIEWICZ J., SYLWESTRZAK H., 1970 — Zależność między przebiegiem głębokich stref tektonicznych a rozmieszczeniem złóż endogenicznych w Sudetach. *Prz. Geol.*, **18**, 5: 219–221.

KANASIEWICZ J., MIKULSKI S.Z., 1989 — O możliwości występowania złóż Mo formacji Cu–Mo w strzegomskim masywie granitowym. *Prz. Geol*., **37**, 3: 129–133.

KAJIWRA Y., KROUSE H.R., 1971 — Sulphur isotope partitioning in metallic sulphide systems. *Can. J. Earth Sci.*, **8**: 1397–1408.

KARNKOWSKI H.P., 1999 — Origin and evolution of the Polish Rotliegend basin. *Polish Geol. Inst. Sp. Papers*, **3**: 93pp.

KARWOWSKI Ł., OLSZYŃSKI W., KOZŁOWSKI A., 1973 — Mineralizacja wolframitowa z okolic Szklarskiej Poręby Huty. *Prz. Geol*., **26**, 12: 633–637.

KEITH J.D., CHRISTIANSEN E.H., MAUGHAN D.T., WAITE K.A., 1998 — The role of mafic alkaline magmas in felsic porphyry-Cu and Mo systems. *In*: Mineralized "Intrusion related" skarn systems (ed. D.R. Leintz). *Mineral. Assoc. Can. Short Course*, **26**: 211–243.

KELLEY K.D., LUDINGTON S., 2002 — Cripple Creek and other alkaline-related gold deposits in the southern Rocky Mountains, USA: influence of regional tectonics. *Miner. Deposita*, **37**: 38–60.

KENNAN P.S., DZIEDZIC H., LORENC M.W., MIERZEJEWSKI M.P., 1999 — A review of Rb–Sr isotope patterns in the Carboniferous granitoids of the Sudetes in Poland. *Geol. Sudet.*, **32**: 49–53.

KERRICH R., 1983 — Geochemistry of gold deposits in the Abitibi greenstone belt. *Can. Inst. of Min. and Metal.*, *Sp. Vol*., **27**: 75pp.

KERRICH R., GOLDFARB R., GROVES D., GARWIN S., 2000 — The geodynamics of World-class gold deposits: characteristics, space-time distribution and origins. *In*: Gold in 2000 (eds. S.G. Hageman, P.E. Brown). *SEG Reviews in Economic Geology*, **13**: 501–551.

KŁOSIEWICZ A., 1987 — Mineralizacja kruszcowa południowych zboczy Gór Ołowianych. M.Sc. Thesis. UW, Warszawa

KOLONIN G.R., POLYANOVA G.A., 1993 — Effect of H_2O-CO_2-NaCl fluid evolution on metal complexing and its transport during ore-formation (with the example of gold). *In*: Proc. 4 Intern. Sympos. Hydrothermal Reactions: 113–115. Nancy.

KONSTANTYNOWICZ E., 1960 — Złoża polimetaliczne Gór Kaczawskich. *In*: Geologia złóż surowców mineralnych Polski (ed. R. Krajewski). Arch. Inst. Geol., Wrocław.

KONSTANTYNOWICZ E., 1971 — Geneza sudeckich polimetalicznych złóż żyłowych ze szczególnym uwzględnieniem mineralizacji miedziowej. *Biul. Inst. Geol.*, **241**: 37–44.

KOSMANN A., 1891 — Gold und Silber in Niederschlesien Erzen. Berg- und Hütten-Ztg. Arch. PIG, Warszawa.

KOSMANN A., 1930 — Gold und Silber in Niederschlesien Erzen. Centr. Arch. Geol. PIG, Warszawa.

KOWALSKI W., 1976 — Geochemia, mineralogia i geneza dolnośląskich złóż i wystąpień barytowych. Część I: Wprowadzenie, metody badań, mineralizacja barytowa na obszarze Synklinorium Śródsudeckiego i Gór Sowich. *Arch. Miner.*, **32**, 2: 5–92.

KOWALSKI W., 1977 — Geochemia, mineralogia i geneza dolnośląskich złóż i wystąpień barytowych. Część II: Mineralizacja barytowa na obszarze Gór Kaczawskich, wyniki badań geochemicznych, uwagi na temat wieku i genezy mineralizacji barytowej w Sudetach. *Arch. Miner.*, **33**, 1: 107–167.

KOTAŃSKI Z. (ed.), 1997 — Atlas geologiczny Polski. Mapy geologiczne ścięcia poziomego. Państ. Inst. Geol., Warszawa.

KOZDRÓJ W., 1995 — Objaśnienia do Szczegółowej mapy geologicznej Sudetów w skali 1:25 000, ark. Wojcieszów. Państ. Inst. Geol., Warszawa.

KOZDRÓJ W., SKOWRONEK A., 1999 — Early Palaeozoic lithostratigraphy of the Góry Kaczawskie (Mountains) metamorphic complex. Exkursionführer und Veröffentlichungen der Gesellschaft für Geowissenschaften (eds. Brauze, Hoth), **206**: 88–97. Görlitz 24–28.9.1999. Berlin.

KOZDRÓJ W., KRENTZ O., OPLETAL M. (eds.), 2001 — Comments on the Geological Map Lausitz–Izera–Karkonosze, 1:100 000. Pol. Geol. Inst., Warszawa.

KOZŁOWSKI A., 1984 — Calcium-rich inclusion solutions in fluorite from the Strzegom pegmatites, Lower Silesia. *Acta Geol. Pol*., **34**: 131–138.

KOZŁOWSKI A., METZ P., 1989 — Fluid inclusion studies in quartz from the reportedly gold-bearing veins from Lower Silesia, SW Poland. Proc. International Symp. on Gold Geology and Exploration, Shenyang: 731–735.

KOZŁOWSKI S., PARACHONIAK W., 1967 — Wulkanizm permski w depresji północnosudeckiej. *Pr. Muz. Ziem., Pr. Petrogr. Geol.*, **11**: 191–221.

KOZŁOWSKI A., KARWOWSKI Ł., OLSZYŃSKI W., 1975 — Tungsten-tin-molybdenum mineralization in the Karkonosze Massif. *Acta Geol. Pol*., **25**, 3: 415–430.

KRAJEWSKI R., 1948 — Złoża rud na Dolnym Śląsku, Oblicze Ziem Odzyskanych, Dolny Śląsk. Inst. Geol., Warszawa.

KRAJEWSKI R., 1960 — Surowce metaliczne. *In*: Geologia złóż surowców mineralnych Polski (ed. R. Krajewski). Inst. Geol., Warszawa.

KRÖNER A., HEGNER E., HAMMER J., HAASE G., BIELICKI K., KRAUSS M., EIDAM J., 1994 — Geochronology and Nd–Sr systematics of Lusatian granitoids: significance for the evolution of the Variscan orogen in east-central Europe. *Geol. Rund*., **83**: 357–376.

KRETSCHMAR U., SCOTT S., 1976 — Phase relations involving arsenopyrite in the system Fe–As–S and their application. *Can. Miner.*, **14**: 364–386.

KRUSCH P., 1907 — Gutachten über die Golderzlagrestatten von Hüsdorf, Wünschendorf, zwischen Lähn und Greifenberg. Centr. Arch. Geol. PIG, Warszawa.

KRYZA R., MUSZYŃSKI A., 1992 — Pre-Variscan volcanic-sedimentary succession of the central southern Góry Kaczawskie, SW Poland: outline. *Geol. An. Soc. Geol. Pol.*, **62**: 117–140.

KRYZA R., MAZUR S., 1995 — Contrasting metamorphic paths in the eastern margin of the Karkonosze–Izera Block, SW Poland. *N. Jahrb. Mineral. Abh*., **169**, 2: 157–192.

KRYZA R., MUSZYŃSKI A., VIELZEUF D., 1990 — Glaucophane-bearing assemblage overprinted by greenschist-facies metamorphism in the Variscan Kaczawa complex, Sudetes, Poland. *J. Metamorphic Geol.*, **8**: 345–355.

KUCHA H., 1974 — Złoto rodzime w złożach miedzi na monoklinie przedsudeckiej. *Rudy i Met. Nież.*, **19**, 4: 174–175.

KUCHA H., 1982 — Platinium-group metals in the Zechstein copper deposits, Poland. *Econ. Geol.*, **77**: 1578–1591.

KUCHA H., LIS J., SYLWESTRZAK H., 1986 — The application of electron microprobe to the dating of U–Th–Pb uraninite from the Karkonosze Granite (Lower Silesia). *Miner. Pol*., **11**: 43–47.

KURAL S., MORAWSKI T., 1968 — Strzegom-Sobótka granitic massif. *Biul. Inst. Geol.*, **227**: 33–85.

LANG J.R., BAKER T., HART C., MORTENSEN J.K., 2000 — An exploration model for intrusion-related gold systems: *SGA Newsletter*, **40**: 1, 6–14.

LANGTHALER K.J., RAITH J.G., CORNELL D.H., STEIN H.J., MELCHER F., 2004 — Molybdenum mineralization at Alpeiner Scharte, Tyrol (Austria): results of in-situ U-Pb zircon and Re-Os molybdenite dating. *Min. and Petrol*., **82**: 33–64.

LÄCHELT S., POKORNY J., FEDAK J. (eds.), 1976 — Metallogenetic map – Bohemian massif and Northern Adjacent regions. Wyd. Geol., Warszawa.

Le MAITRE R.W., BATEMAN P., DUDEK A., KELLER J., LAMEYRE J., Le BAS M.J., SABINE P.A., SCHMID R., SORENSEN H., STRECKEISEN A., WOOLLEY A.R., ZANETTIN B., 1989 — A classification of igneous rocks and glossary of terms. Recommendations of the International Union of Geological Sciences Blackwell, Oxford.

LEAT P.T., JACKSON S.E., THORPE R.S., STILLMAN C.J., 1986 — Geochemistry of bimodal basalt-subalkaline/peryalkaline rhyolite provinces within the southern British Caledonides. *J. Geol. Soc. London*, **143**: 259–273.

LEGIERSKI J., 1973 — Model ages and isotopic composition of ore leads of the Bohemian Massif. *Čas. Miner. Geol*., **18**, 1: 1–23.

LEHMANN B., 1994 — Granite-related rare-metal mineralization: a general geochemical framework. *In*: Metallogeny of collisional orogens focused on the Erzgebirge and comparable metallogenic settings (eds. R. Seltmann *et al.*): 342–349. Proceedings of the IAGOD Erzgebirge meeting Geyer, June 4–6, 1993. Czech Geol. Survey, Prague.

LINDNER M., 1963 — Geochemiczne poszukiwania rud metali w Górach Kaczawskich. *Prz. Geol*., **11**, 4: 192–196.

LINDNER M., 1990 — Arsenic ores. *In*: Geology of Poland. Vol. 6 – Mineral deposits (ed. R. Osika): 189–190. Wyd. Geol., Warszawa.

LIS F., KOSZTOLANYI CH., COPPENS R., 1971 — Etude geochronologique du gisement polymetallique de Kowary (Pologne). *Mineral. Deposita*, **6**: 95–102.

LIS J., SYLWESTRZAK H., 1986 — Minerały Dolnego Śląska. Wyd. Geol., Warszawa.

MACHOWIAK K., MUSZYŃSKI A., 2000 — Geochemistry of igneous rocks in the area of Żeleźniak Hill (the Kaczawa Mountains). *Pr. Specjalne PTM*, **17**: 212–214.

MACHOWIAK K., MUSZYŃSKI A., 2005 — Hipabisalny magmatyzm w zapisie petrograficznym na przykładzie rejonu Żeleźniaka, Góry Kaczawskie. *Prz. Geol.*, **53**, 4: 334.

MACHOWIAK K., WEBER-WELLER A., 2003 — Temperatures of hydrothermal alterations of rocks in the Żeleźniak Hill intrusion (The Kaczawa Mountains, Sudetes, SW Poland) – stable isotope analyses and mineral chemistry. *Miner. Pol.*, **34**, 2: 15–30.

MACIEJEWSKI S., MORAWSKI T., 1975 — Zmienność petrograficzna granitów masywu strzegomskiego. *Kwart. Geol.*, **19**, 1: 47–65.

MacLEAN W.H., 1990 — Rare earth elements and hydrothermal ore formation processes. *Miner. Deposita*, **23**: 231–238.

MACHESKY M.L., ANDRADE W.O., ROSE A.W., 1991 — Adsorption of gold(III)-chloride and gold(I)-thiosulphate anions by goethite. *Geochim. Cosmochim. Acta*, **55**: 769–776.

MAJEROWICZ A., 1972 — Masyw granitowy Strzegom-Sobótka. *Geol. Sudetica*, **6**: 7–96.

MAJEROWICZ A., SKURZEWSKI A., 1987 — Granity z okolic Wojcieszowa w Górach Kaczawskich. *Acta Univ. Wratislaviensis Pr. Geol. Mineral.*, **10**, 788: 69–89.

MANECKI A., 1962a — Grafit w łupkach radzimowickich (okolice Wojcieszowa). *Spraw. z Pos. Kom. Nauk PAN Oddz. w Krakowie*, **5**, 1: 203–205

MANECKI A., 1962b — Mineralizacja miedzią występująca w rejonie Bukowej Góry koło Radzimowic (Dolny Śląsk). *Spraw. z Pos. Kom. Nauk PAN Oddz. w Krakowie*, **5**, 2: 460–461.

MANECKI A., 1963 — Intruzje lamprofirowe w okolicy Radzimowic na Dolnym Śląsku. *Spraw. z Pos. Kom. Nauk PAN Oddz. w Krakowie*, **7**, 2: 538–539.

MANECKI A., 1964 — Dickite from Stara Góra in Lower Silesia. *Bull. Acad. Pol. Sc. Sér. Sc. Géol. Géogr.*, **12**, 1: 41–48.

MANECKI A., 1965 — Studium mineralogiczno-petrograficzne polimetalicznych żył okolic Wojcieszowa (Dolny Śląsk). *Pr. Min. Komisji Nauk Min. PAN Odd. w Krakowie*, **2**: 71pp.

MANECKI A., MŁODOŻENIEC W., 1959 — Kobaltonośne żyły złoża „Stara Góra" na Dolnym Śląsku. *Prz. Geol*., **7**, 10: 466–467.

MANECKI A., MŁODOŻENIEC W., 1960 — Wyniki dotychczasowych badań polimetalicznego złoża Stara Góra. *Rudy i Met. Nież*., **9**: 380–383.

MAPA GEOLOGICZNA LAUSITZ–IZERA–KARKONOSZE (bez osadów kenozoicznych) skala 1:100 000. Praca zbiorowa, 2000. Sächsisches Landesamt für umwelt und Geologie. Państw. Inst. Geol., Česky Geologicky Ustav.

MARCOUX E., Le BERRE, P., COCHERIE A., 2004 — The Meillers Autunian hydrothermal chalcedony: first evidence of a ~295 Ma auriferous epithermal sinter in the French Massif Central. *Ore Geol. Rev*., **25**: 69–87.

MARHEINE D., KACHLIK V., MALUSKI H., PATOCKA F., ŻELAŻNIEWICZ A., 2002 — The Ar–Ar ages from the West Sudetes (NE Bohemian Massif): constrains on the Variscan polyphase tectonothermal development. *In*: Palaeozoic Amalgamation of Central Europe (eds. J.A.Winchester *et al.*). *J. Geol. Soc. London, Spec. Pub.*, **201**: 133–155.

MARKEY R., HANNAH J.L., MORGAN J.W., STEIN H.J., 2003 — A double spike for osmium analysis of highly radiogenic samples. *Chem. Geol.,* **200**: 395–406.

MASTALERZ K., PROUZA V., 1995 — Development of the Intra-Sudetic Basin during Carboniferous and Permian. *In*: Sedimentary record of the Variscan orogeny and climate – Intra-Sudetic Basin, Poland and Czech Republic (eds. K. Mastalerz *et al*.): 5–15. Guide to the excursion B1. XIIIth International Congress on Carboniferous–Permian, August 28–September 2, Kraków, Poland. Państw. Inst. Geol., Warszawa.

MATERIAŁY, 1923 — Hussdorf-Wünschendorf. Material über Gold und Arsenbergwerken. Centr. Arch. Geol. PIG, Warszawa.

MATSUHISA Y., GOLDSMITH R., CLAYTON R.N., 1979 — Oxygen isotopic fractionation in the system quartz–albite–anorthite–water. *Geoch. et Cosmochim. Acta*, **43**: 1131–1140.

MATTE P.H., 2001 — The Variscan collage and orogeny (480–290 Ma) and the tectonic definition of the Armorica microplate: a review. *Terra Nova*, **13**: 122–128.

MATTE P.H., MALUSKI H., RAJLICH P., FRANKE W., 1990 — Terrane boundaries in the Bohemian Massif: Result of large-scale Variscan shearing. *Tectonophysics*, **177**: 151–170.

MATTHÄI S.K., HENLEY R.W., HEINRICH C., 1995 — Gold precipitation by fluid mixing in bedding-parallel fractures near Carbonaceous slates at the cosmopolitan Howley gold deposit, Northern Australia. *Econ. Geol*., **90**: 2123–2142.

MAUGHAN D.T., KEITH J.D., CHRISTIANSEN E.H., PULSIPHER T., HATTORI K., EVANS N.J., 2002 — Contributions from mafic alkaline magmas to the Bingham porphyry Cu–Au–Mo deposit, Utah, USA. *Miner. Deposita*, **37**: 14–37.

McCOY D.T., NEWBERRY R.J., LAYER P., DIMARCHI J.J., BAKKE A., MASTERMAN J.S., MINEHANE D.L., 1997 — Plutonic related gold deposits of interior Alaska. *Econ. Geol. Monograph*, **9**: 191–241.

McCUAIG T.C., KERRICH R., 1998 — P-T-t-deformation-fluid characteristics of lode gold deposits in the Yilgran craton, Western Australia: *Royal Soc. of W. Australia J.*, **79**: 123–129.

MICHNIEWICZ M., 1981 — Próba interpretacji wczesnych etapów tektogenezy Sudetów w nawiązaniu do teorii diapiryzmu wgłębnego oraz koncepcji głębokich rozłamów. *Geol. Sudetica*, **16**, 2: 75–138.

MICHNIEWICZ M., 2003 — Surowce metaliczne Bloku Karkonosko-Izerskiego. *In*: Sudety Zachodnie od wendu do czwartorzędu (eds. A. Ciężkowski *et al.*): 155–168. WIND, Wrocław.

MIERZEJEWSKI M.P., GRODZICKI A., 1982 — O możliwości znalezienia cyny w Karkonoszach. *Prz. Geol.*, **30**, 8: 389–395.

MIERZEJEWSKI M.P., PIN C., DUTHOU J.L., COUTURIE I.P., 1994 — Sr–Nd isotopic study of the Karkonosze granite (Western Sudetes). *In*: Igneous activity and metamorphic evolution of the Sudetes area (ed. R. Kryza): 82p. Uniw. Wroc., Inst. Nauk. Geol., Wrocław.

MIKULSKI S.Z. 1996. Gold mineralization within contact-metamorphic and shear zones in the "Złoty Jar" quarry – the Złoty Stok As–Au deposit area. *Geol. Quart.*, **40**: 407–442.

MIKULSKI S.Z, 1997 — Złoto rodzime w złozu rudy arsenowej w Czarnowie (Sudety Zachodnie). *In*: Metale szlachetne w NE części Masywu Czeskiego i w obszarach przyległych – geneza, występowanie, perspektywy (ed. A. Muszer): 29–33. Konf. Nauk. Jarnołtówek 19–21.06.1997 r. Wrocław.

MIKULSKI S.Z., 1998 — Złotonośna mineralizacja kruszcowa z Barda Śląskiego (Sudety Środkowe). *Prz. Geol.*, **46**, 12: 1261–1267.

MIKULSKI S.Z., 1999 — Złoto z Radzimowic w Górach Kaczawskich (Sudety) – nowe dane geochemiczne i mineralogiczne. *Prz. Geol.*, **47**, 12: 999–1005.

MIKULSKI S.Z., 2000a — Klasyfikacja form wystąpień złota mikroskopowego w złotonośnych rudach polimetalicznych z Sudetów. *Pr. Specjalne PTM.*, **16**: 209–223.

MIKULSKI S.Z., 2000b — Poszukiwania mineralizacji scheelitowo-złotonośnej w rejonie makroenklawy Ptasznika na intruzji kłodzko-złotostockiej w Sudetach. *Biul. Państw. Inst.Geol.*, **391**: 5–88.

MIKULSKI S.Z., 2000c — Magmowe formacje litotektoniczne Gór Kaczawskich jako potencjalne źródło złota pierwotnego w Sudetach. Centr. Arch. Geol. PIG, Warszawa.

MIKULSKI S.Z., 2001 — Late-Hercynian gold-bearing arsenic-polymetallic mineralization within Saxothuringian zone in the Polish Sudetes, Northeast Bohemian Massif. *In*: Mineral deposits at the beginning of the 21st century. (eds. Piestrzyński *et al*.): 787–790. Proceedings of the Joint 6th Biennial SGA-SEG meeting. Kraków, Poland. 26–29 August 2001. A.A. Balkema Publishers, Lisse/Abingdon/Exton/Tokyo.

MIKULSKI S.Z., 2003a — Multiple episodes of magmatic and hydrothermal activity at the Radzimowice gold deposit in the Sudetes Mountains (Bohemian Massif, Poland) *In*: Mineral exploration and sustainable development (eds. D.G., Eliopoulos *et al*.): 339–342. Proceedings of the 7th Biennial SGA meeting. Athens, Greece. 24–28 August 2003. Millpress.

MIKULSKI S.Z., 2003b — Orogenic quartz-sulphide-gold veins from the Klecza–Radomice ore district in the Kaczawa Mountains (Western Sudetes) – NE part of Bohemian Massif. *In*: Mineral exploration and sustainable development (eds. D.G., Eliopoulos *et al*.): 787–790. Proceedings of the 7th Biennial SGA meeting. Athens, Greece. 24–28 August 2003. Millpress.

MIKULSKI S.Z., 2005a — Geological, mineralogical and geochemical characteristics of the Radzimowice Au–As–Cu deposit from the Kaczawa Mountains (Western Sudetes, Poland) – an example of the transition of porphyry and epithermal style. *Miner. Deposita*, **39**, 8: 904–920.

MIKULSKI S.Z., 2005b — The telluride mineralization event(s) within the Late-Variscan gold deposits in the Western Sudetes (NE part of the Bohemian Massif, SW Poland). *In*: Mineral deposit research: Meeting the global challenge (eds. J. Mao, F.P. Bierlein): 1415–1418. Proceedings of the 8th Biennial SGA meeting. Beijing, China. 18–21 August 2005. Springer, Berlin/Hilderberg/New York.

MIKULSKI S.Z., 2005c — The arsenopyrite geothermometer – a difficult application to arsenopyrite from the Radzimowice abandoned Au–As–Cu deposit (Kaczawa Mountains). *Pr. Specjalne PTM*, **26**: 207–210.

MIKULSKI S.Z., 2005d — Metalogeneza złota w Sudetach zachodnich w świetle badań pierwiastków śladowych wybranych waryscyjskich skał magmowych – wyniki wstępne. *Przeg. Geol.*, **53**, 4: 336–337.

MIKULSKI S.Z., STEIN H.J., 2005 — The Re–Os age for molybdenite from the Variscan Strzegom–Sobótka massif, SW Poland. *In*: Mineral deposit research: Meeting the global challenge (eds. J. Mao, F.P. Bierlein): 789–792. Springer, Berlin/Hilderberg/New York.

MIKULSKI S.Z., OLSZYŃSKI W., SPECZIK S., WOJCIECHOWSKI A., 1999 — Primary gold deposits and occurrences in the Sudety Mountains, SW Poland. *In*: Mineral deposits: processes to processing (eds. Stanley *et al.):* 1419–1422. Proceedings of the 5th biennial meeting SGA and 10th Quadrennial IAGOD, London 22–25 August, 1999. A.A. Balkema. Rotterdam/Brookfield.

MIKULSKI S.Z., LEROUGE C., KOZŁOWSKI A., 2003 — Fluid inclusion and preliminary oxygen isotopic studies of quartz from the Radzimowice Au–Cu–As deposit in Sudetes Mountains. *In*: Mineral exploration and sustainable development (eds. D.G. Eliopoulos *et al*.): 343–345. Proceedings of the 7th Biennial SGA meeting. Athens, Greece. 24–28 August 2003. Millpress, Rotterdam.

MIKULSKI S.Z., BAGIŃSKI B., DZIERŻANOWSKI P., 2004 — The CHIME age calculation on monazite and xenotime in aplogranite from the Szklarska Poręba Huta quarry. *PTM Pr. Spec.*, **24**: 287–290

MIKULSKI S.Z., MARKEY R.J., STEIN H.J., 2005a — Re–Os ages for auriferous sulphides from the gold deposits in the Kaczawa Mountains (SW Poland). *In*: Mineral deposit research: Meeting the global challenge (eds. J. Mao, F.P. Bierlein): 793–796. Springer, Berlin/Hilderberg/New York.

MIKULSKI S.Z., SPECZIK S., KOZŁOWSKI A., 2005b — Fluid inclusion study of quartz veins from the orogenic Klecza gold deposit in the Kaczawa Mountains (SW Poland). *In*: Mineral deposit research: Meeting the global challenge (eds. J. Mao, F.P. Bierlein): 553–556. Springer.

MIKULSKI S.Z., BAGIŃSKI B., DZIERŻANOWSKI P., 2005c — Distribution of Co, Ni, and As in pyrites from Klecza and Radomice in the Kaczawa Mountains. *Polskie Towarzystwo Mineralogiczne – Prace Specjalne*, **25**: 211–214.

MIKULSKI S.Z., STEIN H.J., MARKEY R.J., 2005d — Determination of sulphide ages from Lower Silesia using the Re–Os method. *Pr. Specjalne PTM*, **26**: 215–218.

MILEWICZ J., 1962 — Szczegółowa mapa geologiczna Sudetów w skali 1:25 000, ark. Lubomierz. Wyd. Geol., Warszawa.

MILEWICZ J., 1970 — Objaśnienia do Szczegółowej mapy geologicznej Sudetów w skali 1:25 000, ark. Lubomierz. Wyd. Geol., Warszawa.

MILEWICZ J., 1987 — Przyczynek do poznania tektoniki waryscyjskiej wschodniej części depresji północnosudeckiej (Dolny Śląsk). *Prz. Geol*., **35**, 10: 529–530.

MILEWICZ J., FRĄCKIEWICZ W., 1983 — Szczegółowa mapa geologiczna Sudetów w skali 1:25 000, ark. Wleń. Wyd. Geol., Warszawa.

MILEWICZ J., FRĄCKIEWICZ W., 1988 — Objaśnienia do Szczegółowej mapy geologicznej Sudetów w skali 1:25 000, ark. Wleń. Wyd. Geol., Warszawa.

MILEWICZ J., KOZDRÓJ W., 1994a — Szczegółowa mapa geologiczna Sudetów w skali 1:25 000, ark. Proboszczów. Państw. Inst. Geol., Warszawa.

MILEWICZ J., KOZDRÓJ W., 1994b — Objaśnienia do Szczegółowej mapy geologicznej Sudetów w skali 1:25 000. Arkusz Proboszczczów. Państw. Inst. Geol., Warszawa.

MOCHNACKA K., 1982 — Mineralizacja polimetaliczna wschodniej osłony metamorficznej granitu Karkonoszy i jej związek z geologicznym rozwojem regionu. *Biul. Inst. Geol.*, **341**: 273–289.

MOCHNACKA K., 2000 — Prawidłowości wykształcenia mineralizacji kruszcowej w metamorficznej osłonie granitu

Karkonoszy – próba powiązania ze środowiskiem geotektonicznym. *In*: Problemy genezy złóż rud, mineralogia, petrografia, geochemia. *Pr. Specjalne PTM*, **16**: 223–258.

MOCHNACKA K., BANAŚ M., 2000 — Occurrence and genetic relationships of uranium and thorium mineralization in the Karkonosze-Izera Block (the Sudety Mountains, SW Poland). *Ann. Soc. Geol. Pol.*, **70**: 137–150.

MORÁVEK P., 1995 — Gold metallogeny of Central and Western European Variscides. *In*: Mineral deposits from their origin to their environmental impacts (eds. J. Paśava *et al.*): 67–70. Balkema, Rotterdam.

MORÁVEK P., (ed.), PERTOLD Z., PUNČOCHÁR M., STUDNIČNA B., ZACHARIÁŠ J., 1996 — Gold deposits in Bohemia. Czech Geol. Survey, Prague.

MORSEY-PICKARD F., 1898 — Gutachten betreffend die Erzbergwerke "*Eureka*" "*Ottilie*" und "*Kätchen*" im Kreise Löwenberg, Provinz Schlesise. Centr. Arch. Geol. PIG, Warszawa.

MÖLLER O., 1911 — Die Primaren Goldlageerstätten von Hüssdorf-Wünschendorf in Pr. Schlesien. Abschrift aus Erzbergbau. Mater. arch. PIG.

MÖLLER P., KERSTEN G., 1994 — Electrochemical accumulation of visible gold on arsenopyrite and pyrite surfaces. *Miner. Deposita*, **29**: 404–413.

MROCZKOWSKI J., 1992 — A N-trending photolineament in the Rudawy Janowickie Mountains (West Sudetes, Poland) and its tectonic significance. *Ann. Soc. Geol. Pol.*, **62**: 63–73.

MUMIN A., FLEET M., CHRYSSOULIS S., 1994 — Gold mineralization in As-rich mesothermal gold ores of the Bogosu-Prestea mining district of the Ashanti Gold Belt, Ghana: remobilization of "invisible" Au. *Miner. Deposita*, **29**: 445–460.

MURPHY P.J., ROBERTS S., 1997 — Evolution of a metamorphic fluid and its role in lode gold mineralization in the Central Iberian Zone. *Mineral. Deposita*, **32**: 459–474.

MÜLLER D., GROVES D.I., 2000 — Potassic igneous rocks and associated gold-copper mineralization. Springer, Berlin/Heidelberg/New York.

MUSZER A., 1997 — Charakterystyka okruszcowania skał północnej i środkowej części Gór Złotych na tle budowy geologicznej. *Pr. Geol. Miner*., **59**: 104pp.

MUSZYŃSKI A., MACHOWIAK K., KRYZA R., ARMSTRONG R., 2002 — SHRIMP U–Pb zircon geochronology of the Late-Variscan Żeleźniak rhyolite intrusion, Polish Sudetes – preliminary results. *Pr. Specjalne PTM*, **19**: 156–158.

NAWROCKI J., 1998 — Paleomagnetic data and tectonic regime during Permian sedimentation in the Sudety Mountains *Prz. Geol*., **46,** 6: 1023–1027.

NEKRASOV I.Y., 1996 — Geochemistry, mineralogy, and genesis of epigenetic ore deposits. A.A. Balkema, Rotterdam/Brookfield.

NEUHAUS A., 1936 — Űber Vorkommen von Kupfererzfűhrenden Spateisensteingängen im őstlichen Bober-Katzbach-Gebirge (Schlesien). *Chem. D. Erde*, **10**. Jena.

NORONHA F., CATHELINEAU M., BOIRON M., BANKS M.C., DOIRA A., RIBEIRO M.A., NORGUEIRA P., GUEDES A., 2000 — A three stage fluid flow model for Variscan gold metallogenesis in northern Portugal. *J. of Geoch. Expl.*, **71**: 209–224.

OBERC J., 1964 — Główna sudecka dyslokacja diagonalna i jej znaczenie dla stanowiska synklinoriów waryscyjsko-laramijskich. *Kwart. Geol*., **8**, 3: 478–488.

OBERC J., 1972 — Sudety i obszary przyległe. Budowa Geologiczna Polski. T. 4, Tektonika część 2. Wyd. Geol., Warszawa.

OBERC-DZIEDZIC T., ŻELAŹNIEWICZ A., CWOJDZIŃSKI S., 1999 — Granitoids of the Odra Fault Zone: late- post-orogenic Variscan intrusions in the Saxothuringian Zone, SW Poland: *Geol. Sudetica*, **32**, 1: 55–71.

OHMOTO H., 1986 — Stable isotope geochemistry of ore deposits: stable isotopes in high temperature geological processes. *Rev. Mineral*., **16**: 491–559.

OHMOTO H., GOLDHABER B., 1997 — Sulphur and carbon isotopes. *In*: Geochemistry of hydrothermal ore deposits (ed. H.L. Barnes): 517–600. John Wiley & Sons Inc., New York.

OLSZYŃSKI W., MIKULSKI S.Z., 1997 — Złoto rodzime w łupkach krystalicznych z Radomic koło Wlenia. *In*: Metale szlachetne w NE części Masywu Czeskiego i w obszarach przyległych – geneza, występowanie, perspektywy (ed. A. Muszer): 86–90. Mater. Konf. Nauk. Jarnołtówek 19–21.06.1997 r. Wrocław.

OLIVER G.J.H., KELLEY S., 1993 — ^{40}Ar-^{39}Ar fusion ages from the Polish Sudetes: Variscan tectonothermal reworking of Caledonian protoliths. *N.Jb. für Geol. Paläont. Mh*.: 321–344.

OSIKA R., 1987 — Złoto i srebro oraz metale śladowe. *In*: Budowa Geologiczna Polski. T. 6. Złoża surowców mineralnych (ed. R. Osika): 367–368. Wyd. Geol., Warszawa.

OSZCZEPALSKI S., 1999 — Wiek mineralizacji cechsztyńskiej w świetle radiometrycznych badań illitu metodą K–Ar. *In*: Wybrane zagadnienia stratygrafii, tektoniki i okruszcowania Dolnego Śląska (ed. A. Muszer): 75–84. Wrocław.

OSZCZEPALSKI S., RYDZEWSKI A., SPECZIK S., 1999 — Rote Fäule-related Au–Pt–Pd mineralization in SW Poland: new data. *In*: Mineral deposits: Processes to processing (eds. Stanley *et al*.): 1423–1425. A.A. Balkema, Rotterdam.

OSZCZEPALSKI S., NOWAK G., BECHTEL A., ŽÁK K., 2002 — Evidence of oxidation of the Kupferschiefer in the Lubin–Sieroszowice deposit, Poland: Implications for Cu–Ag and Au–Pt–Pd mineralization. *Geol. Quart.*, **46**, 1: 1–23.

PAŃCZYK M., BACHLIŃSKI R., 2004 — Rb–Sr dating of Permian silica-rich volcanic rocks from the North Sudetic Basin – preliminary data. *Pr. Specjalne PTM*, **24**: 307–310.

PAJĄK M., 1997 — Wstępne dane o występowaniu złota rodzimego w Radzimowicach (Góry Kaczawskie): *In*: Metale szlachetne w NE części Masywu Czeskiego i w obszarach przyległych – geneza, występowanie, perspektywy (ed. A. Muszer): 42–47. Konf. Nauk. Jarnołtówek 19–21.06.1997 r. Wrocław.

PAULO A., 1962 — Nowe dane o mineralizacji utworów Palaeozoicznych okolicy Lipy Jaworskiej (Dolny Śląsk). *Spraw. z Pos. Kom. Nauk. PAN Oddz. w Krakowie*, **6**, 2: 518–520.

PAULO A., 1970 — Minerały niklu i bizmutu w żyłach kruszcowych okolicy Chełmca (Góry Kaczawskie, Dolny Śląsk). *Pr. Miner. Kom. Nauk Miner. PAN Oddz. w Krakowie*, **24**: 61–77.

PAULO A., 1972 — Charakterystyka mineralogiczna złoża barytu w Stanisławowie (Dolny Śląsk). *Pr. Miner. Kom. Nauk Miner. PAN Oddz. w Krakowie*, **29**: 76pp.

PAULO A., 1973 — Złoże barytu w Stanisławowie na tle metalogenii Gór Kaczawskich. *Pr. Geol. Kom. Nauk Geol. PAN Oddz. w Krakowie*, **76**: 72pp.

PAULO A., 1994 — Geology of barite veins in the Polish Sudetes. *In*: Metallogeny of collisional orogens (eds. R. Seltmann *et al.*): 383–390. Czech Geological Survey, Prague.

PAULO A., SALAMON W., 1973a — Native gold in ore veins of the Western part of the Góry Kaczawskie Mountains (Sudetes). *Miner. Pol*., **4**: 85–90.

PAULO A., SALAMON W., 1973b — O żyle kruszcowej w Grudnie (Góry Kaczawskie). *Kwart. Geol.*, **17**, 2: 234–241.

PAULO A., SALAMON W., 1974a — A note on freibergite, pyrargyrite and bournonite from Grudno, Lower Silesia. *Miner. Pol.*, **5**, 3: 83–86.

PAULO A., SALAMON W., 1974b — Przyczynek do znajomości złoża polimetalicznego w Starej Górze. *Kwart. Geol.*, **18**, 2: 266–276.

PAWŁOWSKA J., 1973 — Fizyczno-chemiczne warunki powstawania dolnośląskich złóż barytów. *Biul. Inst. Geol.*, **267**: 5–101.

PEARCE J.A., 1983 — Role of the subcontinental lithosphere in magma genesis at active continental margins. *In*: Continental basalts and mantle xenoliths (eds. C.J. Hawkesworth, M.J. Norry): 230–249. Shiva, Nantwich.

PEARCE J.A., HARRIS N.B., TINDLE A.G., 1984 — Trace element discrimination diagrams for the tectonic interpretation of granitic rocks. *J. Petrol.*, **25**: 956–983.

PECCERILLO K., TAYLOR S.R., 1976 — Geochemistry of Eocene calc-alkaline volcanic rocks from the Kastamonu area, northern Turkey. *Contrib. Mineral. Petrol.*, **58**: 63–81.

PENDIAS H., 1965 — Geochemiczne profile w okolicy Radzimowic na Dolnym Śląsku. *Inst. Geol. Biul.*, **170**: 81–145.

PENDIAS H., WALENCZAK Z., 1956 — Objawy okruszcowania w północno-zachodniej części masywu strzegomskiego. *Inst. Geol. Biul.*, **112**: 31–42.

PETRASCHECK W.E., 1933 — Die Erzlagerstätten des Schlesischen Gebirges. *Arch. Lagerst.-Forsch*., **59**: 1–53. Berlin.

PETRASCHECK W.E., 1937 — Die geologische Stellung der Schlesischen Arsen-, Kupfer– und Eisenspatlagerstätten und deren Bedeutung für die neuen Aufschlussarbeiten. *Metal und Erz.*, **34**, 20: 527–532.

PIESTRZYŃSKI A., 1992 — Wybrane materiały do ćwiczeń z petrografii rud. *Skrypty uczelniane,* **1306**: 393pp. Wydawnictwa AGH, Kraków.

PIESTRZYŃSKI A., SAWŁOWICZ Z., 1999 — Exploration for Au and PGE in the Polisch Zechstein copper deposits (Kupferschiefer). *J. Geoch. Expl*., **66**: 17–25.

PIESTRZYŃSKI A., WODZICKI A., 2000 — Origin of the gold deposit in the Polkowice-West Mine, Lubin-Sieroszowice Mining District, Poland. *Mineral. Deposita*, **35**: 37–47.

PIESTRZYŃSKI A., MOCHNACKA K., MAYER W., KUCHA, H., 1992 — Native gold (electrum), Fe–Co–Ni arsenides and sulphides in the mica schists from Przecznica, the Kamienica Range, SW Poland. *Mineralogia Polonica*, **23**: 27–43.

PIESTRZYŃSKI A., WODZICKI A., BANASZAK, A., 1996 — Złoto w złożach miedzi na monoklinie przedsudeckiej (SW Polska). *Prz. Geol*., **44**, 11: 1098–1102.

PIESTRZYŃSKI A., PIECZONKA J., SPECZIK S., OSZCZEPALSKI S., BANASZAK A., 1997 — Noble metals from the Kupferschiefer-type deposits, Lubin–Sieroszowice, SW Poland. *In*: Mineral deposits: research and exploration —Where do they meet? (eds. H. Papunen *et al*.): 563–566. Proc. of the 4th Biennial SGA Meeting. Turku, Finland. 11–13 August 1997. A.A. Balkema, Rotterdam/Brookfield.

PIN C., MIERZEJEWSKI M.P., DUTHOU J.L., 1987 — Wiek izochronowy Rb/Sr granitu karkonoskiego z kamieniołomu Szklarska Poręba Huta oraz oznaczenie stosunku inicjalnego $^{87}Sr/^{86}Sr$ w tymże granicie. *Prz. Geol*., **35**, 10: 512–517.

PIN C., PUZIEWICZ J., DUTHOU J., 1989 — Ages and origins of a composite granitic massif in the Variscan belt. *N. Jb. Mineral.*, *Abh.*, **160**: 71–82.

POPIVNYAK I.V., 1975 — Role of CO_2 in formation of the lodes of the Muy gold ore deposit (North Buryatia). Carbon and its compounds in endogene processes of mineral formation, Lviv: 84–86.

POULSEN K.H., ROBERT F., DUBČ B., 2000 — Geological classification of Canadian gold deposits. *Geol. Sur. Can. Bul.*, **540**: 106pp.

PRONIEWICZ E., 2002 — Mineralizacja kruszcowa w rejonie Stanisławowa w Górach Kaczawskich. M.Sc. Thesis. UW, Warszawa.

PUZIEWICZ J., 1985 — Origin of chemical, structural and textural variations in aplites from Strzegom granite (Poland). *N. Jb. Miner. Abh.*, **153**: 19–31.

PUZIEWICZ J., 1990 — Masyw granitowy Strzegom–Sobótka. *Arch. Miner.*, **50**, 1/2: 135–154.

QUIRING H., 1948 — Geschichte des Goldes: 154–166. F. Enke. Verlag, Stuttgart.

RAMDOHR P., 1969 — The ore minerals and their intergrowths. Pergamon Press, Oxford.

REED M.H., SPYCHER N.F., 1985 — Boiling, cooling and oxidation in epithermal systems: A numerical modeling approach. *In*: Geology and geochemistry of epithermal systems (eds. B.R. Berger, P. Bethke). Society of Economic Geologists, *Reviews in Econ. Geol*., **2**: 249–272.

RICHARDS J.P., 1995 — Alkalic-type epithermal gold deposits - a review. *Miner. Ass. of Canada Short Course Ser.*, **23**: 367–400.

ROBERT F., POULSEN K.H., DUBÉ B., 1997 — Gold deposits and their geological classification. *In*: International Conference on Mineral Exploration. Exploration 97, 4 December 1997, Proceedings (eds. A.G. Gubins): 209–220.

ROCK N.M.S., BOWES D.R., WRIGHT A.E., 1991 — Lamprophyres. Blackie.

ROIG J.Y., BOUCHOT V., MALUSKI H., FAURE M., 2000 — Superimposed hydrothermal events along the Argentant fault (Western French Massif Central). *In*: A GEODE-GEOFRANCE 3D Workshop on orogenic gold deposits in Europe with emphasis on the Variscides (eds. BRGM). Extended abstracts, November 7–8, 2000, Orléans (BRGM), France. *Document du BRGM*, **297**: 66–67. BRGM.

ROEDDER E., 1984 — Fluid inclusions. *Rev. Mineral.*, **12**: 644pp.

ROMBERGER S.R., 1986 — The solution chemistry of gold applied to the origin of hydrothermal deposits. *In*: Gold in the Western Shield (eds. L.A. Clark, D.R. Francis). *Can. Inst. of Mining and Metalurgy.*, *Spec. Vol*., **38**: 168–186.

ROMBERGER S.R., 1988 — Geochemistry of gold in hydrothermal deposits. *U.S. Geol. Survey Bull.*, **1857-A**: 9–25.

ROSENBERG-LIPINSKY V., 1896 — Die Erzfunde und ihre Lagerstätten zwischen Görlitz und Niesky. *Zeitschr. für Prakt. Geol.*: 213–217.

ROSENBERG-LIPINSKY V., 1897 — Die neuen Goldfunde zu Löwenberg in Preussisch-Schlesien. *Zeitschr. für prakt. Geol.*: 156–158.

SACHS 1914 — Die Bildung schlesischer Erzlagerstätten. *Montan. Rundschau*: 489–492.

SAŁACIŃSKI R., 1973 — Ore mineralization in granite at Paszowice. *Acta Geol. Pol.*, **23**: 587–596.

SAŁACIŃSKI R., 1978 — Mineralizacja kruszcowa i jej geneza w granitoidowym masywie strzegomskim. *Biul. Inst. Geol.*, **308**, 41–90.

SAWŁOWICZ Z., 1987 — Framboidal pyrite from the metamorphic Radzimowice schists of Stara Góra (Lower Silesia, Poland). *Miner. Pol.*, **18**: 57–62.

SAVAGE R.S., BIRD D.K., ASHLEY R.P., 2000 — Legacy of the California Gold Rush: Environmental geochemistry of arsenic in the southern Mother Lode Gold District. *Int. Geol. Rev.*, **42**: 385–415.

SCHNEIDERHŐHN H., 1941 — Lehrbuch der Erzlagerstättenkunde. Bd. **1**, Die Lagerstätten der magmatischen Abfolge. Verlag von Gustav Fischer, Jena.

SESTON R., WINCHESTER J.A., PIASECKI M.A.J., CROWLEY Q.G., FLOYD P., 2000 — A structural model for the western-central Sudetes: a deformed stack of Variscan thrust sheets: *J. Geol. Soc. London*, **157**: 1155–1167.

SEWARD T.M., 1973 — Thio complexes of gold and the transport of gold in hydrothermal ore solutions. *Geochim. Cosmochim. Acta*, **37**: 370–399.

SEWARD T.M., 1989 — The hydrothermal geochemistry of gold and its implications for ore formation: boiling and conductive cooling as examples. *Econ. Geol. Monograph*, **6**: 398–404.

SEWARD T.M., 1991 — The hydrothermal geochemistry of gold. *In:* Gold metallogeny and exploration (ed. R.P. Foster): 37–62. Blackie, London.

SEWARD T.M., BARNES H.L., 1997 — Metal transport by hydrothermal ore fluids. *In*: Geochemistry of hydrothermal ore deposits (ed. H.L. Barnes): 435–487. 3rd edition., John Wiley & Sons, Inc., USA.

SHARP Z.D., ESSENE E.J., KELLY W.C., 1985 — A re-examination of the arsenopyrite geothermometer: pressure considerations and applications to natural assemblages. *Can. Miner.*, **23**: 517–534.

SHEPHERD T.J., BOUCH J.E., GUNN A.G., McKERVEY J.A., NADEN J., SCRIVENER R.C., STYLES M.T., LARGE D.E., 2005 — Permo-Triasic unconformity-related Au–Pd mineralization, South Devon, UK: new insights and the European perspective. *Miner. Deposita*, **39**: 24–45.

SIEMIĄTKOWSKI J., 1993 — Mineralogiczna interpretacja wyników analiz chemicznych skał z hałd w Radzimowicach (Stara Góra). *Pos. Nauk. PIG*, **49**: 41.

SILLITOE R.H., 1991 — Intrusion-related gold deposits. *In*: Gold metallogeny and exploration (ed. R.P. Foster): 165–209. Blackie, Glasgow, London.

SILLITOE R.H., 2000 — Gold-rich porphyry deposits: desrcriptive and genetic models and their role in exploration and discovery. *In*: Gold in 2000 (eds. S.G. Hageman, P.E. Brown). *SEG Rev. Econ. Geol.*, **13**: 315–345.

SILLITOE R.H., THOMPSON J.F.H., 1998 — Intrusion-related vein gold deposits: Types, tectono-magmatic settings and difficulties of distinction from orogenic gold deposits. *Res. Geol.*, **48**: 237–250.

SIMMON., KESLER S.F., CHRYSSOULIS S., 1999 — Geochemistry and textures of gold-bearing arsenian pyrite, Twin Creeks, Nevada: Implications for deposition of gold in Carlin-type deposits: *Econ. Geol.*, **94**: 405–421.

SIUDA R., 2005 — Minerały strefy wietrzenia złoża w Starej Górze. Ph.D. Thesis. UW, Warszawa.

SKOWRONEK A., STEFFAHN J., 2000 — The age of the Kauffung Limestone (W Sudetes, Poland) – a revision due to new discovery of microfossils. *N. Jb. Geol. und Paläont. Monatsh.*, **2**: 65–82.

SKURZEWSKI A., 1984 — Wulkanity hercyńskie w rejonie Wojcieszowa. *Kwart. Geol.*, **28**, 1: 39–58.

SMOLIAR M.I., WALKER R.J., MORGAN J.W., 1996 — Re–Os ages of group II1, IIIA, IVA and IVB iron meteorites. *Science*, **271**: 117–133.

SOKOŁOWSKA G., WOJCIECHOWSKI A., 1995 — Złotonośność porfirowego masywu Żeleźniaka k/Radzimowic i skał go otaczających. *Pos. Nauk. PIG*, **51**, 3: 39–40. Warszawa.

SPECZIK S., WOJCIECHOWSKI A., 1997 — Złotonośne utwory z pogranicza czerwonego spągowca i cechsztynu niecki północnosudeckiej w okolicach Nowego Kościoła. *Prz. Geol.*, **45**, 9: 872–874.

SPECZIK S., PIESTRZYŃSKI A., RYDZEWSKI A., OSZCZEPALSKI S., 1997 — Exploration for Cu–Ag and Au–Pt–Pd Kupferschiefer-type deposits in SW Poland. *In*: Mineral deposits: Research and exploration —Where do they meet? (eds. H. Papunen *et al.*): 119–122. Proc. of the 4th Biennial SGA meeting. Turku, Finland. 11–13 August 1997. A.A. Balkema, Rotterdam/Brookfield.

SPRINGER J.S., 1986 — Gold in carbon-rich rocks: improbable protores. *In*: Gold in the Western Shield (ed. L.A. Clark, D.R. Francis). *Can. Inst. of Mining and Metall., Spec. Vol.*, **38**: 104–112.

SPIRIDONOV E.M., 1996 — Granitic rocks and gold mineralization of North Kazakhstan. *In*: Granite-related ore deposits of Central Kazakhstan and adjacent areas (eds. V. Shatov *et al.*): 197–217. Glagol Publishing House, St. Petersburg.

STAHL F., 1935 — Gutachten über die Goldlagerstätten von Hüssdorf-Wünschendorf. Centr. Arch. Geol. PIG, Warszawa.

STAUFFACHER J., 1914 — Der Gangdistrikt von Altenberg in Schlesien auf Grund eigener Aufnahmen der Oberfläche und der unterirdischen Aufschlüsse. *Zeitsch. für prakt. Geol.*, **22**: 12–15.

STAUFFACHER J., 1915 — Der Goldgangdistrikt von Altenberg in Schlesien. *Zeitsch. für prakt. Geol.*, **23**: 53–83.

STEIN H.J., MARKEY R.J., MORGAN J.W., HANNAH J.L., ŽAK K., SUNBLAD K., 1997 — Re–Os dating of shear-hosted Au deposits using molybdenite. *In*: Mineral deposits: research and Exploration —Where do they meet? (eds. H. Papunen *et al.*): 313–317. Proc. of the 4th Biennial SGA meeting. Turku, Finland. 11–13 August 1997. A.A. Balkema, Rotterdam/Brookfield.

STEIN H.J., MORGAN J.W., SCHERESTEN A., 2000 — Re–Os of low level highly radiogenic (LLHR) sulphides: The Harnas gold deposit, southwest Sweden, records continental-scale tectonic events. *Econ. Geol.*, **95**: 1657–1671.

STEIN H.J., MARKEY R.J., MORGAN J.W., HANNAH J.L., SCHERSTÉN A., 2001 — The remarkable Re-Os chronometer in molybdenite: how and why it works. *Terra Nova*, **13**, 6: 479–486.

SYLWESTRZAK H., WOŁKOWICZ K., 1985 — Nowy zespół Sn–W–Mo ze Starej Góry (Dolny Śląsk) i jego znaczenie genetyczne. *Prz. Geol.*, **33**, 2: 73–75.

SZAŁAMACHA J., 1956 — Szczegółowa mapa geologiczna Sudetów w skali 1:25 000, ark. Janowice Wielkie. Wyd. Geol., Warszawa.

SZAŁAMACHA J., 1969 — Objaśnienia do Szczegółowej mapy geologicznej Sudetów w skali 1:25 000, ark. Janowice Wielkie. Wyd. Geol., Warszawa.

SZAŁAMACHA J., 1970 — Szczegółowa mapa geologiczna Sudetów w skali 1:25 000, ark. Stara Kamienica. Wyd. Geol., Warszawa.

SZAŁAMACHA J., 1974 — Szczegółowa mapa geologiczna Sudetów w skali 1:25 000, ark. Siedlęcin. Inst. Geol., Warszawa.

SZAŁAMACHA J., 1978 — Objaśnienia do Szczegółowej mapy geologicznej Sudetów w skali 1:25 000, ark. Siedlęcin. Wyd. Geol., Warszawa.

SZAŁAMACHA M., 1971 — Uwagi o geologii i tektonice serii izerskiej i kaczawskiej w strefie ich kontaktu między Jeżowem i Strzyżowcem. *Kwart. Geol*., **15**, 4: 1026–1027.

SZAŁAMACHA M., 1976 — O złożowej mineralizacji barytowo-fluorytowej w Jeżowie Sudeckim. *Kwart. Geol*., **20**, 2: 215–240.

TAYLOR S.R., McLENNAN S.M., 1985 — The continental crust: Its composition and evolution. Oxford Blackwell Scientific Publications, Oxford.

TEISSEYRE J., 1968 — Budowa geologiczna wschodniej części okrywy granitu Karkonoszy w okolicach Miedzianki (Sudety Zachodnie). *Geol. Sudet.*, **4**: 482–541.

TEISSEYRE H., 1956 — Depresja Świebodzic jako jednostka geologiczna. *Biul. Inst. Geol.*, **106**.

TEISSEYRE H., 1963 — Siodło Bolków–Wojcieszów jako charakterystyczny przykład struktury kaledońskiej w Sudetach. *Pr. Inst. Geol*., **30**, 4: 279–300.

TEISSEYRE H., 1967 — Najważniejsze zagadnienia geologii podstawowej w Górach Kaczawskich. Przew. 40 Zjazdu Pol. Tow. Geol., Zgorzelec: 11–45. Wyd. Geol., Warszawa.

TEISSEYRE H., 1974 — Szczegółowa mapa geologiczna Sudetów w skali 1:25 000, ark. Bolków. Wyd. Geol., Warszawa.

TEISSEYRE H., 1977 — Objaśnienia do Szczegółowej mapy geologicznej Sudetów w skali 1:25 000, ark. Bolków. Wyd. Geol., Warszawa.

TEISSEYRE H., SMULIKOWSKI K., OBERC J., 1957 — Geologia regionalna Polski. Vol. **3**, cz. 1. Kraków.

THOMPSON R.N., 1982 — Magmatism of the British Tertiary Volcanic Province. *Scottish J. Geol*., **18**: 49–107.

THOMPSON J.F.H., NEWBERRY R.J., 2000 — Gold deposits related to reduced granitic intrusions. *SEG Rev. Econ. Geol.*, **13**: 377–400.

THOMPSON J.F.H., SILLITOE R.H., BAKER T., LANG J.R., MORTENSEN J.K., 1999 — Intrusion-related gold deposits associated with tungsten-tin provinces: *Mineral. Deposita*, **34**: 323–334.

TRAUBE H., 1888 — Die Minerale Schlesiens. Breslau.

TURNAU E., ŻELAŻNIEWICZ A., FRANKE W., 2002 — Middle to early late Viséan onset of late orogenic sedimentation in the Intra-Sudetic basin, West Sudetes: miospore evidence and tectonic implication. *Geol. Sudetica*, **34**: 9–16.

TURNIAK K., BRÖCKER M., 2002 — Age of the two-mica granite from the Strzegom Massif: new data from U/Pb monazite and xenotime study. *Pr. Specjalne PTM*, **20**: 211–213.

UBERNA J., 1959 — Kaolin i żyły kwarcowe w rejonie Wądroża Wielkiego. *Prz. Geol*., **12**, 7: 536–537.

URBANEK Z., 1978 — The significance of Devonian conodonts faunas for the stratygraphy of epimetamorphic rocks the northern part of the Góry Kaczawskie. *Geol. Sudetica*, **13**: 7–30.

URBANEK Z., BARANOWSKI Z., 1986 — Revision of age of the Radzimowice schists from the Góry Kaczawskie, Western Sudetes. *Ann. Soc. Geol. Pol.*, **56**, 3/4: 399–408.

URBANEK Z., BARANOWSKI Z., HAYDUKIEWICZ A., 1975 — Geologiczne konsekwencje występowania dewońskich konodontów w metamorfiku północnej części Gór Kaczawskich. *Geol. Sudetica*, **10**: 155–169.

WAJSPRYCH B., 1974 — Strukturalno-geologiczne warunki lokalizacji złóż żyłowych jednostki Chełmca. *Geol. Sudetica*, **9**, 1: 125–133.

WEDEPOHL K.H., 1994 — Composition and origin of the Kupferschiefer bed. *Geol. Quart.*, **38**: 623–638.

WHITE A.J.R. CHAPPELL B.W., 1977 — Ultrametamorphism and granitoid genesis. *Tectonophysics*, **43**: 7–22.

WHITE N.C., HEDENQUIST J.W., 1995 — Epithermal gold deposits: Styles, characteristics, and exploration. *SEG Newsletter*, **23**: 1, 9–13.

WILAMOWSKI A., 1998 — Środowisko geotektoniczne intruzji granitowych Tatr i Karkonoszy w świetle danych geochemicznych. *Arch. Miner.*, **51**, 1/2: 261–271.

WINCHESTER J.A., FLOYD P.A., 1977 — Geochemical discrimination of different magma series and their differentiation products using immobile elements. *Chemical Geol*., **20**: 325–343.

WINCHESTER J.A., FLOYD P.A., CHOCYK M., HOROBOWY K., KOZDRÓJ W., 1995 — Geochemistry and tectonic environment of Ordovician meta-igneous rocks in the Rudawy Janowickie Complex, southwest Poland. *J. Geol. Soc. London*, **152**: 105–115.

WOJCIECHOWSKI A., 2001 — Poziom złotonośny z pogranicza czerwonego spągowca i cechsztynu niecki północnosudeckiej w rejonie Nowego Kościoła. *Prz. Geol.*, **49**, 1: 51–59.

WYMAN D., KERRICH R., 1989 — Archean shoshonitic lamprophyres associated with Superior Province gold deposits, distribution, tectonic setting, noble metal abundances, and significance for gold mineralization. *Econ. Geol. Monograph*, **6**: 651–667.

ZACHARIÁŠ J., STEIN H., 2001 — Re–Os ages of Variscan hydrothermal gold mineralizations, Central Bohemian Metallogenic Zone, Czech Republic. *In*: Mineral deposits at the beginning of the 21st century. (eds. Piestrzyński *et al*.): 851–854. Proceedings of the Joint 6th Biennial SGA-SEG Meeting. Kraków, Poland. 26–29 August 2001. A.A. Balkema Publishers, Lisse/Abingdon/Exton/Tokyo.

ZACHARIÁŠ J., PUDILOVÁ M., ŽÁK K., MORAVEK P., LITOCHLEB J., VÁŇA T., PERTOLD Z., 1997 — P–T conditions, fluid inclusions and O,C,S isotope characteristics of gold-bearing mineralizations within the Central Bohemian Metallogenic Zone. *Acta Universitatis Caroline, Geologia*, **41**, 3/4: 167–178.

ZACHARIÁŠ J., PERTORLD Z., PUDILOVÁ M., ŽÁK K., PERTOLDOVÁ J., STEIN H., MARKEY R., 2001 — Geology and genesis of Variscan porphyry-style gold mineralization, Petráčkova hora deposit, Bohemian Massif, Czech Republic. *Miner. Deposita*, **36**: 517–541

ZIMMERMANN E., 1918 — Erläuterungen zu Blatt von Goldberg und Schönau. Geol. Karte von Preussen. Berlin.

ZIMMERMANN E., HAACK W., 1935 — Geologische Karte von Preussen. Blatt Bolkenhain, **246**. Preuss Geol. Landesanst. Berlin.

ZIMMERMANN E., KÜHN B., 1929 — Geologische Karte von Preussen und benachbarten deutschen Ländern. Blatt Schönau, **292**. Preuss Geol. Landesanst. Berlin.

ZIMMERMANN E., KÜHN B., 1938 — Erläuterungen zu Blatt von Goldberg und Schönau. Geol. Karte von Preussen und benachbarten deutschen Ländern 1:25 000. Lief. **246**. Preuss. Geol. Landesanst., Berlin.

ZIMNOCH E., 1965 — Okruszcowanie złoża Starej Góry w świetle nowych danych. *Biul. Geol. Wydz. Geol. UW*, **5**: 3–38.

ZIMNOCH E., 1978 — Mineralizacja kruszcowa złoża Miedzianka w Sudetach. *Biul. Inst. Geol*., **308**: 91–122.

ZÖLLER A., 1923 — Das Goldbergwerke am Willenberg bei Röversdorf unweit Goldberg in Niederschlesien. Centr. Arch. Geol. PIG, Warszawa.

ZÖLLER A., 1932 — Untersuchungen von Goldvorkommen bei Berbisdorf. Centr. Arch. Geol. PIG, Warszawa.

ZÖLLER A., 1936 — Die Putzenzech am Willenberg. Ein Altes Goldbergwerk bei Röversdorf unweit Schönaus in Niederschlesien. *Zeitschr. für prakt. Geol.*, **44**: 109–112.

ZÖLLER A., 1938 — Bericht über eine Dienstreise von 2–7.II. 1938 zur Untersuchung von Bohrproben aus Bohrungen östlich von Bunslau. Centr. Arch. Geol. PIG, Warszawa.

ŻELAŻNIEWICZ A., 1997 — The Sudetes as a Palaeozoic orogen in Central Europe. *Geol. Mag.*, **134**: 691–702.

ŻELAŻNIEWICZ A., CWOJDZIŃSKI S., ENGLAND P., ZIENTARA P., 1997 — Variscides in the Sudetes and the reworked Cadomian orogen: evidence from the GB-2A seismic reflection profiling in south-western Poland. *Geol. Quart.*, **41**, 3: 289–308.

PLATES

Abbreviations to plates :
ank – ankerite, ant – stibnite, ad – adularia, asp – arsenopyrite, apt – apatite; Au – native gold, Bi – native bismuth, bt – biotite, bo – boulangerite, bs – bismuthinite, bu – bournonite, cab – carbonates, cc – calcite, chlc – chalcedony, chl – chlorites; cov – covellite, chp – chalcopyrite, dol – dolomite; el – electrum, fal – tetrahedrite group, fe – Fe-hydroxides, gra – graphite, ga – galena, gu – gustavite, he – hematite, hes – hessite, ho – hornblende, il – illite; kao-chlc – kaolinite-chalcedony matrix, ti – titanite, mg – magnetite, mrs – marcasite, msc – muscovite; pl – plagioclase, po – pyrrhotite, py – pyrite, ru – rutile, ruc – rucklidgeite; scor – scorodite, ser – sericite, sid – siderite, sls – Pb-Ag-Bi-sulphosalts, sf – sphalerite, sulph – sulphide; ten – tennantite, ti – titanite, tur – tourmaline; q, q1 – quartz;

PLATE I

Types of ore mineralization and host rocks at the Radzimowice Au–As–Cu deposit

Photo 1. Cataclased massive arsenopyrite-pyrite-chalcopyrite ore in the main quartz vein from the –70 m level of the Wilhelm shaft.The youngest generation veinlets of marcasite and porous texture of ores caused by dissolution of carbonates. Sample no. M-22.

Photo 2. Arsenopyrite-chalcopyrite ore in chlorite schists. Sample no. M-22.

Photo 3.Arsenopyrite quartz-carbonate veinlets cutting strongly altered dacite porphyry from the northern ore field. Red-brown colours of veinlets and spots caused by Fe-hydroxides.

Photo 4. Sulphide mineralization (mainly pyrite) of veinlet-impregnation type within the altered dacite porphyry.

Photo 5. Pyrite impregnation of dacite porphyry. Pyrite formed pseudomorphs after biotite, and K-feldspars. Southern ore field. Sample no. Rdz. 7/5

Photo 6. Arsenopyrite mineralization of rhyodacite porphyry of veinlet-impregnation type. Note the massive arsenopyrite vein over 1 cm thick associated with black quartz. Northern ore field. sample no.

Photo 7. Brecciated and mylonitized quartz-sericite schist adjacent to the Miner consolation vein. The various angular rock fragments and sulphide impregnation (pyrite and chalcopyrite) in matrix. Sample no. Rdz. 2/2

Photo 8. Brecciated milky-white quartz vein cut by the younger generation pyrite veinlets hosted by black quartz-graphite schists. Sample no. Rdz. 4/1

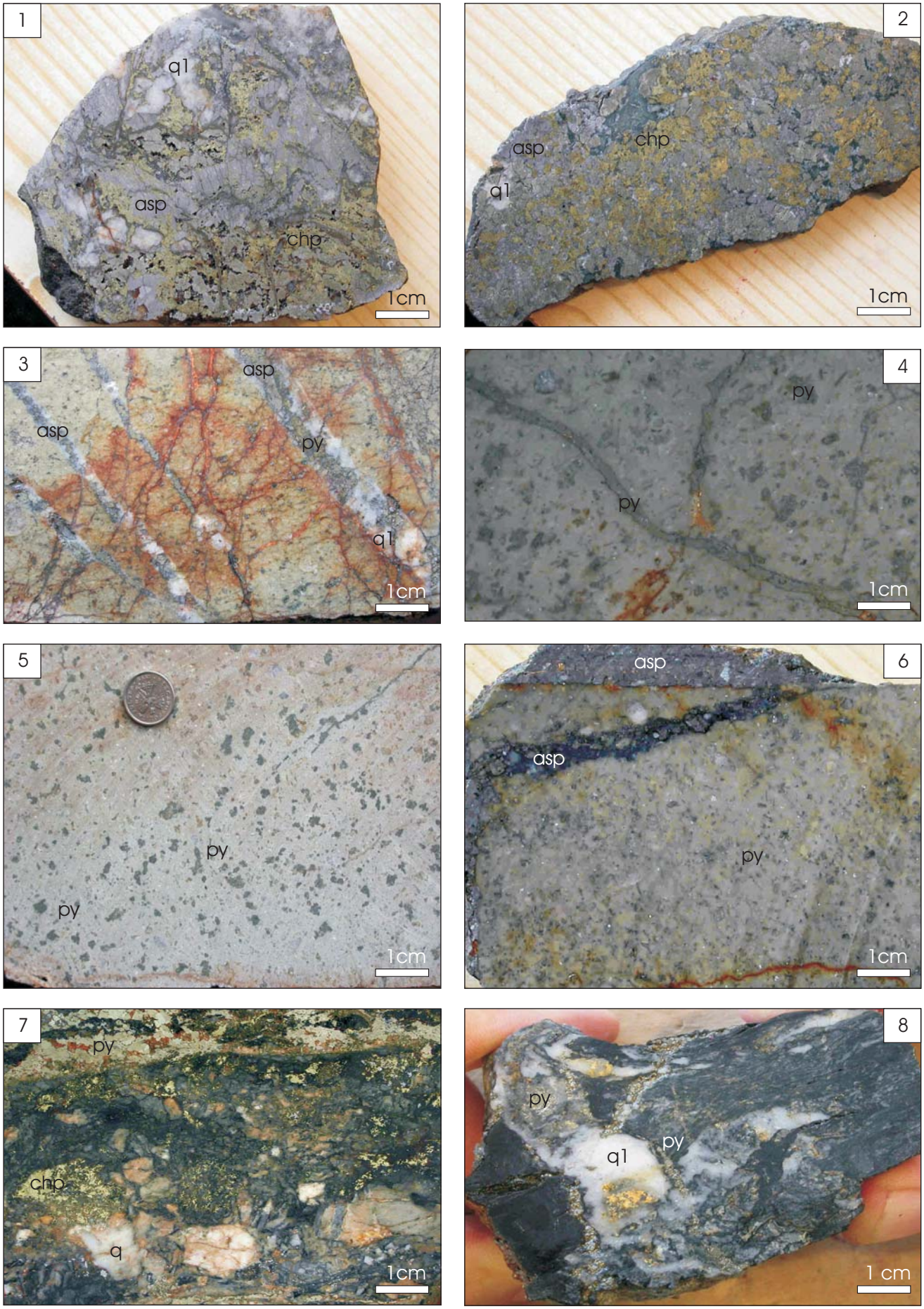

Stanisław Z. Mikulski — The late Variscan gold mineralization in the Kaczawa Mountains, Western Sudetes

PLATE II

The association of Au–Ag–Bi–Te–Pb–S minerals from the Radzimowice Au–As–Cu deposit, reflected light

Photos 1–7. The poly- and monomineral inclusions of different minerals of the Au–Ag–Te–Bi–Pb assemblage. Tellurium minerals are represented mainly by hessite, and gold minerals by electrum and native gold and bismuth minerals by native bismuth and bismuthinite. Co-bearing arsenopyrite and minor pyrite are hosts of the inclusions.

Photo 8. Chalcopyrite with electrum cemented fractured crystal of Co-arsenopyrite.

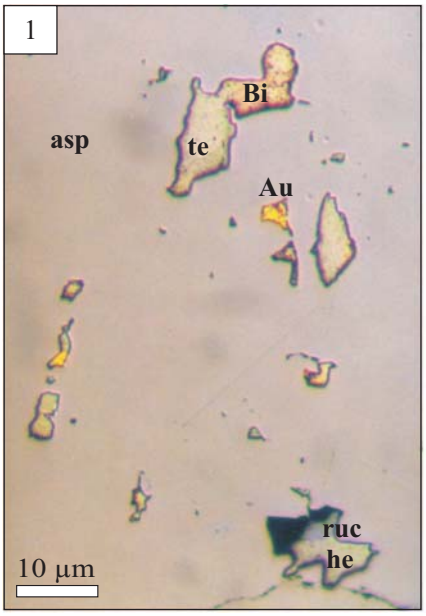
1
asp
Bi
te
Au
ruc
he
10 µm

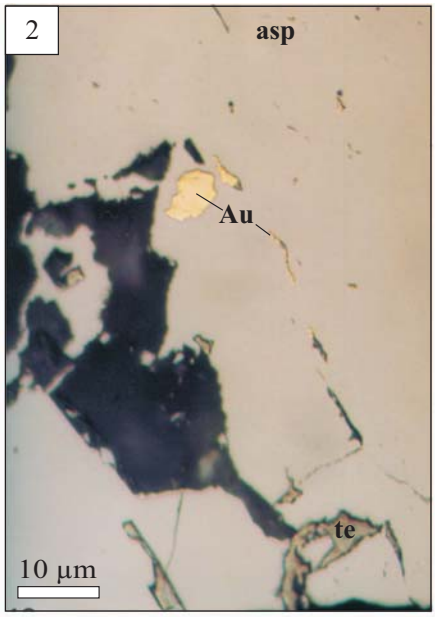
2
asp
Au
te
10 µm


3
el
bs
asp
Au
40 µm

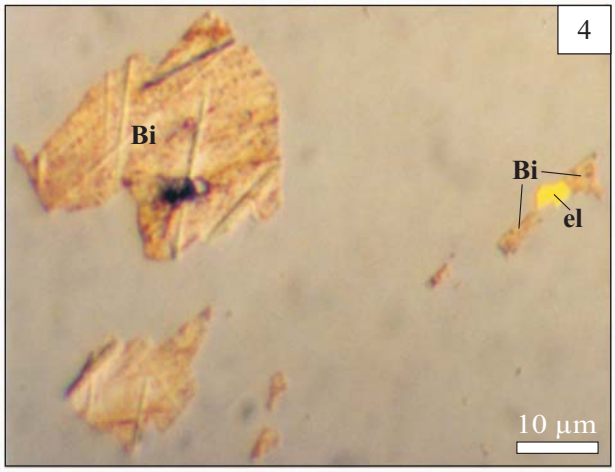
4
Bi
Bi
el
10 µm

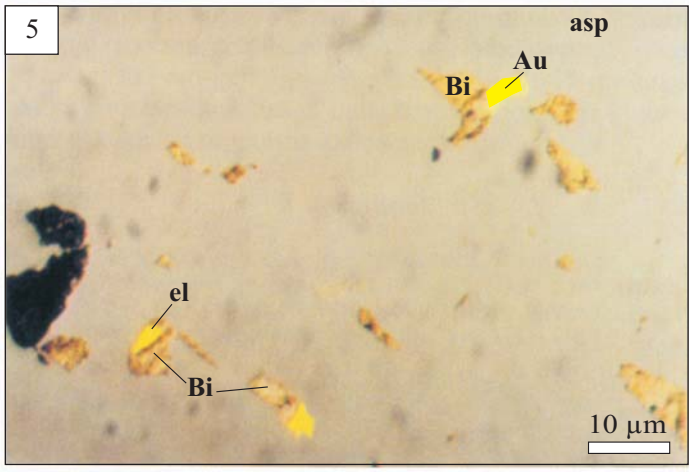
5
asp
Au
Bi
el
Bi
10 µm

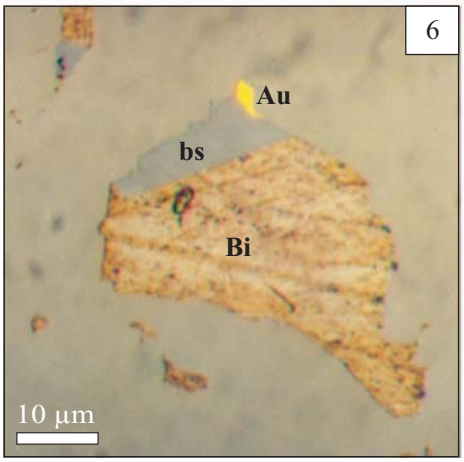
6
Au
bs
Bi
10 µm

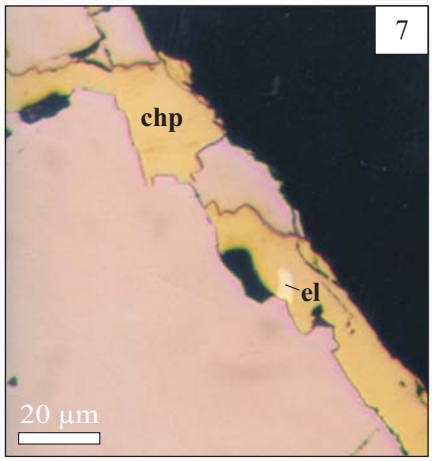
7
chp
el
20 µm

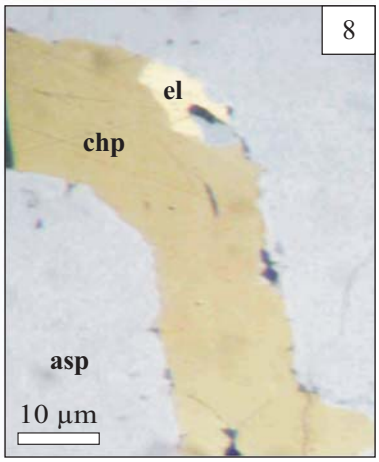
8
el
chp
asp
10 µm

PLATE III

Photographs of ore and associated minerals in igneous rocks under the reflected (Photos 1, 2 and 8) and transmitted lights (Photos 3–7) from the Radzimowice Au–Cu–As deposit

Photo 1. Pseudomorphs of pyrite after biotite phenocrysts with rutile relics (dark gray). Sample no. R34

Photo 2. Poikilitic texture of arsenopyrite with galena and native bismuth inclusions. Sample no. R36.

Photo 3. Quartz phenocrysts with characteristic rim of fine-grained quartz - sericite composition. Note black anhedral and euhedral fine crystals of sulphide (pyrite and arsenopyrite) replacing rock-forming minerals in matrix, and younger quartz-sulphide veinlet cutting dacite (black). Sample no. R29.

Photo 4. Pseudomorphs of sericite and calcite after plagioclase phenocrysts. Note also euhedral crystals of arsenopyrite and quartz-sulphide veinlet cutting dacite (black). Sample no. R6.

Photo 5. Quartz and biotite phenocrysts and sericite pseudomorphs (black) after plagioclase in dacite. Ore minerals are representing by anhedral pyrite and arsenopyrite. Sample no. R13.

Photo 6. Dacite cut by sulphide veinlet (black; pyrite and sphalerite) with adularia, and siderite in surrounding. Sample no. R37.

Photos. 7, 8. Pseudomorphs of pyrite and titanite after biotite and hornblende crystals in lamprophyre. Reflected (7) and transmitted lights (8).

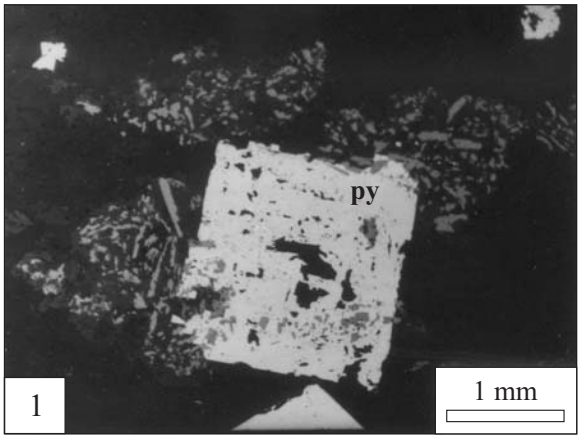
py
1 mm
1

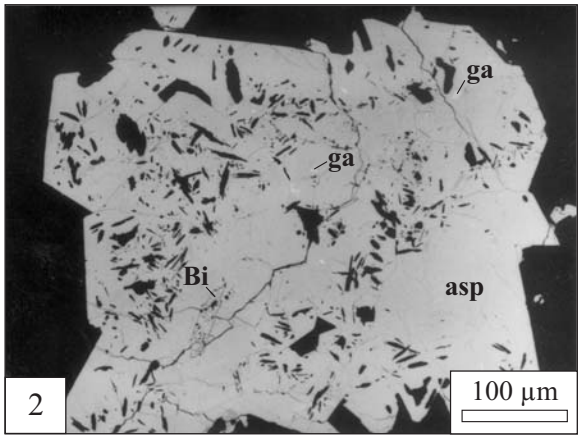
ga
ga
Bi
asp
100 µm
2

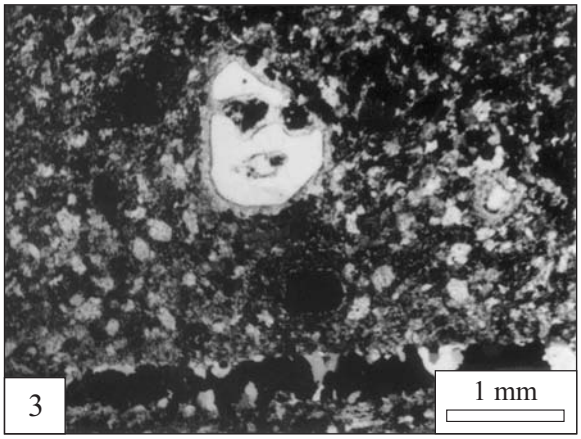
1 mm
3

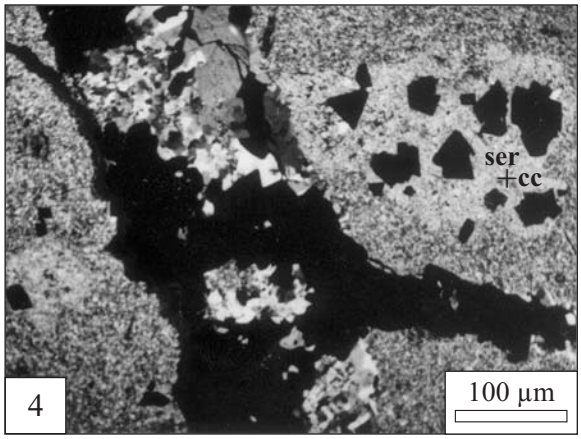
ser
+cc
100 µm
4

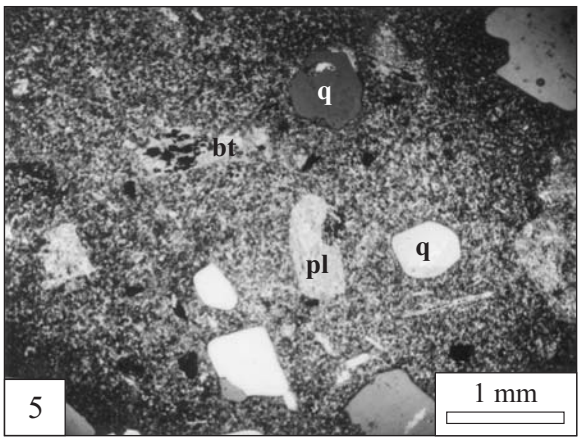
q
bt
pl
q
1 mm
5

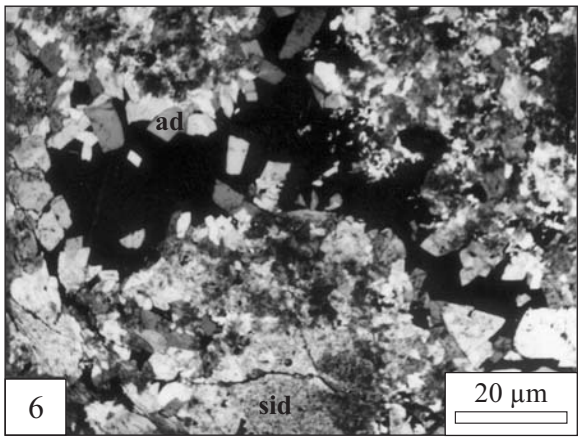
ad
sid
20 µm
6

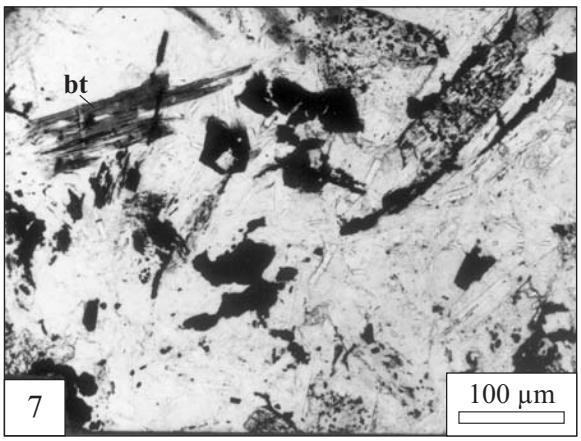
bt
100 µm
7

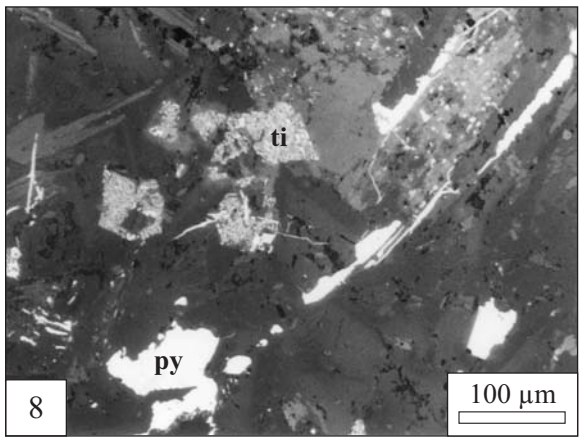
ti
py
100 µm
8

PLATE IV

Photographs with well visible hydrothermal alteration of igneous rocks around the quartz-sulphide veins at the Radzimowice Au–Cu–As deposit.

Photo 1. Porphyric textures of altered dacite are poorly visible. Phenocrysts of plagioclase (light gray) replaced by sericite or muscovite with calcite, and of biotite (black) by epidote with rutile, and/or muscovite, and by pyrite or Fe-hydroxides. Biotite relics contain commonly primary magmatic acicular rutile.

Photo 2. The older generation veinlets of quartz with arsenopyrite are cut by numerous younger generation tiny veinlets of illite and Fe-hydroxides (light brown color)

Photo 3. Carbonate of various compositions represent younger stage of alteration that followed argilitization, feldspathization and silicification of dacite porphyry. Euhedral crystals of dolomite surrounded here by siderite in quartz-sulphide vein from the northern ore field.

Photo 4. Euhedral pyrite (black) is overgrown by calcite and fluorite (violet-blue). Cathodoluminescence light.

Photo 5. Dacite with open space fractures filling of chalcedony. Note common occurrence of pseudomorphs of illite and chalcedony after primary feldspar, and quartz phenocrysts. Pyrite that earlier replaced biotite or plagioclase is almost completely removed during oxidation.

Photo 6. Zonal quartz phenocrysts surrounded by narrow rim of fine-crystalline chalcedony. Cathodoluminescence light.

Photo 7. Dacite moderately sericitized and illitized (tiny white spots) contain numerous euhedral sulphide (dark). Dacite is crosscut by dolomite and low temperature quartz veinlets (white). Enrichment in Fe-hydroxides adjacent to veinlets is marked by orange color.

Photo 8. Fine-crystalline chalcedony filling partly the open space fractures after primary sulphide veinlets. Presence of chalcedony indicating for oxidation condition. Note weak visible phenocrysts of plagioclase and quartz are almost completely replaced by illite and chalcedony.

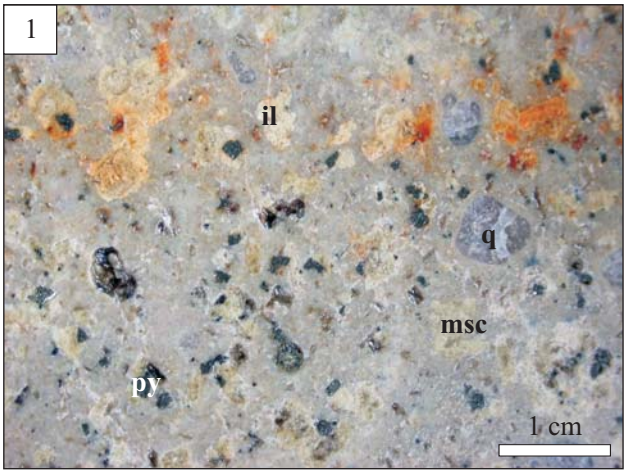
1
il
q
msc
py
1 cm

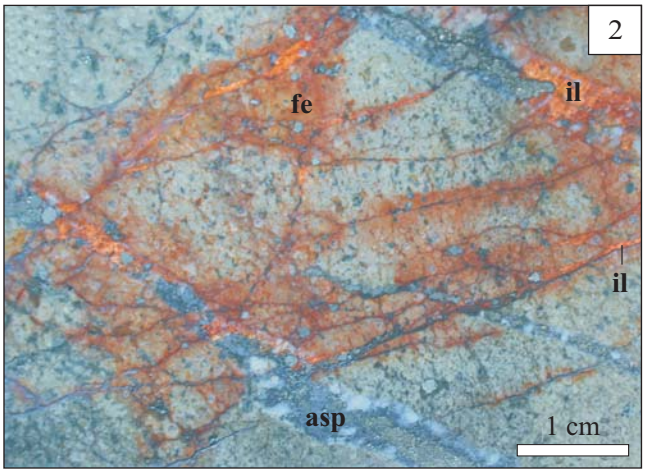
2
fe
il
il
asp
1 cm

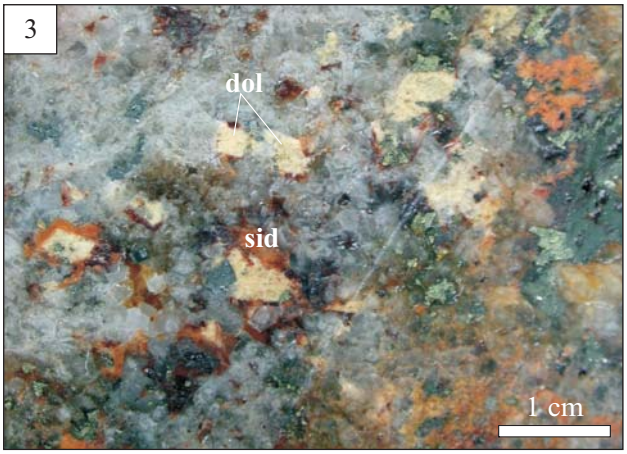
3
dol
sid
1 cm

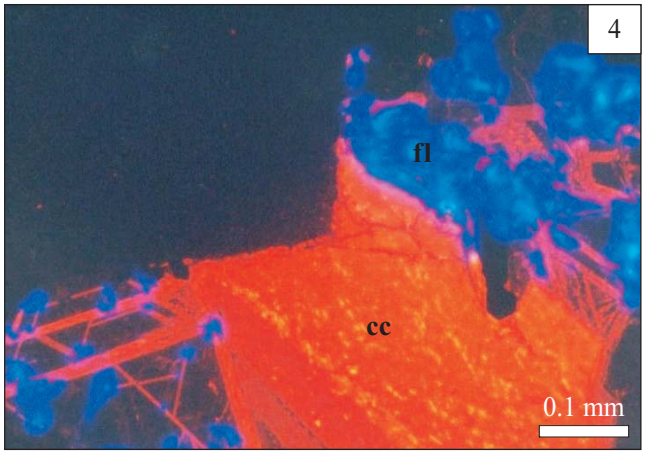
4
fl
cc
0.1 mm

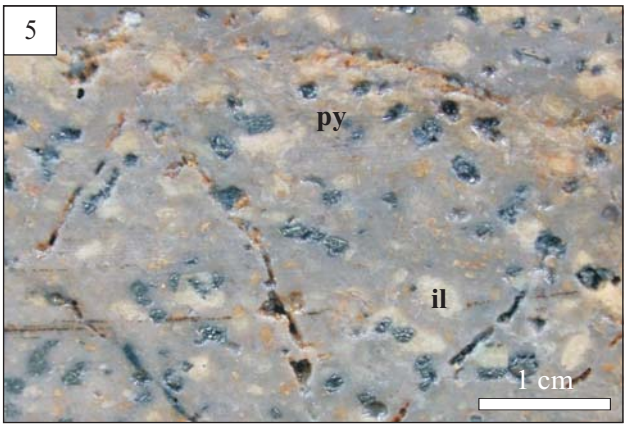
5
py
il
1 cm

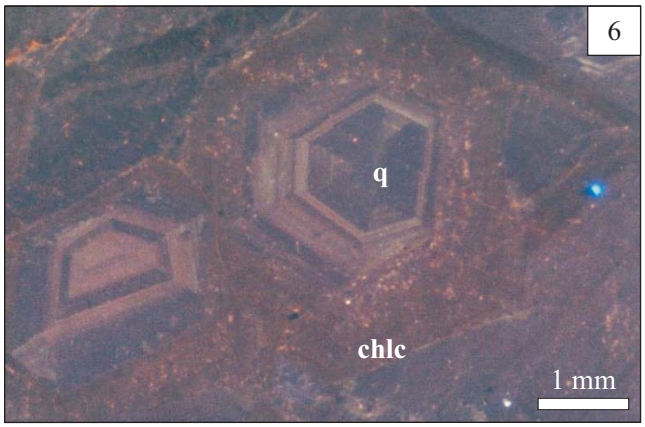
6
q
chlc
1 mm

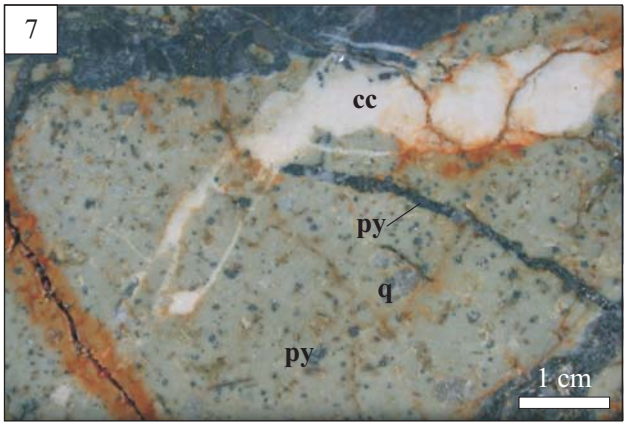
7
cc
py
q
py
1 cm

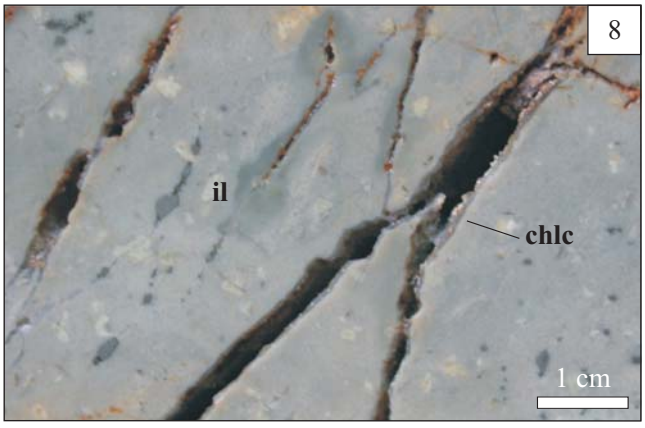
8
il
chlc
1 cm

PLATE V

The representative sulphide from the Radzimowice and Klecza–Radomice abandoned gold mines in the Kaczawa Mountains selected for the age analyses by the Re–Os methods.

Photo 1. Overgrowths of chalcopyrite on pyrite cubic crystal. Radzimowice deposit. Sample no. Rdz 3/1.

Photo 2. Intergrown of euhedral pyrite crystals from Radzimowice deposit. Sample no. M-22.

Photos 3–5. Separated fragments of pyrite and Co-arsenopyrite anhedral crystals from the Radzimowice deposit. Sample no. M-22.

Photo 6. Separated crystals of Co-arsenopyrite from Radzimowice deposit. Sample no. St 3/1-2.

Photos 7, 9, 10. Rhombohedric single and twin crystals of Co-arsenopyrite from the Klecza deposit. Sample no. S-43.

Photo 8. Fragment of pyrite crystal overgrown by quartz. Golejów deposit. Sample no. G-8.

Photo 11. Twin crystals of Co-arsenopyrite from Klecza deposit. Sample no. S-45.

Stanisław Z. Mikulski — The late Variscan gold mineralization in the Kaczawa Mountains, Western Sudetes

PLATE VI

Types of gold-bearing sulphide ore mineralization at the Klecza–Radomice ore district

Photo 1. Massive arsenopyrite ore in the main quartz vein cutting sericite schist from Radomice. Note the cataclased coarse-grained quartz and arsenopyrite big crystals.

Photo 2. Well-visible post-ore brittle deformation. Strongly cataclased quartz vein containing massive arsenopyrite mineralization which was mylonitized and formed so called "arsenic powder". Along the fractures sulphide are replaced by Fe-hydroxides causing red-brownish staining.

Photo 3. Sulphide represented mainly by arsenopyrite cementing brecciated quartz-sericite schist.

Photo 4. Enlarged fragment of Photo 3. Numerous angular fragments of sericite schists are cemented by quartz and sulphide. Note that gray-blue coarse-grained quartz and sulphide was subject of the younger fracturing.

Photo 5. Brecciated massive sulphide (arsenopyrite) with quartz hosted by quartz-sericite schist.

Photo 6. Massive arsenopyrite-pyrite ores. Note numerous angular fragments of quartz-sericite schist in sulphide matrix.

Photo 7. Fractured gray quartz of the 1st generation is filled by micro-veinlets of carbonates (orange – ankerite; white – calcite; red-brown – siderite). Note fine-grained base metal sulphide associated with carbonates.

Photo 8. Strongly fractured white quartz filled by numerous pyrite-marcasite veinlets and fine-crystalline quartz, carbonates, and kaolinite.

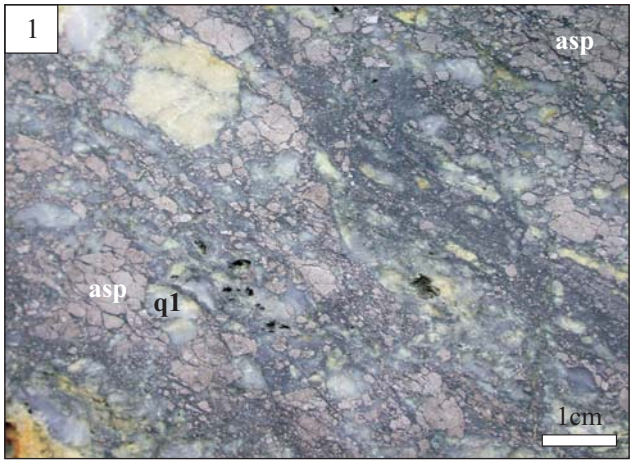

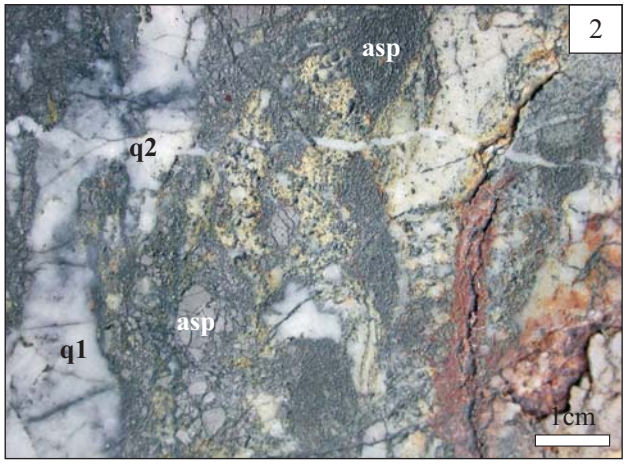

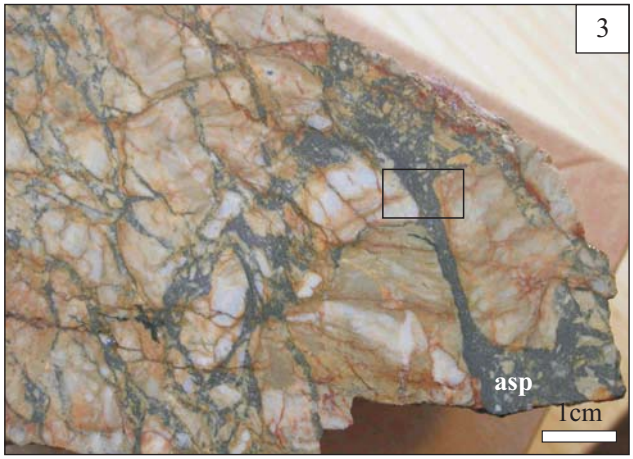

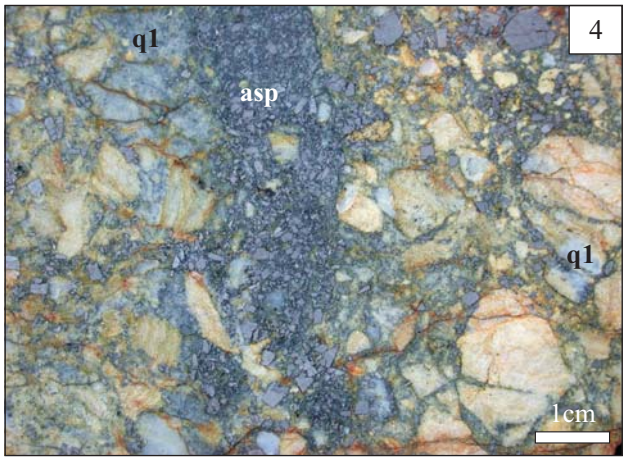

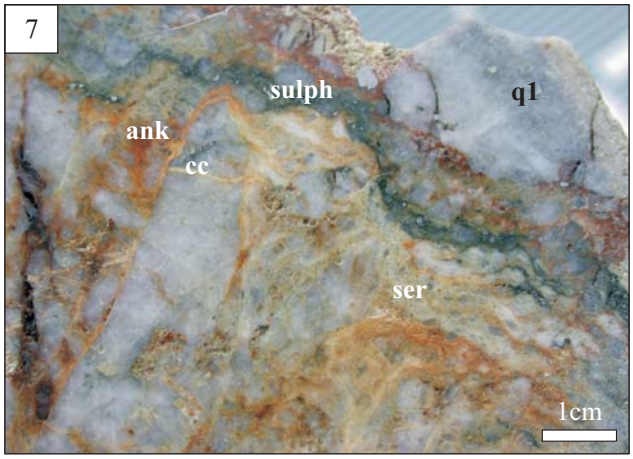

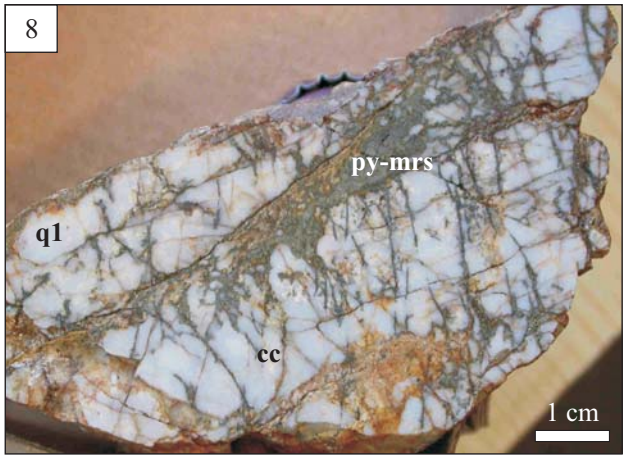

Stanisław Z. Mikulski — The late Variscan gold mineralization in the Kaczawa Mountains, Western Sudetes

PLATE VII

Photographs of ore minerals in transmitted (Photo 2) and reflected (other) lights from the Radomice area.

Photo 1. Quartz vein (black) with strongly fractured and cataclased gold-bearing arsenopyrite (white). Sample no. S-46.

Photo 2. Fractured euhedral medium-grained arsenopyrite (black rhomboids). Note well-visible fine fragments of cataclased arsenopyrite (black) in sericite-chalcedony matrix. Sample no. R62.

Photo 3. Arsenopyrite and pyrite replaced by chalcopyrite and galena. Note numerous inclusions of galena and chalcopyrite micro-veinlets. Black fields, spots are carbonates. Sample no. R44.

Photo 4. Association of chalcopyrite, sphalerite and tetrahedrite intergrowths with carbonates (gray) in cataclastic quartz (black). Note numerous very fine chalcopyrite (white) inclusions in sphalerite (light gray). Sample no. R44.

Photo 5. Poly-mineral inclusions of galena, sphalerite, chalcopyrite and electrum within coarse-grained euhedral arsenopyrite. Sample no. R-44.

Photo 6. Fractured arsenopyrite cut by galena-electrum micro-veinlets. Sample no. S-48a.

Photo 7. Two varieties of hydrothermal pyrite. Fine- and medium-grained crystals of anhedral pyrite with poikilitic core are subject of recrystallization by euhedral pyrite. Sample no. R39.

Photo 8. The hair-like form of marcasite and pyrite that are filling fractures within cataclastic quartz (black) and anhedral arsenopyrite. Sample no. S-46.

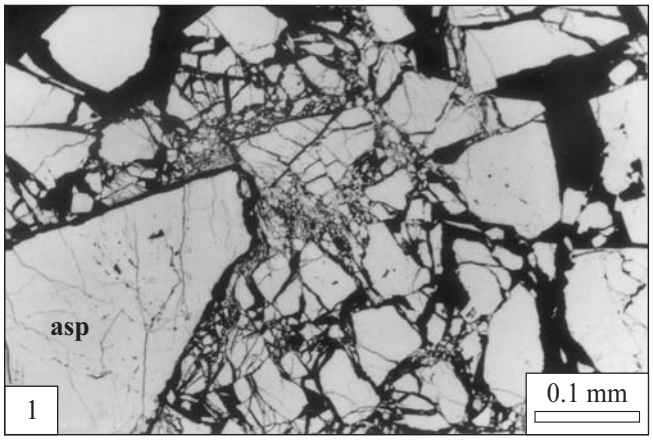
asp
1
0.1 mm

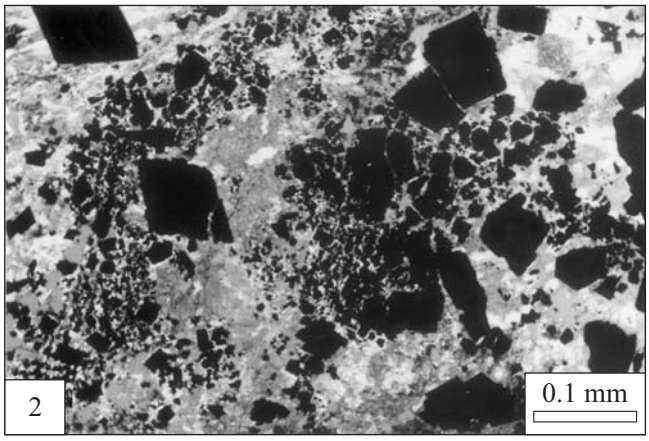
2
0.1 mm

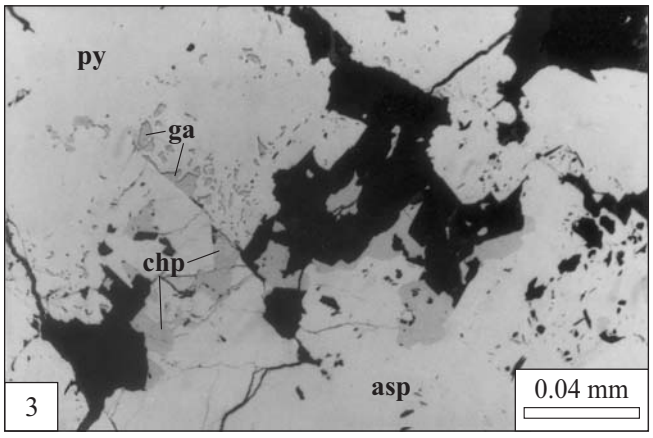
py
ga
chp
asp
3
0.04 mm

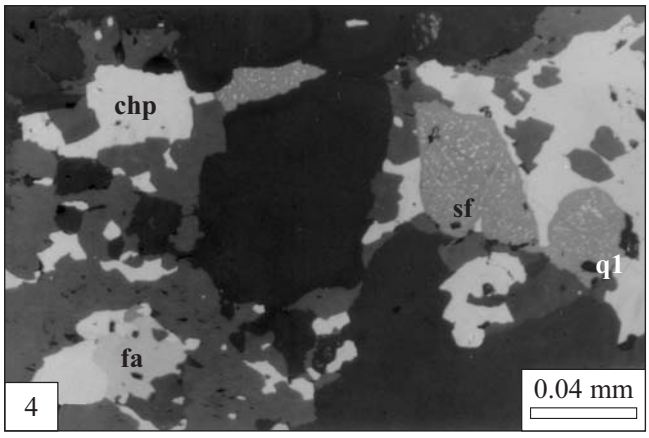
chp
sf
q1
fa
4
0.04 mm

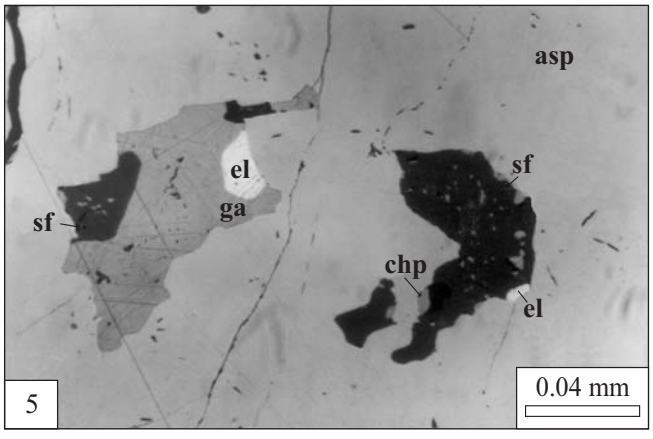
asp
el
sf
ga
sf
chp
el
5
0.04 mm

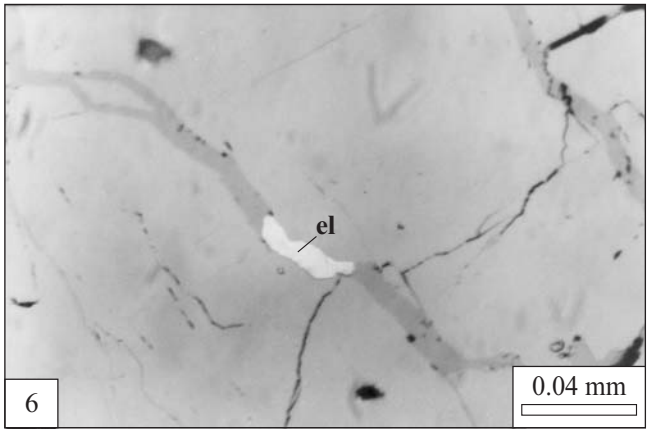
el
6
0.04 mm

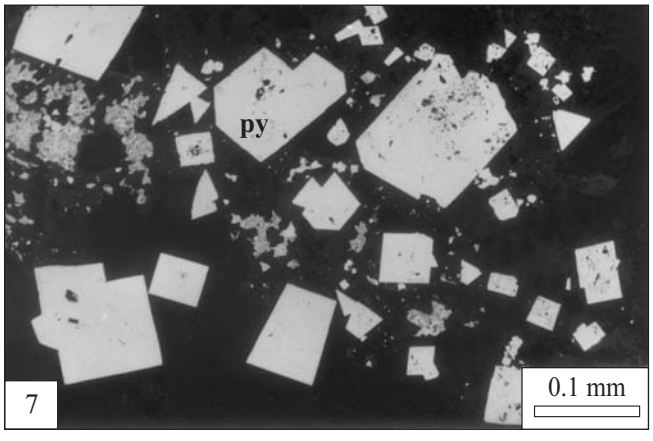
py
7
0.1 mm

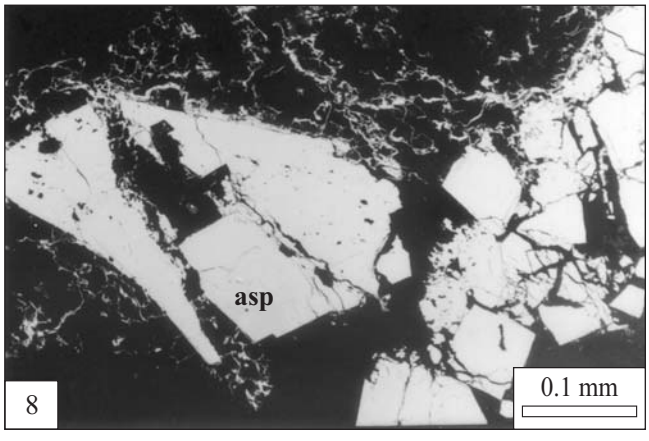
asp
8
0.1 mm

PLATE VIII

Photographs of characteristic host rocks of gold-bearing ore from Klecza and Nielestno (Photos 4 and 5)

Photo 1. Brecciated and fractured form of white quartz of the 1st generation. Note the angular fragments of quartz in red Fe-hydroxides matrix. Numerous micro-fractures are filled by fine-crystalline glossy quartz. White color mineral is kaolinite. Sample no. R59.

Photo 2. Massive coarse-crystalline gray-white quartz vein with abundant sulphide (major pyrite) of impregnation-veinlet character. Big euhedral pyrite crystals and aggregates are fractured. Sample no. G-4.

Photo 3. Strongly cataclased and fractured massive coarse-crystalline gray-white quartz vein with rare sulphide. Numerous fissures are filled by carbonates of various composition associated with base metal sulphides and Fe-hydroxides and electrum. Note the strong sericitization of the hosting schists marked by yellow-green color. Sample no. G-2.

Photo 4. Cataclased coarse-grained quartz cemented by milky quartz, dolomite, hematite and Fe-hydroxides. Sample no. S-60.

Photo 5. Massive vein of white quartz fractured and filled by the younger generation micro-veinlets of glossy quartz and Fe-hydroxides. Sample no. 82.


1
1cm

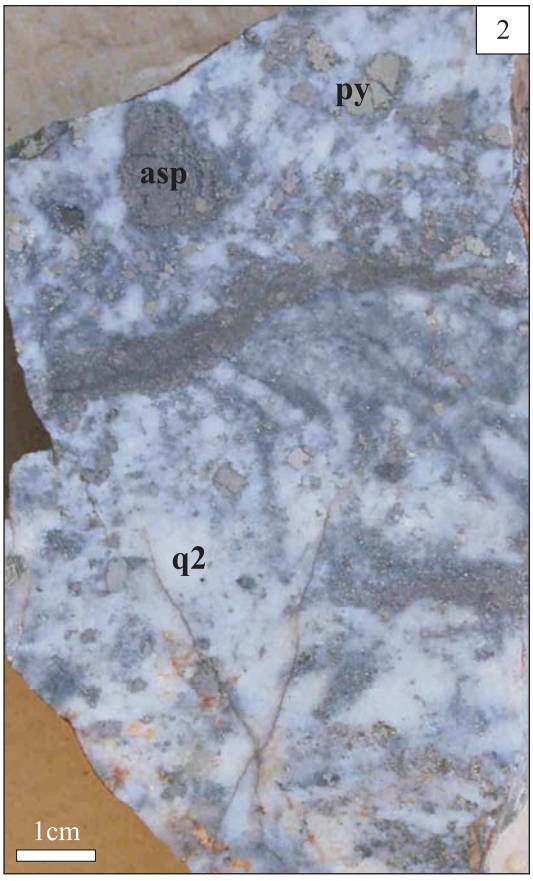
2
py
asp
q2
1cm


4
1cm


3
1cm


5
1cm

PLATE IX

Photographs and BSE images of various generations of pyrite and carbonate
from the abandoned Klecza–Radomice gold ore district.

Photo 1. Different folding of the individual layer of schist. Some of layers are enriched in Fe-hydroxides. F_{2A} open asymmetric folds with vergence to the right (north). Section perpendicular to L_1 lineation and S_1 foliation. Sample from the Klecza area.

Photo 2. Quartz-graphite schist from Klecza enriched in organic matter and framboidal pyrite. Sample no. R65.

Photo 3. Framboidal pyrite (py1a) in graphite schist from Klecza. Sample no. R65.

Photo 4. Big fractured crystals of graphite in association with abundant framboidal pyrite in chlorite. Sample no. R65 from Klecza.

Photo 5. Framboidal pyrite (py1a) is subject of recrystallization by anhedral pyrite (py1b, 2). Sample no. R65.

Photo 6. Enlargement of Photo 5. Recrystallization of framboidal pyrite into younger generation anhedral pyrite (py2). Note the gain of As and lose of Ni in the second generation pyrite in comparison to the framboidal pyrite.

Photo7. Skeletal (anhedral) pyrite (py3a) intergrown with carbonate and euhedral pyrite (py3b) as the last phase of recrystallization of skeletal pyrite to fully idiomorphic forms. Breccia of sericite schists from Radomice. Sample no. R39.

Photo 8. Numerous inclusions of arsenopyrite and rare electrum in pyrite of the 3rd generation (py3b). Radomice, sample (R44) – cataclased sericite/muscovite schist. Note that darker and lighter areas in pyrite crystal reflect also different Ni, Co, and As admixtures.

Photos 3–5, 7 and 8 by P. Dzierżanowski

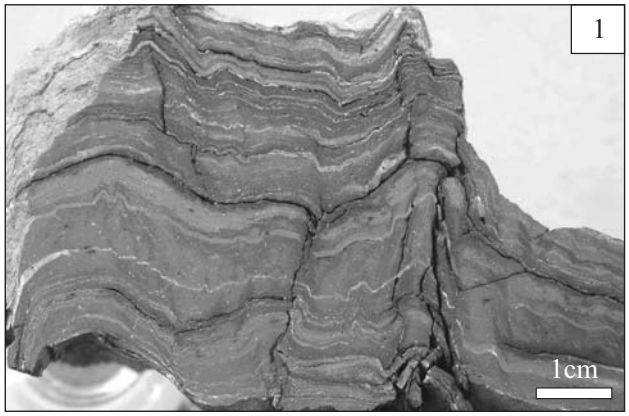
1
1cm

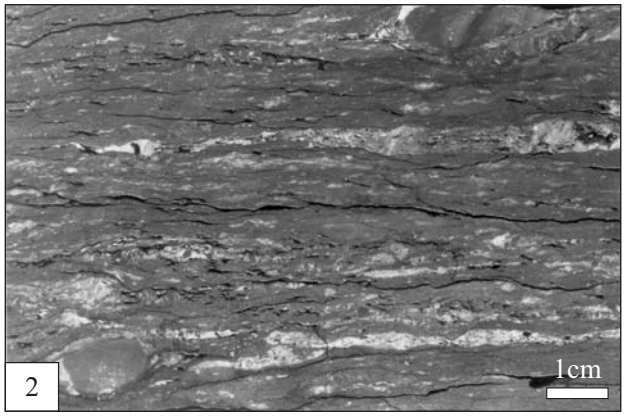
2
1cm

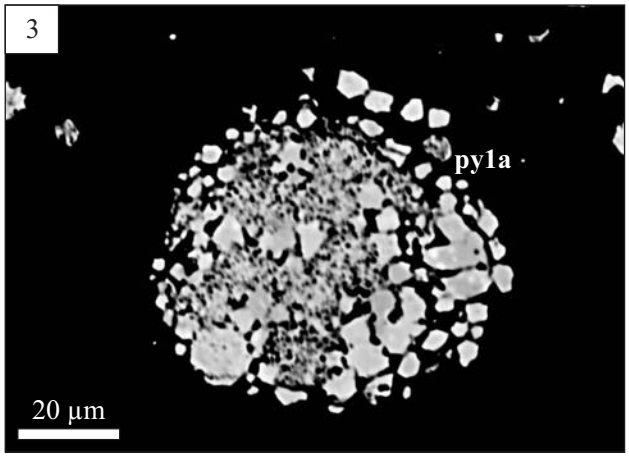
3
py1a
20 µm

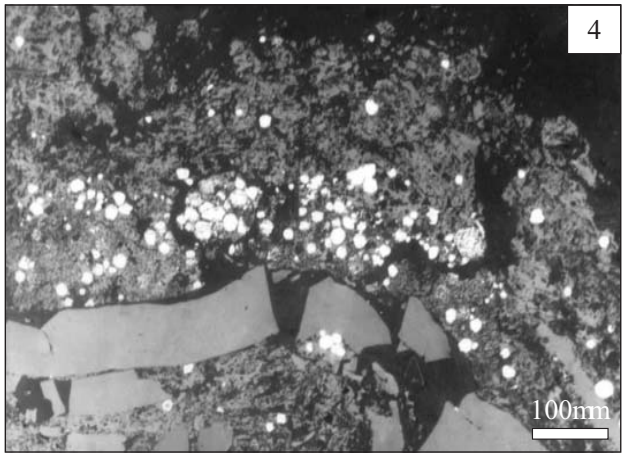
4
100mm

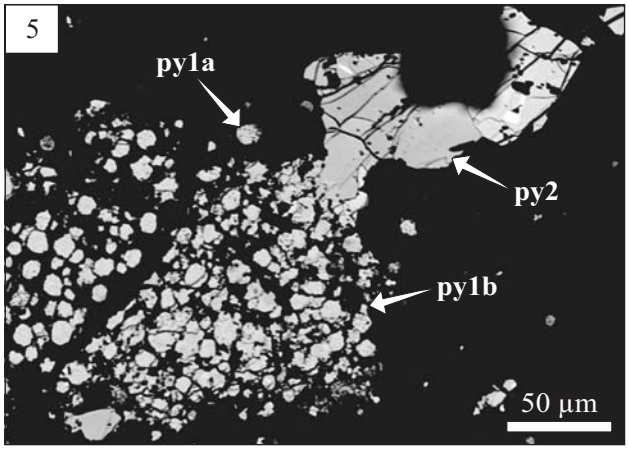
5
py1a
py2
py1b
50 µm

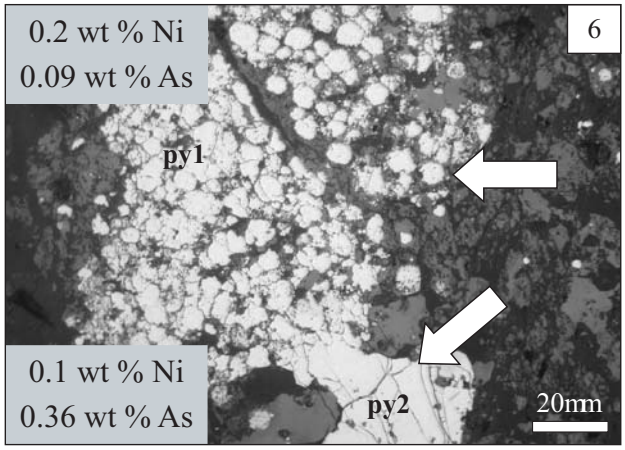
0.2 wt % Ni
0.09 wt % As
6
py1
0.1 wt % Ni
0.36 wt % As
py2
20mm

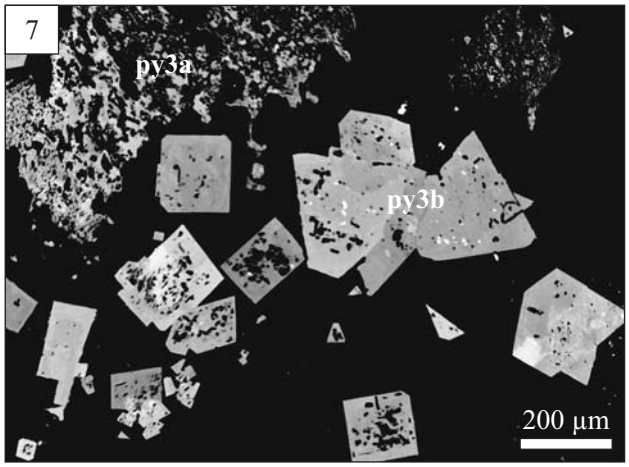
7
py3a
py3b
200 µm

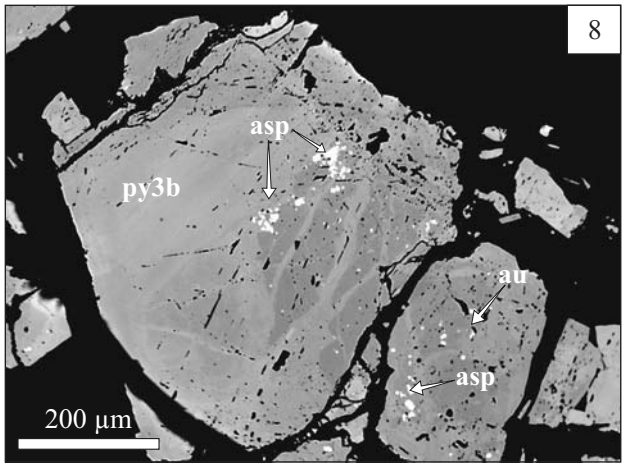
8
asp
py3b
au
asp
200 µm

PLATE X

Photographs of ore minerals in reflected (1–7) and transmitted (8) lights from the Klecza area.

Photo 1. Two generations of pyrite (white) – the framboidal and recrystallized (py2) in quartz-graphite schists. Note a big crystal of graphite (gray). Sample no. R65.

Photo 2. Hematite idioblasts (white) of acicular habit between sericite-rich laminae and in fractures. Sample no. R57.

Photo 3. Quartz vein (black) with strongly fractured and cataclased gold-bearing pyrite (white). Sample no. R63.

Photo 4. Massive quartz vein (black) with cataclased euhedral pyrite cemented by chalcopyrite. Sample no. R62.

Photo 5. Fractured pyrite and euhedral arsenopyrite replaced by galena. Sample no. R63.

Photo 6. Sphalerite (gray) with numerous chalcopyrite (white) inclusions. Note, locally very narrow rims of galena (white) on sphalerite. Sample no. R62.

Photo 7. Marcasite replacements of euhedral pyrite. Sample no. R63.

Photo 8. Ankerite euhedral crystals with narrow rims of Fe-hydroxides (black) in kaolinite/illite-chalcedony matrix. Note anhedral chalcopyrite (black) mineralization between quartz coarse crystals and in association with carbonates. Sample no. R60.

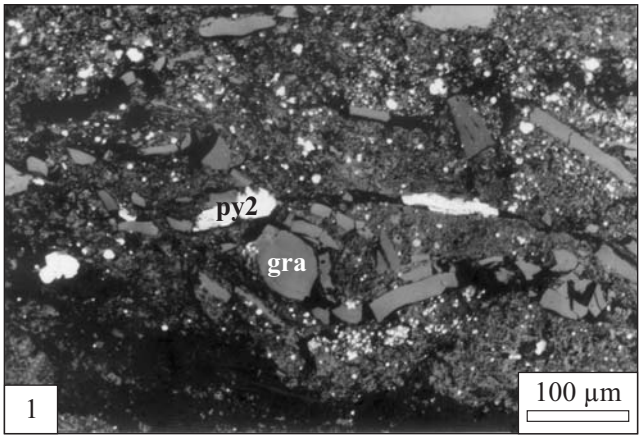
py2
gra
100 µm
1

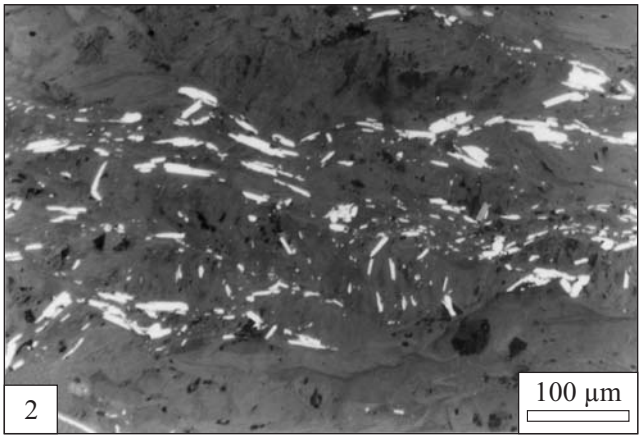
100 µm
2

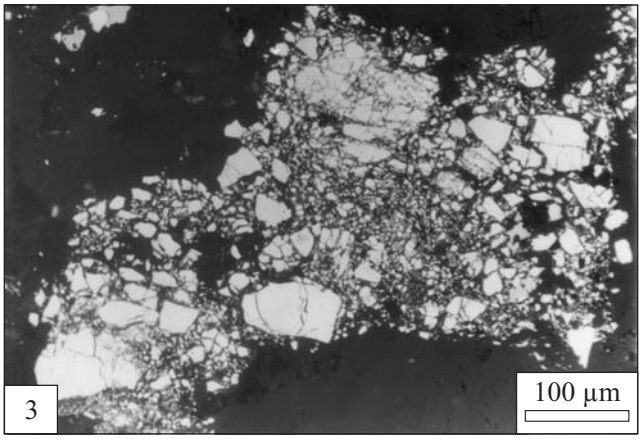
100 µm
3

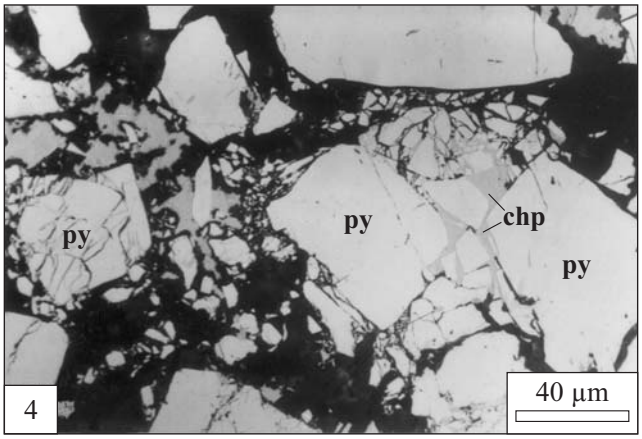
py
py
chp
py
40 µm
4

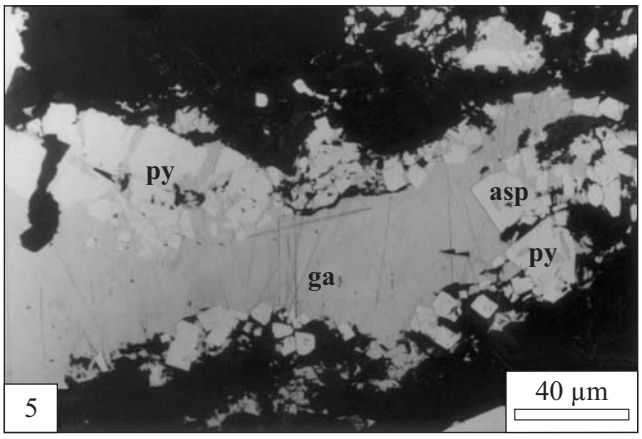
py
asp
py
ga
40 µm
5

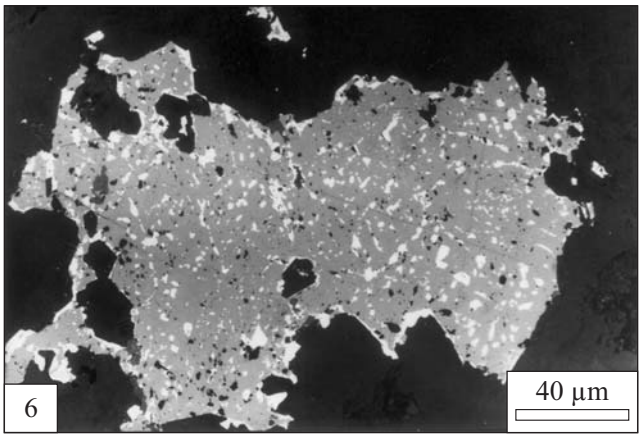
40 µm
6

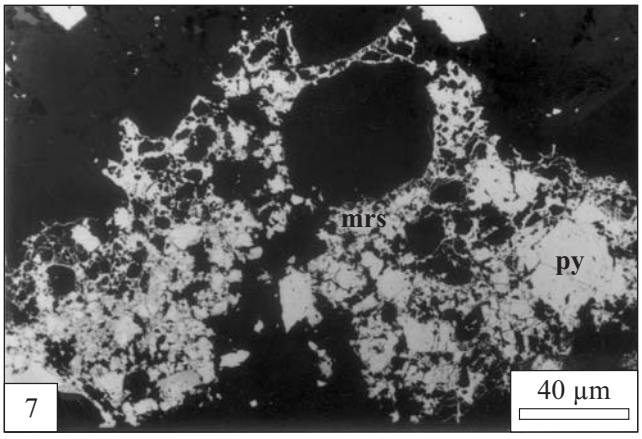
mrs
py
40 µm
7

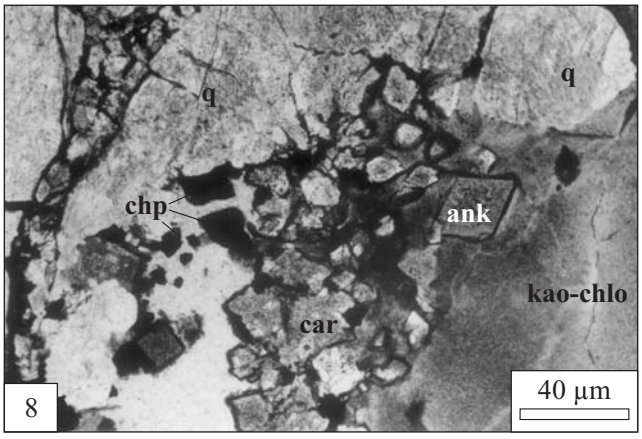
q
q
chp
ank
kao-chlo
car
40 µm
8

PLATE XI

Photographs of ore minerals in transmitted (Photos 1, 2, 7 and 8) and reflected (Photos 3–6) lights from Nielestno area

Photo 1. Folded laminae built of fine-crystalline quartz; sericite and organic matter (black) are subject of younger shearing and micro-faulting. Note also the youngest micro-fracture filled by fine-crystalline quartz. Sample no. R74.

Photo 2. Euhedral fine-grained pyrite (black) in fractures between graphite-muscovite laminae (dark gray) and in quartz (white). Sample no. R53.

Photo 3. Gold and relics of primary sulphide (arsenopyrite and pyrite) in chalcedony. Covellite formed after chalcopyrite. Sample no. R80.

Photo 4. Replacement of arsenopyrite by scorodite (dark gray) and Fe-hydroxides (gray) and of chalcopyrite by covellite. Sample no. R80.

Photo 5. Iron redistribution from primary arsenopyrite and chalcopyrite into the low temperature hematite of acicular habit that is associated with chalcedony. Sample no. Ra 34.

Photo 6. Hematite of fibro-radial aggregates with goethite core in kaolinite-chalcedonic matrix in cataclased quartz vein. Sample no. S-60.

Photo 7. Rhombohedric crystals of dolomite with narrow rims of Fe-hydroxides (black). Sample no. R 68.

Photo 8. Fractured sulphide grains (black) in quartz cemented by chalcedony. Sample no. Ra 34.

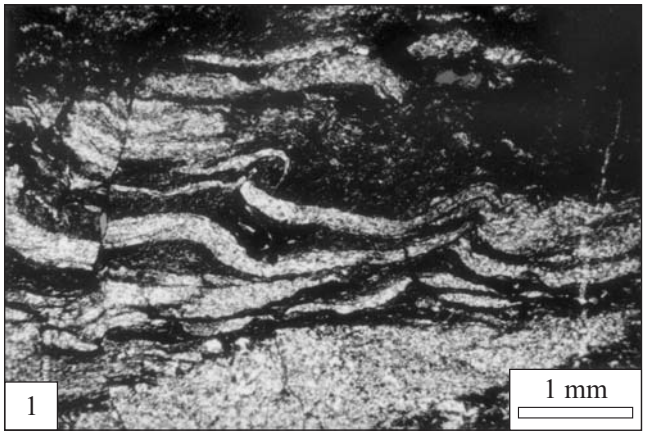
1 mm

1

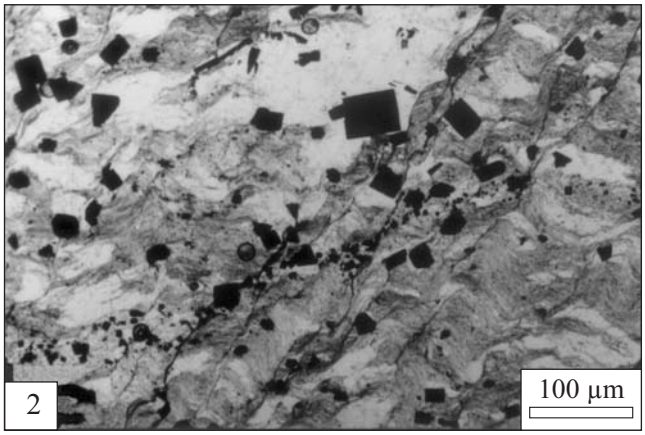
100 µm

2

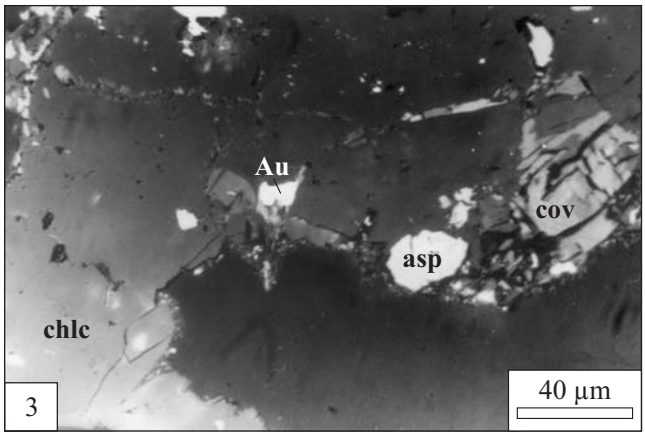
Au
cov
asp
chlc
40 µm

3

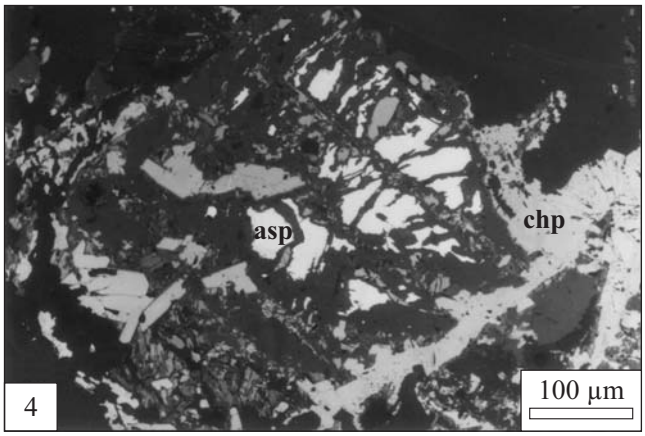
asp
chp
100 µm

4

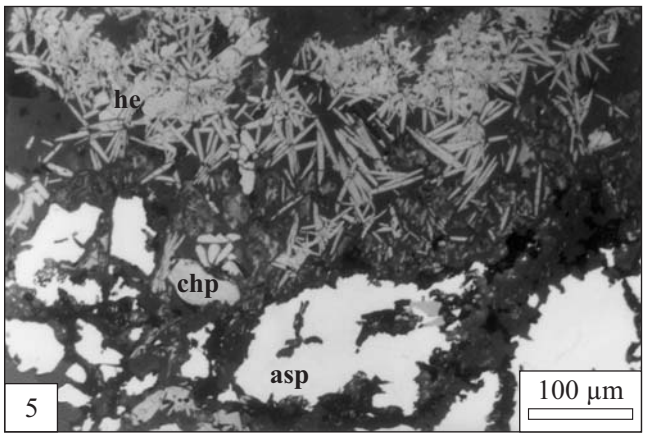
he
chp
asp
100 µm

5

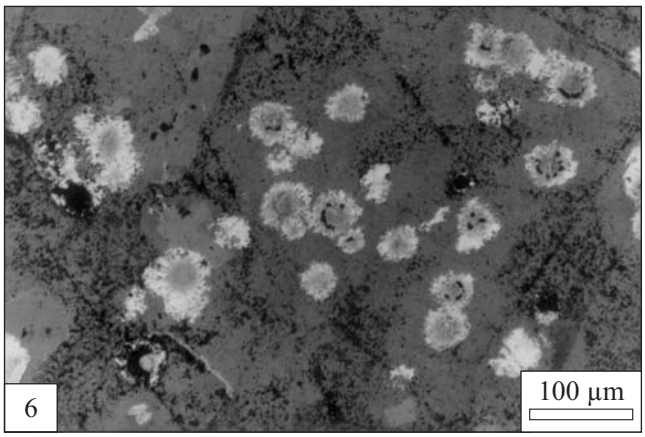
100 µm

6

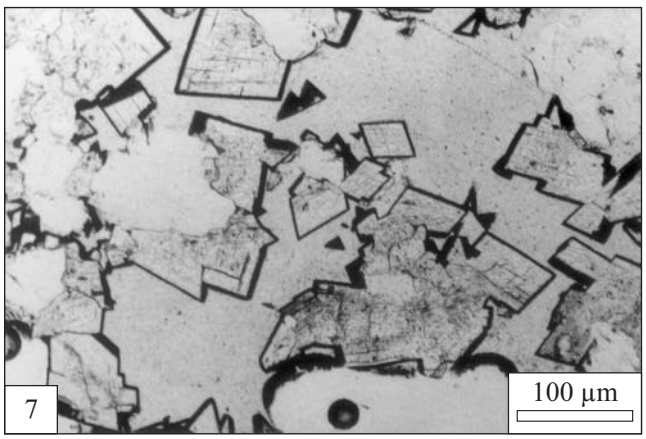
100 µm

7

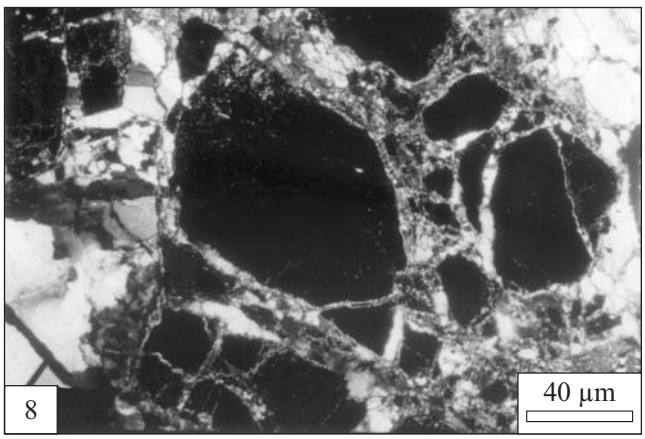
40 µm

8

PLATE XII

Gold in association with sulphide in reflected light (1–8) in the Klecza–Radomice area

Photo 1, 2. Electrum overgrown on arsenopyrite in quartz vein (black). Microphotographs in reflected light, parallel (1) and crossed nicols (2). Sample no. G-7.

Photo 3. Numerous inclusions of electrum hosted by arsenopyrite. Sample no. G-5.

Photo 4. Monomineral inclusions of electrum and galena distributed in micro-fractures of anhedral arsenopyrite. Broken arsenopyrite crystals are cemented by coarse crystalline quartz (black). Sample no. G-7.

Photo 5. Various sulphide inclusions (sphalerite – gray; chalcopyrite – dark yellow; galena – light gray) in association with electrum (light yellow) hosted by arsenopyrite. Note cobaltite euhedral cubic crystal (co) in arsenopyrite. Sample no. G-3.

Photo 6. Association of base metal sulphide with electrum in inclusions hosted by arsenopyrite. Note the elongated inclusions of chalcopyrite and gold in sphalerite. Sample no. R-44.

Photo 7. Micro-veinlets of galena-electrum filling fractures in coarse-grained euhedral arsenopyrite in quartz vein. Sample no. Ra 18.

Photo 8. Electrum filling fracture in coarse-grained arsenopyrite. Sample no. G-7.

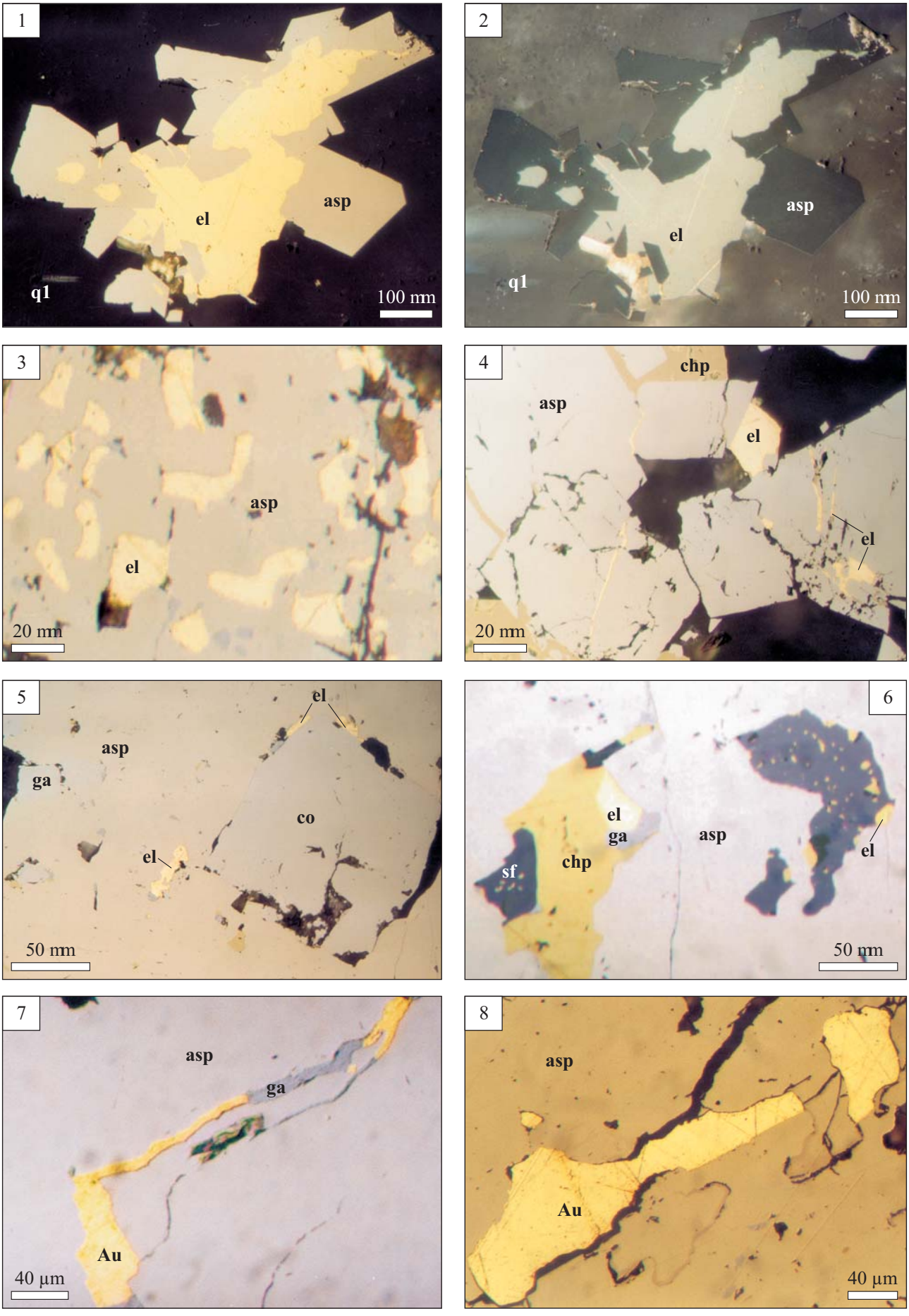

Stanisław Z. Mikulski — The late Variscan gold mineralization in the Kaczawa Mountains, Western Sudetes

PLATE XIII

Intergranular gold with chalcedony in the cataclased quartz-graphite-sericite schist from Klecza (Photos1–4) and Radomice (Photos 5–8)

Photo 1. Free gold in ankerite in association with chalcopyrite and graphite. Sample no. G-7.

Photo 2. Free gold in chalcedony which is cemented fractures in coarse-crystalline quartz. Sample no. R61.

Photo 3. Numerous fine-grained euhedral pyrite and arsenopyrite grains (black) surrounded by chalcedony (light gray). Numerous micro-veinlets of galena with electrum occur in fractured sulphide. Sample no. G-7.

Photo 4. Free gold micro-grains (Au – 82.8 wt%; Ag – 16.3 wt %) in paragenesis with chalcedony (white) filling fractures and intergranular spaces. Note fractured scorodite crystal (gray) cut by fine-crystalline quartz. BSEI. Sample no. R79.

Photos. 5, 6. Native free gold in chalcedony quartz (light gray). Strongly cataclased quartz-sericite-muscovite schist is cemented by chalcedony. Sample no. R79.

Photo 7. Characteristic rosettes of chalcedony which cemented cataclased coarse-grained quartz. Note the black holes which formed after acidic dissolution of primary sulphide. Sample no. R-79.

Photo 8. Chalcedony rim around coarse-grained arsenopyrite (black) which contains micro-veinlets and inclusions of galena, sphalerite and electrum. Sample no. R-44.

Photographs in: reflected light (1, 2, 4–6) and transmitted light (3, 7 and 8).

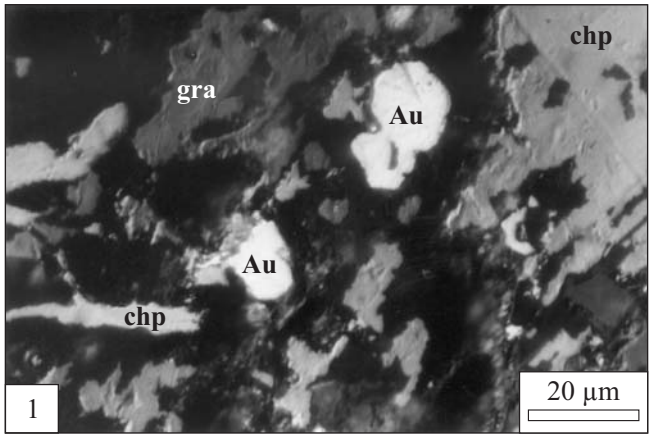
chp
gra
Au
Au
chp
20 µm
1

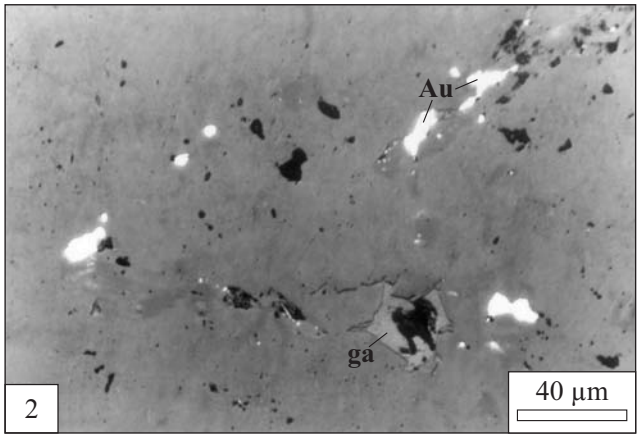
Au
ga
40 µm
2

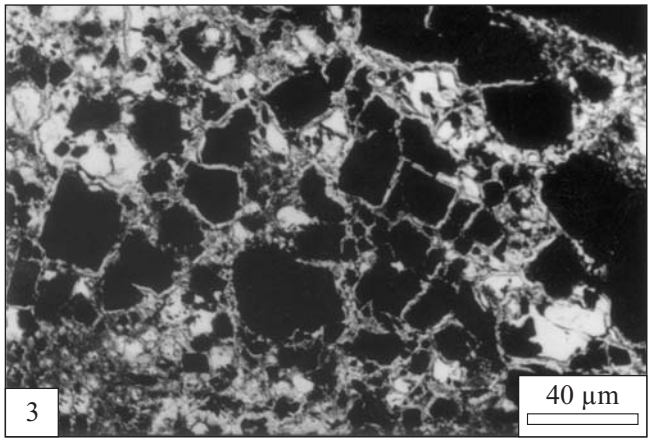
40 µm
3

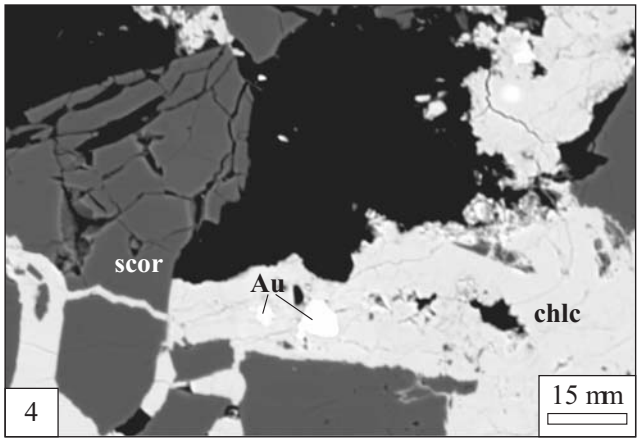
scor
Au
chlc
15 mm
4

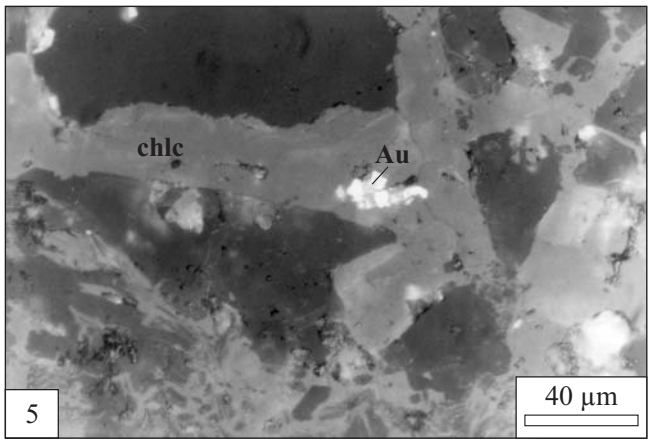
chlc
Au
40 µm
5

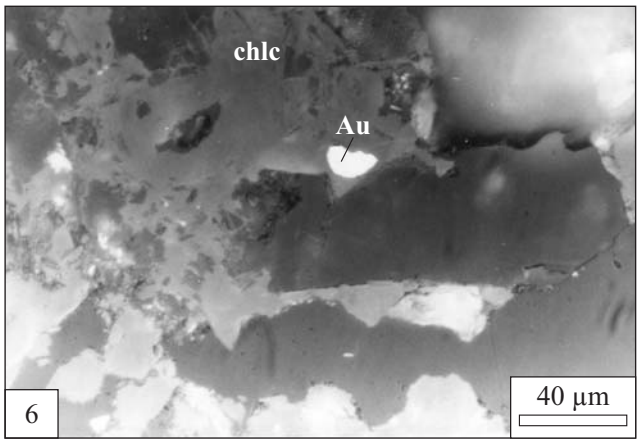
chlc
Au
40 µm
6

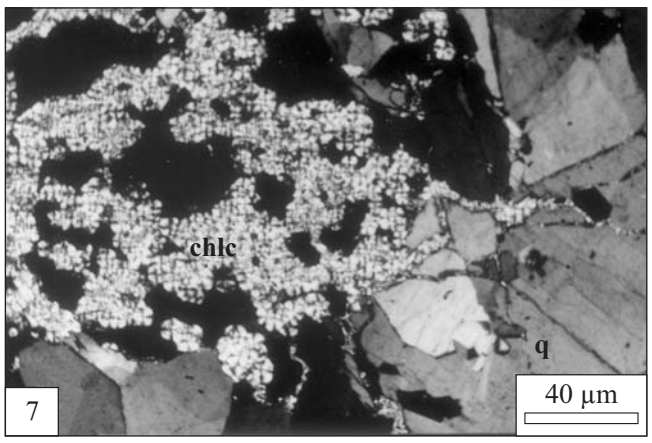
chlc
q
40 µm
7

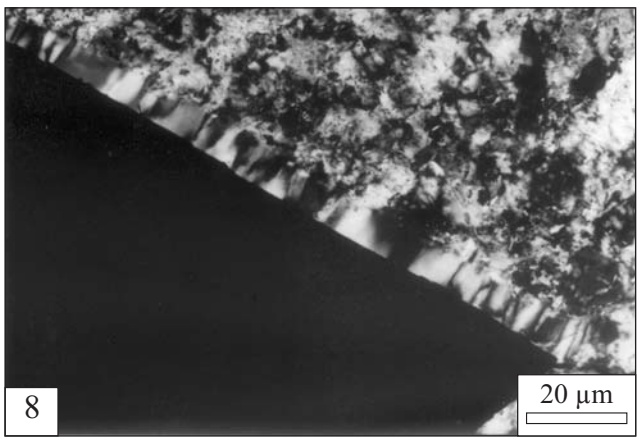
20 µm
8

PLATE XIV

Photographs of the ore minerals association and the host rock alteration at the Klecza–Radomice ore district. Cathodoluminescence and transmitted light (Photos 4 and 8)

Photo 1. Coarse- and fine-crystalline hydrothermal quartz generations with sulphide mineralization (black). Note the various colors of quartz (dark brown – coarse-grained euhedral quartz of the first generation). Sample no. G-1.

Photo 2. Characteristic rim of clay minerals (green – kaolinite) surrounding arsenopyrite euhedral crystal. Note also clay minerals filling micro-fissures in rock. Sample no. R44.

Photo 3. Kaolinite (blue) associated with chalcedony (yellow) are filling fractures and intergranular spaces in sulphide ores represented mainly by pyrite (black). Sericite schist. Sample no. Ra 19.

Photo 4. Euhedral crystals of tourmaline (green) in association with muscovite and chlorite (brown). Sample no. R77.

Photo 5. Fractured coarse-crystalline quartz and pyrite cemented by various composition carbonates. Note the euhedral large crystal of ankerite and fine-grained crystals of dolomite (red) and euhedral hematite in the younger generation calcite. Sample no. Ra 15.

Photo 6. Strong carbonatization (calcite – yellow; dolomite – red) of fractured quartz and sulphide ore (black). Sample no. S-60.

Photo 7. Fractured coarse-crystalline quartz and pyrite cemented by hydrothermal apatite. Note the remnants of fine-grained apatite of sedimentary-metamorphic origin. Sample no. Ra 18.

Photo 8. Euhedral ankerite and dolomite crystals cementing fractured coarse-crystalline quartz. Notice the micro-crystalline quartz between coarse-grained quartz. Kaolinite is the main clay mineral represented mostly as numerous inserts in quartz. Sample no. R68.

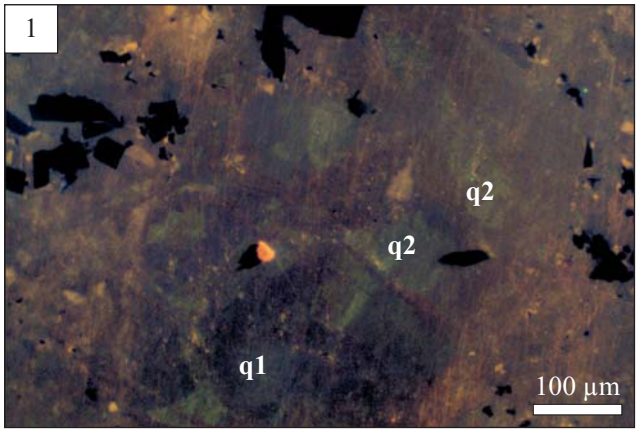
1
q2
q2
q1
100 µm

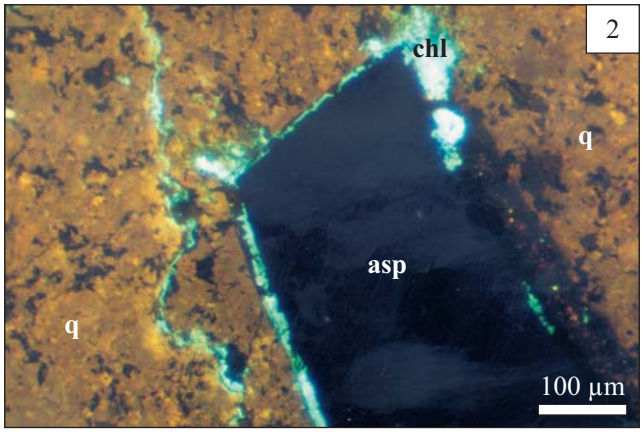
2
chl
q
asp
q
100 µm

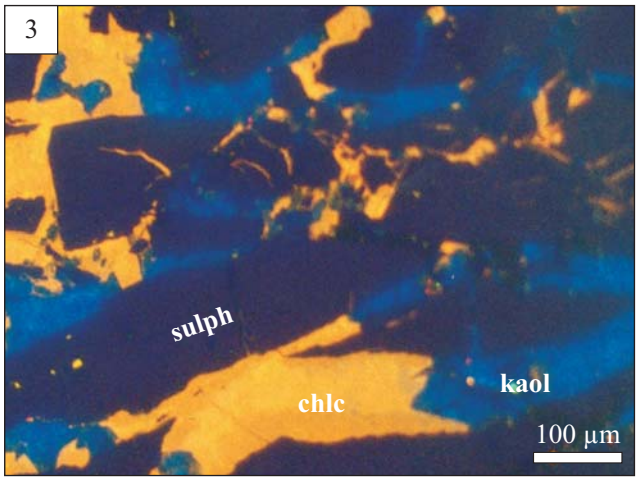
3
sulph
chlc
kaol
100 µm

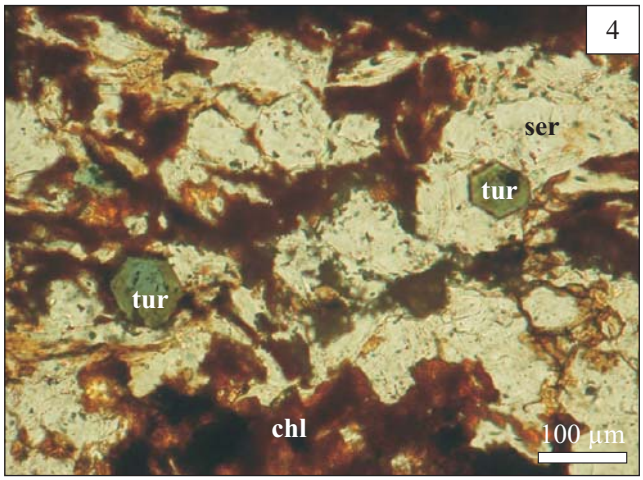
4
ser
tur
tur
chl
100 µm

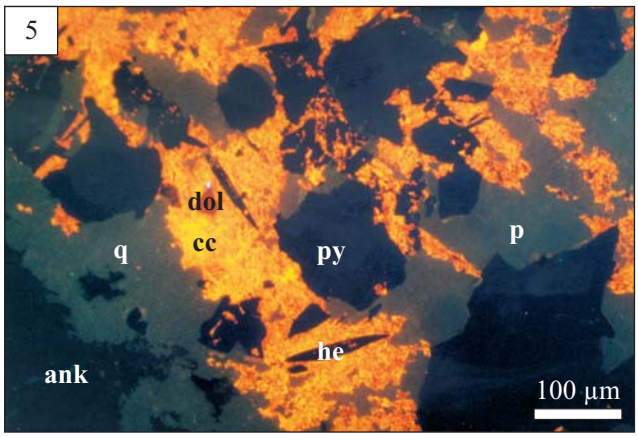
5
dol
cc
q
py
p
he
ank
100 µm

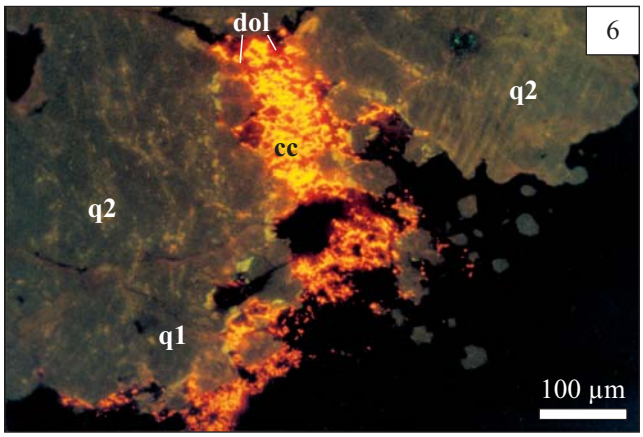
6
dol
q2
cc
q2
q1
100 µm

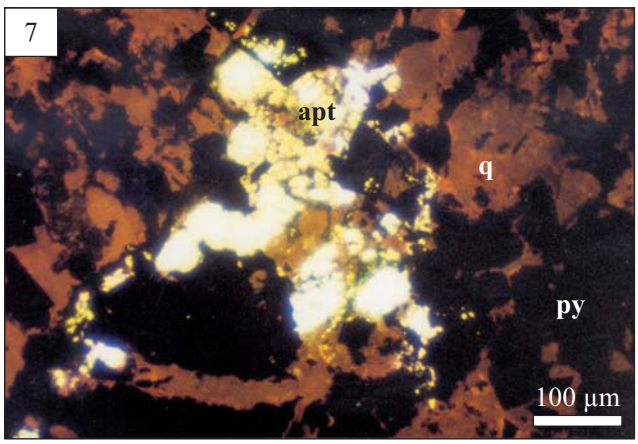
7
apt
q
py
100 µm

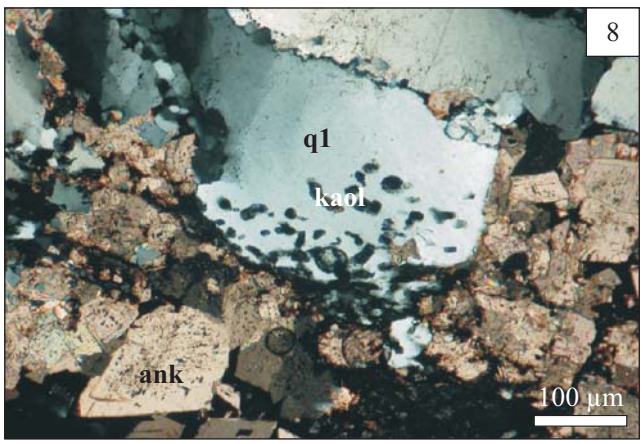
8
q1
kaol
ank
100 µm